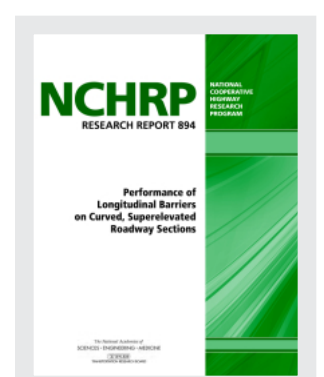


This PDF is available at http://nap.nationalacademies.org/25290









## Performance of Longitudinal Barriers on Curved, Superelevated Roadway Sections (2019)

#### **DETAILS**

138 pages | 8.5 x 11 | PAPERBACK ISBN 978-0-309-48578-4 | DOI 10.17226/25290

#### CONTRIBUTORS

Dhafer Marzougui, Cing-Dao "Steve" Kan, Umashankar Mahadevaiah, Fadi Tahan, Christopher Story, Stefano Dolci, Alberto Moreno, Kenneth S. Opiela, and Richard Powers; National Cooperative Highway Research Program; Transportation Research Board; National Academies of Sciences, Engineering, and Medicine

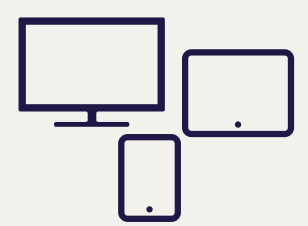
#### SUGGESTED CITATION

National Academies of Sciences, Engineering, and Medicine. 2019. Performance of Longitudinal Barriers on Curved, Superelevated Roadway Sections. Washington, DC: The National Academies Press. https://doi.org/10.17226/25290.



Visit the National Academies Press at nap.edu and login or register to get:

- Access to free PDF downloads of thousands of publications
- 10% off the price of print publications
- Email or social media notifications of new titles related to your interests
- Special offers and discounts



All downloadable National Academies titles are free to be used for personal and/or non-commercial academic use. Users may also freely post links to our titles on this website; non-commercial academic users are encouraged to link to the version on this website rather than distribute a downloaded PDF to ensure that all users are accessing the latest authoritative version of the work. All other uses require written permission. (Request Permission)

This PDF is protected by copyright and owned by the National Academy of Sciences; unless otherwise indicated, the National Academy of Sciences retains copyright to all materials in this PDF with all rights reserved.

#### NATIONAL COOPERATIVE HIGHWAY RESEARCH PROGRAM

# **NCHRP** RESEARCH REPORT 894

# Performance of Longitudinal Barriers on Curved, Superelevated Roadway Sections

Dhafer Marzougui
Cing-Dao "Steve" Kan
Umashankar Mahadevaiah
Fadi Tahan
Christopher Story
Stefano Dolci
Alberto Moreno
Center for Collision Safety and Analysis (CCSA)
George Mason University
Fairfax, VA

#### Kenneth S. Opiela

**CONSULTANT** Springfield, VA

#### **Richard Powers**

CONSULTANT Herndon, VA

Subscriber Categories

Construction • Design • Safety and Human Factors

Research sponsored by the American Association of State Highway and Transportation Officials in cooperation with the Federal Highway Administration

The National Academies of SCIENCES • ENGINEERING • MEDICINE

TRANSPORTATION RESEARCH BOARD

2019

# NATIONAL COOPERATIVE HIGHWAY RESEARCH PROGRAM

Systematic, well-designed, and implementable research is the most effective way to solve many problems facing state departments of transportation (DOTs) administrators and engineers. Often, highway problems are of local interest and can best be studied by state DOTs individually or in cooperation with their state universities and others. However, the accelerating growth of highway transportation results in increasingly complex problems of wide interest to highway authorities. These problems are best studied through a coordinated program of cooperative research.

Recognizing this need, the leadership of the American Association of State Highway and Transportation Officials (AASHTO) in 1962 initiated an objective national highway research program using modern scientific techniques—the National Cooperative Highway Research Program (NCHRP). NCHRP is supported on a continuing basis by funds from participating member states of AASHTO and receives the full cooperation and support of the Federal Highway Administration, United States Department of Transportation.

The Transportation Research Board (TRB) of the National Academies of Sciences, Engineering, and Medicine was requested by AASHTO to administer the research program because of TRB's recognized objectivity and understanding of modern research practices. TRB is uniquely suited for this purpose for many reasons: TRB maintains an extensive committee structure from which authorities on any highway transportation subject may be drawn; TRB possesses avenues of communications and cooperation with federal, state, and local governmental agencies, universities, and industry; TRB's relationship to the National Academies is an insurance of objectivity; and TRB maintains a full-time staff of specialists in highway transportation matters to bring the findings of research directly to those in a position to use them.

The program is developed on the basis of research needs identified by chief administrators and other staff of the highway and transportation departments, by committees of AASHTO, and by the Federal Highway Administration. Topics of the highest merit are selected by the AASHTO Special Committee on Research and Innovation (R&I), and each year R&I's recommendations are proposed to the AASHTO Board of Directors and the National Academies. Research projects to address these topics are defined by NCHRP, and qualified research agencies are selected from submitted proposals. Administration and surveillance of research contracts are the responsibilities of the National Academies and TRB.

The needs for highway research are many, and NCHRP can make significant contributions to solving highway transportation problems of mutual concern to many responsible groups. The program, however, is intended to complement, rather than to substitute for or duplicate, other highway research programs.

#### **NCHRP RESEARCH REPORT 894**

Project 22-29A ISSN 2572-3766 (Print) ISSN 2572-3774 (Online) ISBN 978-0-309-48012-3 Library of Congress Control Number 2019931195

© 2019 National Academy of Sciences. All rights reserved.

#### **COPYRIGHT INFORMATION**

Authors herein are responsible for the authenticity of their materials and for obtaining written permissions from publishers or persons who own the copyright to any previously published or copyrighted material used herein.

Cooperative Research Programs (CRP) grants permission to reproduce material in this publication for classroom and not-for-profit purposes. Permission is given with the understanding that none of the material will be used to imply TRB, AASHTO, FAA, FHWA, FMCSA, FRA, FTA, Office of the Assistant Secretary for Research and Technology, PHMSA, or TDC endorsement of a particular product, method, or practice. It is expected that those reproducing the material in this document for educational and not-for-profit uses will give appropriate acknowledgment of the source of any reprinted or reproduced material. For other uses of the material, request permission from CRP.

#### **NOTICE**

The research report was reviewed by the technical panel and accepted for publication according to procedures established and overseen by the Transportation Research Board and approved by the National Academies of Sciences, Engineering, and Medicine.

The opinions and conclusions expressed or implied in this report are those of the researchers who performed the research and are not necessarily those of the Transportation Research Board; the National Academies of Sciences, Engineering, and Medicine; or the program sponsors.

The Transportation Research Board; the National Academies of Sciences, Engineering, and Medicine; and the sponsors of the National Cooperative Highway Research Program do not endorse products or manufacturers. Trade or manufacturers' names appear herein solely because they are considered essential to the object of the report.

 $Published\ research\ reports\ of\ the$ 

#### **NATIONAL COOPERATIVE HIGHWAY RESEARCH PROGRAM**

are available from

Transportation Research Board Business Office 500 Fifth Street, NW Washington, DC 20001

and can be ordered through the Internet by going to http://www.national-academies.org and then searching for TRB Printed in the United States of America

# The National Academies of SCIENCES • ENGINEERING • MEDICINE

The **National Academy of Sciences** was established in 1863 by an Act of Congress, signed by President Lincoln, as a private, non-governmental institution to advise the nation on issues related to science and technology. Members are elected by their peers for outstanding contributions to research. Dr. Marcia McNutt is president.

The **National Academy of Engineering** was established in 1964 under the charter of the National Academy of Sciences to bring the practices of engineering to advising the nation. Members are elected by their peers for extraordinary contributions to engineering. Dr. C. D. Mote, Jr., is president.

The **National Academy of Medicine** (formerly the Institute of Medicine) was established in 1970 under the charter of the National Academy of Sciences to advise the nation on medical and health issues. Members are elected by their peers for distinguished contributions to medicine and health. Dr. Victor J. Dzau is president.

The three Academies work together as the **National Academies of Sciences**, **Engineering**, **and Medicine** to provide independent, objective analysis and advice to the nation and conduct other activities to solve complex problems and inform public policy decisions. The National Academies also encourage education and research, recognize outstanding contributions to knowledge, and increase public understanding in matters of science, engineering, and medicine.

Learn more about the National Academies of Sciences, Engineering, and Medicine at www.national-academies.org.

The Transportation Research Board is one of seven major programs of the National Academies of Sciences, Engineering, and Medicine. The mission of the Transportation Research Board is to increase the benefits that transportation contributes to society by providing leadership in transportation innovation and progress through research and information exchange, conducted within a setting that is objective, interdisciplinary, and multimodal. The Board's varied committees, task forces, and panels annually engage about 7,000 engineers, scientists, and other transportation researchers and practitioners from the public and private sectors and academia, all of whom contribute their expertise in the public interest. The program is supported by state transportation departments, federal agencies including the component administrations of the U.S. Department of Transportation, and other organizations and individuals interested in the development of transportation.

Learn more about the Transportation Research Board at www.TRB.org.

#### COOPERATIVE RESEARCH PROGRAMS

#### CRP STAFF FOR NCHRP RESEARCH REPORT 894

Christopher J. Hedges, Director, Cooperative Research Programs
Lori L. Sundstrom, Deputy Director, Cooperative Research Programs
Edward T. Harrigan, Senior Program Officer
Sheila A. Moore, Program Associate
Eileen P. Delaney, Director of Publications
Natalie Barnes, Associate Director of Publications
Kami Cabral, Editor

#### **NCHRP PROJECT 22-29A PANEL**

Field of Design—Area of Vehicle Barrier Systems

Chris Poole, Iowa DOT, Ames, IA (Chair)
John C. Durkos, Road Systems, Inc., Stow, OH
Lyman L. "Terry" Hale, III, New York State DOT, Gansevoort, NY
Charles F. McDevitt, McDevitt Consulting, Matthews, NC
David S. Rayburn, National Transportation Safety Board, Washington, DC
Michael J. Smelker, New Mexico DOT, Las Cruces, NM
Teri Soos, Maryland State Highway Administration, Frederick, MD
Ana Eigen, FHWA Liaison
Stephen F. Maher, TRB Liaison

#### **AUTHOR ACKNOWLEDGMENTS**

The George Mason University Research Team wishes to cite its gratitude for contributions to this effort to consultant Dr. Kenneth S. Opiela. His expertise and experience provided invaluable perspectives on barrier design, evaluation, and deployment to maximize their potential to enhance highway safety. Special thanks is also given to the FHWA Office of Safety R&D for allowing testing at the Federal Outdoor Impact Laboratory (FOIL) and to Mr. Eduardo Arispe, who handled all the details to make this possible. The testing addressed questions related to longitudinal barriers deployed on curved, superelevated roadway sections. The Team thanks Gregory Industries (Mr. Andrew Artar) for supplying the test article material for the crash tests conducted under this project and the many individuals from state DOTs, industry, and academia who provided insights, information, and data that was used in this project.

#### FOREWORD

By Edward T. Harrigan Staff Officer Transportation Research Board

This report presents guidance on designing, selecting, and installing longitudinal traffic barriers for curved, superelevated roadways for possible incorporation in the AASHTO *Roadside Design Guide*. The report will be of immediate interest to engineers in state highway agencies with responsibility for design and selection of roadway barrier systems.

Curved, high-speed roadways are usually superelevated to make the curved roadway easier for vehicles to navigate. Several potential concerns and uncertainties arise when longitudinal barriers are installed on curved, superelevated roadway sections (CSRS).

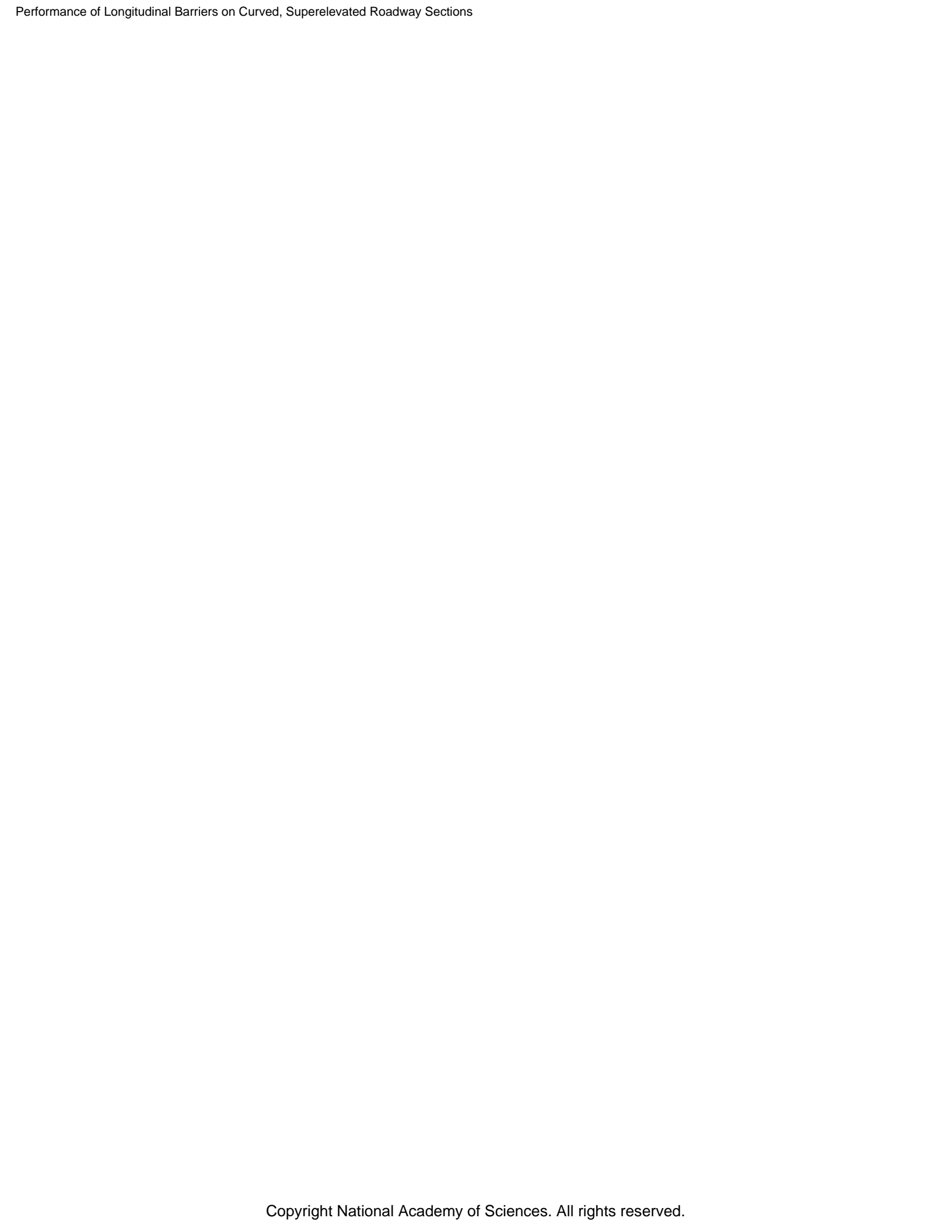
Roadway curvature increases the angle of impact of a vehicle with respect to the barrier. This angle increase can cause an increase in impact loading that may potentially exceed the capacity of barriers designed for impacts along tangent roadway sections. Measures of occupant risk may also increase in magnitude.

The objective of this research was to develop guidance for highway agencies on the design, selection, and installation of longitudinal traffic barriers on CSRS. The research was performed by George Mason University, Fairfax, Virginia, with the support of the FHWA's Federal Outdoor Impact Laboratory (FOIL) at the Turner-Fairbank Highway Research Center, McLean, Virginia.

The research encompassed extensive vehicle dynamics and finite element analyses of vehicle-barrier impacts on CSRS. The analyses were conducted for several different vehicle and barrier types, and for a range of roadway curvature and superelevation; shoulder width and angle; roadside slope; and barrier orientation and placement. The results of the computer analyses were validated by crash tests at the FHWA's FOIL with full-size extended-cab pickup trucks impacting W-beam guardrail on CSRS.

The practical outcome of the project is guidance for the AASHTO Technical Committee on Roadside Safety on the design, selection, and installation of longitudinal barriers on CSRS. This guidance is summarized in Table 8.1 of the report, along with its implications for the design, selection, and installation of concrete and W-beam barriers on CSRS.

This report fully documents the research. The following five appendices can be found on the TRB website (www.TRB.org) by searching for "NCHRP Research Report 894": Appendix A: State DOT Survey Instrument and Instructions; Appendix B: Vehicle Dynamics Simulation Results; Appendix C: Finite Element Model Validations; Appendix D: Finite Element Simulation Results; and Appendix E: Full-Scale Crash Testing Report.



## CONTENTS

1	Summary
14	Chapter 1 Introduction
14	1.1 Background
15	1.2 Project Objectives and Scope
16	1.3 Research Approach
17	1.4 Report Organization
18	Chapter 2 Literature Review and State DOT Survey
18	2.1 Introduction
18	2.2 Barrier Crashworthiness Research
20	2.3 Terrain Effect Studies
23	2.4 General Curve Safety Guidance
24	2.5 Road Design Guidelines
27	2.6 State DOT Survey Results
30	2.7 Summary
31	Chapter 3 Crash Data Analysis
31	3.1 NASS/CDS Data Analyses
35	3.2 NASS/GES Data Analyses
38	3.3 FARS Data Analysis
41	3.4 NCHRP Project 17-22 Data Analysis
42	3.5 Data Analysis Summary
14	<b>Chapter 4</b> Vehicle Dynamics Analysis for Vehicles Leaving the Traveled Way on CSRS
44	4.1 Background
45	4.2 Objective
45	4.3 Research Approach
46	4.4 VDA Considerations
50	4.5 VDA Simulation Results
57	4.6 Conclusions
58	<b>Chapter 5</b> Crash Simulation Analysis of Impacts into Longitudinal Barriers on CSRS
58	5.1 Introduction
58	5.2 Background
58	5.3 FE Modeling and Crash Simulation Analyses
66	5.4 Computer Model Validations
71	5.5 Crash Simulation Parameters
73	5.6 Crash Simulation Results
82	5.7 Conclusions

86	<b>Chapter 6</b> Full-Scale Testing and Results
86	6.1 Introduction
86	6.2 Background
88	6.3 Testing Requirements, Criteria, and Facility
89	6.4 Testing Approach
95	6.5 Preliminary Tests
97	6.6 Full-Scale Crash Testing Results
106	6.7 Test Results Evaluation
111	6.8 Conclusions
112	<b>Chapter 7</b> Development of Guidance for Improved Longitudinal Barrier Design, Selection, and Installation on CSRS
112	7.1 Background
112	7.2 Research Questions
114	7.3 Summary of Findings
114	7.4 Translating Findings and Observations into Guidance
118	Chapter 8 Conclusions
119	8.1 Proposed Guidance
119	8.2 Implications for Current Practice
121	8.3 Needs for Future Research
122	References
124	Appendix A State DOT Survey Instrument and Instructions
125	Appendix B Vehicle Dynamics Simulation Results
126	Appendix C Finite Element Model Validations
127	Appendix D Finite Element Simulation Results
128	Appendix E Full-Scale Crash Testing Report

#### SUMMARY

# Performance of Longitudinal Barriers on Curved, Superelevated Roadway Sections

#### **Background and Objectives**

NCHRP Project 22-29, "Performance of Longitudinal Barriers on Curved, Superelevated Roadway Sections," and Project 22-29A, "Evaluating the Performance of Longitudinal Barriers on Curved, Superelevated Roadway Sections," were initiated to develop a better understanding of the safety performance (i.e., crashworthiness) for barriers used on curved, superelevated roadway sections (CSRS) and to suggest options and guidance for improving barrier selection, design, and deployment in pursuit of enhanced highway safety. CSRS are most commonly found on major interstate-type highways, and they exist on both tight and gentle curves (see Figure 1). The most critical CSRS situations occur on the tight curves associated with interchanges. This research involved a four-phase effort to systematically and comprehensively consider safety for varying CSRS situations. The research (1) reviewed the practices and available knowledge of barriers on curves and their safety performance; (2) analyzed issues associated with vehicle-to-barrier interfaces; (3) simulated crashes with various types of barriers for varying curvature, shoulder configurations, and superelevation conditions; and (4) conducted crash tests to confirm the simulation results. The project resulted in the development of proposed enhancements to barrier design, selection, and deployment for varying CSRS situations.

#### **Research Approach**

During the first phase of the project, the Research Team gathered relevant information pertaining to the safety performance of longitudinal barriers on CSRS from reviewing technical literature and conducting a survey of state DOTs (state DOT survey) to obtain their design standards and practices. The review of domestic and international literature (from TRID) revealed that very little research has been conducted to analyze the safety of designs for barriers used in CSRS situations. For example, current crashworthiness evaluation criteria only apply to straight or tangent sections of barriers, and there have been very few efforts to test barriers on curves. The state DOT survey revealed varying practices for the selection and deployment of barriers on CSRS, but these were essentially similar to those for barriers on tangent sections. Analyses of crash data indicated that there are more crashes on curved road sections, but the details in the data are not sufficient to discern differences by features of the curve (e.g., degree of curvature, superelevation) or the type and placement of barriers where crashes occurred. It was concluded that a clear need exists to develop a deeper understanding of longitudinal barrier safety performance for CSRS.

The research began with applying vehicle dynamics analysis (VDA) to study the effects of surface changes of the roadway, shoulder, and side slopes on the trajectory and orientation

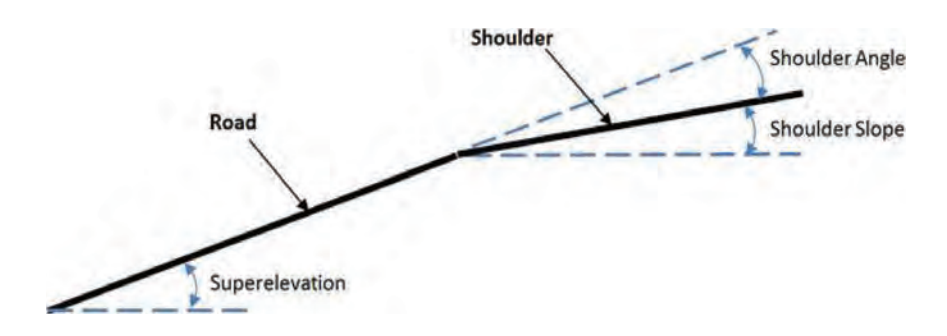


Figure 1. Typical CSRS with longitudinal barriers.

of a vehicle at its interface with varying barrier types and their placement. The underlying premise for these analyses was that a good vehicle-to-barrier interface is necessary for adequate safety performance. Vehicles undergo changes in their roll, pitch, and yaw as they traverse a banked roadway, a shoulder (most likely having a different slope), and then the graded side slope before encountering a barrier. The design features for the Manual for Assessing Safety Hardware (MASH) test vehicles (i.e., the small sedan and large pickup truck) were input into commercially available VDA software to generate trajectory plots for a broad set of conditions. The analyses covered a representative set of conditions as summarized in Table 1 for three common types of longitudinal barriers. Various plots and summaries were generated in the assessment of interface effectiveness.

#### Table 1. Factors considered in the research.

- Barrier Type
  - o Concrete barrier [height ≤ 32 in. (813 mm)]: NJ concrete barrier
  - o Strong-post W-beam guardrail [height < 31 in. (787 mm)]: G4(1S)
  - o Strong-post W-beam guardrail [height ≥ 31 in. (787 mm)]: MGS
- · Vehicle Type
  - o 2270P pickup truck: 2007 Chevrolet Silverado model
  - o 1100C small car: 2010 Toyota Yaris model
- Curvature/Superelevation Combinations
  - o 614 ft (187 m) radius/12% superelevation
  - o 2,130 ft (649 m) radius/12% superelevation
  - 758 ft (231 m) radius/8% superelevation
    2,670 ft (814 m) radius/8% superelevation
  - o 833 ft (254 m) radius/6% superelevation
  - o 3,050 ft (930 m) radius/6% superelevation
- Shoulder Width and Slope
  - o 4 ft (1.22 m), 8 ft (2.44 m), and 12 ft (3.66 m) widths
  - o 0%, 3%, 6%, and 8% shoulder angles
- Roadside Slope
  - o 12H:1V (negative) relative to shoulder for all simulations
- Impact Conditions
  - $\circ$   $\,$  Impact angle:  $25^{\circ}$
  - o Impact speed: 62 mph (100 km/h)
- Barrier Placement Relative to Road Section
  - o Lateral position: at edge of shoulder
  - o Vertical orientation: normal to road, normal to shoulder, or true vertical



Shoulder Angles	6% Superelevation	8 % Superelevation	12 % Superelevation						
Analyzed	Corresponding Shoulder Slope								
0%	6%	8%	12%						
3%	3%	5%	9%						
6%	0%	2%	6%						
8%	-2%	0%	4%						

Figure 2. Shoulder slope conditions relative to the roadway surface analyzed.

The research considered variations in shoulder width and slopes and organized the results based on shoulder angle as noted in Figure 2. This metric reflects the cross section slope changes on the superelevated roadway to the adjacent shoulder. A negative side slope of 12H:1V relative to shoulder was used for all simulations.

The second phase of the analyses involved crash simulation analysis using finite element (FE) models. Simulations of crashes into barriers have been shown to effectively replicate actual events and can provide useful metrics on safety performance. Simulations allow variations of the vehicle-to-barrier interface to be considered as well as the necessary aspects of barrier strength as a function of its detailed design and deployment. A subset of CSRS conditions were selected as candidates for simulation based on results from the VDA. Since detailed crash simulations each take 20 h to 40 h of computer processing time, the VDA simulation results were used to minimize the number of FE cases that needed to be simulated. Approximately 200 FE simulations were run. Various metrics were derived from the simulations, but the focus was on the MASH Test Level 3 (TL-3) crashworthiness measures related to vehicle stability and occupant risk (MASH 2009).

Full-scale crash testing was undertaken as the last step in this research to verify and validate the simulation results. Three tests were conducted to provide a basis for asserting the validity of the simulation results. The tests showed outcomes similar to the simulations for similar conditions, leading to the conclusion that the simulation results were valid.

More details on these analysis efforts are provided in the following sections.

#### **Vehicle Dynamics Analysis**

The VDA research efforts initially involved adapting models to assess the various aspects of vehicle-to-barrier interface performance under different CSRS conditions, as reflected in Table 1. Human-vehicle-environment (HVE) (Engineering Dynamics Corporation 2005)

and CarSim (CarSim 2006) programs for VDA were used to generate vehicle trajectories to gain insights on the influences of surface features on the orientation of the vehicle and the likely barrier interface regions for the various superelevation, slope, shoulder, and backslope conditions. Typical results from these analyses are the plots shown in Figure 3. For the random set of conditions displayed, the VDA-based normalized override (blue curve) and underride curves (green curve) can be noted. The yellow line indicates the "barrier interface region" that would exist for a concrete barrier across positions off the shoulder where they could be placed. The shapes of these curves reflect the maximum and minimum traces of the primary structural regions for the two vehicles and varying speed and impact angles considered. They vary as a result of the differences in curve radius, degree of superelevation, shoulder width and slope, and backslope conditions. It can also be seen that the effective placement areas (shaded green area below curves) vary by conditions. VDA interface curves like these were generated for a range of possible barrier placement practices.

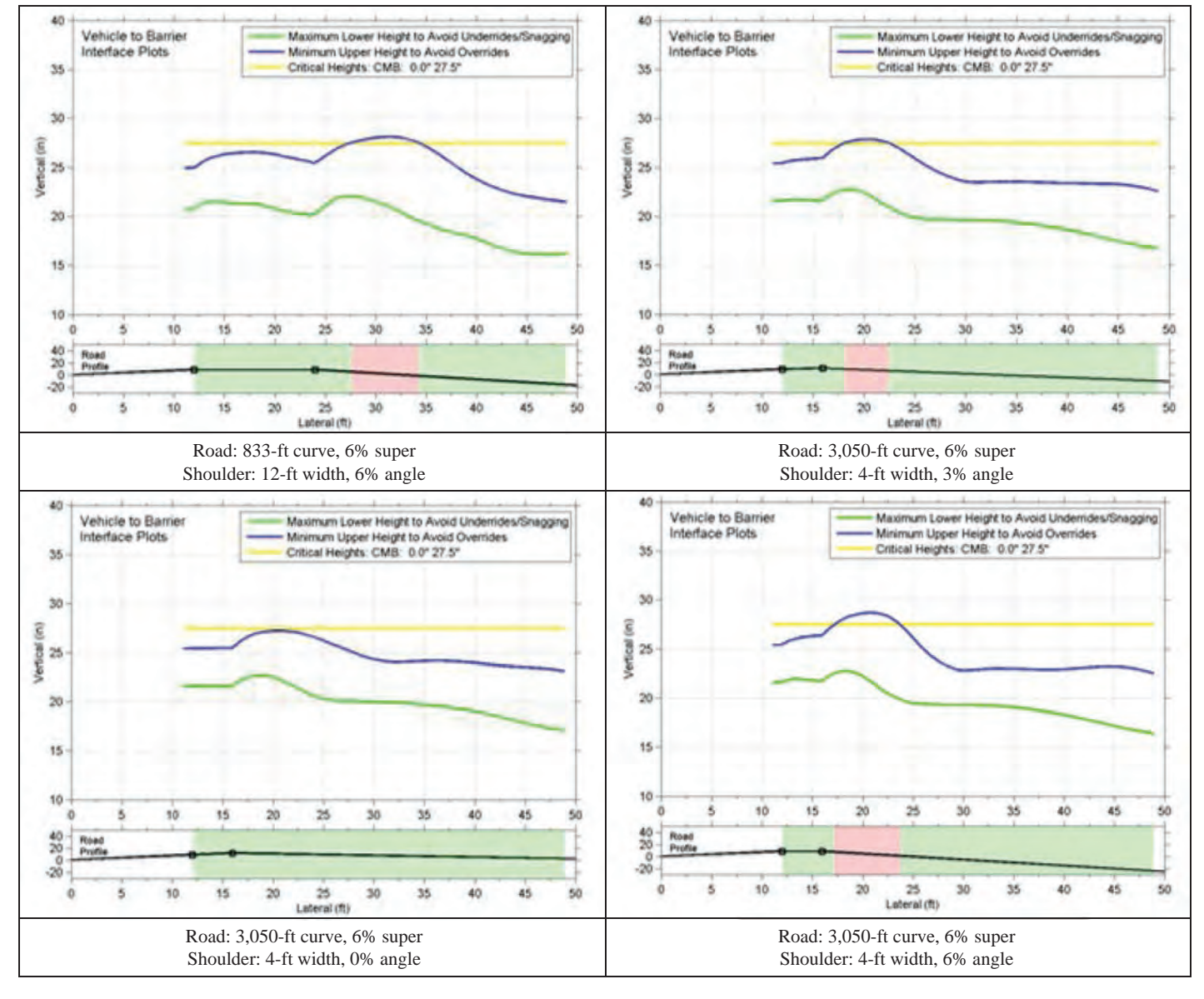


Figure 3. Typical override and underride limits on varying CSRS.

Tabular summaries were also generated of the interface performance for all the specific conditions of interest. The plots and tabular summaries reflect the physics of a vehicle leaving the road on a CSRS and interfacing with barriers positioned at edge of the shoulder. The VDA results were used to determine the maximum and minimum vehicle bumper heights at first contact with the barrier for all combinations of curvature, superelevation, and shoulder width and slope. In Table 2, the maximum and minimum heights are indicated. Each cell represents the vehicle bumper height for the specific conditions. The cells with values in red type indicate those situations where poor interface conditions are likely to exist. These imply that the height is outside the limits (e.g., too high or too low) and there is potential for vehicle overriding or underriding the barrier. This table as well as the interface plots provided insights about conditions where safety issues may occur and were used to decide which cases to evaluate using FE simulations.

The VDA results provide some useful insights about the potential effectiveness of different types of barriers on CSRS. Some possible implications of the VDA results include the following:

- Use barriers offering increased height and depth of their capture area for a CSRS. This may be more important for sharper curves, higher levels of superelevation, and more pronounced changes from roadway to shoulder angles.
- Clear zones beyond the shoulder may be an option where sufficient runout area is available. This analysis only considered nearly level 12H:1V roadside slope conditions.
- Based on the VDA results, it was observed that there is no vehicle-to-barrier interface issue (i.e., potential for override or underride) with concrete median barriers when used on CSRS.
- The simulations show that there may be potential for small vehicle underride with the Midwest Guardrail System (MGS) barriers and potential for override of the pickup truck with the lower height G4(1S) W-beam guardrail systems.

The VDA focused on the vehicle-to-barrier interface. This is a necessary condition, but not sufficient to ensure that the barrier will meet crashworthiness requirements. This is where further analyses using FE models and crash simulation became necessary.

#### **Finite Element Simulation Analyses**

Simulation analysis was undertaken to analyze the impact performance of the three barrier types for the various CSRS and barrier placement options. The LS-DYNA software used validated FE models of barriers and vehicles to simulate crashes. These models were validated by comparisons of crash test data to simulated results for tests on tangent, level sections. Validation efforts indicated that the models effectively replicated the crash tests based on similarities of the motion metrics (e.g., yaw, pitch, roll, and associated velocity and acceleration profiles for the x-, y-, and z-axes) indicating the viability of the simulations.

Figure 4 displays results from the simulation analyses. It shows the predicted behavior of the vehicle and all the pertinent MASH metrics and evaluations. The basic CSRS features, barrier placement, and impact conditions are indicated in the upper part of the table. In this case, a 614-ft-radius curve with a superelevation of 12% is modeled. The curve has a 4-ft-wide shoulder with a 6% slope. At the edge of the shoulder, a New Jersey concrete safety shape barrier (NJ concrete barrier) is placed with a "normal to road" orientation. A MASH 2270P vehicle traverses the CSRS and departs the traveled way and crosses the 4-ft shoulder leading to an impact with the barrier at 100 km/h and 25°. The picture shows "snapshots" of the vehicle position at various points of time during the approximately 2-s "crash event."

Table 2. Summary of results of VDA bumper-barrier interface heights.

				NJ	Concre	ete Bar	rier		MGS W-beam Barrier G4(1S) W-beam b							eam ba	arrier			
	Curvature Radius (ft)		614	2130	758	2670	833	3050	614	2130	758	2670	833	3050	614	2130	758	2670	833	3050
	Super Ele	vation (%)	12	12	8	8	6	6	12	12	8	8	6	6	12	12	8	8	6	6
	Shoulder	Min (in)	20.80	22.05	20.79	21.76	20.75	21.59	20.80	22.05	20.79	21.76	20.75	21.59	20.80	22.05	20.79	21.76	20.75	21.59
	Angle 0%	Max (in)	24.68	25.39	24.55	25.13	24.51	24.98	24.68	25.39	24.55	25.13	24.51	24.98	24.68	25.39	24.55	25.13	24.51	24.98
	Shoulder	Min (in)	21.08	22.11	21.07	21.83	21.04	21.62	21.08	22.11	21.07	21.83	21.04	21.62	21.08	22.11	21.07	21.83	21.04	21.62
4 ft Shoulder	Angle 3%	Max (in)	25.39	25.87	25.27	25.60	25.23	25.46	25.39	25.87	25.27	25.60	25.23	25.46	25.39	25.87	25.27	25.60	25.23	25.46
Width	Shoulder	Min (in)	21.42	22.18	21.39	21.93	21.38	21.72	21.42	22.18	21.39	21.93	21.38	21.72	21.42	22.18	21.39	21.93	21.38	21.72
	Angle 6%	Max (in)	26.15	26.37	26.04	26.10	25.99	25.92	26.15	26.37	26.04	26.10	25.99	25.92	26.15	26.37	26.04	26.10	25.99	25.92
	Shoulder	Min (in)	21.67	22.57	21.63	22.10	21.61	21.85	21.67	22.57	21.63	22.10	21.61	21.85	21.67	22.57	21.63	22.10	21.61	21.85
	Angle 8%	Max (in)	26.68	26.72	26.58	26.42	26.53	26.24	26.68	26.72	26.58	26.42	26.53	26.24	26.68	26.72	26.58	26.42	26.53	26.24
	Shoulder Angle 0%	Min (in)	20.69	22.01	20.67	21.70	20.64	21.54	20.69	22.01	20.67	21.70	20.64	21.54	20.69	22.01	20.67	21.70	20.64	21.54
		Max (in)	24.76	25.46	24.64	25.20	24.59	25.07	24.76	25.46	24.64	25.20	24.59	25.07	24.76	25.46	24.64	25.20	24.59	25.07
	Shoulder	Min (in)	20.77	21.79	20.75	21.49	20.72	21.28	20.77	21.79	20.75	21.49	20.72	21.28	20.77	21.79	20.75	21.49	20.72	21.28
8 ft		Max (in)	25.53	25.86	25.37	25.57	25.30	25.39	25.53	25.86	25.37	25.57	25.30	25.39	25.53	25.86	25.37	25.57	25.30	25.39
Shoulder Width	Shoulder	Min (in)	20.91	21.59	20.89	21.33	20.87	21.13	20.91	21.59	20.89	21.33	20.87	21.13	20.91	21.59	20.89	21.33	20.87	21.13
Width	Angle 6%	Max (in)	26.06	26.06	25.94	25.77	25.88	25.58	26.06	26.06	25.94	25.77	25.88	25.58	26.06	26.06	25.94	25.77	25.88	25.58
	Shoulder	Min (in)	21.03	21.25	21.00	20.92	20.97	20.72	21.03	21.25	21.00	20.92	20.97	20.72	21.03	21.25	21.00	20.92	20.97	20.72
	Angle 8%	Max (in)	26.40	26.17	26.24	25.84	26.19	25.65	26.40	26.17	26.24	25.84	26.19	25.65	26.40	26.17	26.24	25.84	26.19	25.65
		1														1				
	Shoulder	Min (in)	20.51	21.93	20.48	21.61	20.44	21.43	20.51	21.93	20.48	21.61	20.44	21.43	20.51	21.93	20.48	21.61	20.44	21.43
	Angle 0%	Max (in)	24.86	25.56	24.73	25.29	24.65	25.15	24.86	25.56	24.73	25.29	24.65	25.15	24.86	25.56	24.73	25.29	24.65	25.15
12.5	Shoulder	Min (in)	20.35	21.64	20.34	21.30	20.30	21.08	20.35	21.64	20.34	21.30	20.30	21.08	20.35	21.64	20.34	21.30	20.30	21.08
12 ft Shoulder	Angle 3%	Max (in)	25.07	25.41	24.95	25.12	24.88	24.96	25.07	25.41	24.95	25.12	24.88	24.96	25.07	25.41	24.95	25.12	24.88	24.96
Width	Shoulder	Min (in)	20.23	21.40	20.23	21.02	20.20	20.80	20.23	21.40	20.23	21.02	20.20	20.80	20.23	21.40	20.23	21.02	20.20	20.80
	Angle 6%	Max (in)	25.19	25.16	25.03	24.85	24.99	24.66	25.19	25.16	25.03	24.85	24.99	24.66	25.19	25.16	25.03	24.85	24.99	24.66
	Shoulder Angle 8%	Min (in)	20.15	21.26	20.17	20.87	20.14	20.63	20.15	21.26	20.17	20.87	20.14	20.63	20.15	21.26	20.17	20.87	20.14	20.63
	Aligie 0%	Max (in)	25.16	24.98	25.05	24.64	24.99	24.42	25.16	24.98	25.05	24.64	24.99	24.42	25.16	24.98	25.05	24.64	24.99	24.42

Note: Values in red type indicate situations where poor interface conditions are likely to exist.

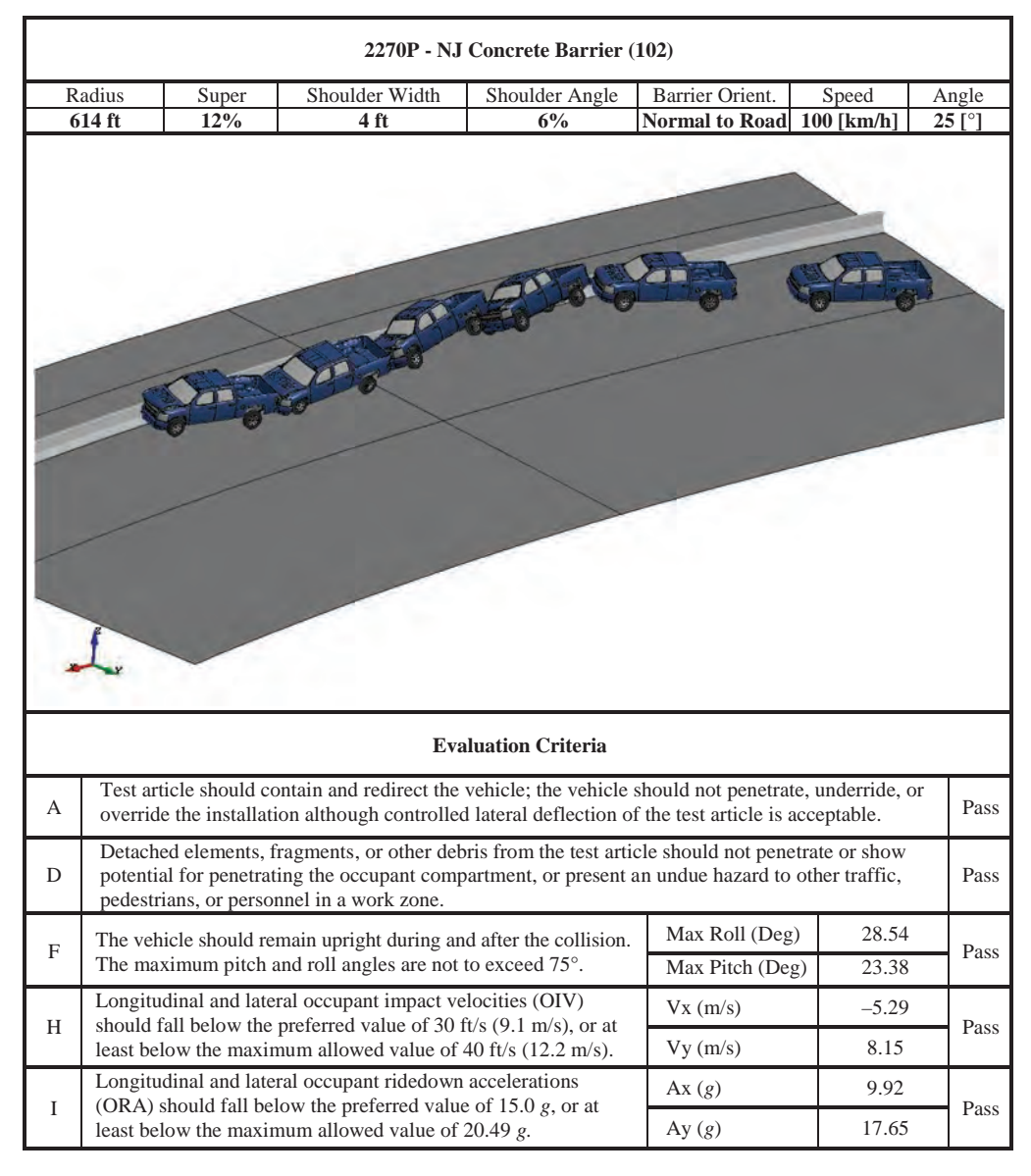


Figure 4. Typical simulation analysis summary report.

The vehicle approaches as if from the inside travel lane on a departure trajectory. The simulation is initiated away from the barrier to allow the vehicle model to be "stabilized" before impact. The point of the 25° impact has the right front side of the pickup truck making first contact with the barrier. Fractions of a second later, the vehicle yaws, leading to a rear-end impact with the barrier while riding up the barrier and beginning an outward roll. About 0.3 s later, the vehicle has been redirected toward the travel lane and down the barrier side. There is greater outward roll, but further contact with the barrier reverses the roll direction. This visual sequence provides a convenient means to compare performance among various conditions. The lower part of the table provides a summary of the MASH crashworthiness evaluation metrics for the conditions simulated.

Similar summaries were generated to allow convenient comparisons of barrier performance under different conditions. For example, Figure 5 compares the vehicle behavior for MASH 3-10 and 3-11 impacts on curves of 758- and 2,670-ft radius with 8% superelevation,

Parameters and Results	Case	Time Sequence View
CSRS: Radius 758 ft, 8% super	224	
Vehicle: 1100C	1100C	
A – Containment (Pass)		
D – Detached Elements (Pass)		
F – Max Roll – 26.59 (Pass)		
Max Pitch – 21.99 (Pass)		
H - OIV - Vx5.47 (Pass)		
Vy – 9.76 (Pass)		
I - ORA - Ax3.19 (Pass)		
Ay – 14.23 (Pass)		
CSRS: Radius 758 ft, 8% super	124	
Vehicle: 2270P	2270P	
A – Containment (Pass)		MAN TON MAN
D – Detached Elements (Pass)		
F – Max Roll – 33.66 (Pass)		7000
Max Pitch – 29.86 (Pass)		STATE OF THE STATE
H - OIV - Vx5.39 (Pass)		
Vy – 8.24 (Pass)		
I - ORA - Ax13.38 (Pass)		
Ay – 18.43 (Pass)		
CSRS: Radius 2,670 ft, 8% super	264	
Vehicle: 1100C	1100C	
A – Containment (Pass)		
D – Detached Elements (Pass)		
F - Max Roll - 25.85 (Pass)		
Max Pitch – 21.72 (Pass)		
H - OIV - Vx5.49 (Pass)		
Vy – 9.72 (Pass)		
I - ORA - Ax3.27 (Pass)		
Ay13.54 (Pass)	464	
CSRS: Radius 2,670 ft, 8% super	164	
Vehicle: 2270P	2270P	
A – Containment (Pass)		
D – Detached Elements (Pass)		
F – Max Roll – 35.84 (Pass)		
Max Pitch – 31.6 (Pass)		548
H – OIV – Vx – –5.57 (Pass) Vy – 8.13 (Pass)		
Vy - 8.13 (Pass) I - ORA - Ax12.09 (Pass)		
Ay - 18.28 (Pass)		
Ay - 10.20 (Fass)		

Figure 5. Sample comparison of radius effects for different vehicles.

and a 4-ft-wide shoulder with an 8% shoulder angle. The barriers were oriented normal to road. The figure shows the vehicle behavior differences observed between the small car and the large pickup truck for these conditions.

A considerable amount of information was generated by the simulations. The outcomes are summarized in a series of tables for each barrier and MASH test condition across the range of conditions simulated. An example is given in Table 3. For each CSRS condition (i.e., curve radius and superelevation; shoulder width and shoulder angle), the results of the simulation runs for impacts with specific types of barriers are provided. Some of these cells are marked with an asterisk (\*) to indicate that the outcome was based on expert judgment derived from the FE simulations and VDA.

The Research Team drew insights from these summaries. The following findings emerged:

- Variations in barrier performance were noted for the various conditions, suggesting that the simulation models and approach reflect the physics of barrier impacts on CSRS.
- After approximately 60 simulations for the NJ concrete barrier (as shown in this table), most have passed the MASH Test 3-11 (the most critical test) requirements for CSRS conditions when the barrier is installed normal to road or shoulder. The simulations

Table 3. Sample performance table based on simulations.

#### 32" NJ Concrete Barrier Performance Table

		Curvature/Superelevation (50 mph Design Speeds)											
			614 ft / 12%			758 ft / 8%			833 ft / 6%				
Shoulder Width	Shoulder Angle	FE True Vertical	FE 上 to Shoulder	FE ⊥to Road	FE True Vertical	FE 上 to Shoulder	FE 上 to Road	FE True Vertical	FE 上 to Shoulder	FE ⊥to Road			
	0%	Pass*	Pass*	Pass*	Pass*	Pass*	Pass*	Pass*	Pass*	Pass*			
4.5	3%	Pass (111)	Pass*	Pass (112)	Pass*	Pass*	Pass*	Pass*	Pass*	Pass*			
4 ft	6%	Fail (101)	Pass (113)	Pass (102)	Pass (121)	Pass*	Pass (122)	Pass*	Pass*	Pass*			
	8%	Fail (103)	Pass (114)	Pass (104)	Fail (123)	Pass (129)	Pass (124)	Pass (131)	Pass*	Pass (132)			
	0%	Pass*	Pass*	Pass*	Pass*	Pass*	Pass*	Pass*	Pass*	Pass*			
	3%	Pass*	Pass*	Pass*	Pass*	Pass*	Pass*	Pass*	Pass*	Pass*			
8 ft	6%	Fail (105)	Pass (115)	Pass (106)	Pass (127)	Pass*	Pass (128)	Pass*	Pass*	Pass*			
	8%	Fail (107)	Pass (116)	Pass (108)	Fail (125)	Pass (130)	Fail (126)	Fail (233)	Pass*	Pass (134)			
	0%	Pass*	Pass*	Pass*	Pass*	Pass*	Pass*	Pass*	Pass*	Pass*			
***	3%	Pass*	Pass*	Pass*	Pass*	Pass*	Pass*	Pass*	Pass*	Pass*			
12 ft	6%	Pass (109)	Pass*	Pass (110)	Pass*	Pass*	Pass*	Pass*	Pass*	Pass*			
	8%	Pass*	Pass*	Pass*	Pass*	Pass*	Pass*	Pass*	Pass*	Pass*			
		Curvature/Superelevation (80 mph Design Speeds)											
			2130 ft / 12%			2670 ft / 8%		3050 ft / 6%					
Shoulder Width	Shoulder Angle	FE	FE	FE					•				
		True Vertical	⊥to Shoulder	⊥to Road	FE True Vertical	FE 上 to Shoulder	FE ⊥to Road	FE True Vertical	FE 1 to Shoulder	FE 上 to Road			
	0%		l	⊥to	True	⊥to	⊥to	True	FE ⊥to	⊥to			
4.5	0% 3%	Vertical	Shoulder	⊥to Road	True Vertical	⊥to Shoulder	⊥to Road	True Vertical	FE 上 to Shoulder	⊥to Road			
4 ft		Vertical Pass*	Shoulder Pass*	⊥to Road Pass*	True Vertical Pass*	±to Shoulder Pass*	⊥to Road Pass*	True Vertical Pass*	FE 1 to Shoulder Pass*	⊥to Road Pass*			
4 ft	3%	Vertical Pass* Pass*	Shoulder Pass* Pass*	⊥to Road Pass*	True Vertical Pass* Pass*	L to Shoulder Pass* Pass*	⊥to Road Pass* Pass*	True Vertical Pass* Pass*	FE	L to Road Pass* Pass*			
4 ft	3% 6%	Vertical Pass* Pass* Fail (145)	Shoulder Pass* Pass* Pass (153)	L to Road Pass* Pass* Pass (146)	True Vertical Pass* Pass* Fail (161)	L to Shoulder Pass* Pass* Pass (165)	L to Road Pass* Pass* Pass (162)	True Vertical Pass* Pass*	FE 1 to Shoulder Pass* Pass*	L to Road Pass* Pass* Pass (172)			
	3% 6% 8%	Vertical Pass* Pass* Fail (145) Fail (147)	Pass* Pass (153) Pass (154)	L to Road Pass* Pass (146) Pass (148)	True Vertical Pass* Pass* Fail (161)	L to Shoulder Pass* Pass (165) Fail (266)	L to Road Pass* Pass (162) Pass (164)	True Vertical Pass* Pass* Pass (171) Pass (173)	FE 1 to Shoulder Pass* Pass* Pass* Pass (175)	L to Road Pass* Pass* Pass (172) Fail (174)			
4 ft 8 ft	3% 6% 8% 0%	Vertical Pass* Pass* Fail (145) Fail (147) Pass*	Shoulder Pass* Pass* Pass (153) Pass (154) Pass*	L to Road  Pass*  Pass*  Pass (146)  Pass (148)  Pass*	True Vertical Pass* Pass* Fail (161) Fail (163) Pass*	L to Shoulder Pass* Pass (165) Fail (266) Pass*	L to Road  Pass*  Pass*  Pass (162)  Pass (164)  Pass*	True Vertical Pass* Pass* Pass (171) Pass (173) Pass*	FE 1 to Shoulder Pass* Pass* Pass (175) Pass*	L to Road  Pass*  Pass*  Pass (172)  Fail (174)  Pass*			
	3% 6% 8% 0% 3%	Vertical Pass* Pass* Fail (145) Fail (147) Pass* Pass*	Shoulder Pass* Pass* Pass (153) Pass (154) Pass* Pass*	L to Road  Pass*  Pass (146)  Pass (148)  Pass*  Pass*	True Vertical Pass* Pass* Fail (161) Fail (163) Pass* Pass*	T to Shoulder Pass* Pass (165) Fail (266) Pass* Pass*	L to Road  Pass*  Pass (162)  Pass (164)  Pass*  Pass*	True Vertical Pass* Pass* Pass (171) Pass (173) Pass* Pass*	FE 1 to Shoulder Pass* Pass* Pass (175) Pass*	L to Road  Pass*  Pass*  Pass (172)  Fail (174)  Pass*  Pass*			
	3% 6% 8% 0% 3% 6%	Vertical Pass* Pass* Fail (145) Fail (147) Pass* Pass* Fail (245)	Pass* Pass (153) Pass (154) Pass* Pass (155)	L to Road  Pass*  Pass (146)  Pass (148)  Pass*  Pass*  Pass (150)	True Vertical Pass* Pass* Fail (161) Fail (163) Pass* Pass*	L to Shoulder Pass* Pass (165) Fail (266) Pass* Pass*	L to Road  Pass*  Pass (162)  Pass (164)  Pass*  Pass*  Pass*	True Vertical Pass* Pass* Pass (171) Pass (173) Pass* Pass* Pass*	FE 1 to Shoulder Pass* Pass* Pass (175) Pass* Pass* Pass*	L to Road  Pass*  Pass (172)  Fail (174)  Pass*  Pass*  Pass*			
8 ft	3% 6% 8% 0% 3% 6% 8%	Vertical Pass* Pass* Fail (145) Fail (147) Pass* Pass* Fail (245) Fail (247)	Pass* Pass (153) Pass (154) Pass* Pass (155) Pass (155) Pass (156)	Pass* Pass (146) Pass (148) Pass (148) Pass* Pass* Pass (150) Fail (152)	True Vertical Pass* Pass* Fail (161) Fail (163) Pass* Pass* Pass* Pass*	T to Shoulder  Pass*  Pass (165)  Fail (266)  Pass*  Pass*  Pass*  Pass*	Pass* Pass (162) Pass (164) Pass* Pass* Pass* Pass*	True Vertical Pass* Pass (171) Pass (173) Pass * Pass* Pass* Pass*	FE 1 to Shoulder Pass* Pass* Pass (175) Pass* Pass* Pass* Pass* Pass*	L to Road  Pass*  Pass*  Pass (172)  Fail (174)  Pass*  Pass*  Pass*			
	3% 6% 8% 0% 3% 6% 8%	Vertical Pass* Pass* Fail (145) Fail (147) Pass* Pass* Fail (245) Fail (247) Fail (249)	Pass* Pass (153) Pass (154) Pass* Pass (155) Pass (155) Pass (156) Pass (157)	Pass* Pass (146) Pass (148) Pass (148) Pass (150) Fail (152) Pass (142)	True Vertical Pass* Pass* Fail (161) Fail (163) Pass* Pass* Pass* Pass* Pass*	L to Shoulder Pass* Pass (165) Fail (266) Pass* Pass* Pass* Pass*	L to Road  Pass*  Pass (162)  Pass (164)  Pass*  Pass*  Pass*  Pass*  Pass*	True Vertical Pass* Pass (171) Pass (173) Pass* Pass* Pass* Pass* Pass*	FE 1 to Shoulder Pass* Pass* Pass (175) Pass* Pass* Pass* Pass* Pass*	L to Road  Pass*  Pass (172)  Fail (174)  Pass*  Pass*  Pass*  Pass*  Pass*			

Note: Asterisk (\*) indicates that the outcome was based on expert judgment derived from the FE simulations and VDA.

- of impacts with the NJ concrete barrier indicated that it is more prone to fail the crash-worthiness requirements for situations where the superelevation is 8% or greater and the shoulder angle is 6% to 8%.
- Performance under less severe CSRS and barrier placement conditions is incrementally
  improved. This suggests that current applications of the concrete barrier are viable. This
  also suggests that there may not be compelling reasons to conduct full-scale crash tests
  on concrete barrier.
- Efforts to simulate G4(1S) W-beam barriers for the various conditions showed consistent results associated with barrier height. The 27¾-in.-high barriers did not perform as well as higher barriers.
- The simulations of vehicle impacts into G4(1S) barriers at a height of 27¾ in. for CSRS applications showed a propensity for override, as the VDA results suggested. There were fewer cases of vaulting for the G4(1S) barriers at 29 in. high. There were no cases where underride was indicated to be a problem.
- Simulations of the MGS barriers (31 in. high) showed no propensity for underride issues with the small car.
- Additional simulations for F-shape concrete barriers indicated improved performance over the NJ concrete barrier.

The simulation efforts included some additional runs to add depth to the analyses and provide a better understanding of the underlying physics. They provide additional metrics or different views of the simulated impacts.

#### **Full-Scale Testing**

There was considerable discussion about which crash tests would be most important to conduct. Ultimately, three tests were conducted:

- Test 16004. G4(1S) barrier at 29 in. high with a 2270P vehicle at 100 km/h for a 254-m (833-ft) radius curve with a 6% superelevation with a –2% shoulder slope, and a 4-ft shoulder. The vehicle impacted the barrier at the desired speed, but there was less drift than anticipated, causing the vehicle to impact 2 ft to 3 ft from the desired Critical Impact Point (CIP), hitting closer to the first downstream post. Consequently, the rail was more rigid and the vehicle traveled along it near the top, but did not vault the barrier as had been seen in the simulation. This was considered a marginal result.
- Test 16010. G4(1S) barrier at 29 in. high with a 2270P vehicle at 100 km/h for a 254-m (833-ft) radius curve with a 6% superelevation with a –2% shoulder slope, and a 4-ft shoulder. The vehicle impacted the barrier at the desired speed near the CIP. Consequently, the rail was less rigid, allowing the vehicle to climb and vault over it. This result was considered to confirm the simulation results.
- Test 16015. G4(1S) barrier at 29 in. high with a 2270P vehicle at 100 km/h for a 254-m (833-ft) radius curve with a 6% superelevation with a –2% shoulder slope, and an 8-ft shoulder. The vehicle impacted the barrier at the desired speed near the CIP. The rail safely redirected the vehicle. This result was considered to confirm the simulation results for 8-ft shoulders.

These tests were conducted for the most common type of W-beam barrier and bracketed the pass/fail limits indicated by the simulations. Because the test results were considered similar, they are believed to provide confirmation that the simulations reflected the real-world safety performance of barriers on CSRS.

# **Development of Guidance for Deployment of Longitudinal Barriers on CSRS**

A considerable amount of information was derived from the VDA, simulation analyses, and crash testing. The challenge was to translate these results into guidance for the design, selection, and installation of longitudinal barriers on CSRS. Table 4 contains the significant implications and guidance derived for the barriers and CSRS conditions analyzed. These are included along with the critical guidance elements (in bold) that evolved from this research.

Table 4. CSRS implications and guidance derived for the barriers and CSRS analyzed.

Aspect	Implications and Guidance Elements
Barrier Design	
General	<ul> <li>Poor vehicle-to-barrier interface limits the barrier functions in a crash.</li> <li>Good interface is a necessary, but not a sufficient condition for selection of a barrier type.         The degree of increased impact severity needs to be assessed.     </li> <li>Consider using interface analyses (i.e., VDA) to evaluate special cases or other types of barriers to increase confidence in the design.</li> <li>Consider higher barriers to better accommodate larger vehicles for CSRS applications.</li> </ul>
Concrete Barriers	<ul> <li>Concrete safety shapes do not have underride problems, but face slopes can induce rollovers.</li> <li>Use higher concrete barriers where there is a concern about override associated with CSRS features.</li> <li>Concrete barriers with an appropriate face slope may be considered the most universally effective design for CSRS conditions.</li> <li>Design concrete barriers with minimum face slope to limit vehicle ride-up and maintain a viable interface area overlap.</li> </ul>
W-Beam Barrier	<ul> <li>The need for a higher barrier is apparent, but increasing the rail height necessitated review of underride potential.</li> <li>Increases in barrier height are most important for tight curves where excessive speeds are likely to occur (e.g., off-ramps, downhill).</li> <li>Follow the FHWA Technical Memorandum of May 17, 2010, that recommends the nominal height for new installations of G4(1S) barrier be 29 in. for CSRS (Nicol 2010).</li> <li>Consider 31-inhigh W-beam barrier designs for CSRS situations.</li> </ul>
Selection	
Curvature and Superelevation	<ul> <li>Conduct deeper analysis of short-radius, high superelevation CSRS situations.</li> <li>Limit the use of tight curves with high superelevations.</li> <li>Consider using higher barriers on CSRS with appropriate underride protection.</li> <li>Limit major changes in shoulder slope to avoid impacting the barrier when the</li> </ul>
Width and Angle	Use wider shoulders where slope changes must be large to allow the suspension to stabilize the vehicle before impact.      Limit shoulder angle to comply with the AASHTO recommendation that melting snow flow away from the road.
Roadside Slope	Limit the variation of slope change on the roadside for situations where the barrier is not placed adjacent to the shoulder to provide an acceptable interface.
Barrier Type	<ul> <li>Consider higher (e.g., 31-in.) W-beam barrier designs for CSRS situations.</li> <li>Select barriers with increased height for tight curves where high speeds are likely to occur.</li> <li>Consider using concrete barriers with minimum face slope (e.g., F-shape) to reduce the risk of rollover.</li> </ul>
Installation	
Orientation Placement	<ul> <li>Promote use of barrier orientation perpendicular to the roadway for concrete barriers.</li> <li>Limit the placement of barriers to the edge of the shoulder on CSRS, particularly where there is a non-trivial slope change going to the roadside slope.</li> <li>Use wider shoulders with lower shoulder angles relative to the road on CSRS with short radii and high superelevation.</li> </ul>
Maintenance	<ul> <li>Analysis on the effectiveness of damaged barriers on CSRS is needed.</li> <li>Further analysis of relative priorities for barrier maintenance on CSRS may be needed.</li> </ul>

Note: Critical guidance elements are shown in bold type.

These are subject to further vetting, rewording, and editing in consultation with AASHTO committees. This construct provides a summary of the findings of the multifaceted analyses that support the proposed guidance for barrier design, selection, and installation.

#### **Conclusions**

In this effort, it was determined that there is limited information on the influences of CSRS features on safety. It was found that there were physics-based criteria for determining appropriate curvature and banking parameters to allow vehicles to safely negotiate curves under varying surface conditions. Criteria for basic curve design are found in the AASHTO's A Policy on Geometric Design for Highways and Streets (Green Book) (AASHTO 2011a). It was noted, however, that there was very limited guidance available for addressing concerns about vehicles leaving the roadway under CSRS conditions. While there is the basic understanding that crashes occur more often on curves than on tangent sections, the influences of CSRS features on crash propensity were not clear. It was noted that there is a fundamental issue with the level of detail associated with crash reporting that limits analysis options. The usual data captured for crashes falls short on details about the features of the road at or upstream of the crash location. In some cases, there are basic features that are provided on crash reports (e.g., pavement condition), but rarely are details on grade or curvature captured. This limits the ability to analyze CSRS crashes because the necessary data is not routinely captured. The problem occurs even when an agency has the road features data but cannot link it to specific crash sites.

There has been a growing understanding of the dynamics of vehicles as they traverse specific surfaces, but such analyses have not typically been undertaken in most crash analysis efforts, despite the availability of software tools for the purpose. Sophisticated simulation tools that allow the physics of vehicle dynamics and vehicle-to-barrier impacts to be analyzed may not be applied due to limited funds. The interest in understanding the safety performance of barriers on CSRS provides the impetus for using advanced tools when ordinary research approaches are limited.

This effort was undertaken in three phases to enhance the understanding of the safety performance of barriers on CSRS and develop guidance for their effective design, selection, and installation. The following insights resulted from this research:

- There has been little effort to determine whether longitudinal barriers adjacent to CSRS perform in the way same as those on tangent sections.
- Current guidance for barrier design, selection, and maintenance is essentially the same as that for tangent sections.
- VDA using commercially available tools provides a means to study the effects of speed, surface features, and vehicle type on the trajectory and orientations of a vehicle departing the traveled way on CSRS.
- Vehicle trajectories for two types of vehicles traveling at 62 mph (10km/h) were examined to determine their interface with barriers at various locations along the roadway.
- The VDA provided useful information on vehicle-to-barrier interfaces for a range of CSRS conditions.
- VDA results were used to determine which situations warranted deeper analyses using simulation.
- FE simulations were undertaken to investigate the impact performance (i.e., physics) of selected vehicles impacting one of three types of barriers placed on a CSRS.
- The simulation analyses focused on MASH impact conditions to evaluate the performance for NJ concrete, G4(1S) W-beam, and MGS barriers.

- The results indicated that there was some potential for failure, but options for addressing the problems existed.
- Three full-scale crash tests were conducted that validated the simulation analyses. These tests also demonstrated approaches for conducting future tests of barriers on CSRS.

The findings from all three phases of the research were summarized into proposed actions that could increase barrier safety on CSRS. The proposed actions will be shared with various groups for feedback and refined for possible incorporation into guidance documents and state practices. Needs for future research were also defined. *NCHRP Research Report 894* documents in detail the analyses and results from this project. These were synthesized into a series of proposals for effective design, selection, and installation of longitudinal barriers on CSRS.

#### CHAPTER 1

## Introduction

Highways consist of tangent and curved roadway sections for which there are well-established geometric design criteria. Curved roadway sections on higher speed roads are generally constructed with superelevation to compensate for the centripetal forces exerted on the vehicles, making it easier for the driver to control the vehicle through the curved section. Guidelines for the design of CSRS are found in the *Green Book*. These indicate superelevation rates for varying degrees of curvature for two speeds. They do not provide design guidance for shoulder features or barriers for superelevated curves.

There is limited guidance for the selection, design, and installation of barriers for CSRS of the road network. While it is well known that crashes occur proportionately more often on curves than tangent sections, the influence of curvature, superelevation, and roadway features on crash propensity or severity is not well understood. Barriers are often deployed on CSRS as a continuation of barriers on adjacent sections or to address situations created by the superelevated curve (i.e., the protection from a drop to the backslope, often associated with the embankment needed to provide the superelevation slope). Guidance for the deployment and testing of barriers on CSRS is limited. The need exists for a better understanding of the behavior of vehicles that leave the traveled way in such situations and the associated performance requirements for barriers deployed on the CSRS.

This report provides an overview of efforts and findings under two NCHRP projects: NCHRP Project 22-29, "Performance of Longitudinal Barriers on Curved, Superelevated Roadway Sections," and NCHRP Project 22-29A, "Evaluating the Performance of Longitudinal Barriers on Curved, Superelevated Roadway Sections." These were initiated to address the limited knowledge and guidance on barrier performance on CSRS through reviews of current agency practices, published research and guidance, accumulated knowledge about crashes and safety issues, and a three-phase effort to analyze the influences of specific CSRS conditions on barrier performance. The research developed insights from comprehensive

VDA, crash simulation, and full-scale testing to develop guidance for improved selection, design, and deployment practices for common longitudinal barriers [e.g., NJ concrete, G4(1S) W-beam guardrail, and the MGS] for CSRS situations.

#### 1.1 Background

The safety performance of longitudinal barriers under current and past crashworthiness evaluation criteria has been assessed under idealized impact conditions where a linear section of the barrier is installed on level terrain and the impacting vehicle is freewheeling with minimum roll and pitch effects. This protocol has evolved to provide a "practical worst-case" impact condition that is reproducible and comparable. In reality, barriers are rarely installed and impacted under ideal conditions, and installations and impacts on CSRS are examples of conditions that are far from ideal.

State DOTs have addressed the installation of barriers for CSRS in varying ways because there is limited guidance in both the *Green Book* and the *Roadside Design Guide* (AASHTO 2011b). Figure 1.1 shows examples of concrete and steel W-beam longitudinal barriers installed on CSRS. Curved roadway sections are generally constructed with superelevation to compensate for the centripetal forces exerted on the vehicles, making it easier for drivers to control their vehicle at higher speeds through the curved section.

Both curvature and superelevation can affect vehicle dynamics and the vehicle's trajectory, orientation, weight distribution, and speed. Recent research has noted that the dynamic effects can significantly affect the interface between the vehicle and the barrier as it leaves the road (Marzougui et al. 2008a, 2010a, 2012a). On curved sections, the vehicle can leave the road at a sharper angle and consequently hit the barrier with higher impact severity. The higher impact severity can lead to increased forces on the occupants, more intrusion into the occupant compartment, ruptured barriers, or unusual interactions between contacted components. In



Figure 1.1. Example CSRS with typical longitudinal barriers.

addition, a sharper impact angle can increase vehicle instability and may lead to vehicle rollover, override, or penetration of the barrier. The sharper angles increase vehicle climb for rigid barriers and tire/post snagging for semi-rigid strongpost barriers. Furthermore, the road superelevation may cause the vehicle to approach the barrier at a different orientation (i.e., roll, pitch, and yaw) and hence impact at a height higher relative to the barrier than would be the case for a flat surface. This is particularly critical when a shoulder has a negative slope relative to the roadway surface.

Background for this research was gathered from reviewing the literature, conducting a state DOT survey, and investigating crash data in search of issues associated with safety performance of CSRS. These efforts revealed that there had been little previous research for longitudinal barriers on CSRS, no common barrier selection, design, or installation practices for barriers on CSRS across the United States, and limited opportunity to discern safety issues due to limited

data for impacts with barriers on CSRS. Thus, there was a need to assess barrier safety performance as a function of curvature, superelevation, shoulder configuration (i.e., width and slope), and impact conditions. The MASH crashworthiness requirements served as the benchmark for the assessment.

#### 1.2 Project Objectives and Scope

The objectives of this research were to (1) evaluate the crash performance of standard longitudinal barriers installed on CSRS; (2) determine if the curvature and superelevation details used by state DOTs degrade the performance of the barriers to the extent that they will no longer meet the crash test criteria for MASH; and (3) develop guidance for the design, selection, and installation of barriers on CSRS. The effort applied state-of-the-art analysis tools to enhance the understanding of the influencing factors and identify possible

future research to study barrier modifications, changes to roadway geometrics, or both in response to any safety issues identified. Under the second phase of the research, the evaluation of crash performance included (1) a review of the development and validation of the crash simulations in NCHRP Project 22-29 using LS-DYNA FE models of four vehicles and three barrier types (G4-1S, MGS, and vertical concrete) and (2) completion of one planned simulation from NCHRP Project 22-29.

The Research Team met these objectives by using simulation analyses and validating the results using crash tests. A wide spectrum of cases was analyzed in detail and cases where the barrier type, design, or placement did not meet requirements were isolated. The following sections describe pertinent accomplishments from NCHRP Project 22-29 and the efforts that were undertaken in this project.

#### 1.3 Research Approach

Curvature and surface slope are known to affect vehicle dynamics and influence vehicle trajectories, orientation, and speed. On curved sections, the vehicle is more likely to leave the road at a sharper angle and impact the barrier with greater force, which could potentially result in a higher impact severity. The degree of superelevation in combination with the shoulder slope can lead to a higher interface with the barrier, which can increase vehicle instability, barrier climb, vehicle rollover, or override. Further, the superelevation with a negative shoulder slope might cause the vehicle to impact the barrier at a different orientation (roll and pitch). Thus, an important starting point for analyses of barriers on CSRS is establishing an understanding of the dynamics of vehicles leaving the roadway and traversing the shoulder and side slope before impacting the barrier.

Much effort has been devoted to analyzing the dynamic effects of vehicles on non-level terrain and the subsequent effects on their trajectories and interfaces with barriers. VDA has been shown to provide new insights on the effects of a vehicle's suspension system on trajectories in all three dimensions. For example, trajectory data in the vertical direction is directly related to the height of the interface of the vehicle and the barrier. This effect is more likely to occur when there is a change in the surface slope between the roadway and the shoulder leading to a shift in the distribution of the vehicle's weight, which could lead to an override or underride of the barrier due to poor interface. The combined effect of the superelevation of the roadway, the slope of the shoulder, and the side slope of the roadside for a vehicle leaving the roadway on a curve can be explicitly analyzed using VDA tools. These tools readily allow the range of combinations of roadway, shoulder, and side slope design features to be analyzed for varying types of vehicles and their paths or trajectories determined. Thus, a VDA approach was proposed as the starting point for this research to cover a broad range of CSRS conditions.

Because VDA only provides insights on the vehicle-tobarrier interface, the second phase of the analyses was to use crash simulation analysis to understand barrier strength and behavior for impacts on varying CSRS. Simulations of crashes into barriers have been shown to effectively replicate actual events and therefore, can provide useful metrics on safety performance. An array of FE models for vehicles and barriers was available to support such analyses. Simulations allow variations of the vehicle-to-barrier interface to be considered, as well as the necessary aspects of barrier strength as a function of its detailed design and deployment. Since simulation runs are time-consuming, it was planned that a subset of CSRS conditions would be selected for simulation based on the VDA results. Various metrics can be derived from the simulations, including the MASH TL-3 crashworthiness measures related to vehicle stability and occupant risk. The simulation analysis supports the generation of many crash metrics as well as digital views of the vehicle-to-barrier impacts. These were considered essential to understanding barrier safety performance on CSRS. These simulation results also provide a means to explain the nature of vehicle-to-barrier interactions, as well as compare the effects of various factors on behavior and performance.

Full-scale crash testing was the last step to verify and validate the simulation results. Tests were conducted to determine the validity of the simulation results. The tests showed outcomes that were similar to the simulations for similar conditions, leading to the conclusion that the simulation results were valid. Since guidelines for the testing and deployment of roadside safety barriers on sloped surfaces and curved sections do not exist, it was recognized that innovative efforts would be needed. Crash testing protocols for barriers have evolved to provide a practical worst-case impact condition that is reproducible and comparable. Barriers had been tested under idealized impact conditions, with the tested barriers being installed on a straight section, having a flat approach terrain, and the impacting vehicle freewheeling with minimum roll and pitch effects. These protocols have evolved to provide important assessments that determine whether safety hardware is "crashworthy." While crash testing protocols have evolved to include tests for a variety of angular impact conditions, one aspect that is not fully addressed is the crashworthiness of barriers installed on CSRS. A review of the literature revealed that only a few efforts had addressed the safety of designs or provided guidance for placement on CSRS. The need existed to understand performance of longitudinal barriers along the CSRS to develop effective barrier designs and appropriate placement guidelines for such locations.

The research approach involved summarizing the research findings in each of the facets to allow translation of the results into guidance on the design, selection, and installation of longitudinal barriers on CSRS. It is planned that guidance derived from these efforts will be presented to AASHTO and FHWA for their critical review and possible integration into the appropriate documents. *NCHRP Research Report 894* describes the findings and explains the rational for the proposed guidelines.

#### 1.4 Report Organization

This report is organized as follows:

- Summary
- Chapter 1—Introduction
- Chapter 2—Literature Review and State DOT Survey
- Chapter 3—Crash Data Analysis

- Chapter 4—Vehicle Dynamics Analysis for Vehicles Leaving the Traveled Way on CSRS
- Chapter 5—Crash Simulation Analysis of Impacts into Longitudinal Barriers on CSRS
- Chapter 6—Full-Scale Testing and Results
- Chapter 7—Development of Guidance for Improved Longitudinal Barrier Design, Selection, and Installation on CSRS
- Chapter 8—Conclusions

The report also includes Appendices A through E as follows:

Appendix A: State DOT Survey Instrument and Instructions; Appendix B: Vehicle Dynamics Simulation Results; Appendix C: Finite Element Model Validations; Appendix D: Finite Element Simulation Results; and Appendix E: Full-Scale Crash Testing Report. These appendices can be found on the TRB website (www.trb.org) by searching for "NCHRP Research Report 894".

#### CHAPTER 2

# Literature Review and State DOT Survey

#### 2.1 Introduction

A detailed literature review was conducted to gather information and synthesize relevant past efforts. The focus was on studies related to the design, performance evaluation, maintenance, and application details of longitudinal barrier systems when placed on CSRS with emphasis on crash testing and computer simulations. TRID was used to identify domestic and international reference materials. The findings from the literature search revealed limited references related to this topic. Summaries of relevant knowledge from domestic and international reference materials are presented in this chapter.

#### 2.2 Barrier Crashworthiness Research

One of the first research efforts to determine the performance of traffic barriers on curved alignments was described in Bridge Rail Retrofit for Curved Structures (Bronstad and Kimball 1986). Three bridge rail systems were installed on a curved, superelevated structure and crash tested. The railings tested were two 813-mm- (32-in.-) tall NJ concrete barriers (one installed true vertical and the other perpendicular to the superelevated bridge deck) and a retrofitted tubular Thriebeam rail (i.e., double-sided Thrie-beam rail), installed perpendicular to the deck (Figure 2.1). Test vehicles included an 820-kg (1,800-lb) sub-compact car (Honda Civic), a 1,020-kg (2,250-lb) compact car (Vega), and a 9,070-kg (20,000-lb) school bus. Impact conditions for all tests were nominally 64 km/h (40 mph) with a 15° impact angle. The simulated bridge deck used in the testing was constructed with a 48.8-m (160-ft) outside radius on a 4.5% downgrade. The superelevation was 12% with no shoulder break.

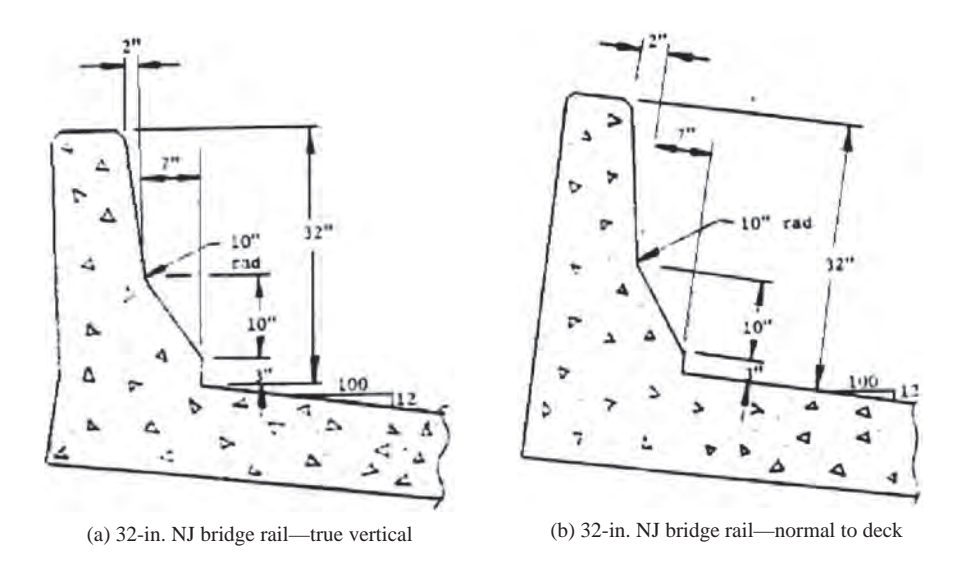
All three barriers contained and redirected the vehicles in the crash tests. There was not a significant difference in performance between the two concrete barrier orientations (i.e., true vertical or perpendicular to the superelevated roadway surface), but vehicle climb was reduced in the perpendicular orientation tests. In all of the concrete barrier tests, the cars climbed at least 460 mm (18 in.) up the barrier. In one test of the vertically oriented barrier, the vehicle nearly climbed to the top of the barrier, even at the relatively low impact speed and angle. The tubular Thrie-beam retrofit design, installed perpendicular to the roadway surface, performed better than the safety shape in all the crashes.

The second and most relevant reference was an FHWA report entitled *Traffic Barriers on Curves, Curbs, and Slopes* dated August 1993 (Stout et al. 1993). This study investigated performance of guardrails on curves, on slopes, and with curbs. The research was conducted in four main phases. In the first phase, previous references on related topics were reviewed. The second phase consisted of analyzing crash datasets to identify issues related to the study topic. Next, a series of crash tests were conducted on guardrails to assess their performance when installed on curves, on slopes, and with curbs. In the final phase, an attempt was made to use computer simulation using the Numerical Analysis of Roadside Design (NARD) program to assess the barrier performance under these conditions.

The literature review revealed that the W-beam and Thriebeam barriers did not meet the *NCHRP Report 230* testing requirements when installed on non-level terrain at the tested offset distances from the edge of the road, while the cable barrier system did meet these requirements. Another finding indicated a similar observation that different lateral barrier offsets and heights could lead to vehicle override and underride in sloped median installations. A third finding was that vehicle behavior is affected by highway features and roadside barriers. A final finding indicated that roadside slopes significantly affect barrier performance.

The data analysis revealed limited information due to the small size of some of the datasets available. Some of the key findings from the crash data analysis are listed as follows:

 Pertaining to curved roadside sections, the accident data showed no evidence that guardrail performance is worse on curved road sections than on straight sections.



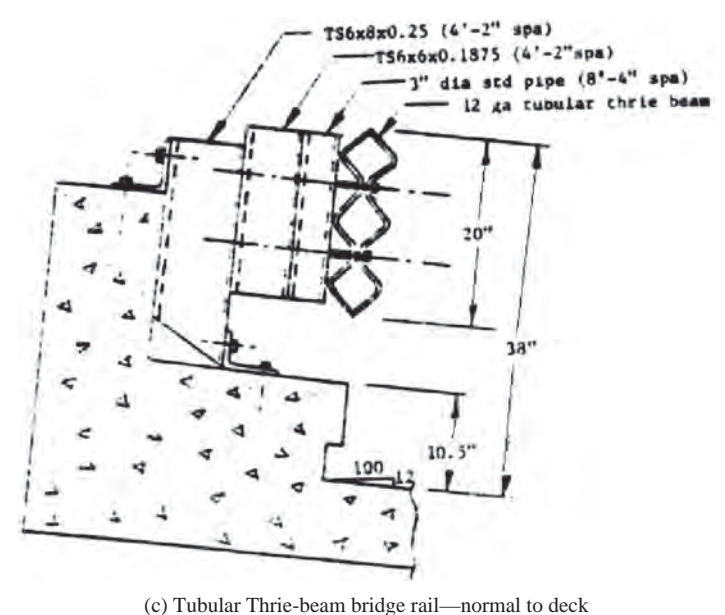


Figure 2.1. Cross sections of tested bridge rails (Bronstad and Kimball 1986).

• For installations on side slopes, the performance of barriers placed behind the hinge point was significantly worse than when placed before the hinge point. This was the case even though all barriers were installed in relatively gentle slopes (shallower than 4H:1V) as recommended by AASHTO guidelines for guardrail installations.

In the third phase of the study, crash tests were conducted. Two tests involved impacts with an 820-kg (1,800-lb) small car and 2,450-kg (5,400-lb) pickup truck, both at 96.5 km/h (60 mph) and 20° impact angle into a standard W-beam guardrail on a 363-m (1,192-ft) radius curve with level terrain. These tests indicated that the barrier would meet the crashworthiness requirements. Four additional tests were

conducted with the 2,450-kg (5,400-lb) pickup at 96.5 km/h (60 mph) and 20° impact angle, but approaching the barrier on the diagonal of a 10% superelevation upslope. Four different barrier and placement conditions were tested as noted in Table 2.1. In all cases for the standard guardrail at normal heights the outcome was negative. Only the high-performance Thrie-beam barrier met the requirements for these crash conditions. The report did not cite specific issues with the vehicle-to-barrier interface that might be a focal point for barrier redesign on curves. While these tests provided some useful insights, they only considered a curve radius of 363 m (1,192 ft), superelevation slope of 10%, speed of 96.5 km/h (60 mph), impact angle of 20°, and a 2,450-kg (5,400-lb) pickup truck. There is a need to consider a broader set of

Test	Barrier	Placement	Outcome				
	Standard W-beam	Beyond 3-m	The vehicle was redirected on the				
1862-6-89	guardrail w/ 1.83-	(10-ft) shoulder	traffic side of the barrier, but rolled				
	m (6-ft) posts		over.				
	Standard W-beam	Beyond 3-m	The vehicle vaulted the rail and rolled				
1862-9-90	guardrail w/ 2.13-	(10-ft) shoulder	over. The lateral torsion in the longer				
	m (7-ft) posts		posts increased buckling.				
1862-10-90	Thrie-beam	Beyond 3-m	The vehicle was redirected by this				
1802-10-90	guardrail	(10-ft) shoulder	high-performance barrier.				
	Standard W-beam	At edge of	This option was intended to eliminate				
	guardrail w/ 1.83-	traveled way	the possibility that the vehicle would				
1862-16-91	m (6-ft) posts		become airborne at the break point of				
			the superelevated section and shoulder,				
			but the vehicle still vaulted and rolled.				

Table 2.1. Full-scale crash tests conducted on 10% superelevation.

impact conditions consistent with updated crashworthiness criteria.

#### 2.3 Terrain Effect Studies

A more recent study, not directly related but relevant to the topic of this research, was conducted at the Texas Transportation Institute (TTI) (Sheikh and Bligh 2006). Using FE simulations, this study investigated the safety performance of 813-mm-(32-in.-) high F-shape concrete barriers when installed on sloped medians. The simulations included different median and barrier placement configurations. In the first configuration, the study focused on barriers installed at the center of symmetric V-shaped medians with side slopes of 6:1 or shallower (Figure 2.2). Horizontal curvatures were not considered in this study.

To identify the most critical impact scenarios for this configuration, simulations without a barrier were conducted to determine the trajectory of the corner of the front bumper relative to the ground as the vehicle traverses the median. This trajectory is shown in Figure 2.3. Two critical barrier placements (i.e., median widths) were identified: (1) when the vehicle is at its highest point relative to the barrier and (2) when the vehicle is at its lowest point relative to the barrier. The first point was found to be 4 m (13.25 ft) from the edge of the road and the bumper point was about 150 mm (6 in.) higher than it would be when the barrier is installed on flat terrain. The second point was identified to be 7.2 m (23.5 ft) from the edge of the road, and the bumper was about 50 mm (2 in.) lower than the flat terrain condition.

Simulations using a 2000P vehicle (represented by a Chevrolet C2500 pickup model) traveling at 100-km/h (62.2-mph) initial speed and 25° impact angle were conducted to assess the barrier performance in these two critical impact configurations. The barrier in these simulations was assumed rigid because it was not expected that it would undergo significant deformation or damage during the impact. Both simulations showed that the barrier met all *NCHRP Report 350* criteria (Ross et al. 1993).

Two additional configurations were investigated where the barrier was placed on one side of the median. In the first configuration, the barrier was placed on the shoulder [Figure 2.4(a)]. In the second configuration, the barrier was placed at the edge of the shoulder as shown in Figure 2.4(b). In the latter case, one side of the median was regraded to accommodate the placement of the 0.61-m (2-ft) base of the barrier. A total median width of 9.1 m (30 ft) [2.2 m (40 ft) (with 1.22-m (4-ft) shoulders] was used in the second case. In both cases, the barrier's vertical alignment was perpendicular to the road surface. The height of the bumper corner point relative to ground level as the vehicle crosses the median is shown in Figure 2.5. The bumper impact height for the first case was 200 mm (8 in.) lower than it would be on flat terrain and about 75 mm (3 in.) higher than it would be for flat terrain installations for the second case. Simulations with the 2000P vehicle traveling at a 100-km/h (62-mph) initial speed and an impact angle of 25° were conducted. In these simulations, the vehicle impacted the back side of the barrier after crossing the symmetric V-shaped 6:1 sloped median. The simulations

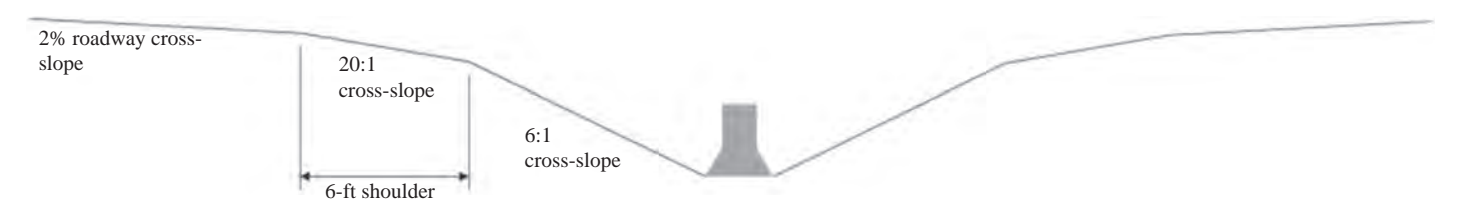


Figure 2.2. Barrier placed in the middle of a 6:1 or shallower sloped median (Sheikh and Bligh 2006).

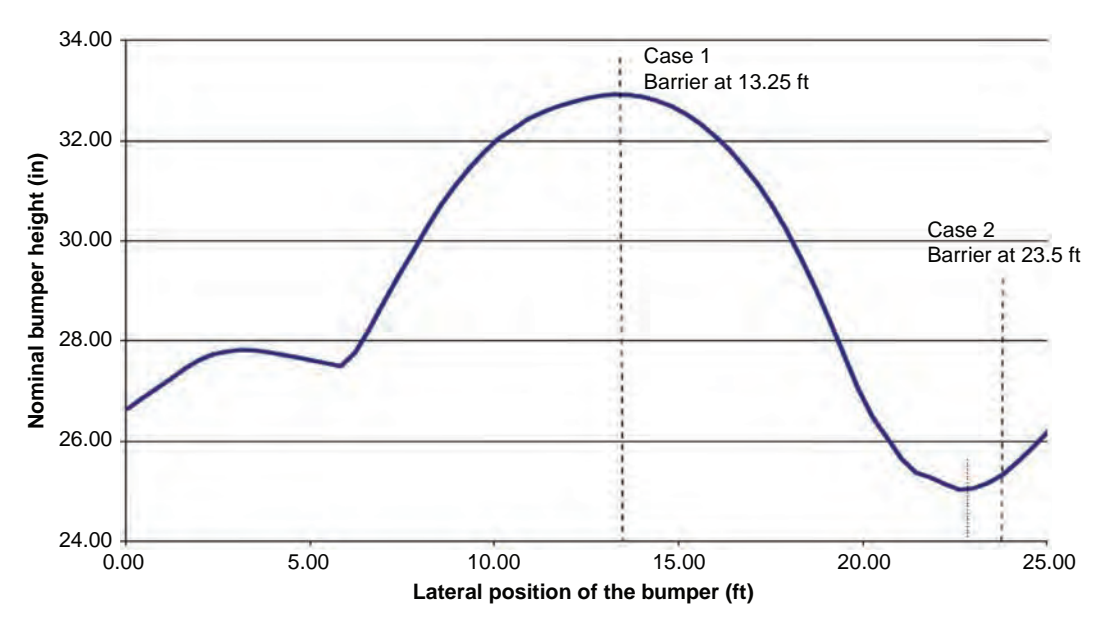


Figure 2.3. Bumper height relative to the ground as vehicle crosses the median (Sheikh and Bligh 2006).

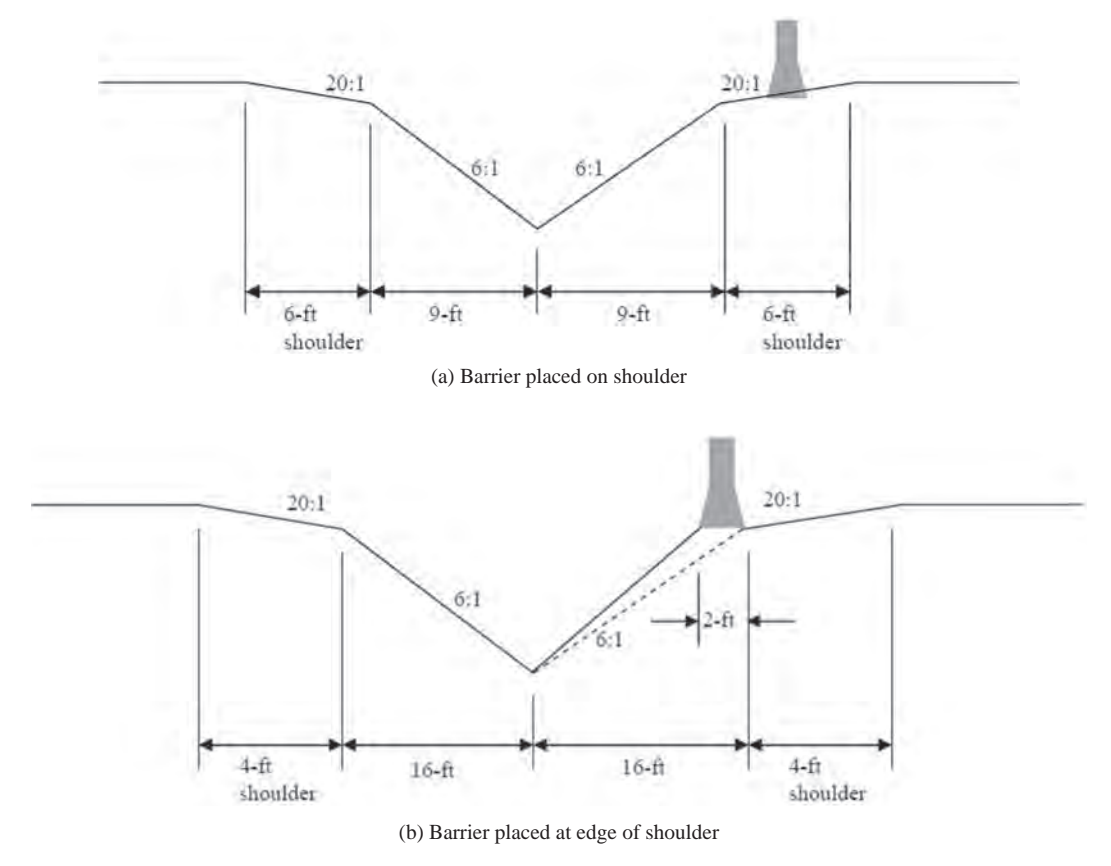


Figure 2.4. Barrier placed at the edge of a 6H:1V or shallower sloped median (Sheikh and Bligh 2006).

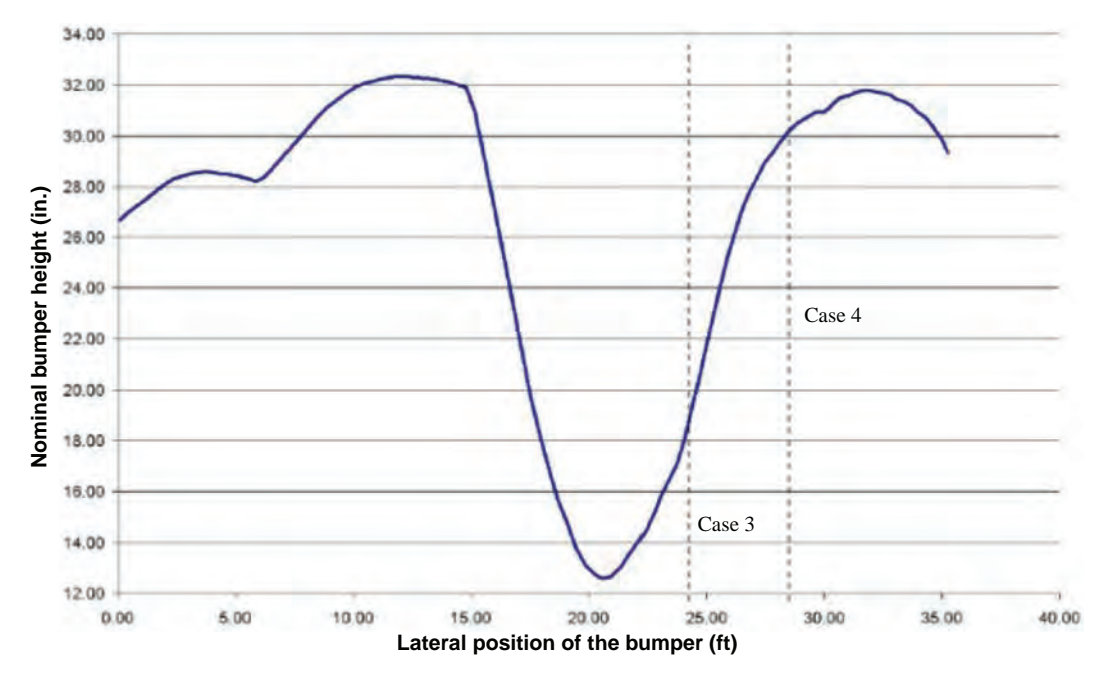


Figure 2.5. Bumper height relative to the ground as vehicle crosses the median (Sheikh and Bligh 2006).

showed that the barrier met all NCHRP Report 350 criteria in both cases.

It is noted from these simulations that the 813-mm (320-in.) F-shape concrete barrier performed adequately, even when the height of the vehicle relative to the barrier was 150 mm (6 in.) higher (Figure 2.3) and 200 mm (8 in.) lower (Figure 2.5) than that of the flat terrain case.

Two full-scale crash tests were conducted to validate the simulation results. The tests were set up in similar configurations to the first two simulation cases (representing barrier placement at the center of V-shaped symmetric medians). Both tests met the NCHRP Report 350 criteria. Based on the simulations and tests, guidelines for the use of concrete barriers on sloped medians were recommended for the Texas DOT (TxDOT) as follows: "The TxDOT cast-in-place permanent F-shape barrier and the precast free-standing F-shape barrier are considered suitable for placement on roadside and median fore-slopes of 6H:1V or less. Additionally, these barriers are suitable to be placed at any lateral offset of the barrier from the roadway edge and for any width of depressed V-ditch median as long as the barrier is placed at its center. Similar or better performance would be expected for placements on more gentle (e.g., 8H:1V) slopes." Testing was not conducted for the cases where the barrier was installed on the shoulder and no recommendations for these cases were included.

In another study conducted at TTI, the effects of barrier vertical orientation (inclination) on the performance of safety shape bridge rail parapets were investigated (Sheikh and Alberson 2005). Simulations with F-shape parapets

installed on five different roadway cross slopes were conducted and compared to study the effects of barrier vertical orientation. The cross slopes studied are shown in Table 2.2. For all cross section profiles, the parapet was modeled plumb to the earth. The simulations were conducted using a 2000P vehicle model impacting the barrier at 100 km/h (62.2 mph) and a 25° angle.

Using the simulation results, the effects of barrier orientation on the vehicle roll and pitch angles and vehicle center of gravity (CG) vertical displacement (representing vehicle climb) were assessed. Figure 2.6 shows plots of these measures for different roadway cross slopes. The simulations showed that the vehicle roll, pitch, and vertical displacement increase with increased cross slope angles (i.e., increased inclination).

Table 2.2. Cross slopes used in the study (Sheikh and Alberson 2005).

Cross-slope	Inclination angle, $\theta$
0	0°
20 1	2,86°
15	3,81°
12,5	4.570
10	5.71°

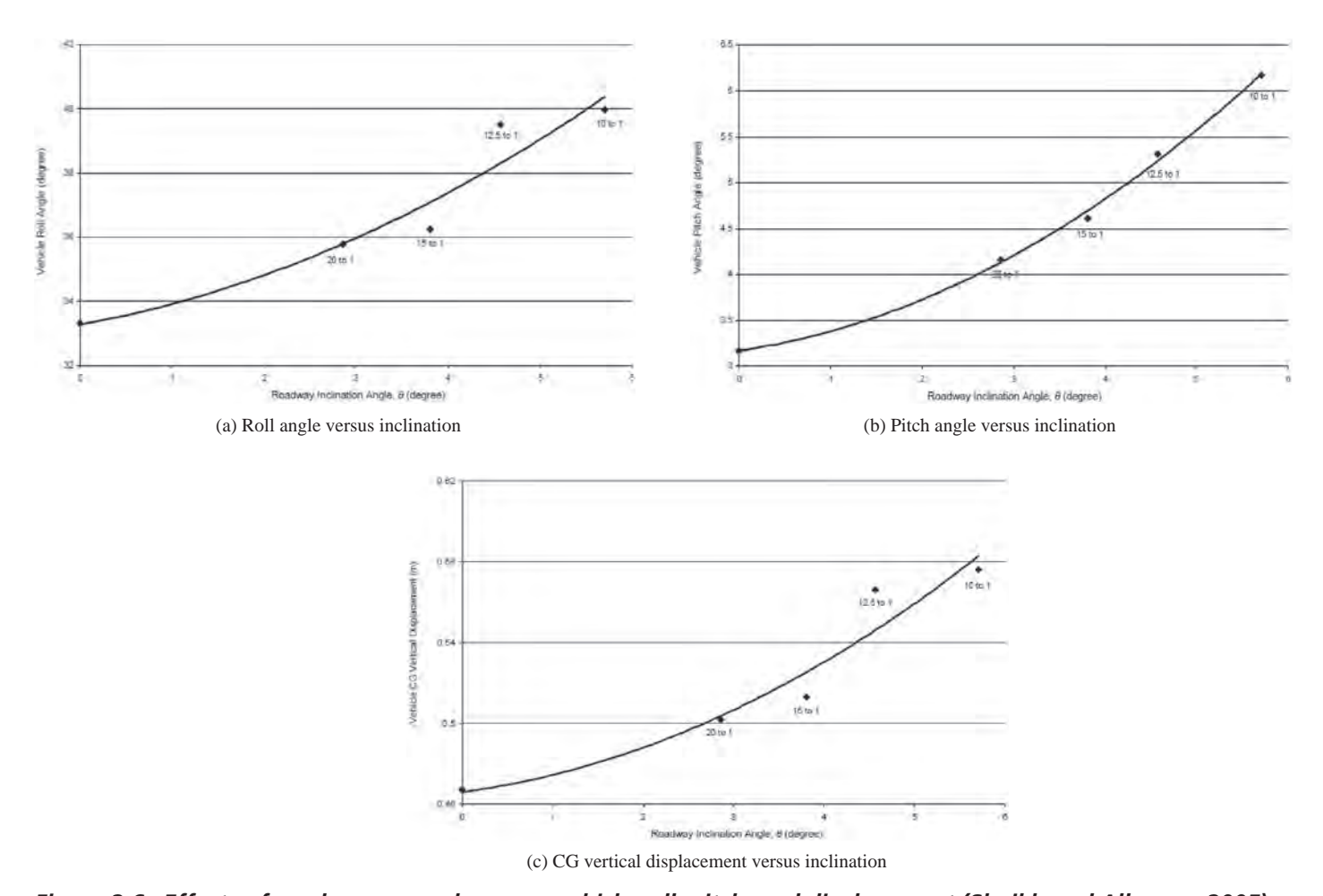


Figure 2.6. Effects of roadway cross slopes on vehicle roll, pitch, and displacement (Sheikh and Alberson 2005).

#### 2.4 General Curve Safety Guidance

Another reference related to the topic of this research is NCHRP Report 500: Guidance for Implementation of the AASHTO Strategic Highway Safety Plan, Volume 7: A Guide for Reducing Collisions on Horizontal Curves (Torbic et al. 2004). This report includes guidelines developed to reduce fatal and serious injuries on curved roads. The guidelines are aimed at reducing the likelihood of a vehicle leaving the road and minimizing the adverse consequences of run-offroad situations at horizontal curves. The guidelines are listed below. The first 15 guidelines are aimed at reducing the number of vehicles leaving the road, while the last 5 are intended to reduce the severity of crashes on curved roads. The last two guidelines specifically address roadside safety hardware; limited information was available in the report on their implementation:

- Provide advance warning of unexpected changes in horizontal alignment
- 2. Enhance delineation along the curve

- 3. Provide adequate sight distance
- 4. Install shoulder rumble strips
- 5. Install centerline rumble strips
- 6. Prevent edge drop-offs
- 7. Provide skid-resistant pavement surfaces
- 8. Provide grooved pavement
- 9. Provide lighting of the curve
- 10. Provide dynamic curve warning system
- 11. Widen the roadway
- 12. Improve or restore superelevation
- 13. Modify horizontal alignment
- 14. Install automated anti-icing systems
- 15. Prohibit/restrict trucks with very long semitrailers on roads with horizontal curves that cannot accommodate truck off tracking
- 16. Design safer slopes and ditches to prevent rollovers
- 17. Remove/relocate objects in hazardous locations
- 18. Delineate roadside objects
- 19. Add or improve roadside hardware
- 20. Improve design and application of barrier and attenuation systems

#### 2.5 Road Design Guidelines

A few guidelines were obtained from respondents of the state DOT survey. An initial review showed that these guidelines are similar to the *Green Book* recommendations summarized in the following subsection. Guidelines pertaining to curved road sections address only geometric aspects of the road. No specific information was found related to longitudinal barrier installations. Few differences were observed between the state DOT survey responses and *Green Book* guidelines for maximum superelevation rates, side friction factors, superelevation design tables, and so forth.

The fundamentals for barrier design and deployment on U.S. highways is provided in the *Green Book* and the *Roadside Design Guide*. These documents were reviewed to understand the prevailing rationale and determine the conditions and parameters cited for when barriers are needed, the recommended types, and where and how they are to be deployed. The focus was on longitudinal barrier installations on high-speed CSRS. The relevant elements from these documents are summarized below. Because states can establish their own standards and practices, a state DOT survey was also conducted.

#### 2.5.1 Green Book

To establish a safe and comfortable driving environment on curved road sections, guidelines for the selection of road curvatures and superelevations, given a selected design speed, are provided in the *Green Book*. The guidelines that are relevant to this research include design speed; maximum superelevation rate; side friction factor; minimum curve radius; superelevation distribution methods and superelevation calculation; and shoulders. These guidelines are used by most states when determining the curvatures and superelevation rates of curved roads. These guidelines were also used in this effort to create the road profiles for the computer simulations. These guidelines are summarized in the following subsections.

#### 2.5.1.1 Design Speed

The Green Book defines design speed as "a selected speed used to determine the various geometric features of the roadway." The design speed should be selected based on the topography, anticipated operating speed, adjacent land use, and functional classification of the highway. The design speed affects many aspects of the roadway geometric elements. It directly influences superelevation and curvatures as well as several other design parameters. The Green Book recommendation for minimum design speed on high-speed roadways (freeways) is 80 km/h (50 mph). The use of design speeds of 100 km/h (60 mph) or higher is encouraged for urban freeways, because it can be achieved with minimal additional costs. A 110 km/h (70 mph) design speed is recommended for rural freeways and interchange locations consistent with higher design speeds. For mountainous terrain, a design speed of 80 to 100 km/h (50 to 60 mph) is recommended. The Green Book gives an approximation of the running speed as a function of design speed as shown in Table 2.3.

Table 2.3. Average running speed versus design speed (AASHTO 2011a).

Met	ric	U.S. Customary						
Design Speed (km/h)	Average Running Speed (km/h)	Design Speed (mph)	Average Running Speed (mph)					
20	20	15	15					
30	30	20	20					
40	40	25	24					
50	47	30	28					
60	55	35	32					
70	63	40	36					
80	70	45	40					
90	77	50	44					
100	85	55	48					
110	91	60	52					
120	98	65	55					
130	102	70	58					
	1	75	61					
		80	64					

#### 2.5.1.2 Maximum Superelevation Rate

Vehicles traveling on curved roads are subjected to a lateral force known as centrifugal force. This lateral force, which pushes the vehicle outward from the curved road center point, increases as the vehicle speed increases or the radius of the curve decreases. Superelevation is the sloping (banking) of the road to oppose this lateral centrifugal force. For high-speed roadways, the *Green Book* recommended range for maximum superelevation rate is 6% to 12%. This range is reduced to 6% to 8% in regions where snow or ice is of concern, because vehicles traveling at low speeds in snowy or icy conditions tend to slide on roads with high superelevations. A superelevation rate of 6% to 8% is also recommended for viaducts; the lower 6% superelevation rate is recommended when freezing and thawing conditions are likely.

#### 2.5.1.3 Side Friction Factor

The side friction factor is defined in the *Green Book* as the "vehicle need for side friction." When a vehicle is traveling on a curved road, the lateral centrifugal force is resisted by a combination of the superelevation and the friction between the tires and the road surface. For a given vehicle speed and curvature radius, an increase in superelevation would lead to

lower lateral friction force (i.e., a larger portion of the centrifugal force is resisted by the superelevation). The side friction factor is the ratio between this lateral friction force and the weight of the vehicle (with a small conservative simplification). The side friction factor *f* is expressed in the *Green Book* as follows:

$$f = \frac{V^2}{15R} - 0.01e$$

where V is the vehicle speed (mph), R is curve radius (ft), and e is the superelevation rate (%).

The side friction factor depends on many variables such as the speed of the vehicle; weight; braking and accelerating; suspension; and tire design and condition. It decreases when the speed of the vehicle increases, and during braking or acceleration. The maximum value of the side friction factor is reached when the vehicle starts to skid. To avoid skidding, the maximum side friction factor used in highway design is much less than the actual value (i.e., roads are designed based on a portion of the maximum side friction available to ensure safety and comfort of the driver). Based on several research studies, the *Green Book* defines a curve for maximum side friction factor versus design speed. This curve is shown in Figure 2.7.

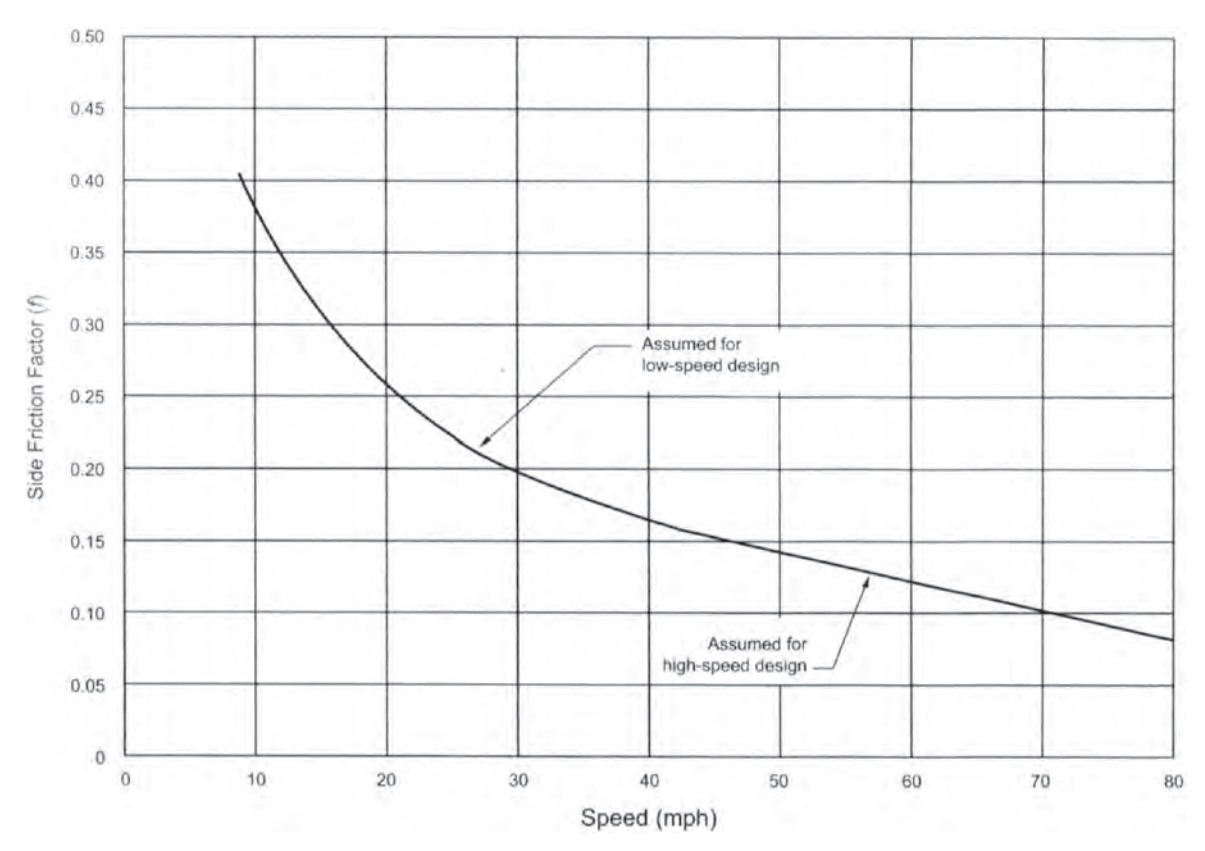


Figure 2.7. Side friction factor assumed for road design (AASHTO 2011a).

#### 2.5.1.4 Minimum Curvature Radius

The minimum curvature radius defines the sharpest curvature for a given design speed, maximum superelevation, and maximum side friction factor. It can be expressed as follows:

$$R_{\min} = \frac{V_D^2}{15(0.01e_{max} + f_{max})}$$

where  $V_D$  is the design speed (mph),  $f_{\text{max}}$  is maximum side friction factor, and  $e_{\text{max}}$  is the superelevation rate (%).

# 2.5.1.5 Superelevation Distribution Methods and Superelevation Calculations

For a given design speed and road curvature, several combinations of superelevation and side friction can be used to resist the lateral centrifugal force. The *Green Book* lists five different methods for the distribution of the superelevation and lateral friction forces. For high-speed roadways, the last method (Method 5) is recommended. In this method, the superelevation and side friction have a curvilinear relationship with respect to the inverse of the curvature radius. Using the maximum side friction factor shown in Figure 2.7 and this method, diagrams of superelevation in relation to curvature radius and design speed for different maximum superelevations are generated. A sample diagram is shown in Figure 2.8. Using the same method, superelevation tables were generated.

A sample superelevation design table is included in Table 2.4. These diagrams and tables are used to determine road curvatures and superelevation rates.

#### 2.5.1.6 Shoulders

The *Green Book* recommends that shoulders in heavily traveled high-speed highways be at least 3 m (10 ft) wide, with a 3.66-m (12-ft) width preferable. On four-lane freeways, the recommended shoulder width on the left side of the road is 1.22 m to 2.44 m (4 ft to 8 ft) and on the right side at least 3 m (10 ft). Asphalt and concrete shoulders should be sloped from 2% to 6%. Gravel or crushed rock shoulder slopes should be from 4% to 6% and turf shoulders should be 6% to 8%.

#### 2.5.2 Roadside Design Guide

A review of the *Roadside Design Guide* revealed no specific recommendations for longitudinal barrier installations on curved and superelevated road sections (i.e., barrier installations on curves follow the same guidelines as on straight roads). A few recommendations related to the research topic are listed as follows:

 A barrier should not be installed on a slope steeper than 6H:1V unless it has been tested and found to meet the NCHRP Report 350 or MASH evaluation criteria.

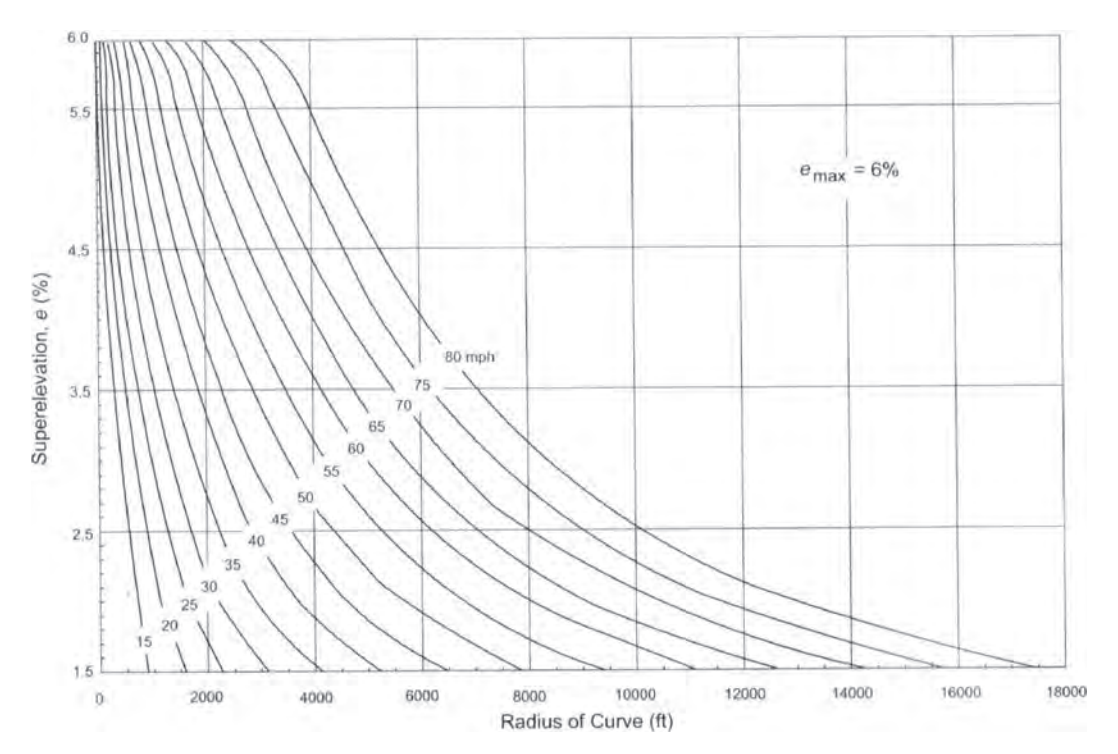


Figure 2.8. Sample design superelevation diagram, for  $e_{max} = 6\%$  (AASHTO 2011a).

						1	J.S. Custo	omary						
	V <sub>d</sub> = 15	V <sub>d</sub> = 20	V <sub>d</sub> = 25	V <sub>d</sub> = 30	V <sub>d</sub> = 35	V <sub>d</sub> = 40 mph	V <sub>d</sub> = 45	V <sub>d</sub> = 50	V <sub>d</sub> = 55	V <sub>d</sub> = 60	V <sub>d</sub> = 65	V <sub>d</sub> = 70	V <sub>d</sub> = 75	V <sub>d</sub> = 80
e (%)	R (ft)	R (ft)	R (ft)	R (ft)	R (ft)	R (ft)	R (ft)	R (ft)	R (ft)					
NC	868	1580	2290	3130	4100	5230	6480	7870	9410	11100	12600	14100	15700	17400
RC	614	1120	1630	2240	2950	3770	4680	5700	6820	8060	9130	10300	11500	12900
2.2	543	991	1450	2000	2630	3370	4190	5100	6110	7230	8200	9240	10400	11600
2.4	482	884	1300	1790	2360	3030	3770	4600	5520	6540	7430	8380	9420	10600
2.6	430	791	1170	1610	2130	2740	3420	4170	5020	5950	6770	7660	8620	9670
2.8	384	709	1050	1460	1930	2490	3110	3800	4580	5440	6200	7030	7930	8910
3.0	341	635	944	1320	1760	2270	2840	3480	4200	4990	5710	5490	7330	8260
3.2	300	566	850	1200	1600	2080	2600	3200	3860	4600	5280	6010	6810	7680
3.4	256	498	761	1080	1460	1900	2390	2940	3560	4250	4890	5580	5340	7180
3,6	209	422	673	972	1320	1740	2190	2710	3290	3940	4540	5210	5930	6720
3.8	176	358	583	864	1190	1590	2010	2490	3040	3650	4230	4860	5560	6320
4.0	151	309	511	766	1070	1440	1840	2300	2810	3390	3950	4550	5220	5950
4.2	131	270	452	684	960	1310	1680	2110	2590	3140	3680	4270	4910	5620
4.4	116	238	402	615	868	1190	1540	1940	2400	2920	3440	4010	4630	5320
4.6	102	212	360	555	788	1090	1410	1780	2210	2710	3220	3770	4380	5040
4.8	91	189	324	502	718	995	1300	1640	2050	2510	3000	3550	4140	4790
5.0	82	169	292	456	654	911	1190	1510	1890	2330	2800	3330	3910	4550
5.2	73	152	264	413	595	833	1090	1390	1750	2160	2610	3120	3690	4320
5.4	65	136	237	373	540	759	995	1280	1610	1990	2420	2910	3460	4090
5.6	58	121	212	335	487	687	903	1160	1470	1830	2230	2700	3230	3840
5.8	51	106	186	296	431	611	806	1040	1320	1650	2020	2460	2970	3560
6.0	39	81	144	231	340	485	643	833	1060	1330	1660	2040	2500	3050

Table 2.4. Sample design superelevation table,  $e_{max} = 6\%$  (AASHTO 2011a).

- Only flexible and semi-rigid barriers should be installed on slopes steeper than 10H:1V.
- A barrier should be placed as far as possible from the traveled way as practical without hindering its proper operation and performance. Barrier offset distances (Shy-Line) range from 1.22 m (4 ft) for a 50-km/h (30-mph) design speed to 3.66 m (12 ft) for a 130-km/h (80-mph) design speed.

#### 2.6 State DOT Survey Results

A state DOT survey was conducted to identify common barriers used on CSRS and to gather information pertaining to specific state standards, guidelines, and practices for the design, installation, and construction for such situations. The survey instrument was designed such that the questions were kept to a minimum but covered needed information and identified where the states had their own standards, guidance, or practices. It deemed more efficient to pursue the details of standards, guidance, or practices only with the states that had them. Thus, there were only eight questions included in

the survey. The questionnaire is included in Appendix A. The survey sought the following information:

- Types of longitudinal barriers currently used or likely to be used in the future on high-speed CSRS.
- The existence of specific criteria for which high-speed CSRS need barriers.
- Existence of specific criteria for the type of barrier to be used.
- Availability of data for crashes in such situations.
- Availability of in-service barrier performance assessments and safety concerns.
- References for the specific standards, guidance, and practices.

Of the 50 states surveyed, 33 responded for a 68% response rate. The responses received are summarized as follows:

**Question 1.** The participants were asked to provide information on the types of longitudinal barriers that are currently in place or are being installed on high-speed CSRS in their state. They were also asked to rank these barriers based on their usage (most to least commonly used). The survey form

Table 2.5. Longitudinal barriers usage on high-speed CSRS.

	Previously Installed Barriers				Curren	tly Being I	nstalled Bar	riers
	# of States Using Barrier <sup>a</sup>	Ranking Factor	Ranking Factor	Global Ranking	# of States Using Barrier <sup>a</sup>	Ranking Factor	Ranking Factor	Global Ranking
W-beam barrier (<31-in. height)	31	1.35	26	1	26	1.77	21	1
Concrete barrier (<32-in. height)	27	2.48	2	2	22	2.82	1	4
Concrete barrier (>32-in. height)	24	3.08	0	3	25	2.80	0	3
Cable barrier system	20	3.70	2	4	20	3.30	1	5
Thrie-beam barrier	15	4.2	1	5	15	4.13	0	6
W-beam barrier (>31-in. height)	9	4.33	0	6	11	2.45	5	2

<sup>&</sup>lt;sup>a</sup> Number of participating states (33 total) that indicated barrier used in high-speed CSRS.

Note: The darker shaded areas indicate the most commonly used longitudinal barrier on CSRS; the lighter shaded areas indicate the second most commonly used barrier.

focused on W-beam, Thrie-beam, and concrete barriers of various heights. The information received was grouped and ranked as shown in Table 2.5. The rankings obtained from the participating states were used to establish a global ranking for all states. A first ranking factor was computed by summing all rankings listed by the states for each barrier and dividing it by the total number of states that use that particular barrier. This factor is shown in the third column of Table 2.5 for "previously installed barriers" and the seventh column for "currently being installed barriers." The smaller this ranking factor, the higher the barrier usage. Another ranking factor used is the total number of states that ranked the barrier as 1 (most commonly used). This factor is shown in columns 4 and 8 for previously installed barriers and currently being installed barriers, respectively. Higher numbers for this factor indicate higher usage. Based on these two factors, a global ranking was determined (columns 5 and 9 in Table 2.5) to identify the most commonly used longitudinal barriers.

The W-beam guardrail, with a height less than 31 in., was ranked as the most commonly used longitudinal barrier on high-speed CSRS. This was the case for both previously installed and currently being installed barriers. All participants indicated that it is used in their state and 26 participants ranked it as the most commonly installed. For previously installed barriers, the concrete barrier with a height less than 32 in. ranked second. This barrier is used by 29 of the 33 participating states and was ranked first (most commonly used) by 2 states. For currently being installed barriers, the W-beam guardrail with a height of 31 in. or higher ranked second. Eleven of the 33 participating states indicated that they are currently installing this

barrier and 5 participants ranked it as the barrier most often currently being installed. Concrete barrier with a height greater than 32 in. was ranked third for both previously installed and currently being installed barriers. Concrete barrier with a height less than 32 in. was ranked fourth for currently being installed barriers. These results were consistent with expectations; however, because higher barriers would increase the likelihood of capturing unstable vehicles, it might have been expected that there would have been more use of higher variations of W-beam and concrete barriers on CSRS.

An unexpected response was in the usage of cable barrier systems on high-speed CSRS. Even though this system was not one of the barriers listed in Question 1, it was added by 20 of the 33 states as previously and currently being installed in their state. Two of the participants indicated that cable barrier was ranked first for previously installed barriers in their state for CSRS, one mentioned it is for roadside application only. One of the participants indicated that cable barrier is currently being installed in their state and is ranked first among the barriers. This response may accurately reflect that cable barriers are increasingly being used in median and roadside applications, which may include CSRS. The focus of this research has been on the outer, roadside applications of barriers. These responses suggest that future analysis should focus on the median barriers in such situations.

**Question 2.** The participants were asked to provide information on the type of barriers that are likely to be the standard applications in high-speed CSRS in future installations. The information from the states was analyzed and grouped as

<sup>&</sup>lt;sup>b</sup> Rating factor based on states' barrier rankings (sum of rankings divided by number of states using barrier).

<sup>&</sup>lt;sup>c</sup> Rating factor based on number of states that ranked barrier as 1 (most commonly used).

Table 2.6. Barriers for future installations.

Longitudinal Barrier Type	# of States That Plan to Use the Barrier in Future Installations
Concrete Barrier (All types)	25
Single slope	10
F-shape	7
• NJ	3
Double-faced	2
W-beam guardrail	15
Cable barrier	13
Strong-post W-beam guardrail	8
MGS	8
Thrie-beam	7
Box-beam	3

shown in Table 2.6. Concrete barriers were listed most often (by 25 of the 33 states). Participants also provided some additional details relative to the barriers' cross sectional shape with single slope and the F-shape concrete barriers being listed by 10 and 7 participants, respectively. The NJ and double-faced concrete barriers were listed by three and two participants, respectively. The W-beam guardrail was listed by 15 of the 33 states. The cable barrier system was mentioned by 13 of the 33 states. The strong-post W-beam and the MGS were each mentioned by 8 of the 33 states. The Thrie-beam barrier was mentioned by 7 states. Three states listed the Box-beam barrier. Detailed descriptions of these barriers and web links to technical drawings were included for most barriers listed by the respondents.

Question 3. The participants were asked if their state has special criteria to determine whether a barrier is warranted on a high-speed CSRS. Eleven states indicated "yes" and 22 indicated "no," suggesting that special criteria may only exist in a third of the states. Five states mentioned that they use the *Roadside Design Guide* for curve adjustment and for clear zone. Three other states indicated that they use their own state road design manual. Four states indicated that they are investigating increasing the clear zone and considering other alternatives based on the specific case. Three states mentioned that they evaluate each site separately and make an engineering judgment on appropriate treatment. One state noted it is considering using 42-in.-high concrete barriers in some applications and Thrie-beam guardrails in others.

**Question 4**. The participants were asked if their state has special criteria for selecting the barrier type and test level for longitudinal barriers to be installed on a high-speed CSRS. Seven participants said "yes" and 26 answered "no." The criteria listed by the seven participants included the following:

- Use NCHRP Report 350 or MASH (2 states),
- Use higher test level than the usual TL-3-based crash history (3 states),

- Use 42-in.-high concrete barrier (1 state), and
- Use own state location and design manuals (4 states).

While the use of prevailing crashworthiness requirements would seem to be the norm, the last three responses suggest that there are considerations for treating high-speed CSRS differently.

**Question 5**. The participants were asked if their state has available data related to crashes involving longitudinal barriers installed on high-speed CSRS. Thirteen states answered "yes" and 20 answered "no." Seven states—Arkansas, Delaware, Iowa, Kansas, Ohio, Oklahoma, and Pennsylvania—indicated that they should be able to pull crash data with some limited parameters from crash reports. North Carolina indicated that it could provide a crash dataset for sections of high-speed roadways with the distinction of curved versus straight roadways (without details of curvature specifications). Montana and New Jersey indicated that their database may contain some of the crash data on superelevated and curved roadways with guardrails, but the superelevations are not reported. Indiana has 825 collisions with guardrail face/end on Interstate highways in 2011, but each crash would then have to be investigated to see if it was on a high-speed curve. Washington State has a State Travel and Collision Data Office (STCDO) that handles crash data.

**Question 6**. The participants were asked if their state is aware of in-service evaluations or accident investigations related to longitudinal barriers installed on high-speed CSRS. Two participants answered "yes" to this question. Illinois mentioned that the crash investigations are confidential, but may be shared if requested for research. North Carolina indicated that many longitudinal barrier analyses have been completed, with before and after crash data evaluations where they installed barriers as a Spot Safety or Hazard Elimination project for roads that have curves. To date, they have evaluated 26 guardrail projects at bridges and 31 guardrail projects for shoulder applications. Alaska mentioned that crash investigations are not widespread, and only site-specific evaluation of installed rail is conducted. The responses indicate that detailed in-service evaluations or case studies for crashes on these types of road sections are not generally available.

**Question 7.** The participants were asked if there are locations in their state where longitudinal barriers placed on a high-speed CSRS did not function as desired. Seven participants answered "yes," 22 said "no," and 4 had no answer. One state had a case where an impacting car encroached into opposite travel lanes through a cable barrier installed in a median on a curve. Another state indicated that a W-beam median guardrail was replaced by a single slope 45-in. concrete

barrier in the median of a CSRS because of repetitive hits on the guardrail. One state had a segment of roadway that was the subject of an improvement project to permit the guardrail removal because motorists rebounded from the guardrail into the traveled way of an opposing lane, or else impacted the guardrail on the opposite shoulder. Another state is replacing a 32-in.-high concrete barrier rail with a 46-in.-high concrete barrier rail on a section of curved roadway in a mountainous location to reduce the likelihood of large trucks penetrating the barrier. Another state reported trucks that either dumped their loads on a curved overpass or tipped over the concrete parapet. One state indicated it had situations where vehicles penetrated through TL-3 cable barriers.

**Question 8.** The participants were asked to list any available additional information related to the performance of longitudinal barriers placed on high-speed CSRS. A few states listed their own state guides (posted on their websites). Two states listed the *Roadside Design Guide* and the *Green Book*.

## 2.7 Summary

A detailed literature review was conducted to gather information and synthesize relevant past efforts. The focus was on studies related to the design, performance, maintenance, and application details of longitudinal barrier systems when placed on CSRS. TRID was used to identify domestic and international reference materials. The literature did not provide much insight about concerns related to the safety performance of barriers placed on curves, much less on CSRS; however, the following insights were gained:

- The nature of impacts on curved sections is not well known. Theoretically, without driver inputs, impacts would occur at shallower angles. The influences of gravitational forces on the impact angle on sloped surfaces have not been analyzed in depth.
- There has been very limited testing of barriers on curved sections. The most significant studies undertaken for the FHWA occurred in 1986 and 1993. These efforts included analyses and tests related to curbs, superelevation, and bridge rails by Bronstad and Kimball (1986) and Stout et al. (1993). Later studies focused on barrier interface issues associated with slopes (Sheikh and Bligh 2006; Sheikh et al. 2008).
- There have been successful efforts using simulation to understand the trajectories of vehicles on sloped surfaces.
   Recent applications of VDA software included efforts to determine effective placement of cable barriers on median slopes (Marzougui et al. 2012a). VDA tools had been applied

- earlier for vehicle performance studies and accident reconstruction.
- Design guidance provided in the *Green Book* focuses on selecting curvatures and superelevation that will allow a vehicle to be driven around a curve at high speeds in comfort and the assurance that under wet conditions vehicles traveling at posted speeds would not be likely to lose control.
- Guidance for the placement of longitudinal barriers is available in the *Roadside Design Guide* for the instances when control is lost, but there is little specific guidance offered for barriers on CSRS.

The literature found and reviewed did not provide much insight about concerns related to the performance of barriers placed on CSRS.

A state DOT survey was conducted to identify common barriers used on CSRS and to gather information pertaining to specific state standards, guidelines, and practices for the design, installation, and construction for such situations.

Representatives from 33 state DOTs responded to the survey (a response rate of 67%). The responses provided useful information relative to current state DOT standards and practices as follows:

- A variety of longitudinal barriers are used for CSRS situations by the states.
- State DOTs do not have specific criteria for longitudinal barriers on CSRS. They tend to accept the *NCHRP Report 350* or MASH crashworthiness requirements as sufficient.
- No state reported knowledge of issues related to crashes on CSRS from in-service performance reviews or other studies.
- State DOTs noted that they plan to use the same types of barriers for future CSRS barrier deployments.
- The longitudinal barriers used varied by type and were about equally split between concrete safety shapes and W- or Thrie-beam designs.
- Some states specify a higher barrier for CSRS deployments where there is evidence of a crash problem.
- Concrete barriers 42 in. high are sometimes specified.

These findings suggest that most state DOTs have not perceived the need for special barrier requirements for CSRS. This might be attributed to the fact that superelevation is more commonly used on high-speed roads that generally have better safety performance. The state DOT survey revealed that most states do not currently have special design, selection, or installation guidance for the installation of longitudinal barriers on CSRS.

# CHAPTER 3

# Crash Data Analysis

Crash data analysis is useful in understanding the frequency and severity of crash events and, when the data is adequate, often allows situational, behavioral, and impact influences to be discerned. This research was initiated on the premise that there is a potential safety problem associated with typical longitudinal barriers when they are installed on curved road sections. The safety problem is believed to be exaggerated when traffic moves at high speeds on roadway sections that are superelevated, which allows drivers to easily negotiate the curves at high speeds. While anecdotal information suggests there is a problem, its magnitude and extent are not clear. This effort began with investigations of several available crash data sources to determine the extent and magnitude of the problem and to gain insights on barrier performance so that effective standards and guidance could be generated. The sources of crash data included the following:

- National Automotive Sampling System/Crashworthiness Data System (NASS/CDS)
- National Automotive Sampling System/General Estimate System (NASS/GES)
- Fatality Analysis Reporting System (FARS)

These are all publicly available datasets maintained by the National Highway Traffic Safety Administration (NHTSA). The NASS/CDS dataset is the most detailed, but has the fewest cases. Its basic data has been supplemented by road features data in many cases through independent research. The NASS/GES is the least detailed or comprehensive, but it reflects the full range of crashes nationwide and as such allows global metrics of specific safety issues to be derived. The FARS dataset provides more detail than GES, but it is only focused on fatal crashes, and its coverage of crash features lacks the detail to directly isolate crashes into longitudinal barriers on high-speed CSRS.

Other data sources exist that could provide useful information, but they fall short of the needs of this research. For

example, if an agency were to have a good highway features inventory, then it would be possible to identify all the locations where CSRS exist. However, specific data on road curvature and the specific starting and ending points of the curves are rare. It is even rarer that features such as superelevation are available in a database. If these locations could be referenced, it might not be possible to accurately determine all the crashes that occurred in proximity of the feature. The process of determining crash locations is not based on GPS coordinates in many places, and often the location data is inexact or inaccurate. Thus, it is not likely that a sound estimate of a crash problem associated with longitudinal barriers on high-speed CSRS can be defined.

Analysis of crash data was undertaken to understand the conditions that influence crash potential and barrier performance. The parameters examined included road curvature, vehicle type, number of road lanes, vertical elevation (i.e., road profile), lighting condition, surface condition, weather condition, and speed limit. Cases where the longitudinal barrier was installed on a curved section were compared with cases where the barrier was installed on a straight section. A summary of the analyses using these three datasets is presented.

# 3.1 NASS/CDS Data Analyses

The NASS/CDS database was used to identify critical factors related to longitudinal barrier performance when installed on CSRS. Datasets from 1988 through 2009 were included in the analysis. The data included a total of 186,465 cases during these 22 years. The datasets were weighted to be representative of the total number of crashes. Both weighted and unweighted data are presented here for comparison. A summary of the results from the analysis is presented below.

The first step in the analysis was to reduce the dataset to the cases involving a longitudinal barrier as a first harmful event. A total of 4,489 vehicles were found to have the first harmful event as collision with a traffic barrier. These cases included

Table 3.1. First harmful event by barrier type (unweighted and weighted).

First Harmful Event	Unweighted		Weighted	
Plist Haililli Event	Number	Percent	Number	Percent
Concrete traffic barrier	2,066	46.02%	726,502	40.70%
Other traffic barrier (includes guardrail)	1,773	39.50%	833,809	46.71%
Bridge rail	650	14.48%	224,743	12.59%
Total longitudinal barrier	4,489	100.00%	1,785,054	100.00%

both curved and straight roads. The variable "OBJCONT1" in the dataset was used to distinguish between "Concrete traffic barrier" (OBJCONT1 = 54), "Other traffic barrier including guardrails" (OBJCONT1 = 56), and "Bridge" (OBJCONT1 = 64). Table 3.1 shows the unweighted and weighted numbers of cases.

Next, the cases were grouped by injury level—[Abbreviated Injury Scale (AIS)]—as shown in Table 3.2. Out of 4,110 cases involving longitudinal barriers (note that 379 cases have missing or unknown injury information), 993 (24%) resulted in serious injuries (AIS  $\geq$  3), 671 (16%) resulted in moderate injury (AIS = 2), 1,684 (41%) resulted in minor injury (AIS = 1), and 762 (19%) had no injury (AIS = 0). When using the weighting factor, the distribution showed 46% no injury, 44% minor injury, 6% moderate injury, and 4% serious injury. It should be noted that NASS/CDS data is biased toward more serious crashes.

The data was then sorted based on curvature alignment (i.e., left or right curvature or straight). Table 3.3 data indicates that 27% of the vehicle crashes with barriers occurred on curved roads while the rest were on straight roads. For the weighted data, the portion of accidents that occurred on curved roads is one-third, while two-thirds occurred on straight roads. The number of cases for right and left curved roads is similar.

The data for impacts with barriers was then used to compare curved versus straight road cases. Table 3.4 and Table 3.5 show the distribution of the vehicle class and the injury classification for curved and straight roads, respectively. The data indicates that 26% of the cases resulted in serious injuries for the curved roads compared with 23%

Table 3.2. Unweighted and weighted cases by AIS.

Classified Abbreviated	Unwe	ighted	Weighted			
Injury Scale	Number	Percent	Number	Percent		
AIS 2-	3,117	75.84%	1,586,921	96.39%		
AIS 3+	993	24.16%	59,396	3.61%		
Total 4,110 100.00% 1,646,317 100.00%						
Missing and Unknown Cases $(109 + 270) = 379$						

Note: AIS has six levels: 1: minor; 2: moderate; 3: serious; 4: severe; 5: critical; and 6: maximal. AIS 2– designates AIS 2 or less injury severity; AIS 3+ designates AIS 3 or higher injury severity.

for the straight roads for unweighted data. When the data is weighted, 3.7% resulted in serious injuries for curved roads, while the straight roads have 3.5% of the serious injuries. The data shows that the percentage of serious crashes on curved roads is similar to that of straight roads. It can be noted as well that the percentage of accidents by vehicle type is similar for curved and straight roads.

Additional parameters examined in the NASS/CDS data included number of road lanes, vertical elevation, surface condition, lighting condition, weather condition, and speed limit. The data based on these parameters is listed in Table 3.6 through Table 3.11, respectively. The tables show the cases involving longitudinal barriers as the first harmful event for curved and straight roads on the left and only curved road cases on the right side for comparison. The following can be noted from the tables:

- Crashes into longitudinal barriers on curved sections are more likely to occur on roads with fewer lanes (narrower roads). Table 3.6 shows that for one- and two-lane roads, the percentage of crashes on curved roads is higher than that of the combined (curved and straight) cases. The reverse is observed for roads with a higher number of lanes (wider roads).
- Crashes into longitudinal barriers on curved roads are more likely to occur on uphill and downhill grades than on flat surfaces. For uphill and downhill roads, Table 3.7 shows that the percentage of crashes on curved roads is higher than that of the combined (curved and straight) road crashes.

Table 3.3. Unweighted and weighted cases by road alignment.

Dood Alianment	Unwe	ighted	Weighted		
Road Alignment	Number	Percent	Number	Percent	
Curved Road	1,201	26.75%	576,478	32.29%	
Curved Road Right	601	13.39%	296,064	16.59%	
Curved Road Left	600	13.37%	280,414	15.71%	
Straight Road	3,288	73.25%	1,208,575	67.71%	
Total	4,489	100.00%	1,785,053	100.00%	

Table 3.4. Unweighted and weighted cases by vehicle and AIS for curved roads.

	Curved Roads						
	AIS 2-	AIS 3+	Total	AIS 2-	AIS 3+	Total	
Vehicle		Unweighted			Weighted		
Class	Number	Number	Total Number	Number	Number	Total Number	
Passenger Cars	562	199	761 (68.99%)	381,705	15,876	397,581 (74.56%)	
Pickups	97	38	135 (12.24%)	52,661	1,774	54,436 (10.21%)	
Utility Vehicles	117	40	157 (14.23%)	58,359	1,798	60,156 (11.28%)	
Vans	37	13	50 (4.52%)	20,692	379	21,072 (3.95%)	
Total	813 (73.71%)	290 (26.29%)	1,103	513,417 (96.28%)	19,828 (3.72%)	533,245	
Unknown A	Unknown AIS and other vehicles cases = 399 unweighted for curved and straight roadways.						

Note: AIS has six levels: 1: minor; 2: moderate; 3: serious; 4: severe; 5: critical; and 6: maximal. AIS 2– designates AIS 2 or less injury severity; AIS 3+ designates AIS 3 or higher injury severity.

Table 3.5. Unweighted and weighted cases by vehicle and AIS for straight roads.

			Straigh	t Roads			
	AIS 2-	AIS 3+	Total	AIS 2-	AIS 3+	Total	
Vehicle		Unweighted			Weighted		
Class	Number	Number	Total Number	Number	Number	Total Number	
Passenger Cars	1,682	499	2,181 (73.02%)	776,569	29,147	805,716 (72.62%)	
Pickups	277	81	358 (11.99%)	156,789	4,732	161,521 (14.56%)	
Utility Vehicles	237	73	310 (10.38%)	98,547	3,425	101,972 (9.19%)	
Vans	93	45	138 (4.62%)	38,166	2,112	40,278 (3.63%)	
Total	2,289 (76.63%)	698 (23.37%)	2,987	1,070,072 (96.45)	39,416 (3.5%)	1,109,487	
Unknown A	IS and other	vehicles cas	es = 399  unw	eighted for cu	arved and str	aight roadways.	

Note: AIS has six levels: 1: minor; 2: moderate; 3: serious; 4: severe; 5: critical; and 6: maximal. AIS 2– designates AIS 2 or less injury severity; AIS 3+ designates AIS 3 or higher injury severity.

Table 3.6. Vehicle cases by number of lanes.

	All barrier im	pacts	Barrier on curved road impacts		
LANES	Frequency	Percent	Frequency	Percent	
One	175	5.62	140	11.66	
Two	1094	35.11	523	43.55	
Three	871	27.95	304	25.31	
Four	598	19.19	164	13.66	
Five	282	9.05	46	3.83	
six	75	2.41	21	1.75	
Seven o	r more 21	0.67	3	0.25	

Frequency Missing = 1373

Table 3.7. Vehicle cases by vertical elevation.

	All barrier impa	Barrier on curved road impacts		
PROFILE	Frequency	Percent	Frequency	Percent
Level	2077	66.98	642	53.86
Uphill gr		15.35	253	21.22
Hillcrest	33	1.06	4	0.34
Downhill .	grade 510	16.45	292	24.50
Sag	5	0.16	1	0.08

Table 3.8. Vehicle cases by road surface condition.

A	ll barrier impa	Barrier on curved road impacts		
SURCOND	Frequency	Percent	Frequency	Percent
Dry	2142	68.79	765	63.75
Wet	662	21.26	290	24.17
Snow or slush	103	3.31	41	3.42
Ice	175	5.62	86	7.17
Sand, dirt or	011 18	0.58	11	0.92
Other	1	0.03	1.	0.08
Unknown	13	0.42	6	0.50

Frequency Missing = 1375

Table 3.9. Vehicle cases by lighting condition.

All barrier impacts			Barrier on curved road impact	
LGTCOND Free	luency	Percent	Frequency	Percent
Daylight Dark Dark, but lighted Dawn Dusk	1456 532 988 85 49	46.82 17.11 31.77 2.73 1.58	533 237 376 34 17	44.53 19.80 31.41 2.84 1.42

Frequency Missing = 1379

Table 3.10. Vehicle cases by weather condition.

All barrier impacts			Barrier on curved road impacts		
WEATHER	Frequency	Percent	Frequency	Percent	
No adverse	2008	79.06	762	77.13	
Rain	378	14.88	155	15.69	
Sleet/hail	19	0.75	8	0.81	
Snow	112	4.41	49	4.96	
Fog	11	0.43	6	0.61	
Rain and for	6	0.24	4	0.40	
Sleet and fo	og 6	0.24	4	0.40	

Frequency Missing = 1949

All barrier impacts Barrier on curved road impacts SPLIMIT Frequency SPLIMIT Frequency Percent Percent 0.16 0.08 0.04 0.25 0.04 32 0.25 16 20 24 40 49 0.09 48 4.61 25 30 10.82 30 32 35 40 69 0.13 72 118 9.90 1.55 80 6.29 130 89 337 45 2.31 146 12.25 97 48 3.45 8.72 105 1.48 13.38 6.09 2.73 50 66 55 597 272 64 122 31 6.21 80 168 81 0.02 89 1139 25.52 10.02 105 113 7.37

Table 3.11. Vehicle cases by posted speed limit (km/h).

- Crashes into longitudinal barriers on curved roads are more likely to occur on wet, snowy, and icy roads than on dry roads. In Table 3.8, the percentages of crashes on wet, snowy, and icy roads are higher on curved roads than that of the combined (curved and straight) roads.
- Other parameters (lighting condition, weather condition, and posted speed) did not show significant effects on the crash distribution when comparing cases on curved roads with those on the combined (curved and straight) roads.

Further analyses of this data for barriers on straight versus curved sections may be useful to isolate the differences.

## 3.2 NASS/GES Data Analyses

Similar analysis was conducted using the NASS/GES database. Datasets from 1988 through 2009 were included in the analysis. The data included a total of 2,065,308 vehicle cases over these 22 years. The datasets were weighted to be representative of the total number of crashes. Both weighted and unweighted data are presented here for comparison. A summary of the results from the analysis is presented below.

The first step in the analysis was to reduce the dataset to the cases involving a longitudinal barrier as a first harmful event. A total of 38,380 vehicles were found to have the first harmful event as a collision with a traffic barrier. These cases included both curved and straight roads. The variable "V\_EVENT" in the dataset was used to distinguish between "Bridge structure" (V\_EVENT = 34), "Guardrail"

(V\_EVENT = 35), and "Concrete traffic barrier or other longitudinal barrier" (V\_EVENT = 36). Table 3.12 shows the unweighted and weighted number of cases.

Next, the cases were divided into two injury groups using the maximum severity in the vehicle (MAX\_VSEV) as shown in Table 3.13. The first group has no injury (O) (MAX\_VSEV = 0), possible injury (C) (MAX\_VSEV = 1), and non-incapacitating evident injury (B) (MAX\_VSEV = 2). The second group has incapacitating injury (A) (MAX\_VSEV = 3) and fatal injury (K) (MAX\_VSEV = 4).

Out of 38,380 cases involving longitudinal barriers, 5,581 (14.54%) resulted in incapacitating (A) and fatal injuries (K); 6,112 (15.92%) resulted in non-incapacitating evident injury (B); 5,854 (15.25%) resulted in possible injury (C); and 19,759 (51.48%) had no injury (O). When using the weighting factor, the distribution showed 163,418 (4.75%) resulted in incapacitating (A) and fatal injuries (K); 377,664 (10.98%) resulted in non-incapacitating evident injury (B); 497,291 (14.46%) resulted in possible injury (C); and 2,286,580 (66.55%) had no injury (O).

Table 3.12. First harmful event by barrier type (unweighted and weighted).

First Harmful Evert	Unwe	ighted	Weighted		
First Harmiul Even	Number	Percent	Number	Percent	
Bridge structure	3,801	9.9%	340,126	9.89%	
Guardrail	19,771	51.51%	1,996,229	58.06%	
Concrete traffic barrier	14,808	38.58%	1,101,994	32.05%	
Total Longitudinal Barrier	38,380	100.00%	3,438,349	100.00%	

Table 3.13. Unweighted and weighted cases by AIS.

Classified Abbreviated	Unwe	ighted	Weighted		
Injury Scale	Number	Percent	Number	Percent	
Non-incapacitating	31,725	82.66%	3,161,536	91.95%	
Incapacitating + K	5,581	14.54%	163,418	4.75%	
Missing and Unknown Cases	1,074	2.80%	113,395	3.3%	
Total	38,380	100.00%	3,438,349	100.00%	

The data was then sorted based on curvature alignment. Table 3.14 indicates that 25.4% of the vehicle crashes occurred on curved roads while the rest occurred on straight roads. For the weighted data, the percentage of accidents occurring on curved roads is 26.71%. Approximately one-quarter of the crashes occurred on curved roads, while approximately three-quarters occurred on straight roads.

The data was then used to compare curved versus straight road cases. Table 3.15 and Table 3.16 show the distribution of the vehicle class and the injury classification for curved and straight roads, respectively. The data indicates that 15.74% of the cases resulted in serious injuries for the curved roads compared with 14.75% for the straight roads for the unweighted data. The data shows that the percentage of cases with serious injuries on curved roads is similar to that on straight roads. The percentage of accidents by vehicle type was found to be similar for curved and straight roads.

Additional parameters examined included number of road lanes, vertical elevation, surface condition, lighting condition, weather condition, and speed limit. The data based on these parameters is listed in Table 3.17 through Table 3.22.

Table 3.14. Unweighted and weighted cases by road alignment.

Road Alignment	Unwe	ighted	Weighted		
Road Alignment	Number	Percent	Number	Percent	
Curved Road	9,750	25.40%	918,393	26.71%	
Straight Road	28,630	74.60%	2,519,956	73.29%	
Total	38,380	100.00%	3,438,349	100.00%	

The tables show the cases involving longitudinal barriers as the first harmful event for curved and straight roads on the left and curved road cases on the right side for comparison. The following can be noted from the tables:

- Crashes into longitudinal barriers on curved sections are more likely to occur on roads with fewer lanes (narrower roads). Table 3.17 shows that for one- and two-lane roads, the percentage of crashes on curved roads is higher than that for the combined (curved and straight) road cases. The reverse is observed for roads with a higher number of lanes (wider roads).
- Crashes into longitudinal barriers on curved roads are more likely to occur on grades than on flat surfaces. For roads with grades, Table 3.18 shows that the percentage of crashes on curved roads is higher than that of the combined (curved and straight) road crashes.
- Crashes into longitudinal barriers on curved roads are more likely to occur on wet, snowy, and icy roads than on dry roads. In Table 3.19, the percentages of crashes on wet, snowy, and icy roads are higher on curved roads than on the combined (curved and straight) roads.

Table 3.15. Unweighted and weighted cases by vehicle and AIS for curved roads.

			Curve	d Roads		
Vehicle	Nonincapacitating	Incapacitating + K	Total	Nonincapacitating	Incapacitating + K	Total
Class		Unweighted			Weighted	
	Number	Number	Total Number	Number	Number	Total Number
Passenger Cars	5,114	826	5,940 (63.83%)	585,109	28,254	613,363 (70.04%)
Pickups + Vans	1,033	168	1,201 (12.90%)	123,510	6,110	129,620 (14.8%)
Utility Vehicles	644	158	802 (8.62%)	74,588	3,621	78,209 (8.93%)
Buses	82	11	93 (1.00%)	9,763	1,125	10,888 (1.24%)
Trucks	749	66	815 (8.75%)	24,196	1,243	25,439 (2.9%)
Motorcycles	220	235	455 (4.90%)	10,520	7,655	18,175 (2.07%)
Total	7,842 (84.26%)	1,464 (15.74%)	9,306	827,686 (94.52%)	48,008 (5.48%)	875,694
	Other vehicle typ	e, missing, and	9	uries = 444 unweight oadways.	ed and 42,699 we	eighted for

Table 3.16. Unweighted and weighted cases by vehicle and AIS for straight roads.

			Straigh	nt Roads			
	Nonincapacitating	Incapacitating + K	Total	Nonincapacitating	Incapacitating + K	Total	
Vehicle Class		Unweighted		Weighted			
	Number	Number	Total Number	Number	Number	Total Number	
Passenger Cars	14,917	2,600	17,517 (63.66%)	1,564,498	74,033	1,638,531 (68.01%)	
Pickups + Vans	3,267	510	3,777 (13.73%)	367,179	16,891	384,070 (15.94%)	
Utility Vehicles	2,529	603	3,132 (11.38%)	268,516	12,482	280,998 (11.66%)	
Single Unit Truck	42	0	42 (0.15%)	1,091	0	1,091 (0.05%)	
Trucks	2,359	168	2,527 (9.18%)	61,236	2,391	63,627 (2.64%)	
Buses	201	21	222 (0.81%)	25,934	1,887	27,821 (1.16%)	
Motorcycles	143	156	299 (1.09%)	8,000	4,970	12970 (0.54%)	
Total	23,458 (85.25%)	4,058 (14.75%)	27,516	2,296,454 ( 95.32%)	112,654 (4.6%)	2,409,108	
Mi	issing and unknown	injuries =1,114 u	nweighted and	110,848 weighted for	or curved roadway	rs.	

Table 3.17. Vehicle cases by number of lanes.

All barrier impacts			Barrier on curved road impac		
LANES	Frequency	Percent	Frequency	Percent	
One	1701	4.43	1109	11.37	
Two	15890	41.40	4869	49.94	
Three	8212	21.40	1274	13.07	
Four	5507	14.35	690	7.08	
Five	1973	5.14	157	1.61	
six	488	1.27	38	0.39	
Seven or	more 113	0.29	8	0.08	
Unknown	4496	11.71	1605	16.46	

Table 3.18. Vehicle cases by vertical elevation.

	All barrier impa	icts	Barrier on curve	ed road impact
PROF ILE	Frequency	Percent	Frequency	Percent
Level Grade Hill crest Sag Unknown	17608 9649 750 149 10224	45.88 25.14 1.95 0.39 26.64	3244 4423 260 65 1758	33.27 45.36 2.67 0.67 18.03

Table 3.19. Vehicle cases by road surface condition.

All barrier impacts			Barrier on curved road impact		
SUR_COND	Frequency	Percent	Frequency	Percent	
Dry	22095	57.57	5085	52.15	
Wet	10010	26.08	3132	32.12	
Snow or Slush	1948	5.08	432	4.43	
Ice/Frost	3904	10.17	965	9.90	
Sand Dirt Mud	Gravel 61	0.16	31	0.32	
Other	122	0.32	47	0.48	
Unknown	240	0.63	58	0.59	

Table 3.20. Vehicle cases by lighting condition.

	All barrier impa	cts	Barrier on curve	ed road impacts
Light_Condition	Frequency	Percent	Frequency	Percent
Daylight	20165	52.54	4990	51.18
Dark	8073	21.03	2161	22.16
Dark but Lighted	8178	21.31	2069	21.22
Dawn	940	2.45	245	2.51
Dusk	688	1.79	207	2.12
Dark - Unknown I	ighting 39	0.10	8	0.08
Unknown	297	0.77	70	0.72

Table 3.21. Vehicle cases by weather condition.

	All barrier impacts			Barrier on curved road impact		
WEATHER	Frequency	Percent	Frequency	Percent		
No Adverse Atmospheric Cor	ndition: 26031	67.82	6431	65.96		
Rain	7676	20.00	2226	22.83		
	539	1.40	129	1.32		
Sleet	3131	8.16	675	6.92		
Snow	251	0.65	94	0.98		
Fog	33	0.09	12	0.12		
Rain and Fog	23	0.06	3	0.03		
Sleet and Fog	307	0.80	.77	0.79		
Other: Smoke, Blowing Sand	Snow 389	1.01	103	1.06		

Table 3.22. Vehicle cases by posted speed limit (km/h).

ved road in	Barrier on curved	All barrier impacts		
y Per	Frequency	Percent	Frequency	Speed_Limit
	5	0.05	18	0
		0.01	4	5
	4	0.02	6	10
F 9	44	0.18	69	15
	55	0.25	97	20
1	449	2.38	914	25
3	358	2.06	792	30
3	798	4.91	1884	35
3	339	2.56	982	40
3	688	5.73	2198	45
)	300	2.77	1064	50
5 2	2686	28.76	11040	55
	634	9.46	3632	60
3	828	16.37	6282	65
9	289	6.65	2553	70
3	18	0.55	210	75
2	2255	17.29	6635	99

• Other parameters (lighting condition, weather condition, and posted speed) did not show significant effects on the crash distribution when comparing cases on curved roads to the combined (curved and straight) road cases.

#### 3.3 FARS Data Analysis

Datasets from the FARS for the years 1982 through 2010 were used in the analysis. These datasets include only cases where one or more fatalities occurred. Years prior to 1982

were not included in the analyses because the variables in these datasets were less descriptive. The 29-year dataset considered in the analysis included a total of 905,289 cases with at least one fatality.

First, the data was truncated to include only the cases where a longitudinal barrier was the first harmful event. A total of 41,634 (4.60%) cases involved a longitudinal barrier as the first harmful event. A variable "HARM\_EV" in the dataset was used to distinguish between "Bridge rail" (HARM\_EV = 23), "Guardrail face" (HARM\_EV = 24), and "Concrete barrier"

Table 3.23. Vehicle crashes by road curvature and barrier type.

Road Alignment	Curved Roads		Straight Roads		Straight and Curved Roads	
C	Number	Percent	Number	Percent	Number	Percent
Bridge Rail	1,508	3.62%	3,354	8.06%	4,862	11.68%
Guardrail and Cable Barrier	13,008	31.24%	17,173	41.25%	30,181	72.49%
Concrete Barrier	2,222	5.34%	4,369	10.49%	6,591	15.83%
Total	16,738	40.02%	24,896	59.79%	41,634	100%

(HARM\_EV = 25). One additional variable, "Cable barrier" (HARM\_EV = 57), was introduced after the year 2008, which was included in the "Guardrail face" (HARM\_EV = 24) category in prior years. Cases with this variable (HARM\_EV = 57) were added to the "Guardrail face" cases to be consistent with prior years. The data was sorted based on roadway alignment and listed in Table 3.23. There were 30,181 (72.49%) fatal crashes involving guardrail barriers, 6,591 (15.8%) involving concrete barriers, and 4,862 (11.7%) involving bridge rails. A total of 16,738 (40.2%) fatal crashes involving longitudinal barriers were on curved roads and the remaining 24,896 (59.8%) cases occurred on straight roads. Although crashes on curved roads account for only one-quarter of the total number crashes (based on the NASS/GES dataset), crashes on curved roads are more severe than crashes on straight roads.

Table 3.24 and Table 3.25 show the distribution of fatal crashes based on the vehicle class and barrier type for curved and straight roads, respectively. Fatal crashes on curved roads are about half (50%) the number of fatal crashes on straight roads for passenger cars, pickups and vans, and

utility vehicles. This figure of occurrence increases to 63% and 76% for Single Unit Trucks (SUT) and large and heavy trucks, respectively, when comparing fatal crashes on curved roads with those on straight roads. About 69% of fatal crashes involving longitudinal barriers on straight roads occur with guardrails, while the remaining crashes occur with bridge rails or concrete barriers. For curved roads, 77% of fatal crashes occur with guardrails and the remaining crashes occur with bridge rails or concrete barriers.

The motorcycle data shows that the fatality numbers on curved roads are twice as high as those on straight roads. This observation is true for bridge rails and guardrails while the concrete barriers have similar values on curved and straight roads.

Additional parameters examined included number of road lanes, vertical elevation, surface condition, lighting condition, weather condition, and speed limit. The data based on these parameters is listed in Table 3.26 through Table 3.31, respectively. The tables show the cases involving longitudinal barriers as the first harmful event for curved and straight

Table 3.24. Vehicle crashes by vehicle and barrier type for curved roads.

Frequency Percent	Bridge rail	Guard- rail	Concrete barrier	Cable barrier	Total
Buses	0.00	0.05	0.01	0.00	0.06
Motorcycles	195 1.17	2827 16.89	531 3.17	0.02	3557 21.25
Other	0.11	93 0.56	0.07	0.00	123 0.73
Passenger Cars	765 4.57	6057 36.19	1029 6.15	0.02	7855 46.93
Pick-Ups-Vans	325 1.94	2093 12.50	255 1.52	0.02	2677 15.99
SingleUnitTruc	15 0.09	110 0.66	18 0.11	0.00	143 0.85
Trucks	92 0.55	808 4.83	128 0.76	0.00	1028 6.14
Utility Vehicl	97 0.58	998 5.96	248 1.48	0.01	1345 8.04
Total	1508 9.01	12994 77.63	2222 13.28	0.08	16738 100.00

Table 3.25. Vehicle crashes by vehicle and barrier type for straight roads.

Frequency Percent	Bridge rail	Guard- rail	Concrete barrier	Cable barrier	Total
Buses	0.01	0.08	0.00	0.00	0.09
Motorcycles	105 0.42	1105 4.44	445 1.79	0.02	1661 6.67
Other	34 0.14	100 0.40	21 0.08	0.00	155 0.62
Passenger Cars	1800 7.23	9545 38.34	2528 10.15	0.09	13896 55.82
Pick-Ups-Vans	914 3.67	3482 13.99	642 2.58	0.02	5042 20.25
SingleUnitTruc	26 0.10	160 0.64	39 0.16	0.00	226 0.91
Trucks	197 0.79	996 4.00	147 0.59	0.00	1340 5.38
Utility Vehicl	276 1.11	1726 6.93	546 2.19	0.02	2553 10.25
Total	3354 13.47	17134 68.82	4369 17.55	39 0.16	24896 100.00

Table 3.26. Vehicle cases by number of lanes.

	All barrier in	ipacts	Barrier on curved road impac				
LANES	Frequency	Percent	Frequency	Percent			
one	825	1.98	601	3.59			
Two	28220	67.81	12281	73.37			
Three	5641	13.55	1763	10.53			
Four	4821	11.58	1428	8.53			
Five	693	1.67	166	0.99			
six	612	1.47	179	1.07			
Seven or	more 203	0.49	43	0.26			
Unknown	602	1.45	277	1.65			

Table 3.27. Vehicle cases by vertical elevation.

	All barrier impa	Barrier on curved road impacts			
PROF ILE	Frequency	Percent	Frequency	Percent	
Level	26262	63.10	18442	74.13	
Grade	13738	33.01	5590	22.47	
Hill crest	727	1.75	346	1.39	
Sag	224	0.54	109	0.44	
Unknown	666	1.60	392	1.58	

Frequency Missing = 17

Table 3.28. Vehicle cases by road surface condition.

	All barrier imp	Barrier on curved road impacts				
SUR_COND	Frequency	Percent	Frequency	Percent		
Dry	33837	81.31	13695	81.82		
Wet	5871	14.11	2394	14.30		
Snow or Slush	597	1.43	211	1.26		
Ice/Frost	994	2.39	282	1.68		
Sand, Dirt, Mud. Gr		0.12	29	0.17		
Water (Standing or	Moying) 6	0.01		- 100 EU		
Other	55	0.13	26	0.16		
Unknown	205	0.49	101	0.60		

Table 3.29. Vehicle cases by lighting condition.

	All barrier impa	Barrier on curved road impacts				
LGT_COND	Frequency	Percent	Frequency	Percent		
Daylight	16286	39.13	6251	37.35		
Dark	15711	37.75	6452	38.55		
Dark but Lighted	7822	18.80	3322	19.85		
Dawn	912	2.19	326	1.95		
Dusk	672	1.61	295	1.76		
Dark - Unknown	Lighting 15	4	0.02			
Unknown	199	0.48	88	0.53		

Frequency Missing = 17

Table 3.30. Vehicle cases by weather condition.

	All barrier imp	Barrier on curved road impacts				
WEATHER	Frequency	Percent	Frequency	Percent		
1 - Clear/Cloud (No Adverse Con	ditions) 35886	86.23	14585	87.14		
2 - Rain (Mist)	3754	9.02	1425	8.51		
3 - Sleet (Hail)	217	0.52	59	0.35		
4 - Snow or Blowing Snow	767	1.84	259	1.55		
5 - Fog, Smog, Smoke	576	1.38	229	1.37		
6 - Severe Crosswinds	80	0.19	43	0.26		
7 - Blowing Sand, Soil, Dirt	9	0.02	1	0.01		
8 - Other	108	0.26	43	0.26		
9 - Unknown	220	0.53	94	0.56		

Frequency Missing = 17

roads on the left and curved road cases on the right side for comparison. The following can be noted from the tables:

- Fatal crashes into longitudinal barriers on curved sections are more likely to occur on roads with fewer lanes (narrower roads). Table 3.26 shows that for one- and two-lane roads, the percentage of crashes on curved roads is higher than that for the combined (curved and straight) road cases. The reverse is observed for roads with a higher number of lanes (wider roads).
- Fatal crashes into longitudinal barriers on curved roads are less likely to occur on grades than on flat surfaces. For roads with grades, Table 3.27 shows that the percentage of crashes on curved roads is lower than that of the combined

- (curved and straight) road crashes. This is opposite to what was found in the NASS/CDS and NASS/GES datasets.
- Other parameters (surface condition, lighting condition, weather condition, and posted speed limit) did not show significant effects on the crash distribution when comparing cases on curved roads with the combined (curved and straight) road cases.

# 3.4 NCHRP Project 17-22 Data Analysis

The dataset from NCHRP Project 17-22, "Identification of Vehicular Impact Conditions Associated with Serious Ran-Off-Road Crashes," was also used to investigate barrier

Table 3.31. Vehicle cases by posted speed limit (km/h).

l road impac	Barrier on curved	All barrier impacts					
Percent	Frequency	Percent	Frequency	SP_LIMIT			
0.20	33	0.15	61	0			
0.01	1	0.00	1	5			
0.02	4	0.02	8	10			
0.20	34	0.13	56	15			
0.41	69	0.23	97	20			
2.62	438	1.85	770	25			
3.63	607	2.76	1147	30			
7.77	1300	5.51	2295	35			
5.57	933	4.09	1702	40			
9.97	1668	7.88	3279	45			
6.43	1077	5.14	2141	50			
45.64	7640	46.34	19285	55			
2.54	425	3.05	1270	60			
9.76	1633	15.33	6380	65			
2.20	368	4.63	1928	70			
0.67	112	0.95	396	75			
	1,35	0.00	1	85			
0.01	2	0.00	2	90			
2.35	394	1.92	798	99			

performance when installed on curved road sections. This dataset supplements existing NASS/CDS data with additional information pertaining to the roadside such as side slope, roadway alignment, curvature, grade, profile, and roadside barrier characteristics (including post-crash measurements). The NCHRP 17-22 dataset was combined with the NASS/CDS data and the cases that involved impacts into longitudinal barriers on curved road sections were identified. Forty crashes were found where the vehicle impacted a longitudinal barrier on a curved road section. These cases were summarized and information containing a description of the crash, a crash diagram, crash scene, barrier, and vehicle pictures, and road characteristics were extracted.

Due to the small number of cases found in the database, no significant conclusions could be extracted from the analysis. The cases were analyzed and grouped into three main categories: (1) barrier redirected the vehicle successfully; (2) barrier (including end terminal) caused rollover; and (3) other special cases. Out of the 40 cases, 32 were included in group 1, where the barrier redirected the vehicle back to the roadway. In 10 of these cases, the driver and occupants had no injuries (only property damage). In 16 of the remaining cases, the crash had no fatalities, but had injuries and property damage. In most of these cases, the vehicle was redirected by the barrier, crossed the travel lane, and remained upright. The remaining six cases had one or more fatalities. In these cases, the vehicle was redirected after the first impact, but impacted another barrier or an obstacle on the opposite side.

The second category (other special cases) had seven cases where the barrier did not safely redirect the vehicle:

- In two of the seven cases, the vehicle hit a concrete barrier and rolled after impact. One case had low injury and the other was fatal (occupant was unbelted).
- In one case, the vehicle hit a W-beam bullnose and rolled
- In one case, the vehicle hit a turned-down end terminal, which caused the vehicle to vault and roll over.
- In one case, the vehicle broke through the end terminal and hit a tree. An AIS 3 injury was recorded.
- In one case, the vehicle impacted a Thrie-beam barrier and rolled over. An AIS 2 injury was recorded.
- In one case, the vehicle hit a W-beam barrier and rolled over. The occupant was unbelted and the crash was fatal.

The last category had only one case where the vehicle hit the back of a Thrie beam barrier. The vehicle vaulted the Thriebeam, continued into the opposite traffic lanes, impacted another Thrie-beam barrier, and came back into the traffic lanes. Two occupants died in the crash.

# 3.5 Data Analysis Summary

Various datasets were analyzed to isolate a specific safety problem. The findings are summarized by dataset as follows:

• NASS/CDS: This represented the most detailed set of data, albeit most of the data items focus on the impact and injury

severities. Data for 1988 through 2009 was analyzed for crashes into concrete barriers, other guardrail, and bridge rails. Of these, 46.7% hit an "other barrier" guardrail and 41% hit a concrete barrier. The analysis involved 4,489 U.S. barrier impact cases, which when weighted reflected 1,785,054 crashes. The weighted results indicated the following:

- Serious injuries (or worse) occurred in 4% of the crashes, moderate injuries in 6%, minor injuries in 44%, and no injuries in 46% of the crashes based on an AIS scale.
- Crashes involved passenger cars 74.6% of the time.
- Crashes occurred on curved roads 32.3% of the time.
- Other analyses isolated frequency of crashes by lighting conditions, road surface condition, number of lanes, and grade. It was noted that crashes into barriers were more likely to occur for narrow roads (two or fewer lanes), on wet or icy pavements, and on uphill or downhill grades.
- Because the data did not include measures of the radii, superelevation, or shoulder features for any of the crash locations, it was not possible to isolate any specific safety problems for barriers on CSRS.
- NASS/GES: This more general dataset provided less detail on crashes and included some different data items. The dataset included 2,065,308 vehicle cases over the same 22-year period:
  - The data for first harmful event includes 38,380 cases of collision with a traffic barrier. Of these, 58% hit a guardrail and 32% a concrete barrier. The differences in percentages can be attributed to variations in data definitions.
  - Incapacitating injuries or fatalities occurred in 4.75% of the crashes, and non-incapacitating injuries in 91.9% of the crashes.
  - Crashes occurred on curved roads 26.7% of the time.
  - The analyses of other conditions led to similar insights related to crashes with barriers as above.
  - The data was also insufficient to isolate any safety problems for barriers on CSRS.
- FARS Data: This dataset was compiled for all fatal crashes and the dataset contained 905,289 cases for the years 1982 through 2010. Fatal crashes with the first harmful event being hitting a longitudinal barrier were isolated. The bar-

riers types included bridge rail, guardrail face, concrete, guardrail end, and cable barriers (after 2008):

- Crashes with guardrail face were represented in 76.3% of the cases and concrete barrier in 15.7% of the cases.
- Crashes occurred on curved roads 40.3% of the time.
- The analyses of other conditions led to similar insights related to crashes with barriers as above, but it was noted that fatalities were more likely to occur on grades.
- The data was also insufficient to isolate any safety problems for barriers on CSRS.
- NCHRP 17-22 Data: This project created a data of CDS cases of longitudinal barrier impacts from three studies. Supplemental data reflecting roadway conditions was added to the 700+ cases. It was hoped that this supplemental data would provide some relevant roadside crash cases. Forty usable cases were isolated, but only seven were related to CSRS conditions. The Team decided that this was too few to derive any meaningful insights.

The analyses of crashes revealed what is generally known, that is, that crashes occur more frequently on curves than on tangent sections. The available data does not, however, allow much mining into the effects of the various design features associated with basic curves, much less with superelevated curves. Given that vehicles are known to leave the road on curves more frequently (e.g., due to loss of side friction, visibility issues), it is appropriate to consider whether the barriers deployed for these situations are providing comparable safety. The available sources of crash data do not typically include sufficient details about the roadway curvature or the barrier type, dimensions, or placement relative to the shoulder to allow safety performance to be analyzed. Further, many state DOTs cannot link their roadway geometry and barrier inventories to crash data. Various sources of data were explored, but none were found to offer useful insights on any variations on the safety of longitudinal barriers installed on CSRS.

It was therefore concluded that available crash data would not be able to provide specific insights on whether typical longitudinal barriers function similarly on CSRS as they do for tangent sections of roadway. The absence of specific data in police crash reports on the types of barrier impacted, the nature of the curve, or details about the shoulder configuration made it necessary to use other means to analyze the safety performance of barriers used in CSRS situations.

# CHAPTER 4

# Vehicle Dynamics Analysis for Vehicles Leaving the Traveled Way on CSRS

## 4.1 Background

The curvature and surface slope on a roadway are known to effect vehicle dynamics and influence vehicle trajectories, orientation, and speed. On curved sections, the vehicle is more likely to leave the road at a sharper angle and consequently impact the barrier with greater force that could potentially result in higher impact severity. The degree of superelevation in combination with the shoulder slope can lead to variations in the vehicle-to-barrier interface which can increase vehicle instability, barrier climb, vehicle rollover, or override/underride. Further, the superelevation with a negative shoulder slope might cause the vehicle to impact the barrier at a different orientation (roll and pitch). Thus, an important starting point for the analysis of barriers on CSRS is understanding the dynamics of vehicles as they leave the traveled way on CSRS and interface with barriers.

A considerable amount of effort has recently been devoted to analyzing the dynamic effects of vehicles on non-level terrain and the subsequent effects on their trajectories and interfaces with barriers. VDA has been shown to provide new insights on the effects of a vehicle's suspension system on trajectories in all three dimensions. For example, trajectory data in the vertical direction is directly related to the interface of the vehicle and the barrier. The slope changes from the roadway to the shoulder could affect the vehicle's trajectory and cause it to contact the barrier too high, which may lead to undesirable override or underride conditions. The combined effect of the superelevation of the roadway, the slope of the shoulder, and the side slope of the roadside for a vehicle leaving the roadway in a curve can be explicitly analyzed using VDA tools. These tools readily allow the range of combinations of roadway, shoulder, and side slope design features to be analyzed for varying types of vehicles, and their paths or trajectories can be determined.

Guidelines for the testing and deployment of roadside safety barriers on sloped surfaces and curved sections are limited. For example, crash testing protocols for barriers have evolved to provide a practical worst-case impact condition that is reproducible and comparable. Thus, barriers are tested under idealized impact conditions, with the barrier being tested installed on a straight and level section minimizing the roll, pitch, and yaw effects on the impacting vehicle. These protocols have evolved to determine whether safety hardware is "crashworthy." While crash testing protocols have evolved to include tests for a variety of angular impact conditions, one aspect that is not fully addressed is the crashworthiness of barriers installed on CSRS. A review of the literature revealed only a few older efforts address the safety of designs or provide guidance for placement on CSRS.

The need exists to systematically analyze a typical set of curved, superelevated roadway situations and the possible paths of errant vehicles to understand (1) the trajectories along the possible vehicle paths, (2) the associated vehicle-to-barrier interfaces for various barrier types and placement, and (3) how the stability of the vehicle (i.e., functions of induced roll, pitch, and yaw effects) may affect the engagement with the barrier and its crashworthiness. VDA results provide a convenient means to understand trajectories and interface scenarios, as well as indicate those critical scenarios that may warrant crash simulation analyses.

The analysis of the overall motion of a vehicle can be very complex, especially at higher speeds. However, vehicle motion is primarily governed by the forces and moments generated by the interaction of the tires and the ground. In vehicle dynamics studies, six degrees of freedom are studied: longitudinal, lateral, and vertical displacement; and roll, pitch, and yaw angles. Generally, the vehicle fixed coordinate system is associated with the CG of the vehicle, but it is possible to generate metrics that allow the frontal interface region for each vehicle to be determined. The data allows the evaluation of potential barrier effectiveness given road departure speed and angle for the surface conditions associated with the roadway, shoulder, transition to the side slope, and the side slope.

Such metrics are important for understanding the position of the frontal region of the vehicle relative to the barrier.

## 4.2 Objective

The objective of the research reported in this chapter was to apply vehicle dynamics tools to assess the trajectories of vehicles leaving the traveled way on CSRS. The intent was to develop a better understanding of the influence of various roadway curvatures, superelevation, shoulder/roadside designs, and barrier features and placement on the dynamic response of vehicles and to assess the safety performance of barriers used in these situations.

## 4.3 Research Approach

Vehicle dynamics simulations were performed to assess vehicles' trajectories as they crossed from the traveled way to varying shoulder and side slope conditions for different roadway curvatures and superelevation. Simulations were conducted with varied vehicles, speeds, and departure angles. The following sections describe the VDA set ups, the software tool used, factors considered, and the cases selected for analyses.

# 4.3.1 Vehicle Dynamics Analysis Applications

The concept of using vehicle dynamics simulation software to analyze run-off-road vehicle behavior and motion is gaining popularity. In 1997, McMillan et al. conducted simulation studies to analyze driver response to roadway departure. This analysis was used to evaluate the ability of collision countermeasure systems to prevent run-off-road accidents. Similar analyses have been performed by Pape et al. (1996) and Hadden et al. (1997) where they extended the VDANL (vehicle dynamics analysis, nonlinear) model of the vehicle/driver to assess the effectiveness of the countermeasure system. Other studies have focused on the results of an off-road crash. Day and Garvey (2000) used EDVSM (Engineering Dynamics Vehicle Simulation Model) to perform rollover simulations. They described the limitations of rollover simulation for on-road and off-road accident reconstruction. The use of simulation software for the analysis of off-road crashes has been broad. Claar et al. (1980) concentrated on suspension modeling for improving off-road ride comfort, whereas some studies have focused on friction influences in the case of water or snow on the road surface, as did Mancosu (2002).

There has been little research using vehicle dynamics simulation software to analyze and enhance the roadway design itself. Sicking and Mak (2004) presented a paper which suggested that efforts should focus on developing better vehicle

and roadside safety hardware models. Also, they indicated that significant effort must be devoted to improving the capability of computer simulations to model run-off-road crashes. The NCAC (National Crash Analysis Center) staff used the HVE simulation program to study the effect of edge drops on guardrail roadside barrier performance (Marzougui et al. 2007). They used varied initial conditions and different vehicles to analyze the behavior of the vehicle encountering various edge drops. The NCAC used VDA to trace two critical points on impacts with W-beam guardrails to determine barrier effectiveness relative to vehicle underride or vaulting. Similarly, the NCAC made extensive use of VDA to analyze the effects of median configurations on the effectiveness of cable barrier placement (Marzougui et al. 2008a, 2009a, 2010a). A major use of VDA that provided the basis for guidelines for the placement of cable median barriers was reported in NCHRP Report 711 (Marzougui et al. 2012a). Last, a study conducted at Pennsylvania State University showed the utilization of commercially available VDA software as a tool to analyze the effect of highway median width and slope on vehicle stability. The researchers used the CarSim programs to run thousands of simulations using different vehicles, median widths and slopes, steering conditions, and initial conditions to generate various metrics, including roll and lateral velocity. The resulting data was used to provide a preliminary assessment of tradeoffs in the size and slope of median profiles versus the types of accidents observed (Brennan and Hamblin 2007).

# 4.3.2 Analyzing Vehicle Dynamics

There is a well-developed body of knowledge about the physics of vehicles that has evolved with the automotive industry. Detailed VDA has been packaged into commercially available software tools. The VDAs in this effort were undertaken with the CarSim software. CarSim is a nonlinear vehicle simulation program capable of analyzing vehicle-roadway interaction and providing a detailed description of the vehicle's trajectory taking into consideration speed, weight, suspension system, surface features, and other factors. It is readily linked to development tools such as MATLAB to extend its functionality. It also allows batch inputs to reflect ranges of conditions that define performance enveloped.

## 4.3.3 Critical Vehicle Interface Analysis Approach

The findings of the literature review, the state DOT survey, reviews of design documents like the *Green Book*, and discussions with the NCHRP Project 22-29A panel led to the identification of factors believed to affect the safety performance of longitudinal barriers placed on CSRS. The initial

set of factors and specific parameters associated with them are indicated below:

- Barrier type
  - Concrete barrier [height ≤ 32 in. (813 mm)]: NJ concrete barrier
  - Strong-post W-beam guardrail [height < 31 in. (787 mm)]:</li>
     G4(1S)
  - Strong-post W-beam guardrail [height≥31 in. (787 mm)]:
     MGS
- Vehicle type
  - 2270P pickup truck: 2007 Chevrolet Silverado Model
  - 1100C small car: 2010 Toyota Yaris Model
- Curvature/superelevation combinations
  - 614 ft (187 m)/12%
  - 2,130 ft (649 m)/12%
  - 758 ft (231 m)/8%
  - 2,670 ft (814 m)/8%
  - 833 ft (254 m)/6%
  - 3,050 ft (930 m)/6%
- Shoulder width and slope
  - 4 ft (1.22 m), 8 ft (2.44 m), and 12 ft (3.66 m) shoulder widths
  - 0%, 3%, 6%, and 8% shoulder angles
- Roadside slope
  - 12H:1V (negative) from the edge of shoulder for all shoulder slopes
- Impact conditions
  - Three impact angles: 20°, 25°, and 30°
  - Three impact speeds: 57 mph, 62 mph, and 67 mph (90 km/h, 100 km/h, and 110 km/h)
- Barrier placement relative to road section
  - Lateral position: at edge of shoulder, 4 ft (1.22 m) offset, and 8 ft (2.44 m) offset

Vertical orientation: normal to road and parallel to true vertical

VDA software was used to model vehicle behavior when traversing the shoulder and side slope for the above range of conditions to obtain trajectories for each case. Aggregating the results across subsets of these parameters allowed the generation of maximum and minimum trajectory traces that provide a means for analyzing the vehicle-to-barrier interface for varying lateral placement. These results provide a basis for identifying critical scenarios for the FE simulations, as well as providing insights useful to generating proposals for improved practices.

#### 4.4 VDA Considerations

Undertaking VDA requires information about vehicles, the barriers to be studied, the effective interface areas, and the terrain or surface conditions associated with CSRS. The following sections describe these aspects as they were defined for this research.

#### 4.4.1 Vehicles Considered

The research focused primarily on two types of vehicles typically found on U.S. highways: a Chevrolet Silverado pickup truck (2,270 kg) and a Toyota Yaris sedan (1,100 kg). These vehicles correspond to test vehicles defined in MASH. The specific weight, size, frontal geometry, and suspension systems of these vehicles were incorporated into the VDA.

In these analyses, two points were defined for each type of vehicle considered to represent the primary interface (engagement) region on the vehicle. These are labeled Point 1 and Point 2 in Figure 4.1. The points are located at positions on





Figure 4.1. Vehicle models used in VDA and their interface points.

the front of the vehicles that represent the engagement point that differentiates between tendencies to override or underride a barrier. Point 1 for the small vehicle is located at a height of 21 in., while Point 2 for the pickup is at a height of 25 in. These point positions were defined by examining the frontal profile of the vehicles and reviewing full-scale crash tests conducted using similar vehicles. The traces of these points are critical in determining the interface with barriers for any vehicle trajectory.

#### 4.4.2 Vehicle-to-Barrier Interface Regions

Three barriers were selected for analysis and an interface region was defined such that if the two critical points (Point 1 and Point 2) are inside this region at the start of the impact, the barrier is considered likely to redirect the vehicle. If Point 1 (from the small car) falls below the interface region, an underride or significant snagging is likely to occur. Similarly, if Point 2 (from the pickup truck) is above the interface region, vehicle override is likely to occur. The interface regions are shown with a shaded box in Figure 4.2 as the maximums and minimums. These regions are based on the geometry of the barrier and a review of full-scale crash tests conducted on these barriers. For the concrete barrier, only the override condition is considered, so there is no minimum. It is important to note that these interface analyses accounted for the effects of vehicle orientation (changes in roll, pitch, and yaw angles) in computations to determine the positions of Points 1 and 2 relative to the vehicle CG. Further, variations in the designs of these barriers, such as the inclusion of rub rails, increased heights, or different shapes for the concrete barrier were not considered. The evaluations based on these interface regions were only used in the VDA as preliminary criteria to identify the set of cases to be simulated in the FE analysis. The actual impact is simulated in the FE evaluations, and the barrier performance is assessed based on these results.

#### 4.4.3 Roadway Curve Conditions

Various degrees of roadway curvature were considered reflecting the range of superelevation applications commonly found on highways. These range from tight curves used on ramps to gentle sweeping curves. Figure 4.3 provides examples of the range of curves considered in the simulation. A total of six roadway curve conditions with different curvature and superelevation were used in the VDA. These conditions were selected based on the *Green Book* design superelevation tables. The analyses incorporated three superelevations (6%, 8%, and 12%). For each superelevation, two curvatures were selected representing the minimum radii at the 50-mph (80-km/h) and 80-mph (130-km/h) design speeds.

# 4.4.4 Analysis of Vehicle Trajectories on CSRS

Figure 4.4 shows the typical path or trajectory (via sequential vehicle images) of a vehicle attempting to negotiate a curve before departing the roadway, as marked by the red line. The cross section of a superelevated curve perpendicular to the centerline (as indicated by the black line) is depicted in the figure. In this case, the banking of the roadway surface is exaggerated. The shoulders can be designed to have the same slope relative to the roadway cross section or a negative slope for drainage purposes. The red line shows the typical path or horizontal trajectory of an errant vehicle leaving the road on a CSRS. It shows a rising surface reflecting a diagonal crossing of the superelevation, followed by diagonally traversing the negative shoulder and side slope.

In the VDA, the vehicle was run a distance of about 1,000 ft (300 m) on this surface to be in a "curve operation" equilibrium state before it was directed off the road. Several predefined departure paths were input into the software to represent various departure angles. Repeated simulations of vehicles traversing such paths were conducted. These were varied to

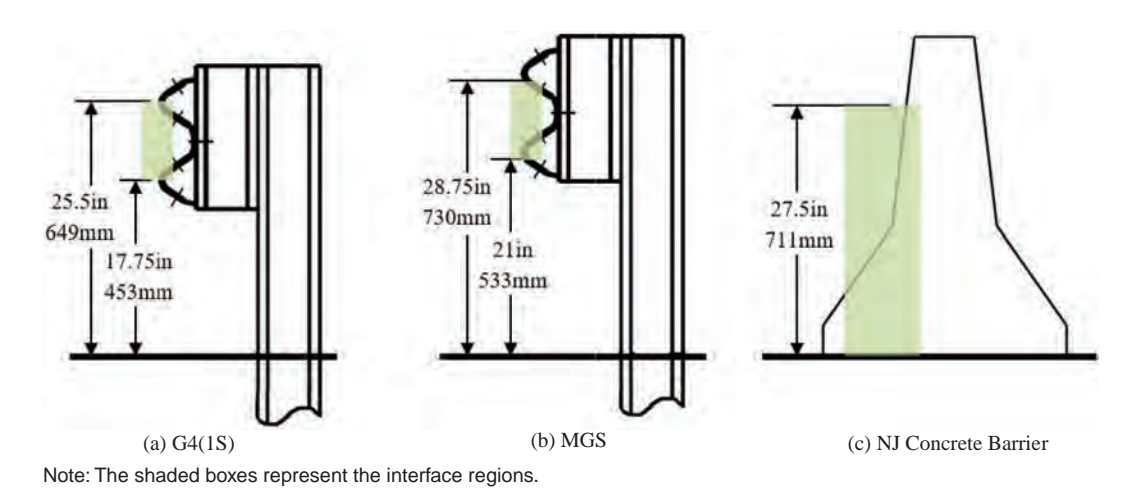


Figure 4.2. Interface regions for the three barriers selected.

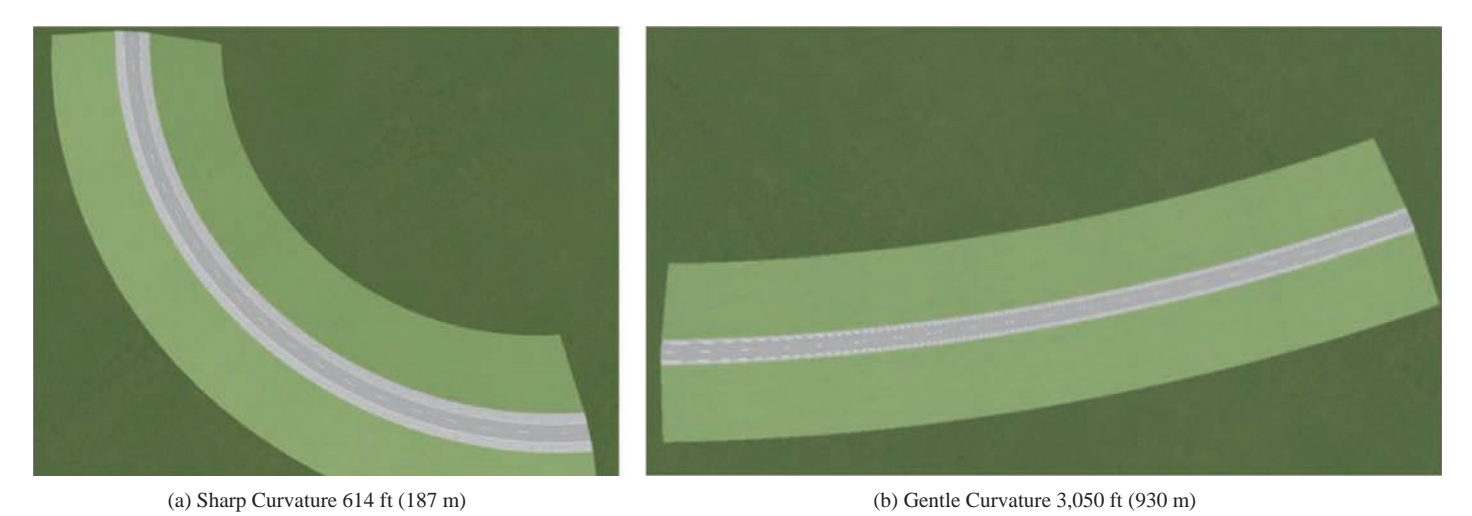


Figure 4.3. Sample variations in roadway curvature.

reflect exit angles of 20°, 25°, and 30° for the vehicles traveling at 57 mph 62 mph, and 67 mph (90km/h, 100 km/h, and 110 km/h). In this research, the roadway to shoulder slopes that were analyzed are depicted in Figure 4.5 with a 12H:1V roadside slope.

It is important to note that these cross sections are consistent with the guidance provided in the *Green Book*. The *Green Book* defines cross slope in Figures 4-2A and 4-2B, which define "roll-over" as the algebraic difference in rate of cross slope. It also notes that "roll-overs" should not exceed 8%. The scheme defined for this research is consistent with these requirements.

A number of different possible conditions for road departures were considered in the VDA with the following underlying assumptions:

- The vehicle carries one average-sized male occupant.
- The roadside has a firm surface, meaning tire furrowing into the surface is negligible.

- Vehicles are "tracking" as they enter the roadside (i.e., vehicle initial speed is in the same direction as its longitudinal axis).
- There are no driver inputs (e.g., steering, braking) that affect the vehicle.
- The tire-to-road friction was made identical in all runs using a friction coefficient of 0.9.
- The simulation software provided dynamics analysis results every thousandth of a second as the vehicle traversed the roadway, shoulder, and side slope.
- There is a smooth transition between the pavement and shoulder, and between the shoulder and side slope, to limit any other effects that might alter vehicle stability.

# 4.4.5 VDA for a Worst-Case Departure Scenario

The dynamic effects on a vehicle traversing a worst-case path for a CSRS without a barrier was undertaken to better

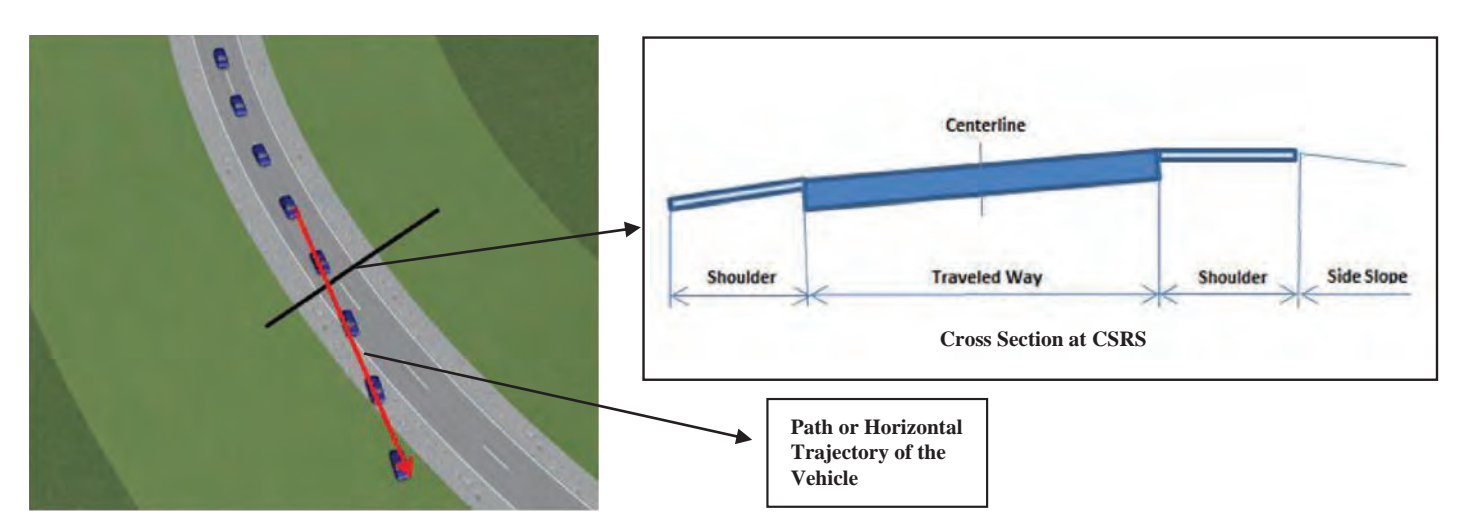
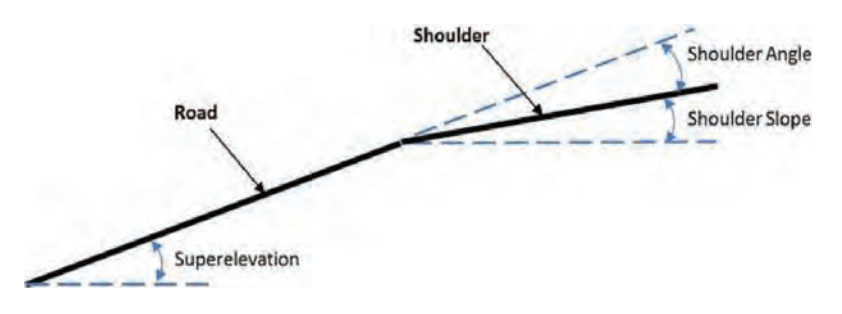
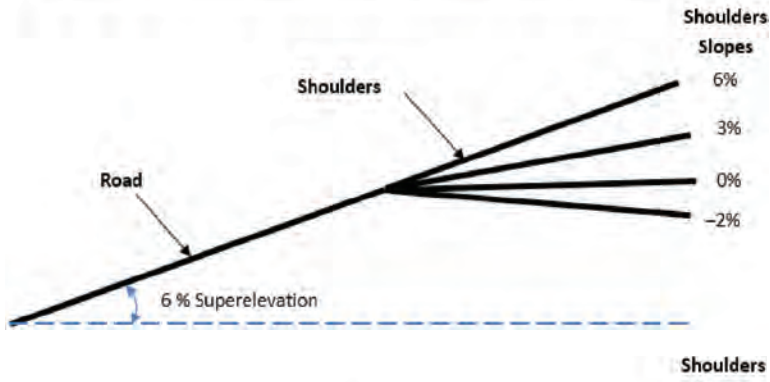
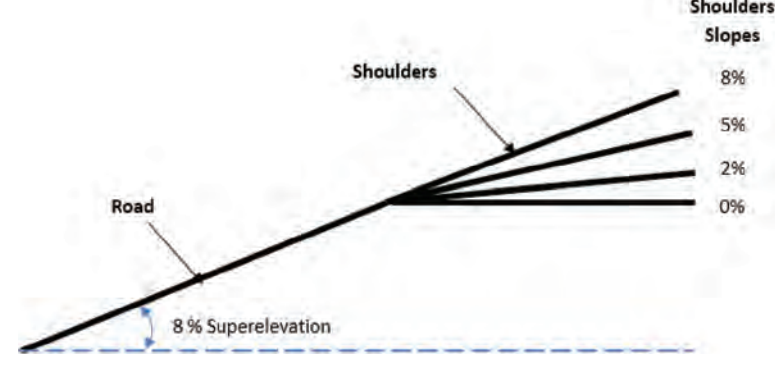


Figure 4.4. Sample VDA perspective of a vehicle leaving the road.



Shoulder Angles	6% Superelevation	8 % Superelevation	12 % Superelevation					
Analyzed	Corres	Corresponding Shoulder Slope						
0%	6%	8%	12%					
3%	3%	5%	9%					
6%	0%	2%	6%					
8%	-2%	0%	4%					





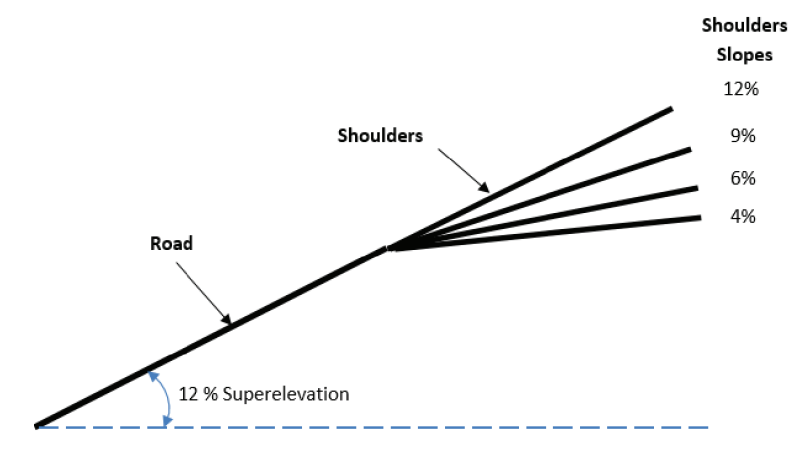


Figure 4.5. Vertical surface cross sections analyzed for superelevated curves.

understand the effects as reflected in changes in the vehicle's trajectory (i.e., x-, y-, and z-coordinates, and the roll, pitch and yaw angles). The effects were considered to be the greatest where the higher slopes and inflection changes took place. The worst case is represented by the cross section in Figure 4.6. The analyses also consider that the vehicle is on a diagonal path, so the right front tire will incur a change before the left front tire and so forth. Such changes imply that the changes at Points 1 and 2 located on the right front will be different for similar points on the left front.

The VDA results shown in Figure 4.7 reflect the differences observed between four cases with two vehicles (1100C small car and 2270P pickup) and two road profiles (with and without superelevation). Figure 4.7(a) shows the effect on the roll angle of the vehicle. This plot covers a duration of 12 s, but the critical period is between 4 s and 7 s (as indicated by the vertical lines) where the vehicle is reaching the shoulder, traversing it, and then encountering the side slope. Similar patterns are noted for both vehicles and for both the superelevated and the non-superelevated cases. A negative roll begins when the tire encounters the shoulder slope, but it is countered as more of the vehicle gets on the shoulder. The roll effect becomes constant once the vehicle gets onto the side slope. The variation between the sets of curves reflects the roll effect induced by the superelevation.

Figure 4.7(b) shows the changes in pitch angle in traversing the cross section with the greatest amount of deviation associated with the shoulder. It must be noted that while the deviations are great, the scale reflects small changes in pitch. The inflection points occur when the shoulder and the side slope are reached for either vehicle. The effect on the pickup is greatest for the pickup without superelevation.

Figure 4.7(c) shows the changes in yaw angle. The dynamics of both vehicles is similar for all cases as the vehicle traverses the shoulder and the reaches the side slope. The pickup shows more change in yaw on the side slope than the small vehicle due to its longer wheelbase.

Figure 4.7(d) shows the effect of the x-value of the vehicle CG, Figure 4.7(e) shows the effect on the y-value, and Figure 4.7(f) shows the changes in z-value. There is little difference in the x- and y-values for the horizontal trajectory. The z-value, while appearing different, only reflects the difference in height associated with the superelevation.

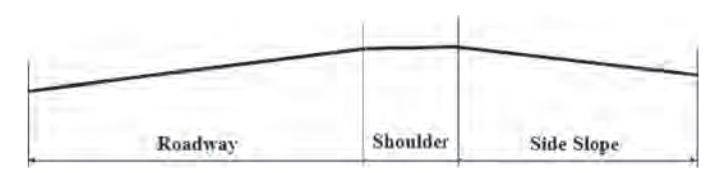


Figure 4.6. Typical profile for path of a vehicle leaving the traveled way.

These metrics for the worst-case scenario show that the vehicle is relatively stable as it traverses the shoulder and initial part of the side slope. It also suggests that the VDA tool is reflecting the variations in surface conditions. It is apparent that there are differences in the vehicle trajectories associated with superelevated and level curves and for various vehicles. It also suggests that there is not likely to be much extraneous variance in the results, leading to the conclusion that there was value to pursuing VDA for the various conditions of interest.

#### 4.5 VDA Simulation Results

The VDA software was used to generate trajectories for each of the vehicles at the selected exit angles and speeds for each road departure condition. The vertical trajectories or trace paths of Point 1 for the 1100C vehicle (brown) and Point 2 for the 2270P vehicle (blue) negotiating a curve and departing onto the roadside of a given configuration are shown in Figure 4.8 by line color and type (note the various vehicle weights, speeds, and exit angles in the legend). These trace paths can be visualized as standing on the roadside downstream from the point a vehicle leaves the roadway and observing the change in elevation of Point 1 or 2. Multiple curves reflect variations in departure speed and angle for each of the vehicles (as noted in the legend). The differences in basic vehicle heights are reflected by the relative positions of the two sets of curves. There is a consistency in the heights with the road profile shown by the black line at the base of the graph. Dynamic effects of the sprung mass cause the curves to vary for the changes in cross section conditions. A similar graph was generated for each set of the conditions in the analysis matrix.

Figure 4.9 provides an example of the normalized representation of the vertical trajectory for the same conditions. In the normalized view, the variations in trajectory are indicated relative to a horizontal plane as opposed to the actual cross section surface. The curve on the bottom shows the road profile or cross section as a reference for the vehicle dynamics traces. The normalized view provides a convenient means to analyze and compare vehicle dynamics effects for different conditions simultaneously. The normalized version is also useful to translate the vertical trajectories to a common plane to allow the aggregation of groups of results to define limits.

Figure 4.10 depicts a primary use of the normalized graphs of the trajectory data. All trajectory traces for a given set of CSRS conditions were plotted from which maximum and minimum limit curves can be derived. In this case, the bold red line represents the maximum trajectory height limit across the entire path. Similarly, the bold green line indicates the minimum trajectory height. These limits indicate requirements for any barrier system in that roadside configuration for all lateral positions beyond the shoulder. This approach

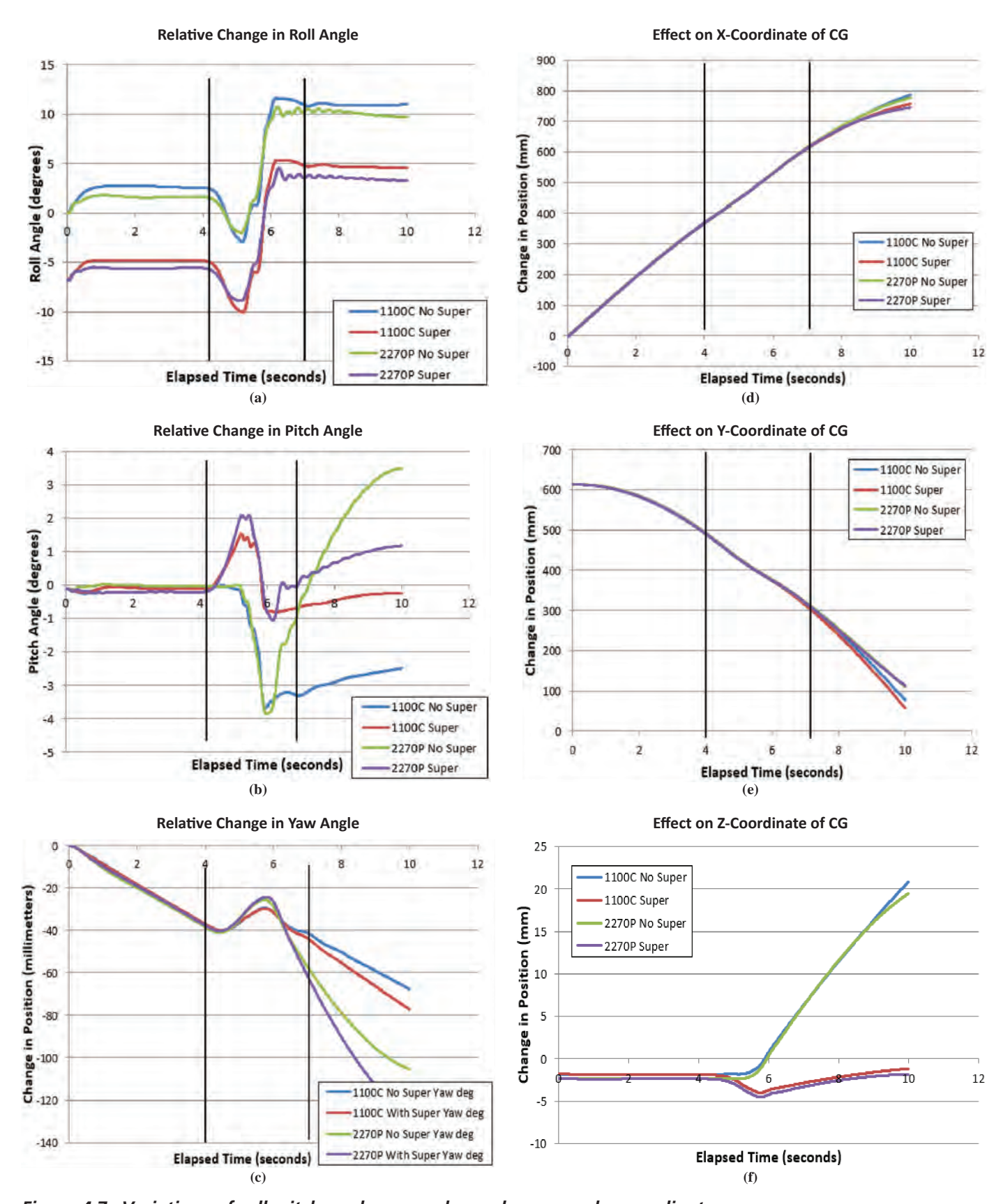


Figure 4.7. Variations of roll, pitch, and yaw angles and x-, y-, and z-coordinates.

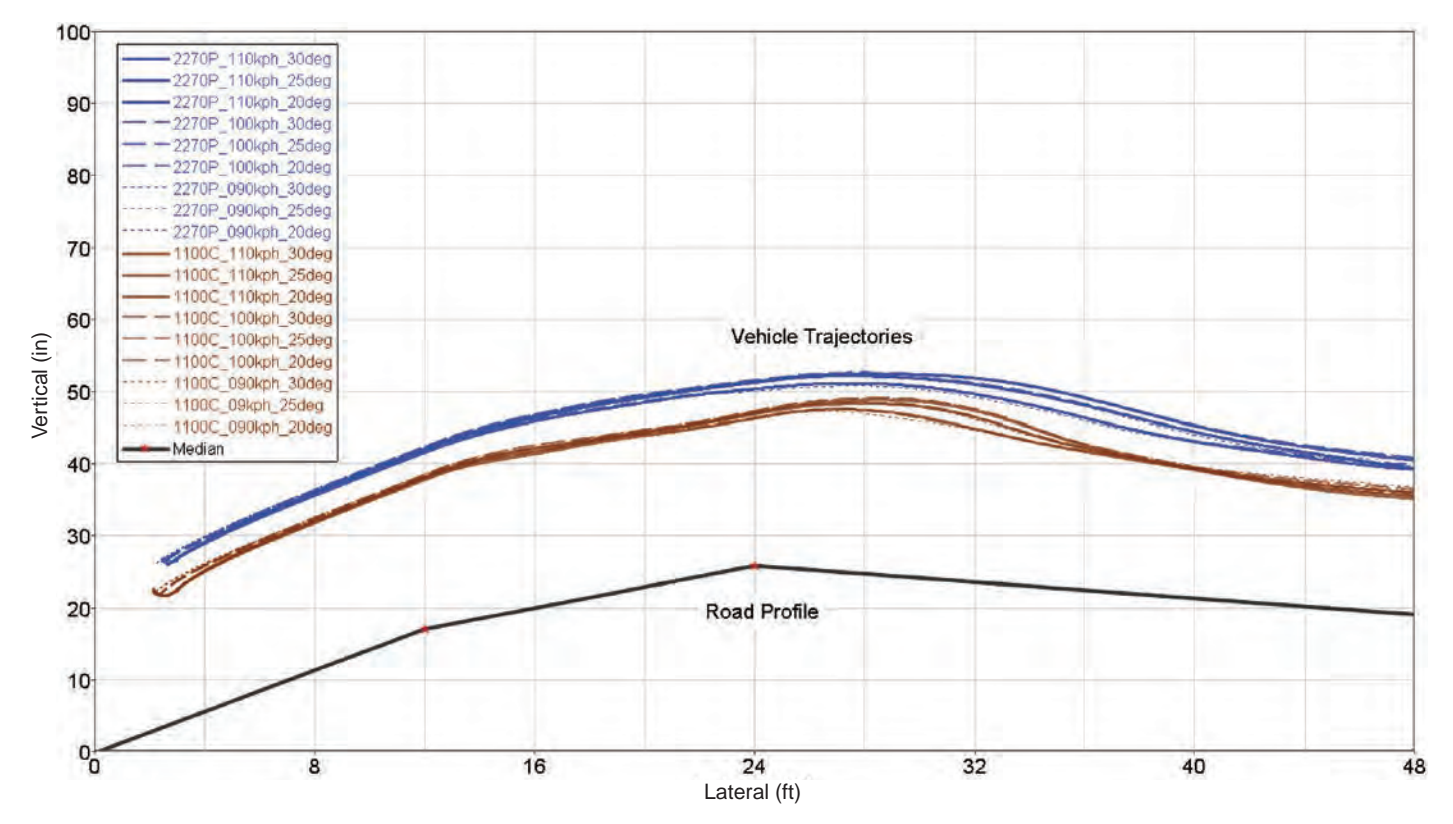


Figure 4.8. Sample plot of non-normalized vehicle trajectories on CSRS.

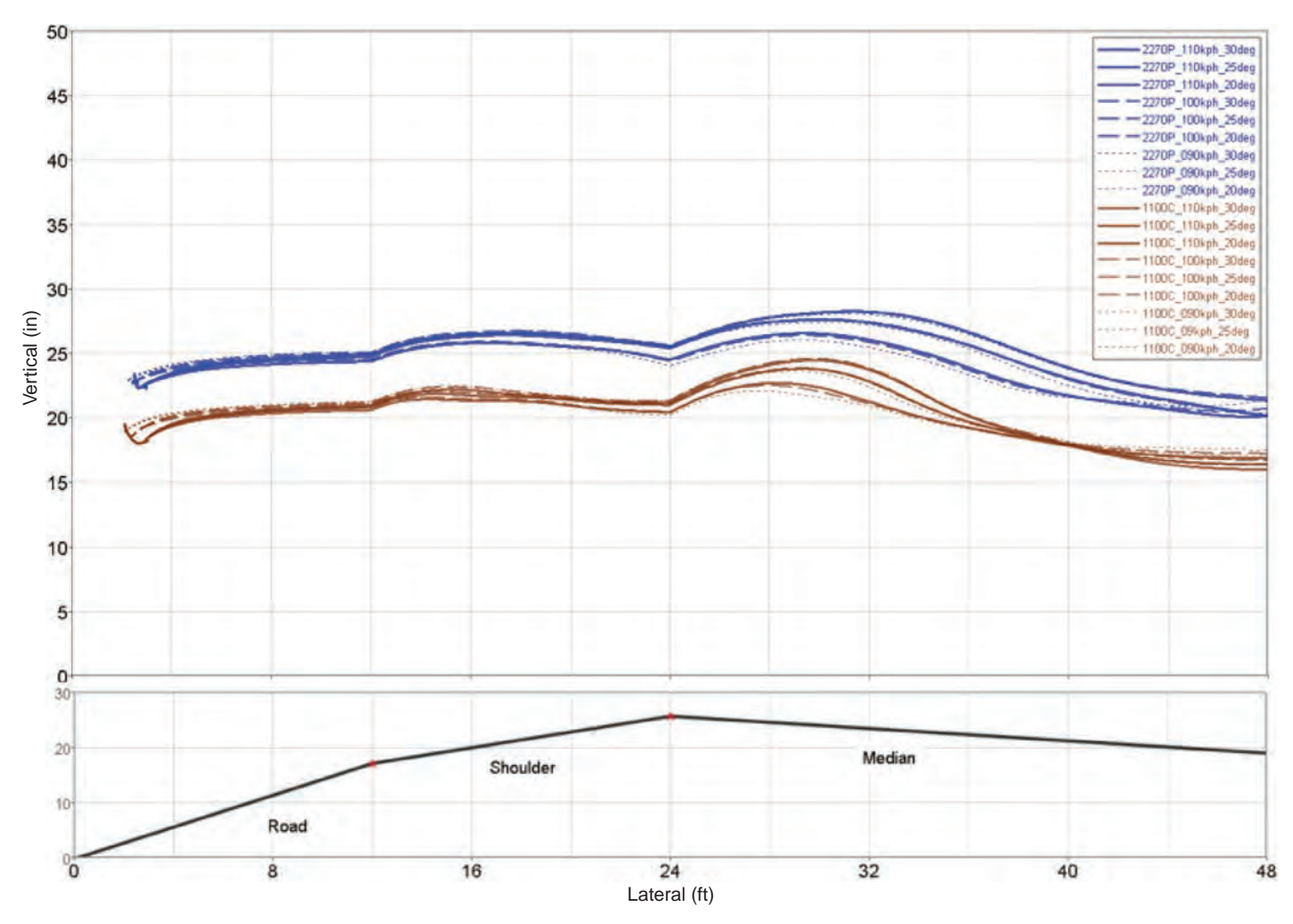


Figure 4.9. Sample plot of normalized vehicle trajectories on CSRS.

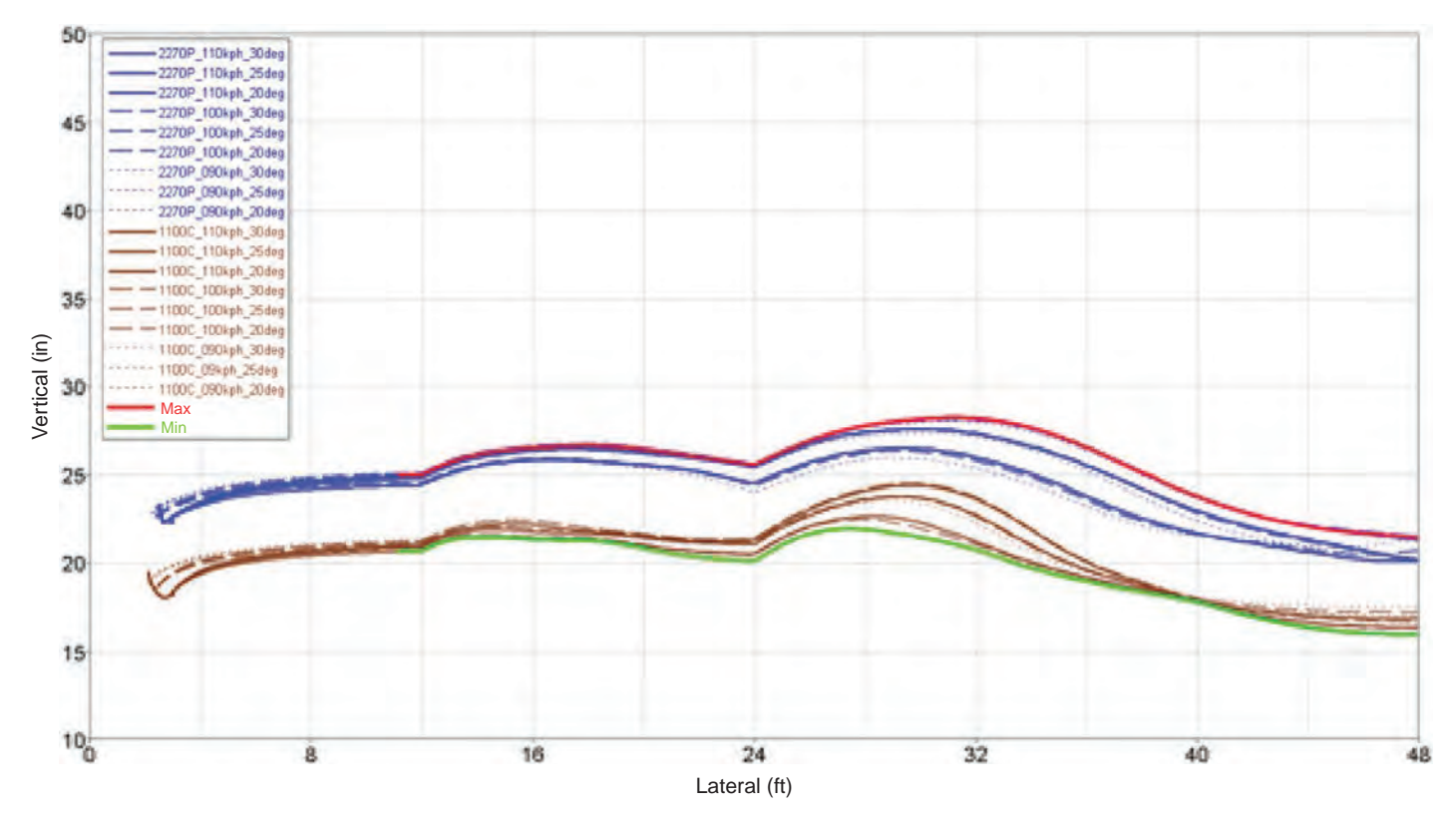


Figure 4.10. Example use of normalized view to show limiting conditions.

can be used to determine the potential effectiveness for varying barrier systems across all possible lateral positions for a given roadside configuration.

Figure 4.11 shows more specific examples of how the plot of maximums and minimums can be applied. For a given superelevated curve and roadside configuration [e.g., 614-ft (187-m) radius curvature and 12% superelevation], the limits can be plotted along with the interface area provided by a specific barrier. These interface areas are represented by the blue and green lines that reflect the maximum and minimum vertical position of the vehicle's critical points as it leaves the roadway and moves onto the roadside. For the barrier to be effective, it must have a good interface for both large and small vehicles at any given lateral position. The two graphs show the limits for the G4(1S) and MGS barriers, respectively, as yellow lines across the graph for various positions where each type of barrier can be placed. If the maximum and minimum limits fall within the yellow lines, then the barrier will have a good interface for both types of vehicles. Where the blue line goes above the top yellow line, there is the opportunity for an override to occur. Where the green line falls below the lowest yellow line, the possibility of an underride exists.

The lower portion of Figure 4.11 shows the profile or cross section of the road related to the upper graph. Effective placement areas are shown in this pane. The red hatched area defines the lateral positions where the specific barrier

has an interface area above the maximum lower height limit (green curve) and/or below the minimum height limit (blue curve). Effective lateral placement occurs where both criteria are met, and this is shown in shaded green. The differences in the effectiveness of the G4(1S) and MGS barriers (by virtue of their design differences) is reflected when the effectiveness areas are compared. These maximum and minimum limits are a unique function of vehicle dynamics for the given configuration, but the yellow barrier isobars reflecting the effective range would depend on the barrier shape/type. These indicate the effective lateral placement options that can serve as guidance for specific CSRS conditions.

Table 4.1 provides a sample summary reflecting the effectiveness results for a barrier (NJ Concrete Barrier) across various CSRS conditions. Plots of this type for all different curve and roadside configurations selected were generated and are presented in Appendix B.

The VDA simulations were used to determine the maximum and minimum heights of the critical points (Points 1 and 2) on the bumper as the vehicle first comes in contact with the barrier. Barrier lateral placement in these evaluations was 1 ft off the shoulder for each of the three barrier systems selected. All combinations of curvature, superelevation, and shoulder width and slope for the different speeds and impact angle were used in the evaluations. The maximum and minimum heights are tabulated in Table 4.2. Each

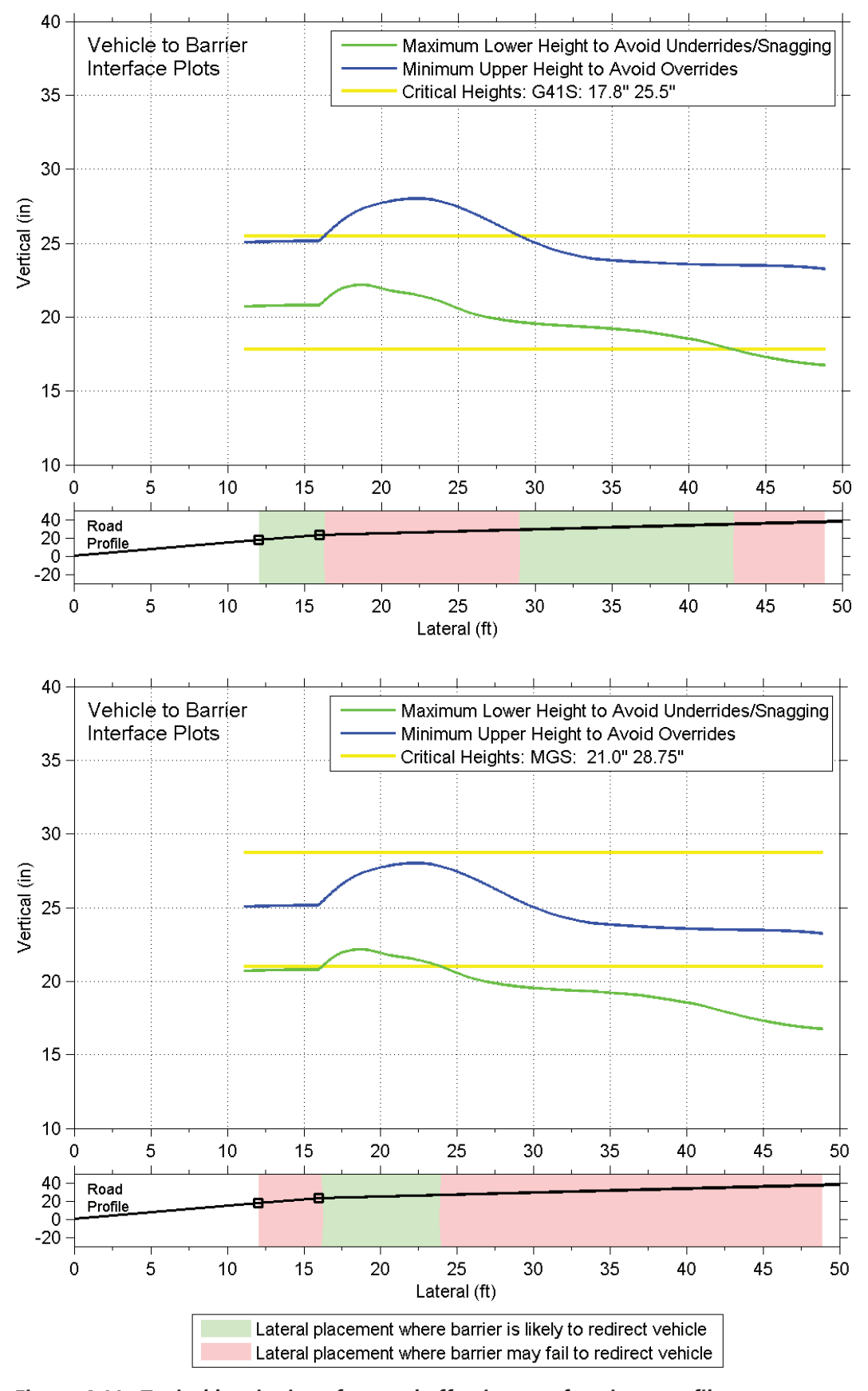


Figure 4.11. Typical barrier interface and effectiveness for given profiles.

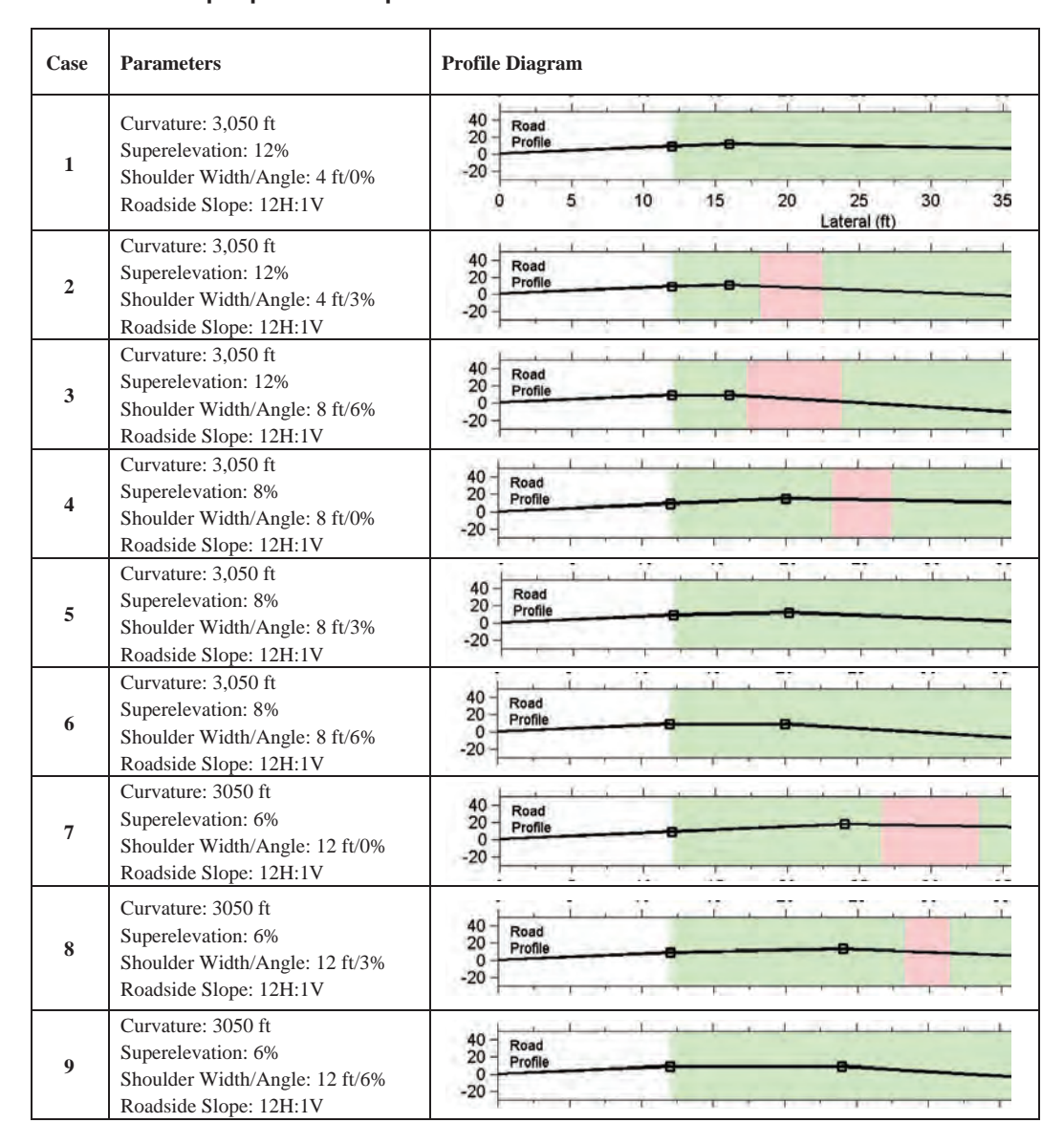


Table 4.1. Sample profile comparisons: NJ concrete barrier.

cell represents the barrier height for the specific conditions. If the value is red, then it implies that the height is outside the limits (e.g., too high or too low) and hence indicates that there is not a good interface. These tables, as well as other interface plots shown in Appendix B, are used to provide the basis for determining those cases or types of cases that need to be analyzed with crash FE simulation.

In Table 4.2, the critical heights range from just under 19 in. to almost 30 in. Examining the results for each type of barrier the following the insights are noted:

#### • NI Concrete Barrier

Since the concrete barrier has a 0-in. minimum interface height, this barrier works for all minimum cases for

- all the curvature, superelevation, shoulder, and placement conditions. Observe that there are no "red" values in any of the minimum rows.
- Similarly, this barrier provides a good interface for all
   1-ft offset placements (no "red" values).
- The highest maximum height value is 29.83 in., which suggests that the use of a concrete barrier with a critical interface higher than 30 in. would provide good interface for all the conditions considered here.
- G4(1S) W-Beam Guardrail Barrier
  - The G4(1S) barrier appears to meet the minimum interface requirements for all cases, as there are no "red" values for any of the Min rows, indicating less susceptibility to underride on the CSRS road profile.

Table 4.2. Vehicle interface results for various CSRS and barriers.

				NJ	Concre	ete Bar	rier			MGS	S W-be	am Ba	rrier			G4(18	S) W-b	eam ba	ırrier	
	Curvature 1	Radius (ft)	614	2130	758	2670	833	3050	614	2130	758	2670	833	3050	614	2130	758	2670	833	3050
	Super Ele	vation (%)	12	12	8	8	6	6	12	12	8	8	6	6	12	12	8	8	6	6
	Shoulder	Min (in)	20.80	22.05	20.79	21.76	20.75	21.59	20.80	22.05	20.79	21.76	20.75	21.59	20.80	22.05	20.79	21.76	20.75	21.59
	Angle 0%	Max (in)	24.68	25.39	24.55	25.13	24.51	24.98	24.68	25.39	24.55	25.13	24.51	24.98	24.68	25.39	24.55	25.13	24.51	24.98
	Shoulder	Min (in)	21.08	22.11	21.07	21.83	21.04	21.62	21.08	22.11	21.07	21.83	21.04	21.62	21.08	22.11	21.07	21.83	21.04	21.62
4 ft	Angle 3%	Max (in)	25.39	25.87	25.27	25.60	25.23	25.46	25.39	25.87	25.27	25.60	25.23	25.46	25.39	25.87	25.27	25.60	25.23	25.46
Shoulder Width	Shoulder	Min (in)	21.42	22.18	21.39	21.93	21.38	21.72	21.42	22.18	21.39	21.93	21.38	21.72	21.42	22.18	21.39	21.93	21.38	21.72
	Angle 6%	Max (in)	26.15	26.37	26.04	26.10	25.99	25.92	26.15	26.37	26.04	26.10	25.99	25.92	26.15	26.37	26.04	26.10	25.99	25.92
	Shoulder	Min (in)	21.67	22.57	21.63	22.10	21.61	21.85	21.67	22.57	21.63	22.10	21.61	21.85	21.67	22.57	21.63	22.10	21.61	21.85
	Angle 8%	Max (in)	26.68	26.72	26.58	26.42	26.53	26.24	26.68	26.72	26.58	26.42	26.53	26.24	26.68	26.72	26.58	26.42	26.53	26.24
	Ch14	Min (in)	20.69	22.01	20.67	21.70	20.64	21.54	20.69	22.01	20.67	21.70	20.64	21.54	20.69	22.01	20.67	21.70	20.64	21.54
	Shoulder Angle 0%	Max (in)	24.76	25.46	24.64	25.20	24.59	25.07	24.76	25.46	24.64	25.20	24.59	25.07	24.76	25.46	24.64	25.20	24.59	25.07
	Shoulder	Min (in)	20.77	21.79	20.75	21.49	20.72	21.28	20.77	21.79	20.75	21.49	20.72	21.28	20.77	21.79	20.75	21.49	20.72	21.28
8 ft	Angle 3%	Max (in)	25.53	25.86	25.37	25.57	25.30	25.39	25.53	25.86	25.37	25.57	25.30	25.39	25.53	25.86	25.37	25.57	25.30	25.39
Shoulder Width	Shoulder	Min (in)	20.91	21.59	20.89	21.33	20.87	21.13	20.91	21.59	20.89	21.33	20.87	21.13	20.91	21.59	20.89	21.33	20.87	21.13
	Angle 6%	Max (in)	26.06	26.06	25.94	25.77	25.88	25.58	26.06	26.06	25.94	25.77	25.88	25.58	26.06	26.06	25.94	25.77	25.88	25.58
	Shoulder	Min (in)	21.03	21.25	21.00	20.92	20.97	20.72	21.03	21.25	21.00	20.92	20.97	20.72	21.03	21.25	21.00	20.92	20.97	20.72
	Angle 8%	Max (in)	26.40	26.17	26.24	25.84	26.19	25.65	26.40	26.17	26.24	25.84	26.19	25.65	26.40	26.17	26.24	25.84	26.19	25.65
		Min (in)	20.51	21.93	20.48	21.61	20.44	21.43	20.51	21.93	20.48	21.61	20.44	21.43	20.51	21.93	20.48	21.61	20.44	21.43
	Shoulder Angle 0%	Max (in)	24.86	25.56	24.73	25.29	24.65	25.15	24.86	25.56	24.73	25.29	24.65	25.15	24.86	25.56	24.73	25.29	24.65	25.15
	Shoulder	Min (in)	20.35	21.64	20.34	21.30	20.30	21.08	20.35	21.64	20.34	21.30	20.30	21.08	20.35	21.64	20.34	21.30	20.30	21.08
12 ft	Angle 3%	Max (in)	25.07	25.41	24.95	25.12	24.88	24.96	25.07	25.41	24.95	25.12	24.88	24.96	25.07	25.41	24.95	25.12	24.88	24.96
Shoulder Width	Shoulder	Min (in)	20.23	21.40	20.23	21.02	20.20	20.80	20.23	21.40	20.23	21.02	20.20	20.80	20.23	21.40	20.23	21.02	20.20	20.80
***************************************	Angle 6%	Max (in)	25.19	25.16	25.03	24.85	24.99	24.66	25.19	25.16	25.03	24.85	24.99	24.66	25.19	25.16	25.03	24.85	24.99	24.66
	Shoulder	Min (in)	20.15	21.26	20.17	20.87	20.14	20.63	20.15	21.26	20.17	20.87	20.14	20.63	20.15	21.26	20.17	20.87	20.14	20.63
	Angle 8%	Max (in)	25.16	24.98	25.05	24.64	24.99	24.42	25.16	24.98	25.05	24.64	24.99	24.42	25.16	24.98	25.05	24.64	24.99	24.42

- There are cases where the maximum requirement is not met (the "red-bold" values), indicating that there is increased chance of override due to the CSRS road profile. These are more noticeable with the higher shoulder slope angles (6% and 8%).
- MGS W-Beam Guardrail Barrier
  - The greater height of the MGS barrier accounts for greater number of good maximum interface indications across a range of conditions, indicating less susceptibility to override due to the CSRS road profile than the G4(1S) system.
  - There is not a corresponding meeting of the minimum requirements. Several of the cells do not meet this criterion, indicating susceptibility to a vehicle going under the barrier and its potential for snagging posts.

These and other insights demonstrate the value of the VDA results. It is important to note here that the VDA gives an indication of the barrier performance based on the vehicle dynamics and geometry of the barrier. It does not account for the increased or decreased severity of the impact resulting from a change in vehicle orientation and speed. FE analyses were performed to investigate these additional effects.

#### 4.6 Conclusions

In this effort, trajectories for vehicles departing from CSRS were determined using VDA tools. VDA tools allowed the entry of data for specific vehicles that reflected differences in size, weight, suspension features, and other factors as well as the cross sectional surface for various conditions under which a vehicle can leave the roadway (i.e., speed, angle). The trace plots generated as the vehicle traverses the various cross sections reflect the effects of the suspension and provide useful insights into effects on the vehicle's interface area relative to the barrier. The latter aspect is a critical metric for assessing the barrier's potential ability to capture and redirect the vehicle. The results from this analysis provide useful insights for identifying critical cases for investigation using FE simulations, as well as proposing guidance on selecting and placing barriers on CSRS.

The VDA results provide some useful insights about the potential effectiveness of different types of barriers on CSRS:

- Barriers offering increased height and depth of their capture area should be used. This is more important for sharper curves and higher levels of superelevation.
- Clear zones beyond the shoulder may be an option where sufficient runout area is available. This analysis only considered nearly level 12H:1V roadside slope conditions.

It is important to remember that these analyses focus strictly on the vehicle-to-barrier interface. This is a necessary condition, but not sufficient to ensure that the barrier will meet crashworthiness requirements. This is where further analyses using FE models and crash simulation become useful.

There are not clear choices for selecting specific cases for crash simulation. The differences in barriers necessitates that crash simulations be conducted for each of them. For each barrier type, the following crash simulations should be considered:

- The most common acceptable interface scenario.
- The most divergent case for comparison of crashworthiness metrics and considerations of options for varying the design.

Based on the results of these crash simulations, decisions can be made on the value of additional simulations, for example, simulations with the following:

- Impacts at shallower impact angles.
- Selected cases where poor interface might suggest a propensity to cause rollovers.
- Variations in the orientation of the barrier to true vertical.
- SUTs to understand higher interface and vehicle weight impacts.

The benefits of these additional simulations will be weighed in the context of providing needed insights or support for the proposals that are to be developed.

# CHAPTER 5

# Crash Simulation Analysis of Impacts into Longitudinal Barriers on CSRS

#### **5.1 Introduction**

This research revealed that there has been little testing or analyses of longitudinal barriers used on CSRS for reasons ranging from the difficulty of testing barriers on such roadways, limited capabilities to employ other approaches, and limited details in crash records that make it hard to isolate incidents involving this specific type of barrier deployment. There have been strides in analyzing barrier effectiveness in varying deployment scenarios using simulation. This research proposed to employ crash simulations based on FE modeling to analyze the performance of longitudinal barriers on CSRS. This approach was offered because crash simulation capabilities have evolved to a point where viable insights can be derived considering the full range of conditions associated with impacting a barrier on a CSRS. This chapter describes the FE modeling and crash simulation that was employed.

Crash simulation results allow determination of effective performance envelopes that can serve as the basis for enhancing or creating new guidance for highway and barrier design and deployment on CSRS. The effectiveness of simulation tools allows many combinations of features and impact conditions to be investigated economically. Simulation has become a common means to understand barrier performance without the cost of multiple, full-scale crash tests. Computer simulations also yield significantly more data than can be extracted from the full-scale crash tests. The simulation results include displacements, velocities, and accelerations of every point on the vehicle during impacts with roadside hardware. The deformations and energies absorbed by each component of the vehicle and the roadside hardware under various impact conditions are also computed and provided in the simulation results. Such information is useful for identifying critical weaknesses in the design and for providing a better understanding of the influences of CSRS conditions and placement features on roadside hardware safety performance.

## 5.2 Background

For more than 20 years, the FHWA has promoted the use of crash simulations based on FE models as a means to develop innovative designs and to evaluate their performance. Doing so requires FE models of vehicles and the roadside hardware. FE models have been developed to describe the vehicle and test articles as a collection of elements that reflect the geometry of the items, the nature of connections between adjacent elements, the characteristics of the element materials, and properties associated with the relationships between elements (e.g., joints, fracture mechanics). FE models for vehicles are developed by reverse engineering. For hardware, the geometries of the components are used to define elements.

Over the years, the vehicle models have become more detailed and complete (e.g., functional representation of suspension systems, interior modeling, and air bag capabilities). This has allowed a broader range of applications. The more recent generation of vehicle models consists of more than 1 million elements when all the interior components are included. Because all structural components are explicitly modeled, these detailed models can be used to study different impact scenarios including frontal, side, rear, oblique, and roof impacts.

The objectives of the simulation efforts were to (1) develop, adapt, and validate FE models for longitudinal barriers typically deployed on CSRS, (2) analyze the effects of curvature, superelevation, shoulder design, and roadside conditions on the MASH performance of the barriers, and (3) use the simulation results to formulate guidance of improved practice for the selection and placement of barriers for such situations. The efforts focused on a set of typical types of CSRS.

# 5.3 FE Modeling and Crash Simulation Analyses

Finite element analysis (FEA) involves the use of FE models of vehicles and barriers in crash simulations. The simulations analyze the physics of each discrete element of

the models for small increments of time (e.g., microseconds) over the duration of an impact event (e.g., the vehicle hitting the barrier). Because elements of the vehicle and the barrier will contact each other and the forces will cause the elements to deform, move, or fail in accordance with the defined material properties and nature of connections between elements, it is possible to replicate the crash dynamics that provide an indication of a barrier's performance. While such simulations do take a considerable amount of time to go through all the elements over the duration of the crash event, they are more economical than using crash testing. Further, the details of the elements in the model and principles of physics allow more detailed data to be derived from the simulation, and multiple simulation runs can permit parametric changes to study a broader range of conditions (e.g., impacts at different speeds and angles).

The LS-DYNA commercial FE package developed by Livermore Software Technology Corporation (LSTC) is used in the simulations (Hallquist 1997, 2006). It uses an explicit Lagrangian numerical method to solve nonlinear, three-dimensional, dynamic, large displacement problems. It has numerous features that allow for the analysis of several nonlinear dynamic engineering problems. It has a large selection of FE types which include one node lumped mass; two node spring; damper and beam elements; three and four node shell elements; and eight node solid and thick shell elements. For each of these element types, a number of element formulations are implemented in the code. As an example, more than 16 different shell formulations are available. These include reduced, fully integrated, and membrane formulations.

LS-DYNA has a library of more than 180 constitutive material models. The majority of these models can be used with all element formulations mentioned above. These models cover a wide range of material behaviors including elasticity, plasticity, thermal effects, and rate dependency. These constitutive models have been successfully used to model several materials including metals, plastics, rubber, soil, concrete, ceramics, composites, foams, and fluids. LS-DYNA has over 20 options for modeling connections including welds, rivets, and joints. Some of these connections incorporate failure. It also has over 50 different methods for modeling initial conditions, boundary conditions, and loadings. Some of these include initial velocity, initial stress, nodal forces, pressure, prescribed accelerations, and fixed nodes. The most advantageous capability of LS-DYNA over other FE codes is its advanced contact algorithm. Over 20 contact interfaces are available in the code including Nodes-to-Surface, Surface-to-Surface, Single-Surface, and Automatic-General. These allow for solving diverse types of impact problems.

The LS-DYNA program has been used by the Research Team in many studies to address transportation safety problems. Several vehicle and roadside hardware models have been developed and used in these studies. Some of these models were used in this research to assess the performance of longitudinal barrier when installed on CSRS. These models and associated validations are presented in the following sections.

#### 5.3.1 Vehicle Models

The crashworthiness analysis under NCHRP Report 350 and MASH involves different test vehicles. For NCHRP Report 350, the small car is represented by an 820-kg vehicle (820C) and the pickup truck by a 2,000-kg vehicle (2000P). Under MASH, the small car is represented by an 1,100-kg vehicle (1100C) and the pickup truck by a 2,270-kg vehicle (2270P). These reflect the trend in the United States that vehicle sizes and weights are increasing (a primary reason for the new MASH requirements). Computer models representing these four vehicles are included in the array of vehicle models available to support crash simulation analyses (National Crash Analysis Center 2012a). Basic information about these FE vehicle models can be found in Table 5.1, but additional information can be obtained from references (National Crash Analysis Center 2012b, 2012c, 2012d, 2012e). Even though the research focuses on MASH evaluations, both sets of models were needed to allow validation against available crash tests for the barriers. It should be noted that the test requirements only give generic vehicle features; different vehicles are often used in the actual testing. The models are believed to be viable surrogates for each of the weight classes. The following sections describe the validation efforts undertaken for the Chevrolet Silverado (representing the 2270P) and Toyota Yaris (representing the 1100C) vehicle models (Marzougui et al. 2012b, 2012c). These reflected the new "extended validation" approach used to create a vehicle model. The other two models (Geo Metro and Chevrolet C2500) were developed earlier and had more usage but less rigorous validation. Because the Silverado and Yaris are the primary models used to assess crashworthiness against the latest criteria, the following additional details are provided.

#### 5.3.1.1 Chevrolet Silverado Model (2270P)

The Silverado model was developed jointly by FHWA and NHTSA to serve multiple purposes in this research and advancement of vehicle and highway safety research. Reverse engineering methods were used to build the FE model and the attention to detail was critical to making it suitable for application for different crash conditions. The model consists of over 950,000 elements including the components of the steering and suspension systems (Marzougui et al. 2009b; National Crash Analysis Center 2009).

Table 5.1. Models representing NCHRP Report 350 and MASH test vehicles.

Description	Vehicle Image
<ul> <li>1997 Geo Metro (820C)</li> <li>Weight: 820 kg (1,806 lb)</li> <li>CG 664 mm (26.14 in.)</li> <li>Model Parameters:         <ul> <li>Parts-230, Nodes-200,348, Elements-193,200</li> </ul> </li> <li>Features: FD, CD, SD</li> <li>Validations: FF, SP</li> <li>Original Release: 12/21/2000</li> </ul>	
2010 Toyota Yaris (1100C)  • Weight: 1,100 kg (2,420 lb)  • CG 1,004 mm rear, 569 mm high  • Model Parameters: Parts-771, Nodes-998,218, Elements-974,348  • Features: FD, CD, SD, IM  • Validations: FF, OF, MDB, SI, IP, SP, SC, ST, OT  • Release Date: 12/02/2011	0
<ul> <li>Weight: 2,000 kg (4,410 lb)</li> <li>CG 664 mm (26.14 in.)</li> <li>Model Parameters:         <ul> <li>Parts-248, Nodes-66,684, Elements-58,400</li> </ul> </li> <li>Features: FD, CD, SD</li> <li>Validations: FF, SP, SC, ST</li> <li>Original Release: 12/12/2000; 11/03/2008</li> </ul>	0
<ul> <li>2007 Chevrolet Silverado Pickup Truck (2270P)</li> <li>Weight: 2,270 kg (5,000 lb)</li> <li>CG 736 mm (28.8 in.)</li> <li>Model Parameters:         <ul> <li>Parts-606, Nodes-261,892, Elements-251,241</li> </ul> </li> <li>Features: FD, CD, SD, IM</li> <li>Validations: FF, IP, SP, SC, ST, OT</li> <li>Original Release: 2/27/2009</li> </ul>	
Validations Legend  FF: NCAP Full Frontal  OF: Offset Frontal  SI: Side Impact  MDB: Modified Deformable Barrier  IP: Inertial Parameters  SP: Spring Response  SC: Suspension Components  ST: Suspension Tests (full-scale)  OT: Other	Features Legend      FD: Fine Detail Version      CD: Coarse Detail Version      SD: Suspension Details      IM: Interior Modeled

This model was initially validated following traditional protocols for comparison of the data from the full frontal impact with a vertical wall required under the New Car Assessment Program (NCAP) administered by NHTSA and the simulated results for that test. In addition, the Silverado model was subjected to validation exercises including the following:

- Comparisons of actual and simulated inertial properties
- Front suspension system component tests
- Rear suspension system component tests
- Full-scale speed bump and terrain traversal tests

Data from these tests was useful in enhancing the model and providing quantitative measures that increased confidence in the predictive capabilities for roadside barrier impacts. The results are believed to indicate that this model will provide a sound basis for many types of crash simulation applications in the future.

The FE model of 2270P vehicle is based on the 2007 Chevrolet Silverado 1500 pickup truck. The vehicle used for creating the model was a 4-door crew cab, short box, vehicle with a 4.8L, V8 engine and an automatic 4-speed transmission weighing 2,298 kg. The model was developed through a reverse engineering process. The vehicle was disassembled



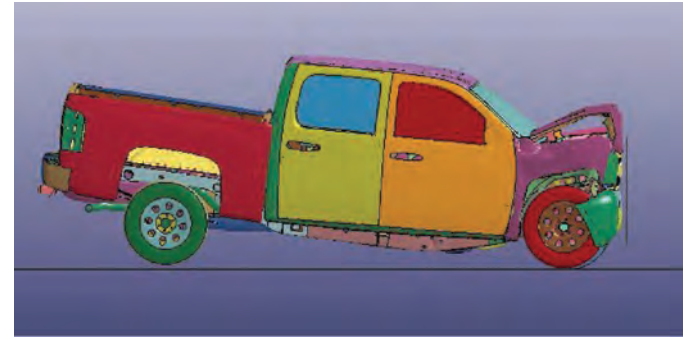
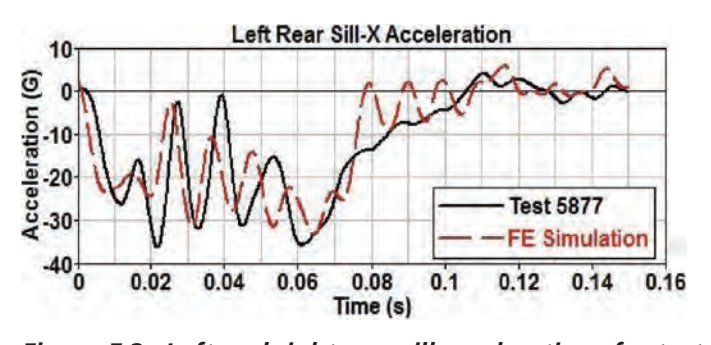


Figure 5.1. Side view of tested vehicle and model after NCAP crash.



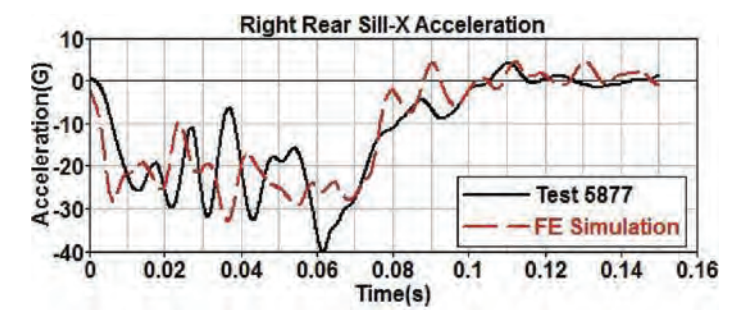


Figure 5.2. Left and right rear sill accelerations for test and simulation.

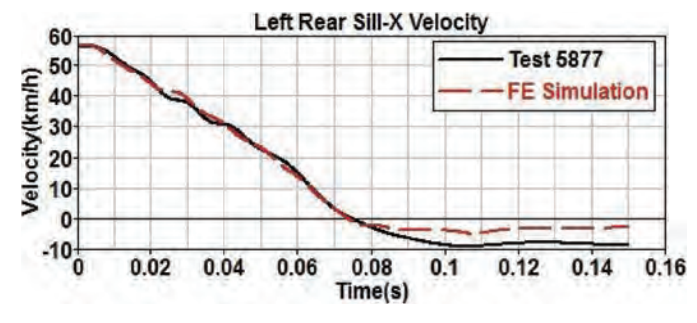
and each part was cataloged, scanned, measured, and classified by material type. Each part was meshed to create an accurate computer model representing the data gathered in the disassembly, including geometry and material properties. Material data and properties were obtained through coupon testing.

Because the Silverado model is primarily used for roadside hardware testing, component testing and simulations were performed to ensure accurate representation of the suspension systems. Over the years, the model has been validated using several full-scale crash tests [NHTSA, NCAP Frontal Barrier Impact—2007 Chevrolet Silverado, NHTSA Test Report 5877; NHTSA, NCAP Side Impact Test—2007 Chevrolet Silverado, NHTSA Test Report 6185; and Insurance Institute for Highway Safety (IIHS) Test CEF0825]. The tests included automotive crashworthiness tests as well as roadside

hardware tests. One sample validation is summarized below. Additional validations are included in Appendix C.

One of the tests that was used for the validations is a NCAP test conducted for NHTSA (Test 5877). The vehicle in this test impacted a rigid wall at 35 mph in a full frontal impact configuration (90° angle). The simulation results were compared with the test results. The simulation yielded similar vehicle kinematics and deformation, as shown in Figure 5.1. Figure 5.2 compares the left and right rear sill accelerations of the test and the simulation. These graphs indicate good correlation between the test and the simulation.

The left and right rear sill velocities were also compared, showing a velocity change of 62 km/h, versus the test, which showed a velocity change of 65 km/h (Figure 5.3). The velocity profiles were similar for both the left and right rear sills, indicating a symmetric response.



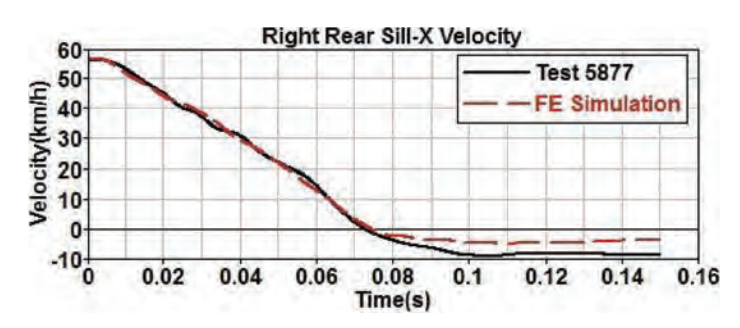


Figure 5.3. Left and right rear sill velocities for test and simulation.





Figure 5.4. Side view of tested vehicle and model after NCAP crash.

#### 5.3.1.2 Toyota Yaris Model (1100C)

This vehicle model was developed to be used in roadside hardware evaluation, as well as in occupant risk and vehicle compatibility analyses (National Crash Analysis Center 2011). It was selected to conform to the MASH requirements for an 1100C test vehicle.

The model was based on a 2010 Toyota Yaris 4-door passenger sedan. Similar to the Silverado model, the vehicle was disassembled and each part was scanned to define its geometry, measured for thickness, and classified by material type. Material data for the major structural components was obtained through coupon testing. A total of 160 tensile tests were performed to generate the material properties for 12 different materials.

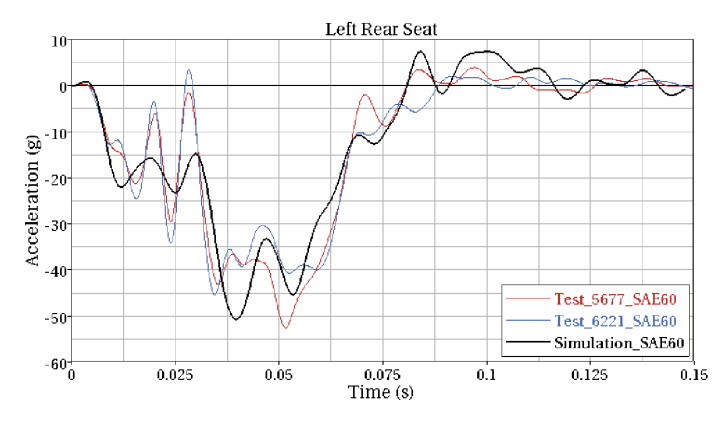
Upon completion of the model development, several automotive full-scale crashworthiness tests were used for validations (NHTSA, NCAP Frontal Barrier Impact—2010 Toyota Yaris, NHTSA Test Report 5677; and NHTSA, NCAP Frontal Barrier Impact—2010 Toyota Yaris, NHTSA Test Report 6221). The model has also been used in roadside hardware impacts as the surrogate for the 1100C test vehicle. A sample validation is summarized below. Additional validations are included in Appendix C.

One of the impact configurations that was used for the Yaris model validations was an NCAP frontal crash into a rigid barrier at 35 mph. Two full frontal NCAP tests were available for validation of the Toyota Yaris FE model in this configuration: Test No. 5677 and Test No. 6221. The overall global deformation pattern of the FE model was very similar to that of the NCAP test, as shown in Figure 5.4. Figure 5.5 compares the left and right rear seat accelerations of the test and the simulation, also indicating similar vehicle behavior between the test and the simulation. The response of the engine during the crash event was captured through two accelerometers. Both the engine top and bottom accelerations in the simulation closely tracked the engine response in the two tests, as shown in Figure 5.6.

#### 5.3.2 Barrier Models

Crash simulation analysis requires FE models of the barriers as well as the impacting vehicles. Three roadside hardware devices were identified as the longitudinal barriers to be studied in this research:

• G4(1S) W-beam guardrail with height < 31 in. Identified as the most commonly used longitudinal barrier for both



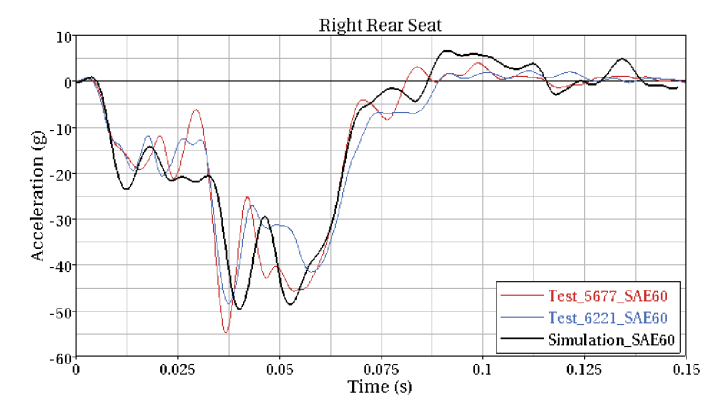
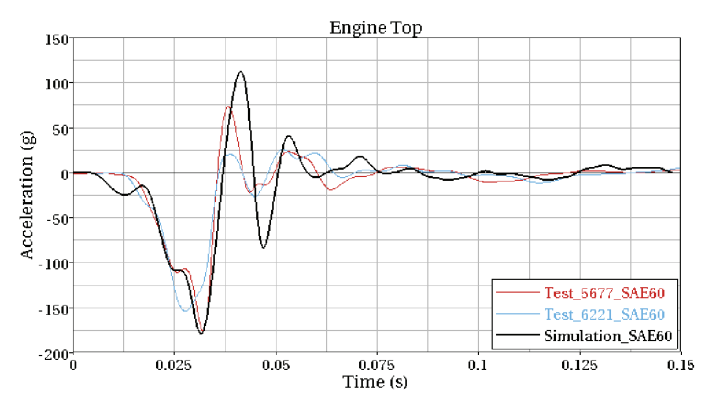


Figure 5.5. Left and right rear sill acceleration for test and simulation.



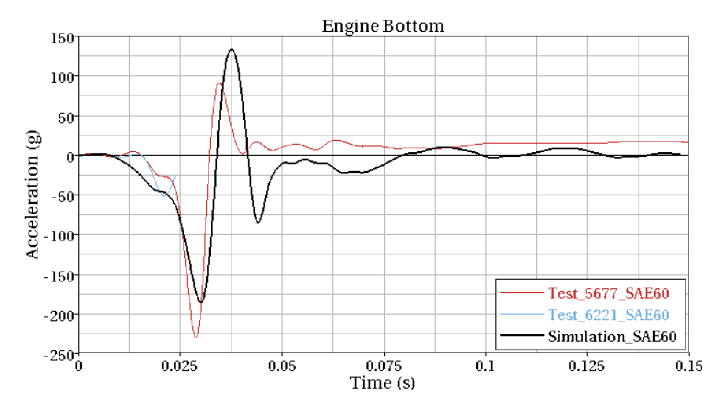


Figure 5.6. Top and bottom engine accelerations for test and simulation.

previously installed and currently being installed barrier on CSRS.

- MGS W-beam guardrail with height ≥ 31 in. Identified as the second most commonly used longitudinal barrier currently being installed on CSRS.
- NJ concrete barriers with heights ≤ 32 in. Identified as the second most commonly used longitudinal barrier for previously installed barrier on CSRS.

FE models that represent the longitudinal barriers listed have been developed and used by the Research Team in previous research (Esfahani et al. 2009; Marzougui et al. 2008b, 2009c, 2010b, 2010c, 2010d, 2011a, 2011b, 2012d). The features of these barrier models are described in the following sections.

#### 5.3.2.1 G4(1S) W-Beam Guardrail Model

This FE model of the G4(1S) was adapted from previous modeling efforts by the Research Team to reflect the specifications for the hardware. This included the specifics for the posts, blockouts, and connectors. The model was based on explicit geometry of all components. Appropriate material and cross sectional properties were assigned to all components to ensure that the correct mass, inertia, and stiffness of the different parts were reflected in the model. The soil was also explicitly modeled using solid elements. The shape of the post was incorporated in the soil mesh to simulate the post/soil interactions. Because the geometry of the bolts was previously found to affect system behavior, the bolts were explicitly incorporated in the model. The model was used in several previous studies and validated against full-scale crash tests.

The rails in this system were made up of standard 12-gauge W-beams with lengths of 3.807 m (12.5 ft). The rails were supported using W150  $\times$  12.6 (W6  $\times$  9) steel posts. These posts were 1,830 mm (72 in.) in length and embedded 1,100 mm

(43.3 in.) into the ground. Wood blockouts were placed between the posts and the W-beam rails and had dimensions of 150 mm  $\times$  200 mm  $\times$  360 mm (6 in.  $\times$  8 in.  $\times$  14 in.). The system level model of the guardrail system was modeled to have a total length of 53.3 m (175 ft) and anchored at both ends using a standard Breakaway Cable Terminal (BCT). The system consisted of 29 posts and 14 W-beam sections. Figure 5.7 depicts some of the details of the model.

#### 5.3.2.2 MGS W-Beam Guardrail Model

The MGS guardrail system used in this research was based on the modified G4(1S) design. A similar modeling approach was used in developing this model with few minor differences. The differences between the two models include the following:

• Rail height was increased to 31 in. by raising the whole G4(1S) system (except for the soil elements) by 2¼ in.

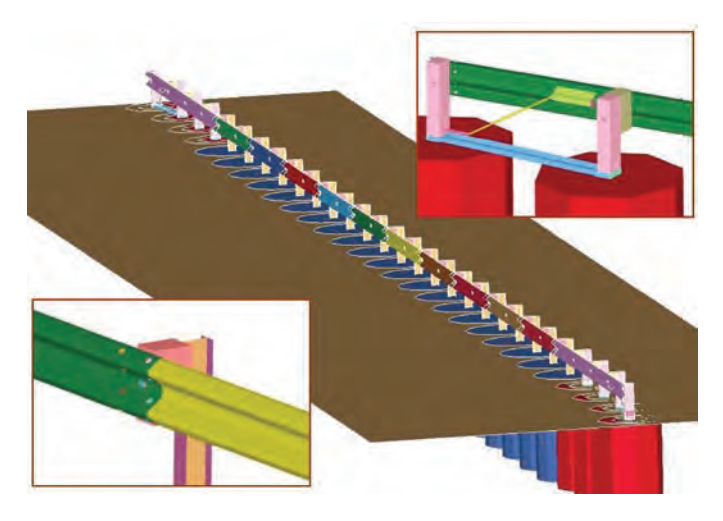


Figure 5.7. G4(1S) strong-post W-beam guardrail model.

64

- Blockouts were changed from 150 mm × 200 mm × 360 mm (6 in. × 8 in. × 14 in.) to 150 mm × 300 mm × 360 mm (6 in. × 12 in. × 14 in.) blocks.
- Rail splices were moved from being at a post to being in between two posts.

The model was also used by the Team in previous studies and validated against full-scale crash tests. Figure 5.8 shows some of the details of the model.

#### 5.3.2.3 NJ Concrete Barrier Model

This FE model of the NJ concrete barrier developed by the Research Team was used for the simulations. The NJ concrete barrier had a height of 32 in. As concrete safety barriers do not deform or deflect even under severe crash conditions, the barrier was modeled using rigid shell elements. For the simulations, the length of barriers was extended to over 150 ft to make sure the vehicle did not reach the end of the barrier before the end of the simulation. The barrier model mesh was refined to sizes between 2 in. and 3 in. to ensure optimum contact between the vehicle and barrier without excessive penetrations. Finer mesh was used at the edges of the barrier. The barrier was fixed to prevent any movement or deformation in the barrier during the crash simulation. The model is shown in Figure 5.9.

# 5.3.3 Barrier Modeling Details

To create the FE models of the barriers, several key features were carefully examined and appropriate modeling techniques were used to ensure that the model was an accurate representation of the actual system. First, explicit geometry of all components of the systems were incorporated in the model. This included the W-beams, posts, blockouts, and

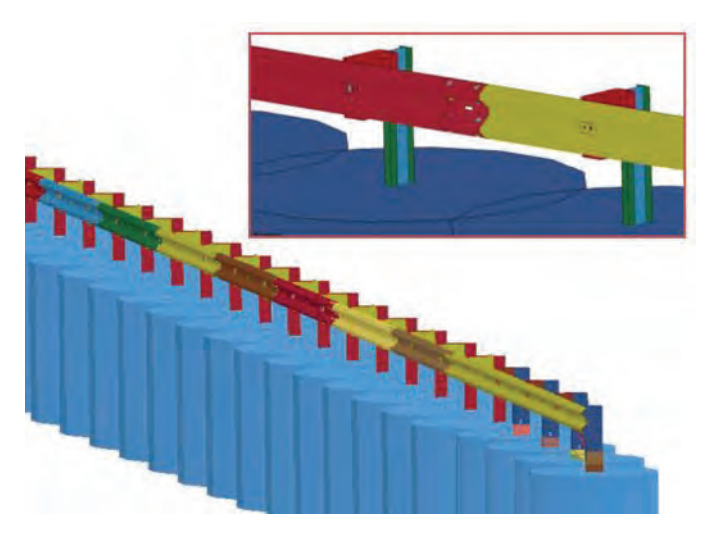


Figure 5.8. MGS strong-post W-beam guardrail model.

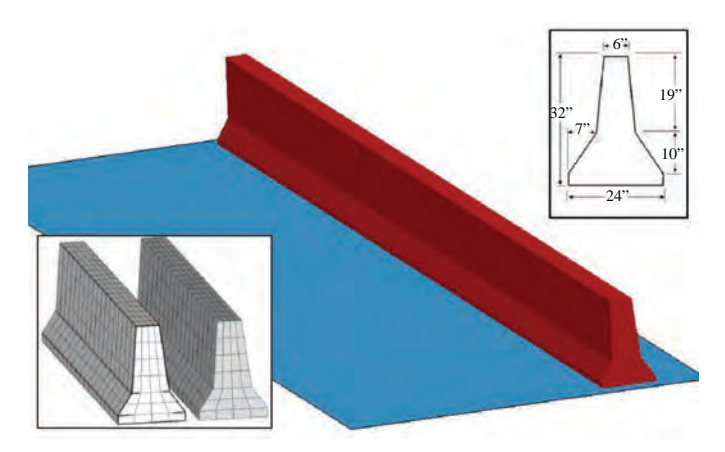


Figure 5.9. NJ concrete median barrier model.

bolts. This ensured the correct mass, inertia, and stiffness of the different parts were reflected in the model. The soil was also explicitly modeled using solid elements. The shape of the post was incorporated in the soil mesh to simulate the post/soil interactions. The geometry of the bolts was found to affect system behavior, so they were explicitly incorporated in the model. These modeling conventions are described in the following paragraphs.

# 5.3.3.1 Modeling of Steel and Soil Elements

Appropriate material and cross sectional properties were assigned to all components of the barrier systems. Rigid material was assumed for the concrete barrier models. For the W-beam guardrail models, two main LS-DYNA material types were used. The metal components, such as the posts and W-beams, were represented as "piecewise linear plasticity" material in LS-DYNA. This material model has been extensively used to represent structural metals, such as steel and aluminum, and it has been fully validated and optimized. The material behavior is isotropic elasto-plastic with strain rate effects and failure. The properties used for these materials were extracted from the literature as well as data from coupon tests that were performed on similar steels. The "soil-andfoam" model in LS-DYNA was used to represent soil properties. The properties used for this model were back-calculated from previously conducted tests. These tests consisted of a bogie vehicle impacting wood and steel posts that are embedded in soil similar to what has been used in the full-scale crash test. Simulations with the same test set ups were performed, and the material properties were varied until acceptable comparisons were achieved between the tests and the simulations.

#### 5.3.3.2 Modeling of W-beam, Post, and Blockouts

A detailed FE model of the steel post with wooden blockout is shown in Figure 5.10(a) and the FE model of the W-beam

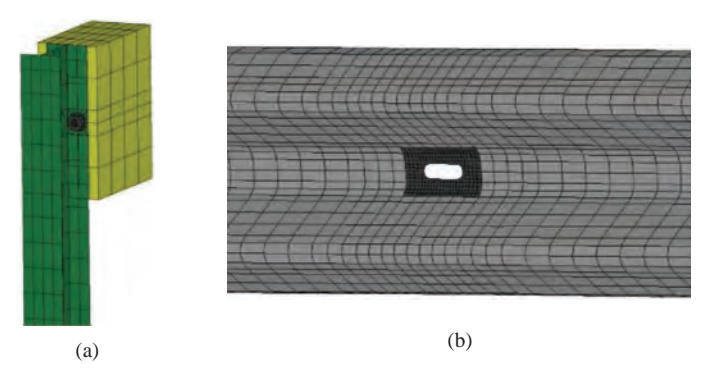


Figure 5.10. FE models of (a) steel post with blockout and (b) W-beam rail.

is shown in Figure 5.10(b). For computational purposes, six rails located at the middle of the entire guardrail system were modeled using fine mesh, while the remaining rails were modeled using coarser mesh. All post and rails were modeled using quadrilateral shell elements. The material formulation used for the rail and post is the isotropic piecewise linear elastic plastic model. Wooden blockouts were modeled using eight node reduced integration hexahedral solid elements. These elements capture the behavior of the model at much less cost, because they consume much less computer time and memory.

# 5.3.3.3 Bolts Modeling

Eight short bolts were used to connect the W-beams together and a long bolt was used to connect the rails to the wooden blockout and post as shown in Figure 5.11. For the small bolts, the material formulation selected for the bolts and nuts was the rigid material formulation. This assumption was made to reduce the computation time, because small elements are needed to capture the geometry of the bolts. These elements would control the time step and lead to larger computation time. By assuming the rigid material model for the bolts, their element size was no longer critical, because rigid elements did not control the time step. A spring was placed between

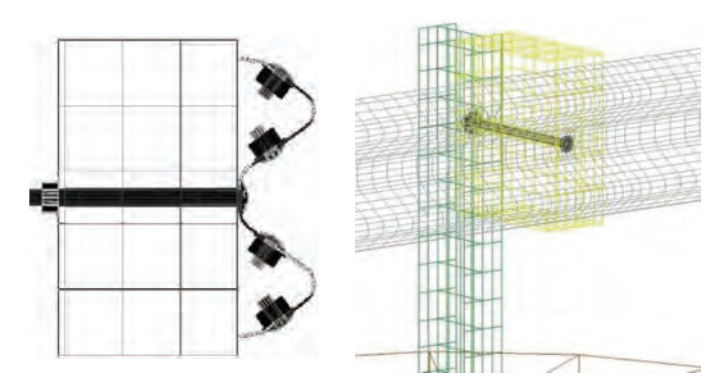


Figure 5.11. FE models of short and long bolts.

the bolt head and the nut to represent the stiffness of the bolt. The properties of these springs were determined from the material properties, cross sectional area, and length of the bolt.

The long bolts have significant effects on the behavior of the system and had to be modeled in detail. To accurately and efficiently represent these bolts, a special modeling technique was utilized in which the bolt was modeled with beam elements to capture its tensile, bending, and shear behavior. By using beam elements, the time step was not controlled by the cross sectional geometry of the bolt. Hence, a larger simulation time step and smaller computation time was needed to reach a solution. An elasto-plastic material model with failure was assigned to the beam elements to simulate the nonlinear and failure behavior of the bolt. The geometry of the bolt is represented by shell elements with "null" material properties. The null shell elements had no effect on the stiffness of the bolts, and their size did not affect the simulation time step. They are used to represent the bolt geometry for only contact purposes. Nodes from shell elements were tied to the beam element nodes to transfer the contact forces.

#### 5.3.3.4 Soil and Soil/Post Model

The soil was modeled as a cylindrical block 2.7 m (9 ft) in diameter and 2.02 m (6.5 ft) in length as shown in Figure 5.12. These dimensions were chosen so that the behavior of the soil and post/soil interaction is accurately captured with reasonable computation time. The outer boundaries of the soil model were constrained using the non-reflection boundary constraint option. This option is often used in modeling an infinite domain and prevents the stress wave from reflecting

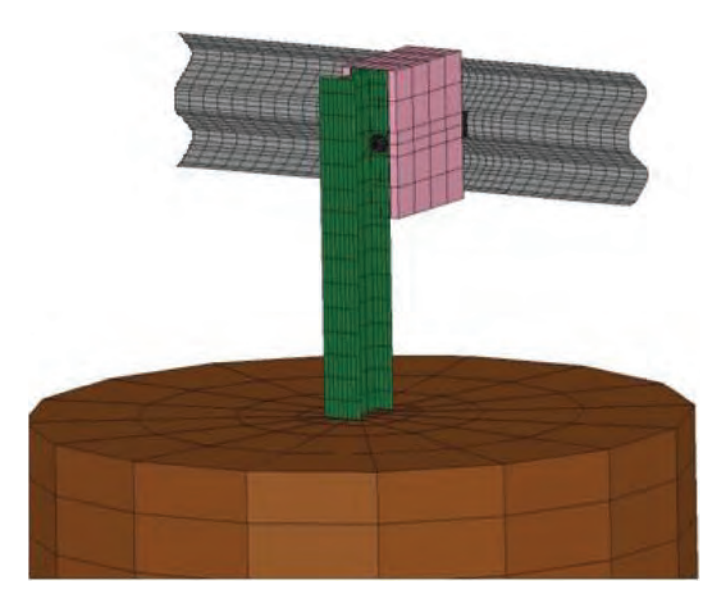


Figure 5.12. Soil model with post and wooden blockout.

at the fixed boundary. The soil block was modeled using eight node hexahedral solid elements. The shape of the post was incorporated into the soil mesh with appropriate flange and web thickness to avoid penetration between post and soil and to have full representation of the post/soil interaction. An automatic single surface sliding interface was defined between the outer faces of the post and inner faces of the soil block to simulate the contact between the post and the soil, and friction between the post and the soil was also included. The material constitutive model used for the soil is the "soil and crushable foam" model.

#### 5.3.4 Crash Simulation Software

The crash simulations were performed using the LS-DYNA nonlinear explicit FE code Version MPP971sR6 on an Intel MPI 3.1 Xeon 64 parallel computer platform. The simulation run times would be expected to vary for other facilities depending on hardware, LS-DYNA version, and precision used.

# **5.4 Computer Model Validations**

Model validation involves simulating a known crash test and comparing the results. A solid validation effort provides confidence that reasonable variations of the model reflecting other situations will yield representative results. For this effort, there were multiple validations for each of the barriers selected for analysis. These made use of the best available crash test data existing at the time of the analysis. Table 5.2 lists the crash tests used for the model validations.

A rigorous verification and validation (V&V) effort was undertaken to provide confidence that the models for each of the three barriers are viable in replicating crashes into barriers on CSRS. The results from the eight comparisons detail the viability or strengths of the validations based on the V&V results. A summary of the validation efforts is provided in Table 5.3, which includes the graphic of vehicle roll, pitch,

and yaw angular rotations and change in vehicle velocity along the x-, y-, and z-directions. Additional comparisons from all seven cases, including side-by-side images from test and simulation at different stages of impact and overlay plots are shown in Appendix C.

V&V analytic comparisons for all seven validation cases were also undertaken based on *NCHRP Web-Only Document 179* (Ray et al. 2010). Roadside Safety Verification and Validation Program (RSVVP) Tables and Phenomena Importance Ranking Tables (PIRTs) were generated. Sample V&V results are included in the next sections. Full V&V reports for each of the seven cases selected are provided in Appendix C.

The validity of the models was assessed by analyzing the distribution of energy associated with the crash event. The laws of physics dictate that the total energy be balanced. Typically, an energy balance graph is generated to assess changes in kinetic, internal, sliding, hourglass, and total energy. All of the comparisons were characterized by the following:

- Relatively constant energy balances were noted suggesting there are no unusual characterizations in the structure of the model that would be an unrealistic sink (point of dissipation) of energy.
- The kinetic energy associated with the motion of the vehicle dropped off as the velocity decreased during the crash.
- Internal energy increased as components of the vehicle absorbed energy through deformation.
- Sliding energy, which is associated to the friction between the vehicle and barrier, increased as expected during the simulations.

All of the V&V criteria for energy balance were met. These aspects led to the conclusion that the model met the fundamental requirements for crash simulation.

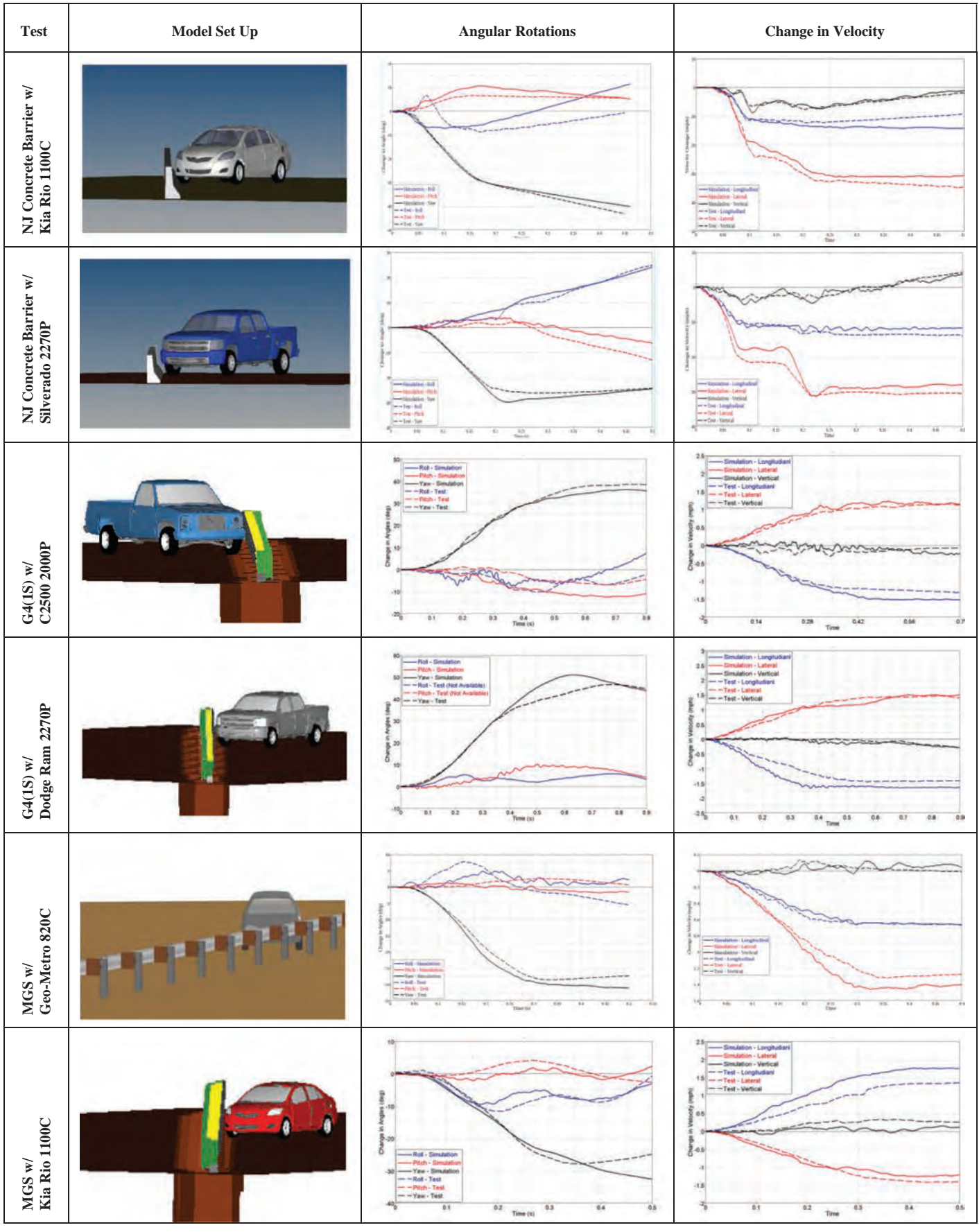
Sample metrics derived from the RSVVP procedure in accordance to NCHRP Web-Only Document 179 are included

Table 5.2. Full-scale crash tests used for validations.

Barrier	Vehicle	Test	Date	Place	Evaluation	Ref
NJ	2002 Kia Rio	2214NJ-1	5/28/04	MwRSF	MASH	Polivka et al. 2006b
Concrete	2007 Silverado	476460-1-4	1/10/09	TTI	MASH	Bullard et al. 2009
G4(1S)	1989 C2500	405421-1	11/16/95	TTI	NCHRP Report 350	Bullard et al. 1996
	2002 RAM	2214WB -2	4/08/05	MwRSF	MASH	Polivka et al. 2006a
MGS	2002 Kia Rio	2214MG-3	11/08/04	MwRSF	MASH	Polivka et al. 2006c
	1994 Geo Metro	NPG-1	6/29/01	MwRSF	NCHRP Report 350	Polivka et al. 2004
	2002 Dodge Ram	2214MG-2	10/06/04	MwRSF	MASH	Polivka et al. 2006d

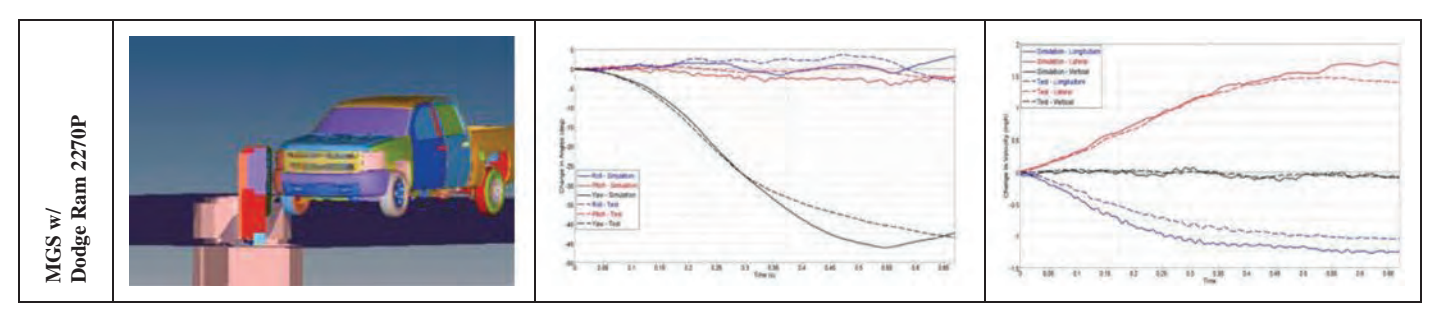
Note: MwRSF = Midwest Roadside Safety Facility; TTI = Texas A&M Transportation Institute.

Table 5.3. Summary validation results—change in vehicle velocities and rotations.



(continued on next page)

Table 5.3. (Continued).



in Figure 5.13. The RSVVP procedure consists of applying statistical tests to determine how well the simulation curves compare with data collected from the test. The figure shows sample results of RSVVP for single-channel (graphs a through f) and multichannel (graph g) comparisons. Various means of comparing the data are shown in each comparison, including the following (moving from the upper left to the lower right):

- Time history plot. The red line indicates the simulated data and the blue line indicates the test data for the crash event. Each data point is a measure of the acceleration recorded.
- Plot of integrated time histories. Integrating the change of acceleration data allows the changes in velocity to be plotted. A general decrease in velocity is noted, as expected, although there is some deviation between the test and the simulation after the impact.
- MPC metrics. This statistical metric provides a measure of "goodness of fit" between the two curves. Three parameters are used for the evaluation: the magnitude (M), phase (P), and comprehensive (C, combined magnitude and phase). A value of less than 40 for M, P, and C is considered passing the criteria.
- ANOVA metrics. Analysis of variance (ANOVA) is also used to compare the test and simulation curves goodness of fit. Two parameters are used for the comparison: the average residual between the curves and the standard deviation of the residuals. Values of less than 5% for the average residual and 35% for the standard deviation are considered passing the criteria. In this example, the metric meets the criteria and hence the boxes are labeled "pass."
- Residuals plots (time history, histogram, and cumulative). These plots show the residual (i.e., difference between the two curves in different forms). In the first plot, time history, the residual is shown versus time. In the second, the residual is shown in a histogram format where the percentage of the residual is plotted against the percentage of its occurrence. In the third plot, the cumulative sum of residuals is plotted.

The program allows various types of single-channel data to be analyzed. The common crash test and simulation metrics compared are as follows:

- X-acceleration: change in acceleration in the original direction of travel of the vehicle
- Y-acceleration: change in acceleration in the lateral direction of travel of the vehicle
- Z-acceleration: change in acceleration in the vertical direction of travel of the vehicle
- Yaw rate: rate of change in original direction of travel of the vehicle
- Roll rate: rate of change in lateral direction of travel of the vehicle
- Pitch rate: rate of change in vertical direction of travel of the vehicle

Because not all measurements have the same importance in the tests, (e.g., in some tests little roll, pitch, or x-acceleration observed), these low magnitude channels could fail the evaluation metrics even if the simulation is valid. To overcome this problem, a multichannel comparison is incorporated in the validation process, where each channel is given a weighting factor based on magnitude. A sample multichannel is shown in Figure 5.13. In this case, the figure indicates that the simulation passes on the multichannel comparison metrics. In addition to graphs shown for the single-channel comparisons, this graph includes relative weights that were computed for each of the channels used on the evaluation. These are used to weight the importance to the overall comparison of the two sets of data (test and simulations).

In addition to RSVVP evaluations comparing the time history from the transducers mounted on the vehicle, *NCHRP Web-Only Document 179* procedure establishes PIRTs aimed at comparing other aspects of the impact such as occupant risk numbers, barrier maximum deflections, and rotations. Table 5.4 shows a sample PIRT comparison. PIRTs for each of the seven cases selected are provided in Appendix C.

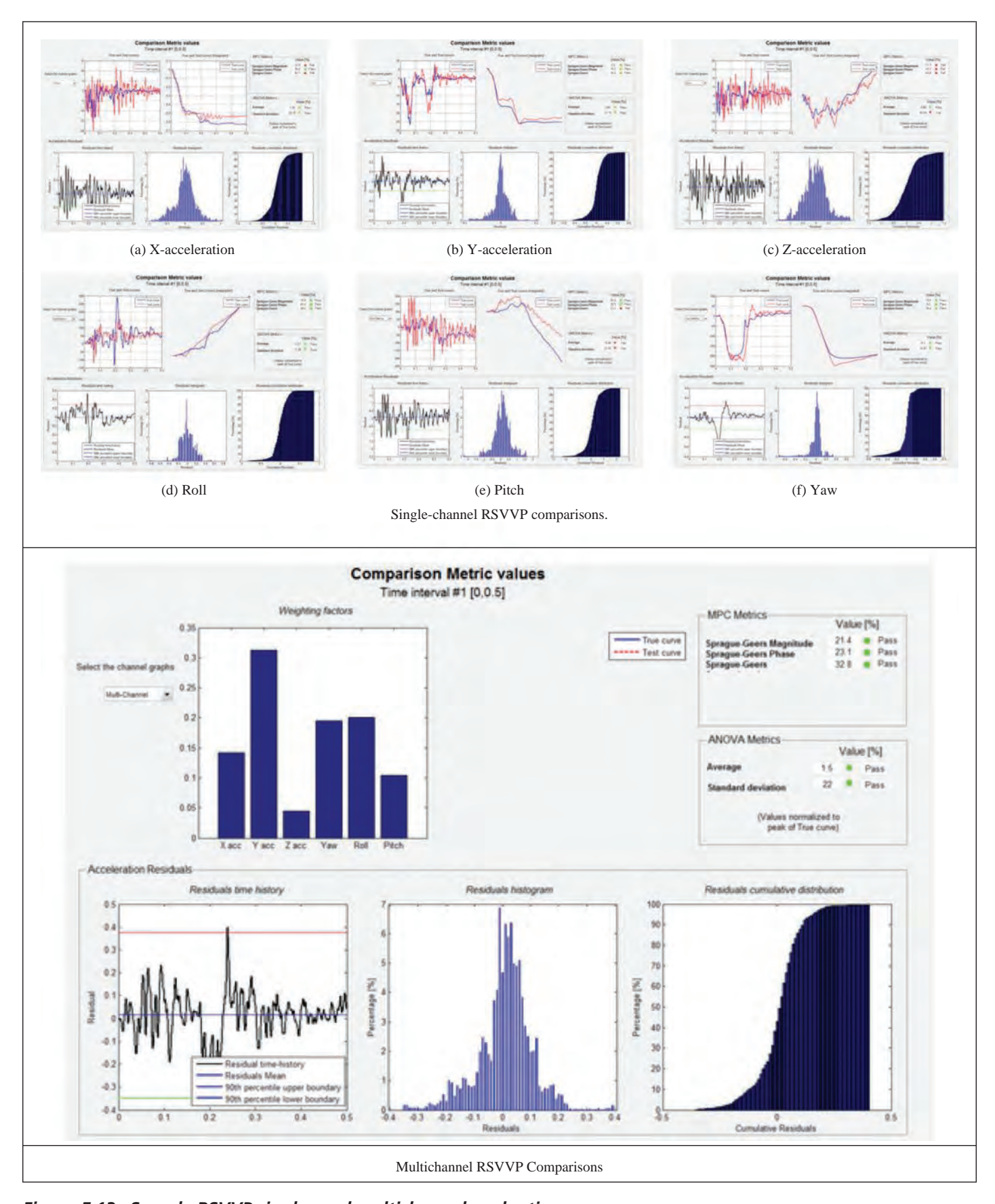


Figure 5.13. Sample RSVVP single- and multichannel evaluations.

Table 5.4. Sample PIRT results from the validations.

			Evaluation Criteria	Known Result	Analysis Result	Relative Diff. (%)	Agree?
		A1	Test article should contain and redirect the vehicle; the vehicle should not penetrate, underride, or override the installation, although controlled lateral deflection of the test article is acceptable.	Yes	Yes		YES
cy		A2	The relative difference in the maximum dynamic deflection is less than 20%.	1 m	0.960 m	4.0 %	YES
Structural Adequacy		A3	The relative difference in the time of vehicle-barrier contact is less than 20%.	0.7 s	0.65 s	7.1 %	YES
ıral A	A	A4	The relative difference in the number of broken or significantly bent posts is less than 20%.	4	4		YES
uct		A5	Barrier did not fail (Answer Yes or No).	Yes	Yes		YES
Str		A6	There were no failures of connector elements (Answer Yes or No).	Yes	Yes		YES
		A7	There was no significant snagging between the vehicle wheels and barrier elements (Answer Yes or No).	No	No		YES
		A8	There was no significant snagging between vehicle body components and barrier elements (Answer Yes or No).	Yes	Yes		YES
	Ī	D	Detached elements, fragments, or other debris from the test article should not penetrate or show potential for penetrating the occupant compartment, or present an undue hazard to other traffic, pedestrians, or personnel in a work zone (Answer Yes or No).	Yes	Yes		YES
		F1	The vehicle should remain upright during and after the collision. The maximum pitch and roll angles are not to exceed 75°.	Yes	Yes		YES
	F	F2	Maximum vehicle roll: relative difference is less than 20% or absolute difference is less than 5°.	10 (0.45 s)	9 (0.35 s)	10% 1°	YES
lisk	_	F3	Maximum vehicle pitch: relative difference is less than 20% or absolute difference is less than 5°.	7 (0.67 s)	12 (0.67 s)	71% 5°	YES
Occupant Risk		F4	Maximum vehicle yaw: relative difference is less than 20% or absolute difference is less than 5°.	38 (0.8 s)	36 (0.72 s)	5.2% 2°	YES
Occu		L1	The occupant impact velocity in the longitudinal direction should not exceed 12 m/sec and the occupant ridedown acceleration in the longitudinal direction should not exceed 20 g.	Yes	Yes		YES
	_	L2	Longitudinal OIV (m/s): Relative difference is less than 20% or absolute difference is less than 2 m/s.	7.1	6.4	9.8% 0.7 m/s	YES
	L	L3	Lateral OIV (m/s): Relative difference is less than 20% or absolute difference is less than 2 m/s.	4.4	5.4	22.7% 1.0 m/s	YES
		L4	Longitudinal ORA (g): Relative difference is less than 20% or absolute difference is less than 4 g.	7.9	11.5	45.6% 3.6 g	YES
		L5	Lateral ORA (g): Relative difference is less than 20% or absolute difference is less than 4 g.	8.4	10.1	20.2% 1.7 g	YES
Vehicle Trajectory	M	M1	The exit angle from the preferable test article should be less than 60% of test impact angle, measured at the time of vehicle loss of contact with test device.	No	No		YES
Veł Traje		M2	Exit angle at loss of contact: relative difference is less than 20% or absolute difference is less than 5°.	16	18	11% 2°	YES

#### **5.5 Crash Simulation Parameters**

The research was initiated to answer a variety of questions over a range of conditions for barriers on CSRS. Over the course of the research, the questions were refined and the focus on critical conditions or situations sharpened. The following sections describe the simulation approach used to establish useful insights and details to get answers to the research questions.

# 5.5.1 Analysis Conditions

The findings of the literature review, state DOT survey, and crash data analysis indicated that there was a large set of parameters that potentially affect the safety performance of longitudinal barriers when placed on CSRS. These were discussed with NCHRP Project 22-29A panel in a review of the VDA. The VDA showed that there are differences in interface effectiveness that can be attributed to the degree of curvature and superelevation, shoulder width and slope, as well as barrier type and placement.

The following sections describe the critical factors associated with roadway conditions, barrier types and placement, and impact conditions that were identified. These parameters and associated ranges were the focus of the simulation efforts. Other parameters were considered after the basic influences were determined.

# 5.5.1.1 Roadway Design Conditions

Deliberations with NCHRP Project 22-29A panel led to defining the primary road design conditions to be analyzed, including curvature and superelevation, shoulder width and slope, and side slope. Various degrees of roadway curvatures reflect the range of superelevation applications commonly found on the highway. These range from tight curves used on ramps to gentle sweeping curves. A total of six roadway curve conditions with different curvatures and superelevations were used in the VDA. These conditions were selected based on the *Green Book* design superelevation tables. The analyses incorporated three superelevations (6%, 8%, and 12%). For each superelevation, two curvatures were selected representing the minimum radii at the 50-mph (80-km/h) and 80-mph (130-km/h) design speeds. The curvatures/superelevation combinations were as follows:

- 614 ft (187 m)/12%
- 2,130 ft (649 m)/12%
- 758 ft (231 m)/8%
- 2,670 ft (814 m)/8%
- 833 ft (254 m)/6%
- 3,050 ft (930 m)/6%

To investigate the effects of roadside shoulder, different shoulder angles and widths were analyzed. Three shoulder widths were considered in the analyses: 4 ft (1.22 m), 8 ft (2.44 m), and 12 ft (3.66 m). Four shoulder angles were included in the analyses: 0%, 3%, 6%, and 8%. An important note here is that the shoulder angle is different than the conventional shoulder slope defined relative to true horizontal plane (see Section 4.4.4). A negative roadside/median slope of 12H:1V relative to shoulder was to be used for all simulations.

# 5.5.1.2 Barrier Types and Placement

The following three types of barriers were investigated (a concrete safety shape and two variations of the strong-post W-beam guardrail based on the state DOT survey responses):

- Concrete barrier: NJ concrete barrier with a height of 32 in. (813 mm)
- Strong-post W-beam guardrail: G4(1S) with heights of 27¾ in. and 29 in. (705 mm and 737 mm)
- Strong-post W-beam guardrail: MGS with a height of 31 in. (787 mm)

Selections of these barriers were made considering the following:

- NJ Concrete Barrier. This classic, widely used concrete safety-shape barrier was a starting point, because vehicle vaulting and rollovers have been attributed to the sloping sides of the barrier profile. The VDA indicated that there would be no underride or override interface issues for the 1100C or 2270P vehicles. However, the NCHRP Project 22-29A panel expressed the concern that the two-stage slopes of the barrier had been seen to cause small vehicle rollovers, so these were simulated. The simulations included both the small car and the pickup truck.
- **G41S W-Beam Barrier**. This widely used barrier was first accepted after the adoption of *NCHRP Report 350*, and it has been widely deployed. Its original design has a height of 27¾ in. The VDA indicated that there could be interface issues for the larger vehicle. Tests with the Silverado and the G4(1S) resulted in vaulting of the barrier. An FHWA technical memorandum in 2010 recommended a nominal height of 29 in. for new installations (Nicol 2010). The simulations were run at both the original height and the 29-in. height recommended by FHWA.
- MGS Barrier. This newer W-beam barrier was designed to accommodate vehicles with higher centers of gravity with a rail height of 31 in. This barrier was accepted by the FHWA in 2005. The VDA indicated that there could be underride interface issues for the small car, so the focus of the simulations was on the 1100C vehicle. There were no simulations for the pickup.

The barriers in all FE simulations were placed at the edge of the "operational" shoulder. Placement further off the shoulder was found to be an uncommon practice.

Three barrier vertical orientations were analyzed including true-vertical orientation, perpendicular to the shoulder surface, and perpendicular to the road surface.

#### 5.5.1.3 Impact Conditions

The following impact conditions were based on MASH for the vehicle types, speed, and angle:

- Vehicle Type
  - 2270P pickup truck: 2007 Chevrolet Silverado model
  - 1100C small car: 2010 Toyota Yaris model
- Impact Conditions
  - Impact angle 25°
  - Impact speed 62 mph (100 km/h)

To limit the number of simulation runs required, the strategy was to use VDA simulation to bracket the potential problem conditions. Based on the VDA results, cases in which there was (1) very poor interface between the vehicle and the barrier and (2) the vehicle was likely to override the barrier were not simulated. Cases that showed marginal or good performance were evaluated using the FE simulations. Other factors that were used to minimize the number of simulations included the following:

- Curvature. There is evidence that the sharper the curvature (smaller radius), the more likely serious crash problems will result. Therefore, the plan was to simulate the midrange curvatures and superelevations [i.e., 758 ft (231 m)/8% and 2,670 ft (814 m)/8%] and, based on the outcome from these simulations, the other curvatures/superelevations would be simulated.
- Impact Angle. Only the usual 25° impact angle was used in the simulations. Higher impact angles were initially investigated, but it was determined that these barriers are not designed for these impact angles and would not likely meet the MASH criteria even for flat surfaces and straight barriers.

- Barrier Offset. Barrier lateral placement was limited to the break point between the shoulder and roadside/median. Even though other placements were initially considered, after consultation with the NCHRP Project 22-29A panel, it was decided that other lateral placements are uncommon.
- **Barrier Height.** Simulations were limited to the standard barrier heights.

Taken together, these factors resulted in more than 150 simulation runs. After summarizing the results and discussing them with the NCHRP Project 22-29A panel, a second round of simulations was undertaken to address concerns. This involved another 100 simulations to investigate other shape concrete barriers and to add depth to the insights developed on the safety performance of barriers on CSRS. Each simulation took between 20 h and 40 h of CPU time to provide detailed analyses of crash events involving typical barriers on CSRS with varying features. Table 5.5 shows the distribution of these simulations. Each simulation has been assigned a case number to facilitate the evaluation process and outline useful analyses and comparisons.

The number of runs in each cell is unequal for various reasons. A main reason was that when the VDA results indicated that there was a "poor interface," the need for FE simulations was less critical. Because it was infeasible to simulate every CSRS condition under consideration given the amount of computing time that would be required, a selection was made based on realistic operational limits.

## 5.5.1.4 Analysis Assumptions

A number of different conditions for road departures were considered. The following assumptions were made prior to the analyses:

- The roadside had a firm surface. Ploughing into the surface by tires was negligible.
- Vehicles were "tracking" as they entered the roadside (i.e., vehicle initial speed is in the same direction as its longitudinal axis).

Table 5.5. Summary of simulation runs.

	Concrete Barrier		G41S W-Beam B	MGS Barrier	
Vehicle	NJ	F Shape	27¾-in. Height	29-in. Height	31-in. Height
Small Car (1100C)	59 Runs (Cases 101–175)	0 Runs	0 Runs	0 Runs	22 Runs (Cases 601–652)
Pickup (2270P)	50 Runs (Cases 201–274)	45 Runs (Cases 901–963)	38 Runs (Cases 801–876)	50 Runs (Cases 301–358)	0 Runs

- There were no driver inputs (e.g., steering, braking) that affect the vehicle.
- The road friction was made identical in all runs using a friction coefficient of 0.9.
- There was a smooth transition between the pavement and shoulder and the shoulder and side slope.

Where these assumptions do not hold, other effects will occur that will alter the stability of the vehicle. Other conditions related to these assumptions could be modeled, but they were not at this stage.

#### 5.5.2 Evaluation Criteria

The performance of the longitudinal barriers in the crash simulations was evaluated in accordance with the criteria presented in MASH. The simulations replicated MASH Test 3-10 for the small car (1,100-kg test vehicle) and MASH Test 3-11 for the pickup truck (2,270-kg test vehicle). The fundamental criteria for crashworthiness evaluation are shown in Table 5.6. These ensure that there is adequate structural integrity of the barrier, all occupant risk metrics are met, and vehicle trajectories are acceptable. The primary difference in this effort was that the barrier was deployed on one of the CSRS configurations previously defined.

For this research, the MASH tests provide a useful immediate and long-term value in the assessment of the performance of barriers used on CSRS. The implications of the MASH (and its predecessors) on performance are well understood because highway engineers have considered a common group of metrics in a structured approach for many years. The simulation approach also provides data that allows other metrics to be analyzed including deformations (barrier

and post deflection), barrier component forces and stresses, and vehicle lift. In addition, simulation technology allows unique views of the vehicle-to-barrier contacts to be generated to better understand unusual results.

# **5.6 Crash Simulation Results**

# 5.6.1 Simulation Analysis Summaries

Figure 5.14 depicts a typical summary of the simulation results. It provides a pictorial view of the impact with a barrier on a CSRS and the resulting behavior of the vehicle. It documents the CSRS conditions including radius, superelevation rate, shoulder width and slope, barrier orientation, and speed and angle of impact. The diagram depicts the time sequence of vehicle and barrier interaction in the crash event. Below the diagram is the MASH evaluation summary, which shows the key metrics generated by the simulation and whether the results passed or failed the MASH criteria. Similar summaries were generated for each of the FE simulations run. The full set of summaries is included in Appendix D.

# 5.6.2 General Comparative Analyses

The simulation results permitted considerations of the influences of curvature, road profile, barrier vertical orientation, impact angle, impact speed, and combinations of these factors on safety performance. The findings provided the basis for formulating barrier design, selection, and installation guidelines. Multiple metrics were generated in the analysis, but all are not documented here. The following sections describe the findings from types of analyses that were undertaken.

Table 5.6. MASH crashworthiness evaluation criteria for simulation analyses.

Structural Adequacy	<b>A:</b> Test article should contain and redirect the vehicle; the vehicle should not penetrate, underride, or override the installation, although controlled lateral deflection of the test article is acceptable.
Occupant Risk	<b>D:</b> Detached elements, fragments, or other debris from the test article should not penetrate or show potential for penetrating the occupant compartment, or present an undue hazard to other traffic, pedestrians, or personnel in a work zone.
	<b>F:</b> The vehicle should remain upright during and after the collision, although moderate roll, pitching, and yawing are acceptable.
	<b>H:</b> The OIV in the longitudinal direction should not exceed 40 ft/s and the ORA in the longitudinal direction should not exceed 20 g.
	<b>I:</b> Longitudinal and lateral ORA should fall below the preferred value of 15.0 <i>g</i> , or at least below the maximum allowed value of 20.49 <i>g</i> .
Vehicle Trajectory	For redirective devices, the vehicle shall exit within the prescribed box.

		2270P - NJ	Concrete Barrier	(102)		
	dius Super 4 ft 12%	Shoulder Width 4 ft	Shoulder Angle 6%	Barrier Orient.  Normal to Road	Speed <b>100 [km/h]</b>	Angle 25°
	Test article should co	entain and redirect the	luation Criteria vehicle; the vehicle	should not penetra	te, underride, o	r
A		on although controlled				Pass
D	potential for penetrat	ragments, or other del				
	pedestrians, or persor	nnel in a work zone.				Pass
Б	The vehicle should re	main upright during a		Max Roll (°)	28.54	
F		main upright during a		Max Roll (°)  Max Pitch (°)	28.54	Pass Pass
	The vehicle should re collision. The maximu 75°.  Longitudinal and later	main upright during a um pitch and roll angl ral OIV should fall be	es are not to exceed low the preferred	` ` `		Pass
F	The vehicle should re collision. The maximu 75°.	main upright during as um pitch and roll anglar ral OIV should fall be a/s), or at least below t	es are not to exceed low the preferred	Max Pitch (°)	23.38	
	The vehicle should re collision. The maximu 75°.  Longitudinal and later value of 30 ft/s (9.1 m	main upright during a um pitch and roll anglar ral OIV should fall be /s), or at least below t /s (12.2 m/s). ral ORA should fall be	low the preferred he maximum	Max Pitch (°) Vx (m/s)	23.38	Pass

Figure 5.14. Sample simulation analysis summary report.

#### 5.6.2.1 Influence of Barrier Orientation

Figure 5.15 depicts typical results for situations with the same radius, superelevation, and shoulder configurations for the NJ concrete barrier but different barrier orientations. The barriers were installed with normal and vertical orientations. The first and second panels provide the MASH results and time sequence diagram for a 2270P vehicle impacting the barrier on a CSRS at 25° and 100 km/h for a tight curve with similar shoulder width conditions. It can be seen that the barrier impact event results in failure due to vehicle roll for the true-vertical orientation case, while the normal orientation case shows a pass. The MASH evaluation results reflect similar unacceptable degrees of maximum vehicle roll (91.77°, exceeding the MASH maximum 75° roll criterion) for the true-vertical orientation and acceptable (28.54°) roll angle for the normal orientation case. The values for OIV and ORA in the longitudinal and lateral directions are similar for both vertical and normal orientation cases and are below the MASH maximum values. Similarly, panels 3 and 4 compare the impact event for the 2270P vehicle for the normal and vertical orientation with a slight shoulder angle change. The results reflect similar patterns, but failures for the true-vertical orientation for both

cases. These results suggest that the normal orientation shows better performance than the true-vertical one for these CSRS conditions using the NJ concrete barrier. The true-vertical orientation also has a higher propensity for vehicle instability.

# 5.6.2.2 Influence of Curvature

Figure 5.16 depicts simulation results from two different radius conditions with similar shoulder configurations for the NJ concrete barrier installed with a normal orientation. The first and third panel provide the MASH results and time sequence diagram for an 1100C vehicle impacting the barrier on a CSRS at 25° and 100 km/h. While there are some scaling differences in the diagrams, it can be seen that the barrier impact event results in similar performance for the 758-ft and 2,670-ft curvatures. The MASH evaluation results also reflect similar degrees of maximum vehicle roll and pitch (e.g., roll 26.59° and 25.85°, and pitch 21.99° and 21.72°). Similarly, the values for OIV and ORA in the longitudinal and lateral directions are the same order of magnitude. Panels 2 and 4 compare the results for the 2270P vehicle. The results reflect comparable degrees of maximum vehicle roll and pitch (e.g.,

	crete; Or	ion: 12%; Shoulder Width: 4 ft; Shoulder Angle: 6% ientation: Normal (N) or True Vertical (V); Speed/Angle: 100kmh/25°
Parameters and Results	Case	Time Sequence View
CSRS: Radius 614 ft, 12% super Vehicle: <b>2270P</b> A – Containment (Pass) D – Detached Elements (Pass) F – Max Roll – 91.77 (Fail) * Max Pitch – 61.09 (Fail) * H – OIV – Vx – -4.67 (Pass) Vy – 7.61 (Pass) I – ORA – Ax –12.34 (Pass) Ay – 18.65 (Pass)	101 V	
CSRS: Radius 614 ft, 12% super Vehicle: 2270P A – Containment (Pass) D – Detached Elements (Pass) F – Max Roll – 28.54 (Pass) Max Pitch – 23.38 (Pass) H – OIV – Vx – -5.29 (Pass) Vy – 8.15 (Pass) I – ORA – Ax – 9.92 (Pass) Ay – 17.65 (Pass)	102 N	
		ion: 6%; Shoulder Width: 4 ft; Shoulder Angle: 8% ation: Normal; Impact Speed/Angle: 100kmh/25°
CSRS: Radius 614 ft, 12% super Vehicle: <b>2270P</b> A – Containment (Pass) D – Detached Elements (Pass) F – Max Roll – 81.65 (Fail)* Max Pitch – 55.67 (Fail)* H – OIV – Vx – -4.73 (Pass) Vy – 7.65 (Pass) I – ORA – Ax – -15.12 (Pass) Ay – -16.55 (Pass)	103 V	
CSRS: Radius 614 ft, 12% super Vehicle: <b>2270P</b> A – Containment (Pass) D – Detached Elements (Pass) F – Max Roll – 29.15 (Pass) Max Pitch – 26.25 (Pass) H – OIV – Vx – -5.47 (Pass) Vy – 8.19 (Pass) I – ORA – Ax – -10.16 (Pass) Ay – 17.69 (Pass)	104 N	

<sup>\*</sup>The combination of high simulated roll and pitch reflect considerable vehicle instability that can result in a rollover in the time after the simulation is terminated.

Figure 5.15. Comparison of barrier orientation effects.

roll 33.66° and 35.84°, and pitch 35.84° and 31.6°). The values for OIV and ORA for the longitudinal and lateral directions are also of a similar order of magnitude. These results suggest that for these CSRS conditions, the NJ concrete barrier performance was similar for these two curvatures.

Figure 5.17 depicts the results for two different radius conditions with similar shoulder configurations for the NJ concrete barrier installed with a true-vertical orientation. The first and third panel provide the MASH results and time sequence diagram for an 1100C vehicle impacting the barrier on a CSRS

at 25° and 100 km/h. It can be observed that the barrier impact event resulted in different performances for the 758-ft and 2,670-ft curvatures. The MASH evaluation results reflect high vehicle roll and pitch for both curvatures (e.g., roll 53.93° and 70.93°, and pitch 58.68° and 81.87°), but only the impacts for the small car on the large radii curve exceeded allowable levels. The values for OIV and ORA for the longitudinal and lateral directions are the same order of magnitude. Panels 2 and 4 compare the impact event for the 2270P vehicle. The results reflect similar degrees of maximum

		relevation: 8%; Shoulder Width: 4 ft; Shoulder Angle: 8%
Parameters and Results	Case	ation: Normal; Impact Speed/Angle: 100kmh/25° Time Sequence View
CSRS: Radius 758 ft, 8% super Vehicle: <b>1100C</b> A – Containment (Pass) D – Detached Elements (Pass) F – Max Roll – 26.59 (Pass) Max Pitch – 21.99 (Pass) H – OIV – Vx – -5.47 (Pass) Vy – 9.76 (Pass) I – ORA – Ax – -3.19 (Pass) Ay – 14.23 (Pass)	224	
CSRS: Radius 758 ft, 8% super Vehicle: 2270P A – Containment (Pass) D – Detached Elements (Pass) F – Max Roll – 33.66 (Pass) Max Pitch – 29.86 (Pass) H – OIV – Vx – 5.39 (Pass) Vy – 8.24 (Pass) I – ORA – Ax – 13.38 (Pass) Ay – 18.43 (Pass)	124	
		vation: 8%; Shoulder Width: 4 ft; Shoulder Angle: 8% tation: Normal; Impact Speed/Angle: 100kmh/25°
CSRS: Radius 2,670 ft, 8% super Vehicle: 1100C A - Containment (Pass) D - Detached Elements (Pass) F - Max Roll - 25.85 (Pass) Max Pitch - 21.72 (Pass) H - OIV - Vx5.49 (Pass) Vy - 9.72 (Pass) I - ORA - Ax3.27 (Pass) Ay13.54 (Pass)	264	
CSRS: Radius 2,670 ft, 8% super Vehicle: <b>2270P</b> A – Containment (Pass) D – Detached Elements (Pass) F – Max Roll – 35.84 (Pass) Max Pitch – 31.6 (Pass) H – OIV – Vx – -5.57 (Pass) Vy – 8.13 (Pass) I – ORA – Ax – -12.09 (Pass) Ay – 18.28 (Pass)	164	

Figure 5.16. Comparison of radius effects for NJ concrete barrier with normal orientation.

vehicle roll and pitch (e.g., roll 57.53° and 59.73°, and pitch 42.15° and 47.05°) for the pickup. The values for OIV and ORA for the longitudinal and lateral directions are the same order of magnitude. These results show a more pronounced roll effect due to the barrier orientation, but not a significant effect due to the difference in curvature.

## 5.6.2.3 Influence of Barrier Type

Figure 5.18, 5.19, and 5.20 depict the different barriers analyzed for increasing curve radii and otherwise similar conditions. Because not all combinations of CSRS conditions were simulated, it is not possible to make impact comparisons across the three barrier types. Variation in the

crash behaviors is apparent, demonstrating that the varying of CSRS parameters influences the vehicle-to-barrier interface and the performance of the barrier. These figures show that the response for the small car and pickup truck varied. For all cases, the OIV and ORA values for the longitudinal and lateral directions are of a similar order of magnitude and direction for the similar barrier type. This may suggest that current barriers can function effectively across a variety of CSRS conditions.

These comparisons show that it is possible to analyze the performance differences across a range of CSRS conditions for typical barriers. It may also be possible to analytically define the influence patterns for safety performance, but that was not possible without simulation results for all combina-

		erelevation: 8%; Shoulder Width: 4 ft; Shoulder Angle: 8%
Parameters and Results	Case	ion: True Vertical; Impact Speed/Angle: 100kmh/25° Time Sequence View
CSRS: Radius 758 ft, 8% super Vehicle: 1100C A – Containment (Pass) D – Detached Elements (Pass) F – Max Roll – 53.93 (Pass) Max Pitch – 58.68 (Pass) H – OIV – Vx – -5.33 (Pass) Vy – 9.59 (Pass) I – ORA – Ax – -4.42 (Pass) Ay – 11.14 (Pass)	223	
CSRS: Radius 758 ft, 8% super Vehicle: <b>2270P</b> A – Containment (Pass) D – Detached Elements (Pass) F – Max Roll – 57.53 (Fail)* Max Pitch – 42.15 (Fail)* H – OIV – Vx – 4.75 (Pass) Vy – 7.89 (Pass) I – ORA – Ax – 10.47 (Pass) Ay – 17.64 (Pass)	123	
		ation: 8%; Shoulder Width: 4 ft; Shoulder Angle: 8%
Barrier: NJ Concrete; C CSRS: Radius 2,670 ft, 8%	Drientation 263	on: True Vertical; Impact Speed/Angle: 100kmh/25°
super Vehicle: 1100C A - Containment (Pass) D - Detached Elements (Pass) F - Max Roll - 70.93 (Fail)* Max Pitch - 81.87 (Fail)* H - OIV - Vx5.14 (Pass) Vy - 9.43 (Pass) I - ORA - Ax4.44 (Pass) Ay - 10.41 (Pass)		L.
CSRS: Radius 2,670 ft, 8% super Vehicle: <b>2270P</b> A – Containment (Pass) D – Detached Elements (Pass) F – Max Roll – 59.73 (Fail)* Max Pitch – 47.05 (Fail)* H – OIV – Vx – –4.83(Pass) Vy – 7.95 (Pass) I – ORA – Ax – 9.71 (Pass) Ay – 18.12 (Pass)	163	

<sup>\*</sup>The combination of high simulated roll and pitch reflect considerable vehicle instability that can result in a rollover in the time after the simulation is terminated.

Figure 5.17. Comparison of radius effects for NJ concrete barrier with true-vertical orientation.

tions of factors. The simulation analysis generated summary tables to reflect the pass/fail patterns across the various CSRS conditions analyzed.

# 5.6.3 Barrier-Specific Results

Performance envelopes were also generated to provide a quantitative assessment of the influence of roadway and barrier design elements on the outcome of the crashes. These included the influences of curvature, road profile, barrier lateral position, barrier vertical orientation, and combinations thereof. The following sections provide a summary of the observations, comparisons, and conclusions drawn from the simulation analyses for each type of barrier. A global set of conclusions is generated to provide a basis for decisions about testing in the next phase of the project and for the development of guidance.

#### 5.6.3.1 Concrete Barrier Results

Table 5.7 contains a summary of the simulation runs that were made for the NJ concrete barrier under the designated

	•	evation: Variable; Shoulder Width: 4 ft; Shoulder Angle: 8% tation: Vertical; Impact Speed/Angle: 100kmh/25°
Parameters and Results	Case	Time Sequence View
CSRS: Radius 614 ft, 12% super Vehicle: 2270P A - Containment (Pass) D - Detached Elements (Pass) F - Max Roll - 54.42 (Pass) Max Pitch - 26.43 (Pass) H - OIV - Vx5.02 (Pass) Vy - 7.86 (Pass) I - ORA - Ax12.32 (Pass) Ay - 17.26 (Pass)	107	
CSRS: Radius 758 ft, 8% super Vehicle: <b>2270P</b> A – Containment (Pass) D – Detached Elements (Pass) F – Max Roll – 62.37 (Fail) Max Pitch – 25.18 (Fail)* H – OIV – Vx – -5.05 (Pass)* Vy – 7.97 (Pass) I – ORA – Ax – -14.75 (Pass) Ay – 17.22 (Pass)	125	
CSRS: Radius 833 ft, 6% super Vehicle: 2270P A - Containment (Pass) D - Detached Elements (Pass) F - Max Roll - 49.51 (Pass) Max Pitch - 20.67 (Pass) H - OIV - Vx4.89 (Pass) Vy - 8.02 (Pass) I - ORA - Ax9.34 (Pass) Ay18.30 (Pass)	133	
CSRS: Radius 2,130 ft, 12% super Vehicle: 2270P A - Containment (Pass) D - Detached Elements (Pass) F - Max Roll - 34.13 (Pass) Max Pitch - 31.01 (Pass) H - OIV - Vx5.14 (Pass) Vy - 8.04 (Pass) I - ORA - Ax10.13 (Pass) Ay - 17.39 (Pass)	151	

<sup>\*</sup>The combination of high simulated roll and pitch reflect considerable vehicle in stability that can result in a rollover in the time after the simulation is terminated.

Figure 5.18. Barrier type effects: NJ concrete barrier.

CSRS parameters and provides the evaluation results derived for the 2270P and 1100C vehicles. The runs covered six different curvatures and superelevation conditions. Four shoulder angles (i.e., slope) and three shoulder width conditions were analyzed. Three barrier orientation conditions were also considered: true vertical, perpendicular to the shoulder surface, and perpendicular to the roadway surface. The cells of the matrix are shaded based on the MASH evaluations for the Test 3-10 and Test 3-11 impact conditions. The cases highlighted in red failed the MASH criteria and those in dark green met the criteria. All cases

that are shaded in light green (with "\*") were assumed to meet the MASH requirements based on having less severe conditions. The clustering of the dark green-shaded cells around the red cell indicate attempts to assess the degree of effects leading to failures.

The following observations are made from the data for cases depicted in this table:

 All failures to meet the MASH requirements for the 1100C and 2270P vehicles resulted from exceeding the maximum allowable roll angle.

		tion: Variable; Shoulder Width: 12 ft; Shoulder Angle: 8%
		: Normal; Impact Speed/Angle: 100kmh/25°
Parameters and Results	Case	Time Sequence View
CSRS: Radius 614 ft, 12%	603	
super	1100C	
Vehicle: 1100C		
A – Containment (Pass)		100
D – Detached Elements (Pass)		
F – Max Roll – 5.23 (Pass)		
Max Pitch – 3.85 (Pass)		
H - OIV - Vx6.74 (Pass)		
Vy – 5.83 (Pass)		
I - ORA - Ax15.50 (Pass)		
Ay – 12.17 (Pass)		
CSRS: Radius 758 ft, 8%	611	
super	1100C	
Vehicle: 1100C		
A – Containment (Pass)		
D – Detached Elements (Pass)		All Control of the Co
F – Max Roll – 5.30 (Pass)		
Max Pitch – 4.52 (Pass)		
H - OIV - Vx6.78 (Pass)		
Vy – 5.88 (Pass)		
I - ORA - Ax17.26 (Pass)		TUITE
Ay – 10.98 (Pass)		
CSRS: Radius 853 ft, 6%	627	
super	1100C	
Vehicle: 1100C	11000	
A – Containment (Pass)		
D – Detached Elements (Pass)		
F – Max Roll – 5.23 (Pass)		
Max Pitch – 5.45 (Pass)		UNIO
H - OIV - Vx8.86 (Pass)		
Vy – 5.68 (Pass)		- A-F
I - ORA - Ax12.42 (Pass)		
Ay – 10.45 (Pass)		
CSRS: Radius 2,670 ft, 8%	641	
super	1100C	
Vehicle: 1100C		
A – Containment (Pass)		
D – Detached Elements (Pass)		
F – Max Roll – 5.21 (Pass)		
Max Pitch – 3.23 (Pass)		
H - OIV - Vx6.88 (Pass)		
Vy – 5.71(Pass)		
I - ORA - Ax18.56(Pass)		C PRO
Ay – 11.86 (Pass)		0-07
CSRS: Radius 3,050 ft, 6%	651	
super	1100C	
Vehicle: 1100C		
A – Containment (Pass)		
D – Detached Elements (Pass)		700
F – Max Roll – 5.30 (Pass)		
Max Pitch – 4.70 (Pass)		
H - OIV - Vx9.98 (Pass)		
Vy – 5.52 (Pass)		
I - ORA - Ax11.77 (Pass)		- Control
Ay – 10.54 (Pass)		
• '	•	

Figure 5.19. Barrier type effects: MGS barrier.

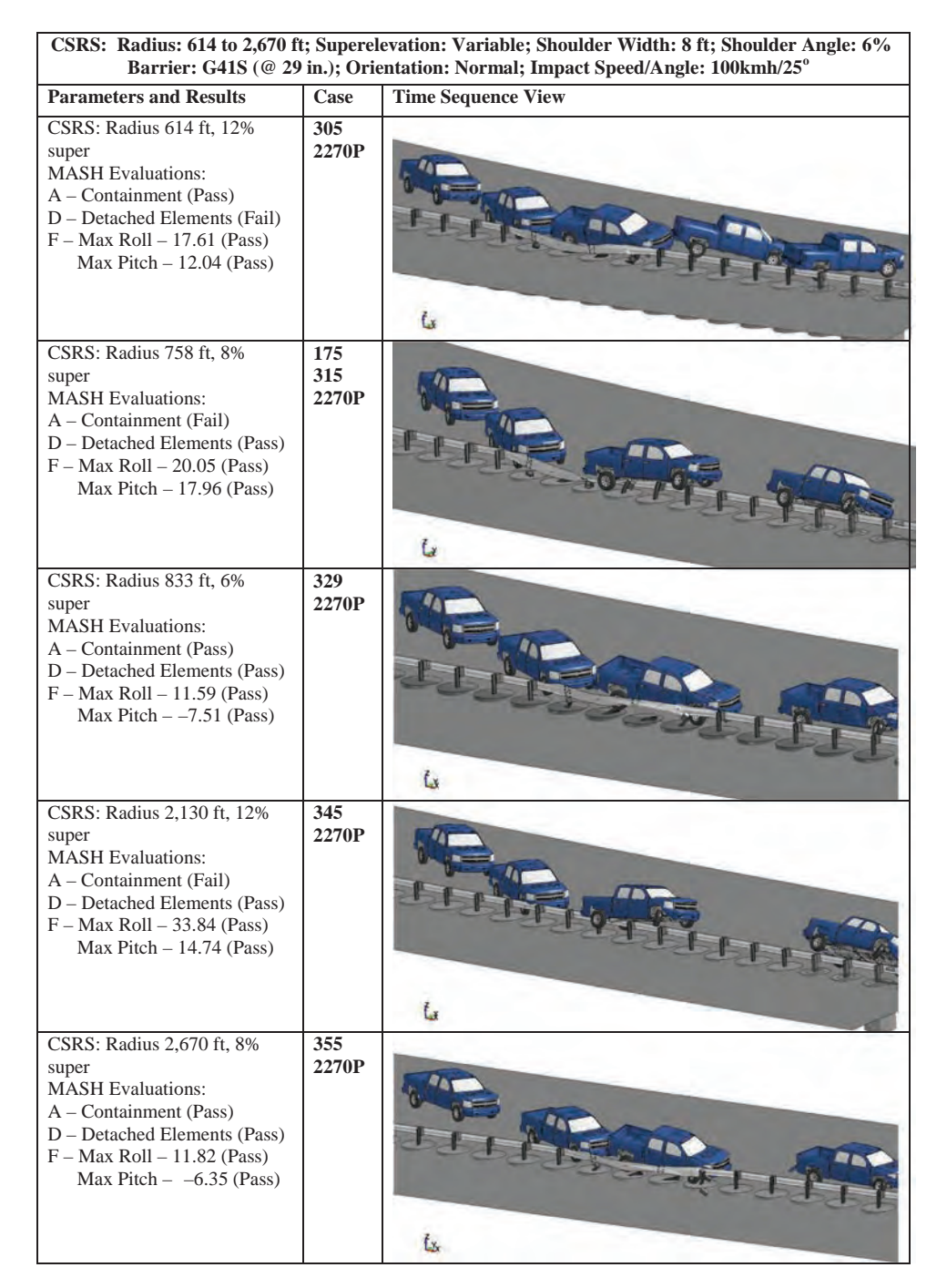


Figure 5.20. Barrier type effects: G41S barrier.

- Most failures occurred when barriers were in true-vertical orientation. There was only one failure when the barrier was oriented normal to shoulder (for the 1100C vehicle) and one when normal to road for the large vehicle.
- More failures were noted with higher superelevation: 12% superelevations had larger number of failures than the 8%, and the 6% superelevation had the lowest number of failures.
- Narrower shoulder widths had more failures than the wider shoulder widths; more failures were noted with the 4-ft than

- the 8-ft shoulder widths, and the 12-ft shoulder width had the lowest number of failed cases.
- The larger the shoulder angle (i.e., the larger the difference in angle between the road and shoulder), the higher the number of failures. The 8% shoulder angle had more cases that failed than the 6%, which had more failed cases than the 3%, and the 0% had the lowest number of failures.

These observations do not reflect the degree of failure. Determining that would be possible by looking at the results

Table 5.7. Performance table for 32-in. NJ concrete barrier.

				Curva	ature/Superel	levation (50 m	nph Design Sp	eeds)		
			614 ft / 12%			758 ft / 8%			833 ft / 6%	
Shoulder Width	Shoulder Angle	FE True Vertical	FE L to Shoulder	FE 1 to Road	FE True Vertical	FE L to Shoulder	FE 1 to Road	FE True Vertical	FE 1 to Shoulder	FE 1 to Road
	0%	Pass*	Pass*	Pass*	Pass*	Pass*	Pass*	Pass*	Pass*	Pass*
	3%	Pass (111)	Pass*	Pass (112)	Pass*	Pass*	Pass*	Pass*	Pass*	Pass*
4ft	6%	Fail (101)	Pass (113)	Pass (102)	Pass (121)	Pass*	Pass (122)	Pass*	Pass*	Pass*
	8%	Fail (103)	Pass (114)	Pass (104)	Fail (123)	Pass (129)	Pass (124)	Pass (131)	Pass*	Pass (132
	0%	Pass*	Pass*	Pass*	Pass*	Pass*	Pass*	Pass*	Pass*	Pass*
	3%	Pass*	Pass*	Pass*	Pass*	Pass*	Pass*	Pass*	Pass*	Pass*
8 ft	6%	Fail (105)	Pass (115)	Pass (106)	Pass (127)	Pass*	Pass (128)	Pass*	Pass*	Pass*
	8%	Fail (107)	Pass (116)	Pass (108)	Fail (125)	Pass (130)	Fail (126)	Fail (233)	Pass*	Pass (134)
	0%	Pass*	Pass*	Pass*	Pass*	Pass*	Pass*	Pass*	Pass*	Pass*
	3%	Pass*	Pass*	Pass*	Pass*	Pass*	Pass*	Pass*	Pass*	Pass*
12 ft	6%	Pass (109)	Pass*	Pass (110)	Pass*	Pass*	Pass*	Pass*	Pass*	Pass*
	8%	Pass*	Pass*	Pass*	Pass*	Pass*	Pass*	Pass*	Pass*	Pass*
				Curva	ature/Superel	evation (80 m	nph Design Sp	eeds)		
			2130 ft / 12%		ature/Superel	evation (80 m 2670 ft / 8%	2000200	eeds)	3050 ft / 6%	
Shoulder Width	Shoulder Angle	FE True Vertical	2130 ft / 12% FE 		FE True Vertical		2000200	FE True Vertical	3050 ft / 6%  FE L to Shoulder	FE Lto Road
	100000000000000000000000000000000000000	FE True	FE ±to	FE 1 to	FE True	2670 ft / 8% FE 	FE Lto	FE True	FE 1 to	FE Lto
Width	Angle	FE True Vertical	FE 1 to Shoulder	FE 1 to Road	FE True Vertical	2670 ft / 8% FE 1 to Shoulder	FE L to Road	FE True Vertical	FE 1 to Shoulder	FE L to Road
	Angle 0%	FE True Vertical Pass*	FE 1 to Shoulder Pass*	FE 1 to Road	FE True Vertical Pass*	2670 ft / 8%  FE	FE 1 to Road	FE True Vertical Pass*	FE 1 to Shoulder Pass*	FE 1 to Road Pass*
Width	Angle 0% 3%	FE True Vertical Pass*	FE 1 to Shoulder Pass*	FE 1 to Road Pass*	FE True Vertical Pass*	2670 ft / 8%  FE	FE 1 to Road Pass*	FE True Vertical Pass*	FE 1 to Shoulder Pass*	FE 1 to Road Pass*
Width	Angle 0% 3% 6%	FE True Vertical Pass* Pass*	FE 1 to Shoulder Pass* Pass* Pass (153)	FE 1 to Road Pass* Pass* Pass (146)	FE True Vertical Pass* Pass*	2670 ft / 8%  FE	FE 1 to Road Pass* Pass*	FE True Vertical Pass* Pass* Pass (171)	FE 1 to Shoulder Pass* Pass*	FE L to Road Pass* Pass*
Width 4 ft	Angle 0% 3% 6% 8%	FE True Vertical Pass* Pass* Fail (145) Fail (147)	FE 1 to Shoulder Pass* Pass* Pass (153) Pass (154)	FE 1 to Road Pass* Pass* Pass (146) Pass (148)	FE True Vertical Pass* Pass* Fail (161) Fail (163)	2670 ft / 8%  FE	FE 1 to Road Pass* Pass* Pass (162) Pass (164)	FE True Vertical Pass* Pass* Pass (171) Pass (173)	FE 1 to Shoulder Pass* Pass* Pass* Pass (175)	FE 1 to Road Pass* Pass* Pass (172 Fail (174)
Width	Angle 0% 3% 6% 8% 0%	FE True Vertical Pass* Pass* Fail (145) Fail (147)	FE Lto Shoulder Pass* Pass* Pass (153) Pass (154) Pass*	FE 1 to Road Pass* Pass* Pass (146) Pass (148) Pass*	FE True Vertical Pass* Pass* Fail (161) Fail (163)	2670 ft / 8%  FE	FE 1 to Road Pass* Pass* Pass (162) Pass (164) Pass*	FE True Vertical Pass* Pass* Pass (171) Pass (173) Pass*	FE Lto Shoulder Pass* Pass* Pass* Pass (175) Pass*	FE Lto Road Pass* Pass* Pass (172 Fail (174) Pass*
Width 4 ft	Angle 0% 3% 6% 8% 0% 3%	FE True Vertical Pass* Pass* Fail (145) Fail (147) Pass*	FE 1 to Shoulder Pass* Pass* Pass (153) Pass (154) Pass*	FE 1 to Road Pass* Pass* Pass (146) Pass (148) Pass*	FE True Vertical Pass* Pass* Fail (161) Fail (163) Pass*	2670 ft / 8%  FE	FE 1 to Road Pass* Pass* Pass (162) Pass (164) Pass*	FE True Vertical Pass* Pass (171) Pass (173) Pass*	FE 1 to Shoulder Pass* Pass* Pass* Pass (175) Pass*	FE 1 to Road Pass* Pass* Pass (172 Fail (174) Pass*
Width 4 ft	Angle 0% 3% 6% 8% 0% 3% 6%	FE True Vertical Pass* Pass* Fail (145) Fail (147) Pass* Pass* Fail (245)	FE I to Shoulder Pass* Pass* Pass (153) Pass (154) Pass* Pass (155)	FE 1 to Road Pass* Pass* Pass (146) Pass (148) Pass* Pass* Pass (150)	FE True Vertical Pass* Pass* Fail (161) Fail (163) Pass* Pass*	2670 ft / 8%  FE	FE 1 to Road Pass* Pass* Pass (162) Pass (164) Pass* Pass*	FE True Vertical Pass* Pass (171) Pass (173) Pass # Pass* Pass*	FE Lto Shoulder Pass* Pass* Pass* Pass (175) Pass* Pass* Pass*	FE I to Road Pass* Pass (172 Fail (174) Pass* Pass*
Width  4 ft	Angle 0% 3% 6% 8% 0% 3% 6% 8%	FE True Vertical Pass* Pass* Fail (145) Fail (147) Pass* Pass* Fail (245) Fail (247)	FE 1 to Shoulder Pass* Pass* Pass (153) Pass (154) Pass* Pass (155) Pass (155)	FE 1 to Road Pass* Pass* Pass (146) Pass (148) Pass* Pass (150) Fail (152)	FE True Vertical Pass* Pass* Fail (161) Fail (163) Pass* Pass* Pass*	2670 ft / 8%  FE	FE 1 to Road Pass* Pass* Pass (162) Pass (164) Pass* Pass* Pass*	FE True Vertical Pass* Pass (171) Pass (173) Pass* Pass* Pass*	FE 1 to Shoulder Pass* Pass* Pass* Pass (175) Pass* Pass* Pass* Pass*	FE I to Road Pass* Pass* Pass (172 Fall (174) Pass* Pass* Pass*
Width 4 ft	Angle 0% 3% 6% 8% 0% 3% 6% 8% 0%	FE True Vertical Pass* Pass* Fail (145) Fail (147) Pass* Pass* Fail (245) Fail (247)	FE 1 to Shoulder Pass* Pass (153) Pass (154) Pass* Pass (155) Pass (155) Pass (156) Pass (157)	FE 1 to Road Pass* Pass* Pass (146) Pass (148) Pass* Pass* Pass (150) Fail (152) Pass (142)	FE True Vertical Pass* Pass* Fail (161) Fail (163) Pass* Pass* Pass* Pass*	2670 ft / 8%  FE	FE 1 to Road Pass* Pass* Pass (162) Pass (164) Pass* Pass* Pass* Pass*	FE True Vertical Pass* Pass (171) Pass (173) Pass* Pass* Pass* Pass* Pass*	FE 1 to Shoulder Pass* Pass* Pass* Pass (175) Pass* Pass* Pass* Pass* Pass*	FE 1 to Road Pass* Pass (172 Fail (174) Pass* Pass* Pass* Pass* Pass*

Notes: \* = Barrier performance extrapolated based on other simulation results. Simulation case numbers are shown in parentheses.

for each of the failed cases. Some efforts to discern the effects of CSRS conditions using analytical means were not successful, given the dispersion effects and interrelationship between factors investigated. These would not reflect other differences in speeds, impact angle, vehicle loading, and driver reactions that are associated with real crashes.

Simulations were also performed for the F-shape concrete barrier. Since the F-shape is known to introduce less vehicle instability than the NJ concrete barrier, only cases where the NJ concrete barrier did not meet MASH requirements were simulated. The results are shown in Table 5.8. When comparing Table 5.7 with Table 5.8, it can be seen that the F-shape shows improved performance over the NJ concrete barrier, although not in a consistent way across all orientations.

#### 5.6.3.2 W-Beam Barrier Results

Table 5.9 contains a summary of the simulation runs made for the W-beam barriers (i.e., G41S and MGS) for various parameters and their results. The runs covered the curvatures and superelevation conditions selected. The same set of shoulder slope and width conditions as the concrete barriers was analyzed. Because W-beam barriers are traditionally installed in a true-vertical orientation, only this case was considered in the performance table. These results are based on analysis of the most critical vehicle. Because there were concerns about underride and pocketing of the small vehicle for the MGS, the simulations were undertaken with the 1100C vehicle. The larger and consequently higher vehicle (2270P) was used for the G4(1S) simulations, because this barrier is more susceptible to overrides. The G4(1S) barrier was initially analyzed based on a barrier height of 27¾ in. All simulation runs made for the barrier at that height led to unacceptable results. The FHWA Technical Memorandum dated May 17, 2010, indicated FHWA's preference for using 29-in.-high barriers over 27¾-in.-high ones and recommended that agencies consider adopting 31-in. barrier designs (Nicol 2010). Consequently, for barrier heights less than 31 in., a height of 29 in. was used in the simulations.

The following observations are made from the data in this table:

- Narrower shoulder widths had more failed cases than the wider shoulders. More failures were noted with the 4-ft shoulder width than the 8-ft shoulder width, and the 12-ft shoulder width had the lowest number of failed cases.
- Larger shoulder angles (i.e., higher difference in angle between the road and shoulder) led to more failures. The 8% shoulder angle had more cases that failed than the 6%, which had more failed cases than the 3%, and the 0% had the fewest failed cases.

- G4(1S) W-beam barriers at 27¾ in. high did not meet MASH requirements for the range of conditions simulated. It was concluded that their performance would not be acceptable for CSRS conditions.
- The G4(1S) W-beam barrier 29 in. high met MASH requirements for most cases where there were wider shoulders. There were 11 failures and 2 marginal results for 4-ft wide shoulders compared with 2 failures for 8-ft shoulders. These all occurred across all radii and superelevations analyzed.
- The higher MGS met the MASH requirements for all cases.
   The 11 simulations undertaken covered a valid cross section of CSRS conditions without a failure.

These observations do not reflect the degree of failure. That would be possible by comparing the detailed simulation results for each of the cases. Marginal passes are indicated by orange shading. Efforts to discern the effects of CSRS conditions using analytical means were not successful given the dispersion effects and interrelationship between factors. These would not reflect other differences in speeds, impact angle, vehicle loading, and driver reactions that are associated with real crashes.

#### 5.7 Conclusions

This effort successfully applied the FE models and crash simulation to analyze the safety performance of longitudinal barriers typically used on CSRS under varying impact conditions. The effort led to the following observations and conclusions:

- For the most part, the VDA results were similar to the selected FE simulations. There was evidence in some cases that the vehicle-to-barrier interface data did not fully reflect safety performance. This can be attributed to the effects of barrier design and placement (e.g., face shape and orientation) that were not explicitly considered in the VDA, as well as the inherent barrier "strength" that was able to redirect a vehicle even if the interface was not ideal.
- These simulations focused on MASH conditions for the general norm of TL-3 for impacts of longitudinal barriers placed on the outside edge of CSRS curves. Thus, the results cover only impacts by the MASH defined small car (1100C) and large pickup truck (2270P).
- This analysis focused on longitudinal barriers deployed on the outside of level curves on typical CSRS across a range of parameters. It focused on meeting MASH TL-3 evaluation criteria that are useful for barrier selection decisions. Deeper analyses of the crash impact dynamics would be needed to assess critical severities and determine means to improve barrier design and placement guidelines.

Table 5.8. Performance table for 32-in. F-shape concrete barrier.

				Curva	ature/Superel	levation (50 m	iph Design Spe	eeds)		
			614 ft / 12%			758 ft / 8%			833 ft / 6%	
Shoulder Width	Shoulder Angle	FE True Vertical	FE 1 to Shoulder	FE 1 to Road	FE True Vertical	FE 1 to Shoulder	FE 1 to Road	FE True Vertical	FE 1 to Shoulder	FE 1 to Road
	0%	Pass*	Pass*	Pass*	Pass*	Pass*	Pass*	Pass*	Pass*	Pass*
	3%	Pass*	Pass*	Pass*	Pass*	Pass*	Pass*	Pass*	Pass*	Pass*
4 ft	6%	Fail (901)	Pass (903)	Pass (902)	Pass*	Pass*	Pass*	Pass*	Pass*	Pass*
	8%	Fail (904)	Pass (906)	Pass (905)	Pass (921)	Pass (923)	Fail (922)	Pass*	Pass*	Pass*
	0%	Pass*	Pass*	Pass*	Pass*	Pass*	Pass*	Pass*	Pass*	Pass*
**	3%	Pass*	Pass*	Pass*	Pass*	Pass*	Pass*	Pass*	Pass*	Pass*
8 ft	6%	Pass (907)	Pass (909)	Pass (908)	Pass*	Pass*	Pass*	Pass*	Pass*	Pass*
	8%	Pass (910)	Fail (912)	Pass (911)	Pass (924)	Pass (926)	Pass (925)	Pass*	Pass*	Pass*
	0%	Pass*	Pass*	Pass*	Pass*	Pass*	Pass*	Pass*	Pass*	Pass*
***	3%	Pass*	Pass*	Pass*	Pass*	Pass*	Pass*	Pass*	Pass*	Pass*
12 ft	6%	Pass*	Pass*	Pass*	Pass*	Pass*	Pass*	Pass*	Pass*	Pass*
	8%	Pass*	Pass*	Pass*	Pass*	Pass*	Pass*	Pass*	Pass*	Pass*
				Curva	ature/Superel	levation (80 m	ph Design Spe	eeds)		
			2130 ft / 12%	47.5	ature/Superel	levation (80 m 2670 ft / 8%	nph Design Spe	eeds)	3050 ft / 6%	
Shoulder Width	Shoulder Angle	FE True Vertical	2130 ft / 12% FE 1 to Shoulder	47.5	FE True Vertical	55 1 S. Cold Total	ph Design Spo FE 1 to Road	FE True Vertical	3050 ft / 6%  FE  L to  Shoulder	FE ⊥to Road
The state of the s	The State of the State of	FE True	FE Lto	FE 1 to	FE True	2670 ft / 8% FE 	FE ⊥to	FE True	FE 1 to	1 to
Width	Angle	FE True Vertical	FE 1 to Shoulder	FE 1 to Road	FE True Vertical	2670 ft / 8% FE to Shoulder	FE 1 to Road	FE True Vertical	FE 1 to Shoulder	⊥to Road
The state of the s	Angle 0%	FE True Vertical Pass*	FE 1 to Shoulder Pass*	FE 1 to Road	FE True Vertical Pass*	2670 ft / 8%  FEt to	FE 1 to Road	FE True Vertical Pass*	FE 1 to Shoulder Pass*	1 to Road Pass*
Width	Angle 0% 3%	FE True Vertical Pass*	FE 1 to Shoulder Pass*	FE 1 to Road Pass*	FE True Vertical Pass*	2670 ft / 8%  FE	FE 1 to Road Pass*	FE True Vertical Pass*	FE 1 to Shoulder Pass*	L to Road Pass* Pass*
Width	Angle 0% 3% 6%	FE True Vertical Pass* Pass*	FE 1 to Shoulder Pass* Pass* Pass (933)	FE 1 to Road Pass* Pass*	FE True Vertical Pass* Pass*	2670 ft / 8%  FE	FE 1 to Road Pass* Pass* Pass (952)	FE True Vertical Pass* Pass*	FE 1 to Shoulder Pass* Pass*	L to Road Pass* Pass*
Width 4 ft	Angle 0% 3% 6% 8%	FE True Vertical Pass* Pass* Fail (931) Fail (934)	FE 1 to Shoulder Pass* Pass* Pass (933) Pass (936)	FE 1 to Road Pass* Pass* Pass (932) Pass (935)	FE True Vertical Pass* Pass* Fail (951) Pass (954)	2670 ft / 8%  FE	FE 1 to Road Pass* Pass* Pass (952) Pass (955)	FE True Vertical Pass* Pass* Pass* Pass*	FE 1 to Shoulder Pass* Pass* Pass* Pass (963)	L to Road Pass* Pass* Pass*
Width	Angle 0% 3% 6% 8% 0%	FE True Vertical Pass* Pass* Fail (931) Fail (934)	FE	FE 1 to Road Pass* Pass* Pass (932) Pass (935) Pass*	FE True Vertical Pass* Pass* Fail (951) Pass (954) Pass*	2670 ft / 8%  FE	FE 1 to Road Pass* Pass* Pass (952) Pass (955) Pass*	FE True Vertical Pass* Pass* Pass* Pass (961) Pass*	FE	L to Road Pass* Pass* Pass* Pass (962 Pass*
Width 4 ft	Angle 0% 3% 6% 8% 0% 3%	FE True Vertical Pass* Pass* Fail (931) Fail (934) Pass*	FE 1 to Shoulder Pass* Pass (933) Pass (936) Pass* Pass*	FE 1 to Road Pass* Pass (932) Pass (935) Pass*	FE True Vertical Pass* Pass* Fail (951) Pass (954) Pass*	Pass* Pass (953) Pass (956) Pass*	FE 1 to Road Pass* Pass* Pass (952) Pass (955) Pass*	FE True Vertical Pass* Pass* Pass* Pass (961) Pass*	FE 1 to Shoulder Pass* Pass* Pass* Pass (963) Pass*	L to Road Pass* Pass* Pass (962 Pass* Pass*
Width 4 ft	Angle 0% 3% 6% 8% 0% 3% 6%	FE True Vertical Pass* Pass* Fail (931) Fail (934) Pass* Pass* Pass (937)	FE 1 to Shoulder Pass* Pass (933) Pass (936) Pass* Pass* Fail (939)	FE 1 to Road Pass* Pass (932) Pass (935) Pass* Pass (938)	FE True Vertical Pass* Pass* Fail (951) Pass (954) Pass* Pass*	2670 ft / 8%  FE	FE 1 to Road Pass* Pass (952) Pass (955) Pass* Pass*	FE True Vertical Pass* Pass* Pass (961) Pass* Pass*	FE 1 to Shoulder Pass* Pass* Pass (963) Pass* Pass* Pass*	L to Road Pass* Pass* Pass (962 Pass* Pass*
Width 4 ft	Angle 0% 3% 6% 8% 0% 3% 6% 8%	FE True Vertical Pass* Pass* Fail (931) Fail (934) Pass* Pass* Pass (937) Pass (940)	FE 1 to Shoulder Pass* Pass (933) Pass (936) Pass* Pass* Fail (939) Fail (942)	FE 1 to Road Pass* Pass (932) Pass (935) Pass* Pass (938) Pass (941)	FE True Vertical Pass* Pass* Fail (951) Pass (954) Pass* Pass* Pass*	Pass* Pass* Pass* Pass* Pass* Pass* Pass (953) Pass (956) Pass* Pass* Pass*	FE I to Road Pass* Pass* Pass (952) Pass (955) Pass* Pass* Pass*	FE True Vertical Pass* Pass* Pass (961) Pass* Pass* Pass* Pass*	FE 1 to Shoulder Pass* Pass* Pass* Pass (963) Pass* Pass* Pass* Pass*	Pass* Pass* Pass* Pass* Pass* Pass* Pass* Pass*
Width 4 ft	Angle 0% 3% 6% 8% 0% 3% 6% 8% 0%	FE True Vertical Pass* Pass* Fail (931) Fail (934) Pass* Pass Pass (937) Pass (940) Fail (943)	FE 1 to Shoulder Pass* Pass (933) Pass (936) Pass* Pass* Fail (939) Fail (942) Pass (945)	FE 1 to Road Pass* Pass (932) Pass (935) Pass* Pass (938) Pass (941) Pass (944)	FE True Vertical Pass* Pass* Fail (951) Pass (954) Pass* Pass* Pass* Pass*	Pass* Pass* Pass* Pass* Pass (953) Pass (956) Pass* Pass* Pass* Pass* Pass*	FE 1 to Road Pass* Pass* Pass (952) Pass (955) Pass* Pass* Pass* Pass*	FE True Vertical Pass* Pass* Pass (961) Pass* Pass* Pass* Pass* Pass*	FE 1 to Shoulder Pass* Pass* Pass (963) Pass* Pass* Pass* Pass* Pass* Pass*	L to Road Pass* Pass* Pass (962 Pass* Pass* Pass* Pass* Pass* Pass*

Notes: \* = Barrier performance extrapolated based on other simulation results. Simulation case numbers are shown in parentheses.

Table 5.9. Performance table for W-beam guardrails.

				Curv	ature/Superel	evation (50 m	ph Design Sp	eeds)		
		614 ft / 12%			758 ft / 8%			833 ft / 6%		
Shoulder Width	Shoulder Angle	MGS (31")	G415 (29")	G41S (27.75")	MGS (31")	G41S (29")	G41S (27.75")	MGS (31")	G41S (29")	G41S (27.75")
4ft	0%	Pass*	Pass*	Fail (806)	Pass*	Pass*	Fail*	Pass (621)	Pass (321)	Fail*
	3%	Pass*	Fail (301)	Fail*	Pass*	Pass*	Fail*	Pass*	Pass*	Fail*
	6%	Pass*	Fail (303)	Fail*	Pass*	Fail (311)	Fail*	Pass*	Fail (323)	Fail*
	8%	Pass*	Fail (305)	Fail*	Pass*	Fail (313)	Fail*	Pass*	Fail (325)	Fail*
	0%	Pass*	Pass*	Fail*	Pass*	Pass*	Fail*	Pass (623)	Pass (327)	Fail*
22	3%	Pass*	Pass*	Fail*	Pass*	Pass*	Fail*	Pass*	Pass*	Fail*
8 ft	6%	Pass*	Pass (307)	Fail*	Pass*	Fail (315)	Fail*	Pass (625)	Pass*	Fail*
	8%	Pass*	Pass (309)	Fail*	Pass*	Pass (317)	Fail*	Pass*	Pass (329)	Fail*
	0%	Pass*	Pass*	Fail*	Pass*	Pass*	Fail*	Pass*	Pass*	Fail*
.2.1	3%	Pass*	Pass*	Fail*	Pass*	Pass*	Fail*	Pass*	Pass*	Fail*
12 ft	6%	Pass (601)	Pass*	Fail*	Pass*	Pass*	Fail*	Pass*	Pass*	Fail*
	8%	Pass (603)	Pass*	Fail (808)	Pass (611)	Pass*	Fail*	Pass (627)	Pass*	Fail*
				Curv	ature/Superel	evation (80 m	ph Design Sp	eeds)		
			2130 ft / 12%		ature/Superel	A TOTAL STREET	ph Design Sp	eeds)	3050 ft / 6%	
Shoulder Width	Shoulder Angle	MGS (31")	2130 ft / 12% G415 (29")		MGS	2670 ft / 8% G41S (29")	ph Design Sp 641S (27.75")	MGS	3050 ft / 6% G41s (29")	G41S (27.75")
		MGS		G41S		2670 ft / 8% G41S	G41S		G41S	(27.75")
	Angle	MGS (31")	G41S (29")	G41S (27.75")	MGS (31")	2670 ft / 8% G41S (29")	G41S (27.75")	MGS (31")	G41S (29")	(27.75")
	Angle 0%	MGS (31") Pass (631)	G41S (29") Pass*	G41S (27.75") Fail*	MGS (31") Pass*	2670 ft / 8% G41S (29") Pass*	641S (27.75") Fail*	MGS (31") Pass*	G41S (29") Pass*	(27.75") Fail (801
Width	Angle 0% 3%	MGS (31") Pass (631) Pass*	G41S (29") Pass*	G41S (27.75") Fail*	MGS (31") Pass*	2670 ft / 8%  G41S (29")  Pass*  Fail*	G41S (27.75") Fail*	MGS (31") Pass*	G41S (29") Pass* Pass*	(27.75") Fail (801 Fail*
Width	Angle 0% 3% 6%	MGS (31") Pass (631) Pass*	G41S (29") Pass* Pass* Fail (331)	G41S (27.75") Fail* Fail*	MGS (31") Pass* Pass*	2670 ft / 8%  G41S (29")  Pass*  Fail*  Fail (341)	G41S (27.75") Fail* Fail*	MGS (31") Pass* Pass*	G41S (29") Pass* Pass* Mar. (351)	(27.75") Fail (801 Fail* Fail* Fail*
Width 4 ft	Angle 0% 3% 6% 8%	MGS (31") Pass (631) Pass* Pass*	G41S (29") Pass* Pass* Fail (331) Fail (333)	G41S (27.75") Fail* Fail* Fail*	MGS (31") Pass* Pass* Pass*	2670 ft / 8%  G41S (29")  Pass*  Fail*  Fail (341)  Fail (343)	G41S (27.75") Fail* Fail* Fail*	MGS (31") Pass* Pass* Pass*	G41S (29") Pass* Pass* Mar. (351) Mar. (353)	(27.75") Fail (801 Fail* Fail* Fail*
Width	Angle 0% 3% 6% 8% 0%	MGS (31")  Pass (631)  Pass*  Pass*  Pass*	G41S (29") Pass* Pass* Fail (331) Fail (333)	G41S (27.75") Fail* Fail* Fail* Fail*	MGS (31") Pass* Pass* Pass* Pass*	2670 ft / 8%  G41S (29")  Pass*  Fail*  Fail (341)  Fail (343)  Pass*	G41S (27.75") Fail* Fail* Fail*	MGS (31") Pass* Pass* Pass* Pass*	G41S (29") Pass* Pass* Mar. (351) Mar. (353) Pass*	(27.75") Fail (801 Fail* Fail* Fail* Fail (802
Width 4 ft	Angle 0% 3% 6% 8% 0% 3%	MGS (31") Pass (631) Pass* Pass* Pass* Pass*	G41S (29") Pass* Pass* Fail (331) Fail (333) Pass*	G41S (27.75") Fail* Fail* Fail* Fail*	MGS (31") Pass* Pass* Pass* Pass* Pass*	2670 ft / 8%  G41S (29")  Pass*  Fail*  Fail (341)  Fail (343)  Pass*  Pass*	G41S (27.75") Fail* Fail* Fail* Fail*	MGS (31") Pass* Pass* Pass* Pass* Pass*	G41S (29") Pass* Pass* Mar. (351) Mar. (353) Pass*	(27.75") Fail (801 Fail* Fail* Fail* Fail (802 Fail*
Width 4 ft	Angle 0% 3% 6% 8% 0% 3% 6%	MGS (31")  Pass (631)  Pass*  Pass*  Pass*  Pass*  Pass*	G41S (29") Pass* Pass* Fail (331) Fail (333) Pass* Pass*	G41S (27.75")  Fail*  Fail*  Fail*  Fail*  Fail*  Fail*	MGS (31") Pass* Pass* Pass* Pass* Pass* Pass*	2670 ft / 8%  G41S (29")  Pass*  Fail (341)  Fail (343)  Pass*  Pass*  Pass*	G41S (27.75") Fail* Fail* Fail* Fail* Fail*	MGS (31") Pass* Pass* Pass* Pass* Pass* Pass*	G41S (29") Pass* Pass* Mar. (351) Mar. (353) Pass* Pass*	(27.75") Fail (801 Fail* Fail* Fail* Fail (802 Fail*
Width  4 ft  8 ft	Angle 0% 3% 6% 8% 0% 3% 6% 8%	MGS (31")  Pass (631)  Pass*  Pass*  Pass*  Pass*  Pass*  Pass*  Pass*  Pass (633)	G41S (29")  Pass*  Pass*  Fail (331)  Fail (333)  Pass*  Pass*  Pass (335)	G41S (27.75") Fail* Fail* Fail* Fail* Fail* Fail*	MGS (31") Pass* Pass* Pass* Pass* Pass* Pass* Pass* Pass*	2670 ft / 8%  G41S (29")  Pass*  Fail*  Fail (341)  Fail (343)  Pass*  Pass*  Pass*  Pass (345)	G41S (27.75") Fail* Fail* Fail* Fail* Fail* Fail*	MGS (31") Pass* Pass* Pass* Pass* Pass* Pass* Pass*	G41S (29") Pass* Pass* Mar. (351) Mar. (353) Pass* Pass* Pass*	(27.75") Fail (801 Fail* Fail* Fail (802 Fail* Fail*
Width 4 ft	Angle 0% 3% 6% 8% 0% 3% 6% 8% 0%	MGS (31")  Pass (631)  Pass*  Pass*  Pass*  Pass*  Pass*  Pass*  Pass (633)  Pass*	G41S (29")  Pass*  Pass*  Fail (331)  Fail (333)  Pass*  Pass*  Pass (335)  Mar. (337)	G41S (27.75")  Fail*  Fail*  Fail*  Fail*  Fail*  Fail*  Fail*  Fail*	MGS (31") Pass* Pass* Pass* Pass* Pass* Pass* Pass* Pass* Pass*	2670 ft / 8%  G41S (29")  Pass*  Fail*  Fail (341)  Fail (343)  Pass*  Pass*  Pass*  Pass (345)  Pass*	G41S (27.75")  Fail*  Fail*  Fail*  Fail*  Fail*  Fail*  Fail*  Fail*	MGS (31") Pass* Pass* Pass* Pass* Pass* Pass* Pass* Pass* Pass*	G41S (29")  Pass*  Pass*  Mar. (351)  Mar. (353)  Pass*  Pass*  Pass (355)  Pass*	(27.75") Fail (801 Fail* Fail* Fail (802 Fail* Fail* Fail* Fail*

Notes: \* = Barrier performance extrapolated based on other simulation results. Simulation case numbers are shown in parentheses. Mar. = marginal pass.

- The G41S barrier with a height of 27¾ in. had demonstrated vaulting failures in tests and simulations undertaken in other efforts conducted to demonstrate the efficacy of the MASH requirements. The FHWA also issued a technical memorandum recommending that the height of the barrier be raised to 29 in. to address such problems. These problems were noted in the early simulations for deployments on CSRS, so no further runs were performed. There was no evidence of underride or snagging issues with the small vehicle. The MGS analysis was conducted last and began with a concern of underride issues. The early FE simulation runs showed no evidence of this, so the number of runs was limited.
- Analysis of barrier orientation was an objective of this research. It was noted in the performance envelopes that concrete barriers oriented in true vertical were most likely to fail. It can be noted that there appears to be less vehicle instability for the larger radius curves for either vehicle type, and the impact metrics are similar.
- The number of factors identified at the outset created a very large analysis matrix making it hard to isolate individual effects. For example, the combined effects of shoulder width and slope for the six CSRS curvature and superelevation conditions for the three barriers for large and small vehicles would have required close to 600 simulations. Some additional benchmarking runs might make it possible to get further insights on relative effects.

- The NJ concrete barrier provided sufficient containment and redirection of the large and small impacting vehicles, but there were many cases where rollovers occurred for the small vehicle, probably due to the influence of the barrier's orientation. These rollovers were lower for orientations normal to road surface. There was no indication of vaulting problems for the situations analyzed.
- Secondary analysis of the 32-in. F-shape concrete barrier indicated that their variations in face slope resulted in fewer failures. The analysis did not attempt to determine the specific influence of face slope differences on safety performance.
- The efficacy of the G4(1S) at the 27¾-in. height was assessed in the simulation runs, and a similar pattern of failures for 4-ft shoulders suggests a problem. Given this has been a widely used barrier, additional investigations may be warranted.
- The MGS barrier showed no indication of override issues in the VDA, so there was limited effort to simulate impacts with the large vehicle. The simulations for the small car suggested that underride and snagging are not issues.

These results suggest that there may be isolated safety performance issues associated with the deployment of standard longitudinal barriers on CSRS. In general, the results indicate that current practices provide for reasonable safety expectations for the vehicles considered.

# CHAPTER 6

# **Full-Scale Testing and Results**

## **6.1 Introduction**

Most longitudinal barriers used on U.S. highways have been tested to the generalized requirements under NCHRP Report 350 or MASH. These testing procedures focus on protocols that allow repeatability and convenient comparison of the performance results to the requirements. Because it is considered impractical to test for all conditions under which a barrier might be placed, tests are typically conducted on straight sections and level surfaces because these are the most common. Longitudinal barriers are subjected to impacts with large and small vehicles at the specific speeds associated with a given test level. This implies that not all possible impact conditions are evaluated. Longitudinal barriers used in applications where the road is curved, banked, or the barrier is placed on a surface adjacent to the road are among those situations that have had very limited testing. The literature review found very few references to research or testing for barriers on or near slopes, and there is no known "acceptance" testing for applications in such situations. A clear indication of a safety problem could not be discerned from available crash data, because the crash reports provide limited details about the barriers and the conditions under which they were deployed. However, it would seem that there may be different vehicle-to-barrier interfaces and consequently impacts on the safety performance of the barrier. Further, it was noted that under current practice there seems to be limited guidance for the design, placement, and installation of barriers for CSRS. The limited understanding of the influences of varying curve, roadway, barrier, and placement features provided the impetus for this NCHRP project to analyze barrier performance for deployments of longitudinal barriers on CSRS.

# 6.2 Background

Different types of longitudinal barriers are typically used on CSRS and the roadway and placement conditions vary. The VDA and simulation analyses provided quantitative measures of the barriers and the conditions under which they were likely to have safety issues. While there are many conditions that were candidates for testing, it was possible to conduct a small set of full-scale crash tests to validate the simulation analyses. The results of the simulation analyses were used to select the test cases.

The analyses showed that the NJ concrete barriers were the most override prone of the concrete barriers, so it did not warrant crash testing. Similarly, the MGS barrier due to its greater height showed limited tendency to have safety performance issues. The most common barrier analyzed, the G4(1S) W-beam guardrail, did indicate serious problems in the initial analyses at the 273/4-in. height, and to a lesser degree at the 29-in. height. Thus, the decision was made to focus the testing on the G4(1S) W-beam barrier. The analyses indicated that the propensity for barrier override or underride was lower for higher radius curves across all superelevation conditions. Because the sharpest 641-ft radius curves with 12% superelevation were noted to be rarely used, the focus for the testing was on the 833-ft radius curves with 6% superelevation. Two shoulder widths—4 ft and 8 ft—were selected for testing with the barrier placed at the edge of the shoulder. These cases are highlighted in Table 6.1. These conditions were considered to lie on either side of the boundary between passing and failing. The testing for these options was conducted under the current MASH crashworthiness requirements.

The Research Team recognized that testing the performance of longitudinal barriers on CSRS would present challenges. Therefore, a testing scheme was proposed that would focus on the most critical aspects that influence viability. The essentials of this scheme included the following:

- Select the critical cases for testing, recognizing that it is likely that only two or three tests will be possible under the available project funds.
- Define the critical CSRS conditions to determine the extent of construction needed (e.g., if two different curve radii are

Table 6.1. Simulation summary of the cases selected for testing.

				Curv	ature/Superel	evation (50 m	ph Design Sp	eeds)		
		614 ft / 12%			758 ft / 8%			833 ft / 6%		
Shoulder Width	Shoulder Angle	MGS (31")	G41S (29")	G41S (27.75")	MGS (31")	G41S (29")	G41S (27.75")	MGS (31")	G415 (29")	G415 (27.75")
4 ft	0%	Pass*	Pass*	Fail (806)	Pass*	Pass*	Fail*	Pass (621)	Pass (321)	Fail*
	3%	Pass*	Fail (301)	Fail*	Pass*	Pass*	Fail*	Pass*	Pass*	Fail*
	6%	Pass*	Fail (303)	Fail*	Pass*	Fail (311)	Fail*	Pass*	Fail (323)	Fail*
	8%	Pass*	Fail (305)	Fail*	Pass*	Fail (313)	Fail*	Pass*	Fail (325)	Fail*
	0%	Pass*	Pass*	Fail*	Pass*	Pass*	Fail*	Pass (623)	Pass (327)	Fail*
122	3%	Pass*	Pass*	Fail*	Pass*	Pass*	Fail*	Pass*	Pass*	Fail*
8 ft	6%	Pass*	Pass (307)	Fail*	Pass*	Fail (315)	Fail*	Pass (625)	Pass*	Fail*
	8%	Pass*	Pass (309)	Fail*	Pass*	Pass (317)	Fail*	Pass* (	Pass (329)	Fail*
12 ft	0%	Pass*	Pass*	Fail*	Pass*	Pass*	Fail*	Pass*	Pass*	Fail*
	3%	Pass*	Pass*	Fail*	Pass*	Pass*	Fail*	Pass*	Pass*	Fail*
	6%	Pass (601)	Pass*	Fail*	Pass*	Pass*	Fail*	Pass*	Pass*	Fail*
	8%	Pass (603)	Pass*	Fail (808)	Pass (611)	Pass*	Fail*	Pass (627)	Pass*	Fail*
				Curv	ature/Superel	evation (80 m	ph Design Sp	eeds)		
			2130 ft / 12%		ature/Superel	di anno en circo	ph Design Sp	eeds)	3050 ft / 6%	
Shoulder Width	Shoulder Angle	MGS (31")	2130 ft / 12% 641S (29")		MGS (31")	2670 ft / 8% G41S (29")	ph Design Sp G41S (27.75")	MGS (31")	3050 ft / 6% G41S (29")	641S (27.75")
	the second second second	MGS	G41S	G41S	MGS	2670 ft / 8% G41S	G41S	MGS	G41S	(27.75")
Width	Angle	MGS (31")	G41S (29")	G41S (27.75")	MGS (31")	2670 ft / 8% G415 (29")	G41S (27.75")	MGS (31")	G41S (29")	(27.75")
	Angle 0%	MGS (31") Pass (631)	G41S (29") Pass*	641S (27.75") Fail*	MGS (31") Pass*	2670 ft / 8% G41S (29") Pass*	641S (27.75") Fail*	MGS (31") Pass*	G41S (29") Pass*	(27.75") Fail (801
Width	Angle 0% 3%	MGS (31") Pass (631) Pass*	G41S (29") Pass* Pass*	G41S (27.75") Fail*	MGS (31") Pass*	2670 ft / 8% G41S (29") Pass* Fail*	G41S (27.75") Fail*	MGS (31") Pass* Pass*	G41S (29") Pass*	(27.75") Fail (801 Fail*
Width	Angle 0% 3% 6%	MGS (31") Pass (631) Pass*	G41S (29") Pass* Pass*	G41S (27.75") Fail* Fail*	MGS (31") Pass* Pass*	2670 ft / 8%  G41S (29")  Pass*  Fail*  Fail (341)	G41S (27.75") Fail* Fail*	MGS (31") Pass* Pass*	G41S (29") Pass* Pass* Mar. (351)	(27.75") Fail (801 Fail* Fail* Fail*
Width 4 ft	Angle 0% 3% 6% 8%	MGS (31") Pass (631) Pass* Pass*	G41S (29") Pass* Pass* Fail (331) Fail (333)	G41S (27.75") Fail* Fail* Fail*	MGS (31") Pass* Pass* Pass*	2670 ft / 8%  G41S (29")  Pass*  Fail*  Fail (341)  Fail (343)	G41S (27.75") Fail* Fail* Fail*	MGS (31") Pass* Pass* Pass*	G41S (29") Pass* Pass* Mar. (351) Mar. (353)	(27.75") Fail (801 Fail* Fail* Fail*
Width	Angle 0% 3% 6% 8% 0%	MGS (31")  Pass (631)  Pass*  Pass*  Pass*	G41S (29") Pass* Pass* Fail (331) Fail (333)	G41S (27.75") Fail* Fail* Fail* Fail*	MGS (31") Pass* Pass* Pass* Pass*	2670 ft / 8%  G41S (29")  Pass*  Fail*  Fail (341)  Fail (343)  Pass*	G41S (27.75") Fail* Fail* Fail* Fail*	MGS (31") Pass* Pass* Pass* Pass*	G41S (29") Pass* Pass* Mar. (351) Mar. (353) Pass*	(27.75") Fail (801 Fail* Fail* Fail* Fail (802
Width 4 ft	Angle 0% 3% 6% 8% 0% 3%	MGS (31") Pass (631) Pass* Pass* Pass* Pass* Pass*	G41S (29") Pass* Pass* Fail (331) Fail (333) Pass*	G41S (27.75") Fail* Fail* Fail* Fail*	MGS (31") Pass* Pass* Pass* Pass* Pass*	2670 ft / 8%  G41S (29")  Pass*  Fail*  Fail (341)  Fail (343)  Pass*  Pass*	G41S (27.75") Fail* Fail* Fail* Fail*	MGS (31") Pass* Pass* Pass* Pass* Pass*	G41S (29") Pass* Pass* Mar. (351) Mar. (353) Pass*	(27.75") Fail (801 Fail* Fail* Fail* Fail (802 Fail*
Width 4 ft	Angle 0% 3% 6% 8% 0% 3% 6%	MGS (31")  Pass (631)  Pass*  Pass*  Pass*  Pass*  Pass*	G41S (29") Pass* Pass* Fail (331) Fail (333) Pass* Pass*	G41S (27.75") Fail* Fail* Fail* Fail* Fail* Fail* Fail*	MGS (31") Pass* Pass* Pass* Pass* Pass* Pass*	2670 ft / 8%  G41S (29")  Pass*  Fail*  Fail (341)  Fail (343)  Pass*  Pass*	G41S (27.75") Fail* Fail* Fail* Fail* Fail* Fail* Fail*	MGS (31") Pass* Pass* Pass* Pass* Pass* Pass*	G41S (29") Pass* Pass* Mar. (351) Mar. (353) Pass* Pass*	(27.75") Fail (801 Fail* Fail* Fail* Fail (802 Fail*
Width  4 ft  8 ft	Angle 0% 3% 6% 8% 0% 3% 6% 8%	MGS (31")  Pass (631)  Pass*  Pass*  Pass*  Pass*  Pass*  Pass*  Pass*  Pass (633)	G41S (29")  Pass*  Pass*  Fail (331)  Fail (333)  Pass*  Pass*  Pass (335)	G41S (27.75") Fail* Fail* Fail* Fail* Fail* Fail*	MGS (31") Pass* Pass* Pass* Pass* Pass* Pass* Pass* Pass*	2670 ft / 8%  G41S (29")  Pass*  Fail*  Fail (341)  Fail (343)  Pass*  Pass*  Pass*  Pass (345)	G41S (27.75")  Fail*  Fail*  Fail*  Fail*  Fail*  Fail*  Fail*  Fail*	MGS (31") Pass* Pass* Pass* Pass* Pass* Pass* Pass* Pass*	G41S (29") Pass* Pass* Mar. (351) Mar. (353) Pass* Pass* Pass*	(27.75") Fail (801) Fail* Fail* Fail (802) Fail* Fail* Fail*
Width 4 ft	Angle 0% 3% 6% 8% 0% 3% 6% 8% 0%	MGS (31")  Pass (631)  Pass*  Pass*  Pass*  Pass*  Pass*  Pass*  Pass*  Pass (633)  Pass*	G41S (29")  Pass*  Pass*  Fail (331)  Fail (333)  Pass*  Pass*  Pass (335)  Mar. (337)	G41S (27.75")  Fail*  Fail*  Fail*  Fail*  Fail*  Fail*  Fail*  Fail*  Fail*	MGS (31") Pass* Pass* Pass* Pass* Pass* Pass* Pass* Pass* Pass*	2670 ft / 8%  G41S (29")  Pass*  Fail*  Fail (341)  Fail (343)  Pass*  Pass*  Pass*  Pass (345)  Pass*	G41S (27.75")  Fail*  Fail*  Fail*  Fail*  Fail*  Fail*  Fail*  Fail*  Fail*	MGS (31")  Pass*  Pass*  Pass*  Pass*  Pass*  Pass*  Pass*  Pass*  Pass*	G41S (29")  Pass*  Pass*  Mar. (351)  Mar. (353)  Pass*  Pass*  Pass (355)  Pass*	(27.75") Fail (801) Fail* Fail* Fail (802) Fail* Fail* Fail* Fail*

Notes: \* = Barrier performance extrapolated based on other simulation results.

Simulation case numbers are shown in parentheses.

Mar. = marginal passing.

considered, it will be necessary to incur expenses to tear down the first road set up and build a second roadway set up).

- Use vehicle dynamics analyses results to determine the appropriate vehicle launch position and speed to reflect the desired impact conditions in the "free-wheeling" mode. Simulation would be used to estimate the necessary "launch" or "release" speed from the track accelerator to attain the required MASH speed at the barrier impact point (or at least within speed tolerances).
- A sloped transition section (ramp or inclined plane) from the release point on the track accelerator to the impact point was constructed to represent the CSRS. The preliminary VDA suggested that the incline should rise about 2 ft over a 30-ft to 60-ft paved transition section that leads into a 24-ft-wide paved CSRS segment with shoulder.
- The VDA results were used to identify critical combinations of barriers and curve features that may represent critical cases as candidates for testing.
- The CSRS segment was constructed accommodate the installation of an adequate length of barrier for testing. A gentle back slope was placed behind the barrier using fill. Accommodations were made to prevent the impact testing from disrupting the road base or foundation to allow for multiple tests across the roadway.
- Preliminary trajectory tests without barriers were conducted to define the degree of side drift and speed loss that might occur so that barriers could be impacted at or near a 25° angle.
- The barrier was set up to be tested with provisions to capture the normal metrics and any additional items that may be useful to understand barrier safety performance on CSRS.

Specific details were finalized after the preliminary tests confirmed the necessary post positions to meet MASH requirements.

The objective of this task was to provide test data for the analyses of barriers on CSRS to rigorously validate the simulation results of the most critical cases. The critical cases were determined using simulation analysis and the experience of the Team and the NCHRP Project 22-29A panel. Table 6.1 shows the conditions analyzed for the G4(1S) barriers that were considered the most important to test. The 254-m (833-ft) radius with 6% superelevation was a mid-range condition and the tests were bracketed to fall in the area where "pass" and "fail" conditions were noted in the simulation analysis. This was necessary because the project budget limited the efforts to two or three tests. The preliminary launch tests without impacts allowed the vehicles to be reused and thus allowed multiple runs to assess speeds and trajectories that greatly increased the probability that the tests would

be successful. The tests were designed and set up to capture the typical data needed to evaluate TL-3 crashworthiness, as well as additional data to understand vehicle dynamics and barrier interface physics that could be useful in determining critical factors that would influence design and placement for the selected CSRS applications.

This chapter describes the efforts to set up and execute the full-scale tests at the FHWA's Federal Outdoor Impact Laboratory (FOIL) to validate the results of the simulation analyses.

# 6.3 Testing Requirements, Criteria, and Facility

Three full-scale crash tests were conducted. The project costs included three test vehicles, construction of the road section with an 833-ft radius and 6% superelevation for two shoulder widths, and installations of an appropriate length of G4(1S) longitudinal barrier for each test. The two shoulder widths required that the positioning of the posts consider the prescribed critical impact points. The barrier was installed by a commercial barrier contractor following standard practices. The tests were conducted in accordance with MASH requirements. Complete details of the testing are provided in Appendix E. The following sections provide an overview of the tests and the results.

# **6.3.1 MASH Requirements**

The tests were conducted in accordance with the current crashworthiness evaluation protocols and requirements under MASH. The MASH testing requirements and protocols included the following (with variations in italics):

## • Test Set Up.

- Ordinarily, the barrier should be installed so that the impact test can occur on level terrain with an unrestricted area to observe vehicle redirection trajectory after impact per MASH (AASHTO 2009, page 57). These tests varied in that a sloped surface was constructed to represent the condition for a vehicle traversing a CSRS prior to barrier impact.
- Minimum barrier installation lengths shall be sufficient to indicate the maximum deflections and opportunities for snagging or vaulting. The lengths need to be sufficiently long to develop the necessary rail tensions. These vary by type of barrier. For W-beam guardrail (semirigid), the length needs to be no less than 100 ft.
- Soil used for embedment must comply with AASHTO "strong soil" (M 147). Tests were conducted to demonstrate adequate strength.

• Testing Required for Various Test Levels and Applicable Criteria from MASH (AASHTO 2009, Table 2-2). The tests outlined in MASH have varying purposes. Test 10 at any test level is intended to demonstrate that the barrier will provide a continuous strength and capability to redirect the errant vehicle. Concerns focus on underride, wheel snag, rollover, and head slap issues. Test 11 focuses on demonstrating the barrier has adequate strength to restrain heavier vehicles. Rollovers and occupant risk are critical concerns. The test requirements are given in the table below:

Test	Test	Vehicles	Impact Speed	Impact	Evaluation
Level	Number			Angle	Criteria
TL-3	3-10	1100C	62 mph (100 kph)	25°	A, D, F. H, I
	3-11	2270P	62 mph (100 kph)	25°	A, D, F. H, I

- Impact Conditions.
  - Speeds and tolerance limits (62 mph  $\pm$  2.5 mph)
  - Angle  $(25^{\circ} \pm 1.5^{\circ})$
- Test Vehicles (Table 2-1).
  - -1100C: small car (2,450 lb ± 55 lb)
  - 2270P: pickup truck (5,000 lb ± 110 lb)
- · CIPs.
  - Semi-rigid barriers: CIP is determined from charts 2.8 and 2.9 to reflect the design features of the device measured from a hard point such as a post.
- Evaluation Metrics and Instrumentation. The vehicle and test article need to be instrumented according to MASH protocols to capture data in a manner that will allow comparison to similar tests and with the appropriate levels of accuracy.

MASH does not have any specific requirements for testing barriers for installation on curves, but there is general language suggesting that barriers should be tested for non-typical applications (AASHTO 2009, Section 2.2.5). It is assumed that while curvature might influence impact angles, the impacts should be within similar tolerance ranges.

#### 6.3.2 MASH Evaluation Criteria

The performance of the longitudinal barriers in the crash simulations was evaluated in accordance with the criteria presented in MASH. The barrier performance was evaluated on the basis of three factors: structural adequacy, occupant risk, and post-impact vehicle trajectory. For longitudinal barriers, the following evaluation criteria have to be met:

## **Structural Adequacy**

A. Test article should contain and redirect the vehicle or bring the vehicle to a controlled stop; the vehicle should

not penetrate, underride, or override the installation, although controlled lateral deflection of the test article is acceptable.

# Occupant Risk

- D. Detached elements, fragments, or other debris from the test article should not penetrate or show potential for penetrating the occupant compartment, or present an undue hazard to other traffic, pedestrians, or personnel in a work zone. Deformation of, or intrusions into, the occupant compartment should not exceed limits set forth in Section 5.3 and Appendix E of MASH.
- F. The vehicle should remain upright during and after collision. The maximum roll and pitch angles are not to exceed 75°.
- H. OIV should satisfy the following: longitudinal and lateral OIV 30 ft/s (preferred), 40 ft/s (maximum).
- I. ORA should satisfy the following: longitudinal and lateral ORA should be less than 15.0 *g* (preferred), 20.49 *g* (maximum).

# **Vehicle Trajectory**

L. The vehicle shall exit the barrier within the exit box.

The results from each test were used to evaluate the barrier safety performance based on these criteria.

#### 6.3.3 FOIL Test Facility

The FOIL is a full-scale outdoor crash test facility primarily designed to test the impacts of vehicles on roadside safety hardware. The test vehicles are propelled into the barriers using a specially designed hydraulic propulsion system. The vehicles are accelerated on a 220-ft fixed concrete track. The propulsion system is capable of pulling an 8,000-kg vehicle up to 60 mph. A 2270P test vehicle can be brought to a speed in excess of 70 mph. The test vehicles are released into a runout area that is 160 ft  $\times$  320 ft. Barriers up to 450 ft in length (usually at 25° relative to the track) can be installed in the runout area at the end of the track. Figure 6.1 provides an aerial view of the layout of the FOIL facility.

# **6.4 Testing Approach**

# 6.4.1 Roadway Segment Construction and Barrier Installation

Figure 6.2 shows the set up for the preliminary and full-scale tests. A representation of a CSRS (including sloped shoulder) was constructed at the end of the FOIL track adjacent to the runout area. The road section and shoulder were placed at an angle relative to the FOIL track to achieve the



Figure 6.1. Aerial view of the FHWA FOIL facility.

desired impact angle with the barrier. The longitudinal barrier was installed adjacent to the road section at the desired lateral locations and vertical orientation. A transition section was constructed between the track and road section to reflect CSRS conditions and achieve the desired vehicle position and orientation for impact. Prior to barrier installation, iterative preliminary tests were conducted to verify that the desired vehicle release speed (at the end of the FOIL track) and vehicle-to-barrier impact angle could be achieved. The barrier posts were set using these parameters to achieve critical impact point requirements in the tests. The G4(1S) barrier was placed at 4-ft and 8-ft offsets to reflect the selected shoulder widths.

The following were some of the challenges in this set up that influenced construction of the tests:

- The elevation along the barrier line will be uniform for at least the length of the longitudinal barrier installation.
- The area along this line must be wide enough to allow for post installation and provide sufficient operating space for barrier construction equipment.
- The raised inclined plane area needs to have sufficient side slopes to ensure stability of the barrier installation for the impact tests.
- The actual paved area does not need to cover the entire length of the barrier installation but should be wide enough to allow assessment of the exit box.
- The slope and barrier line need to be set to ensure impacts at the nominal 25° angle when the vehicle is launched in a free-wheeling mode.

The exact construction plan was refined in discussions with contractors and barrier installation experts. Ultimately, a CSRS roadway/shoulder section was represented by an asphalt pad that was  $12.2 \text{ m} (140.0 \text{ ft}) \times 7.3 \text{ m} (24.0 \text{ ft})$ . The roadway

portion of the asphalt pad was 4.9 m (16.0 ft) with a 6% super elevation. The shoulder portion of the asphalt pad was 3 m (10.0 ft) with a 2% decline. The entire roadway/shoulder was installed with a 254-m (833-ft) radius road curvature.

# 6.4.2 Test Vehicles

Test vehicles conforming to MASH requirements for 2270P pickup trucks were procured considering age and vehicle features. Older pickups and other vehicles were procured for preliminary tests. The vehicles were inspected to ensure that there was no damage that would influence the test. Measurements were made, instrumentation installed, and all fluids and the battery removed. The dummy, instrument tray, battery box, data acquisition system, and brake system were installed as prescribed. The final weights were recorded on standard forms for recording test data. Instrumentation was certified to have valid current calibrations. Protocols for accelerometers were followed to meet MASH requirements. Other instrumentation was installed to FOIL protocols. A typical test vehicle is shown in Figure 6.3. A description of the test instrumentation and data acquisition systems was fully documented (see Appendix E).

#### 6.4.3 Test Articles

Test articles, namely the G4(1S) barrier, were installed by an established roadside hardware contractor and labeled to monitor the impact effects on parts of the system. Critical to effective testing for this novel roadway set up was ensuring that the critical impact point was achieved. The preliminary tests determined the range of drift that might be expected as the vehicle is in free-wheeling mode traversing the transition section. Using this range of drift, the barrier position was chosen such that the vehicle would make first contact as close

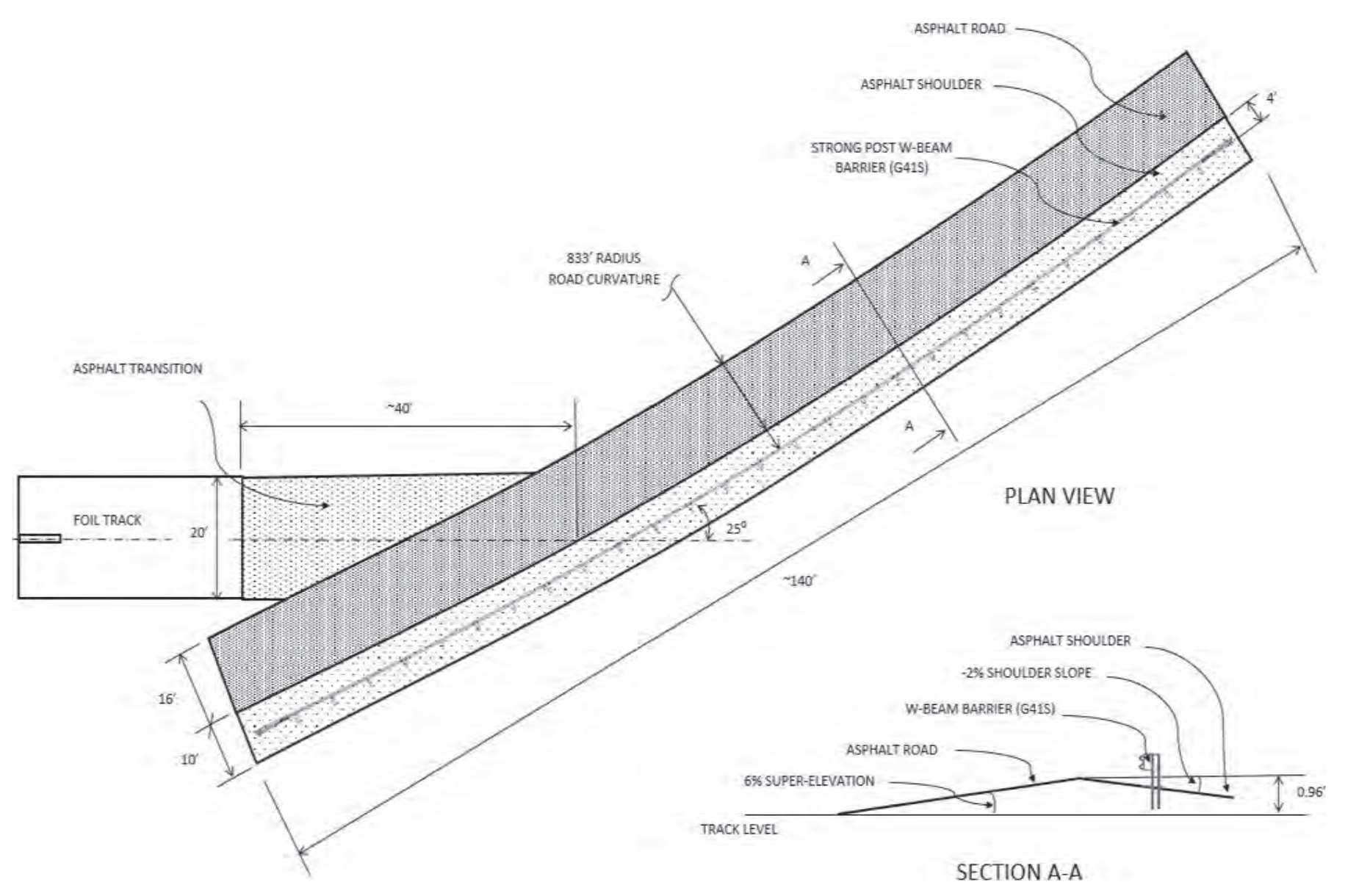


Figure 6.2. Test set up plan for CSRS section constructed for testing at FOIL.



Figure 6.3. Typical MASH 2270P vehicle for crash testing.

as possible to the critical impact point. This was achieved by identifying the intersection point between the expected vehicle trajectory and the barrier line and using it to determine where the first impacted post needed to be installed. The other posts were then positioned relative to this post for the length of the test article installation.

The tested articles consisted of a G4(1S) W-beam guard-rail with 25 standard steel posts and blockouts with 2 Type-T anchor assembly end terminations for a total of 29 posts (Figure 6.4). The spacing of each post was 1.9 m (6 ft 3 in.) for a total length of 53.3 m (175 ft). The top height of the G4(1S) W-beam rail was set at 73.7 cm (29 in.). The posts were embedded with a hydraulic hammer in Virginia Department of Transportation (VDOT) 21A soil, which conforms to the standard for strong soil (Figure 6.5). The photos show multiple views of the installation process and resulting test article and test bed. This process was repeated for tests representing 4-ft and 8-ft shoulders.

Since MASH requires that soil conditions meet specific requirements when the barrier function depends on strength developed through in-ground embedment, an area around each post location was excavated with a 3-ft diameter auger for a depth greater than the expected post embedment. The soil from each of these pits was replaced with strong soil. The strong soil was compacted in 6-in. lifts and nuclear density meter readings were used to ensure full compaction. Additional pendulum testing was conducted as necessary to provide soil condition data.

Soil strength was determined by the specification required in MASH that must be verified before the test is conducted (AASHTO 2009, Chapter 3 and Appendix B). Prior to the full-scale crash testing, dynamic pendulum and static pull testing were conducted in accordance with MASH recom-

mendations to ensure that the soil used in the tests complied with the MASH criteria. The tests consisted of impacting (dynamic) or pulling (static) a W6  $\times$  15 post that is 1.8 m (6 ft) in length and embedded 101.6 cm (40 in.) in standard strong soil. The post was impacted/pulled at a height of 63.5 cm (25 in.) and the load was measured to verify the minimum soil resistance. The minimum dynamic load required for post deflections between 12.5 cm (5 in.) and 63.5 cm (25 in.) is 33-kN (7.5-kip) force. The soil type and compaction procedure were then used for all G4(1S) installations. Static pull tests were conducted the day of the crash test and compared with the previously conducted static pull tests to ensure an adequate strength (higher than 90% of the initial test). These posts were compacted the same day as the test article installation and using the same soil material.

#### 6.4.4 Test Procedures

The tests were set up and performed in accordance with the recommended MASH procedures. High-speed cameras, accelerometers, rate transducers, and speed measuring devices were used to capture the vehicle and barrier responses during the impact. Eight high-speed cameras were used for full-scale crash tests. One camera was placed over the impact region to capture an overhead view. Seven additional cameras were placed at different locations surrounding the impact region to capture left, right, front, rear, and isometric views of the crash event. Two tri-axial accelerometers were mounted at the vehicle center of gravity to measure the x-, y-, and z-accelerations of the vehicle. This data was used to compute the ORAs and OIVs. Additionally, two tri-axial rate transducers were used to measure the vehicle roll, pitch, and yaw. Contact switches were installed on the vehicle and test article to synchronize time zero during the impact for the sensor data and high-speed movies.

For each test, details of the set ups, test execution, and results were documented. The documentation followed the standard protocols established for the FOIL that comply with MASH requirements. The test documentation includes materials describing the test set up and results, as well as various digital images and data from physical measurements or instrumentation installed on the test vehicles and articles. These are provided in Appendix E.

A detailed report documenting all aspects of the tests was generated that included the following information:

- Test Background: A detailed description of the test with multiple images of the test article is provided.
- Test Set Up Description: A detailed description of the set up of the test article in the test setting is provided including description of the elements, their locations, proximity to the test track, and other details. Pictures are also included.

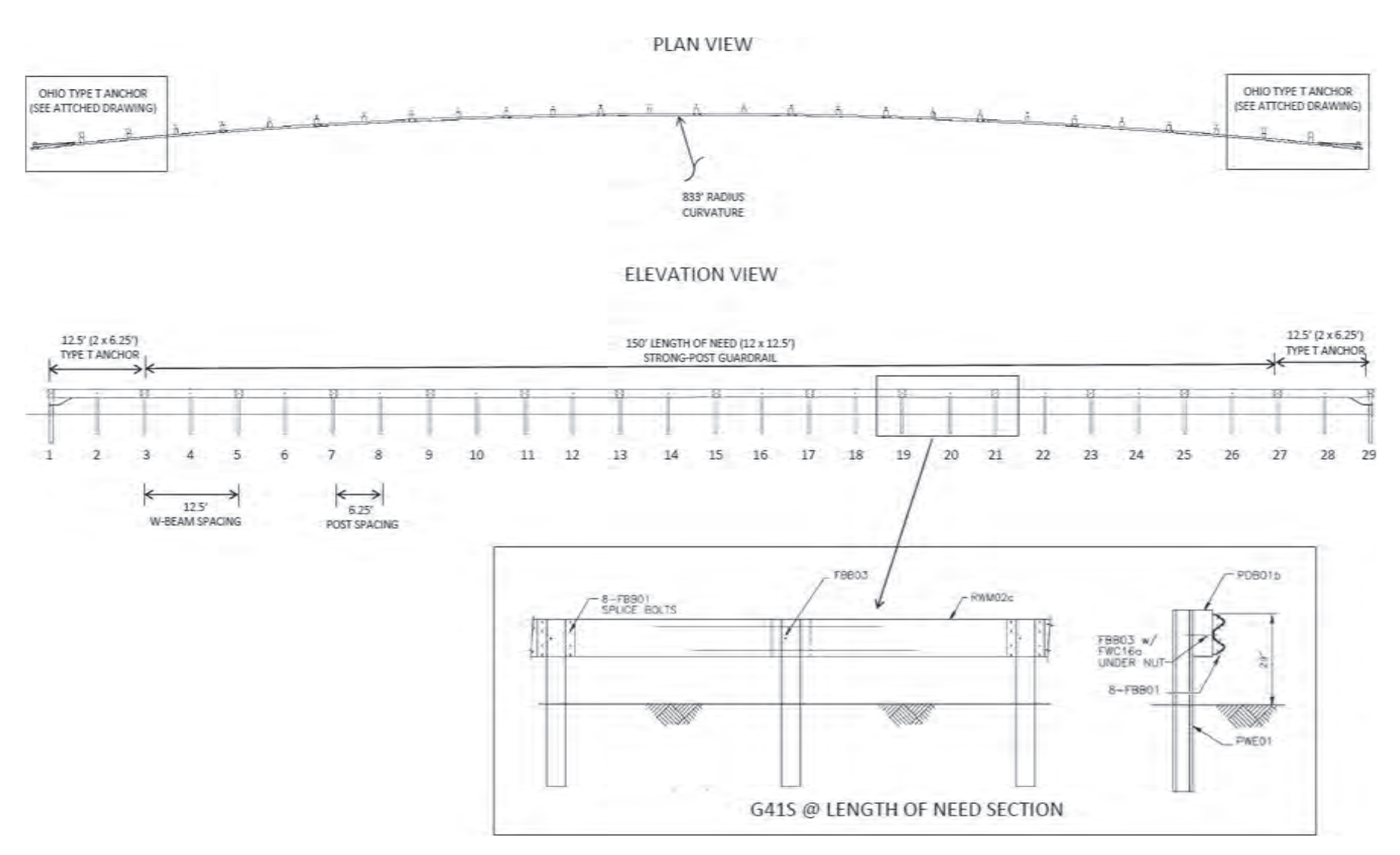


Figure 6.4. CSRS W-beam test article set up.

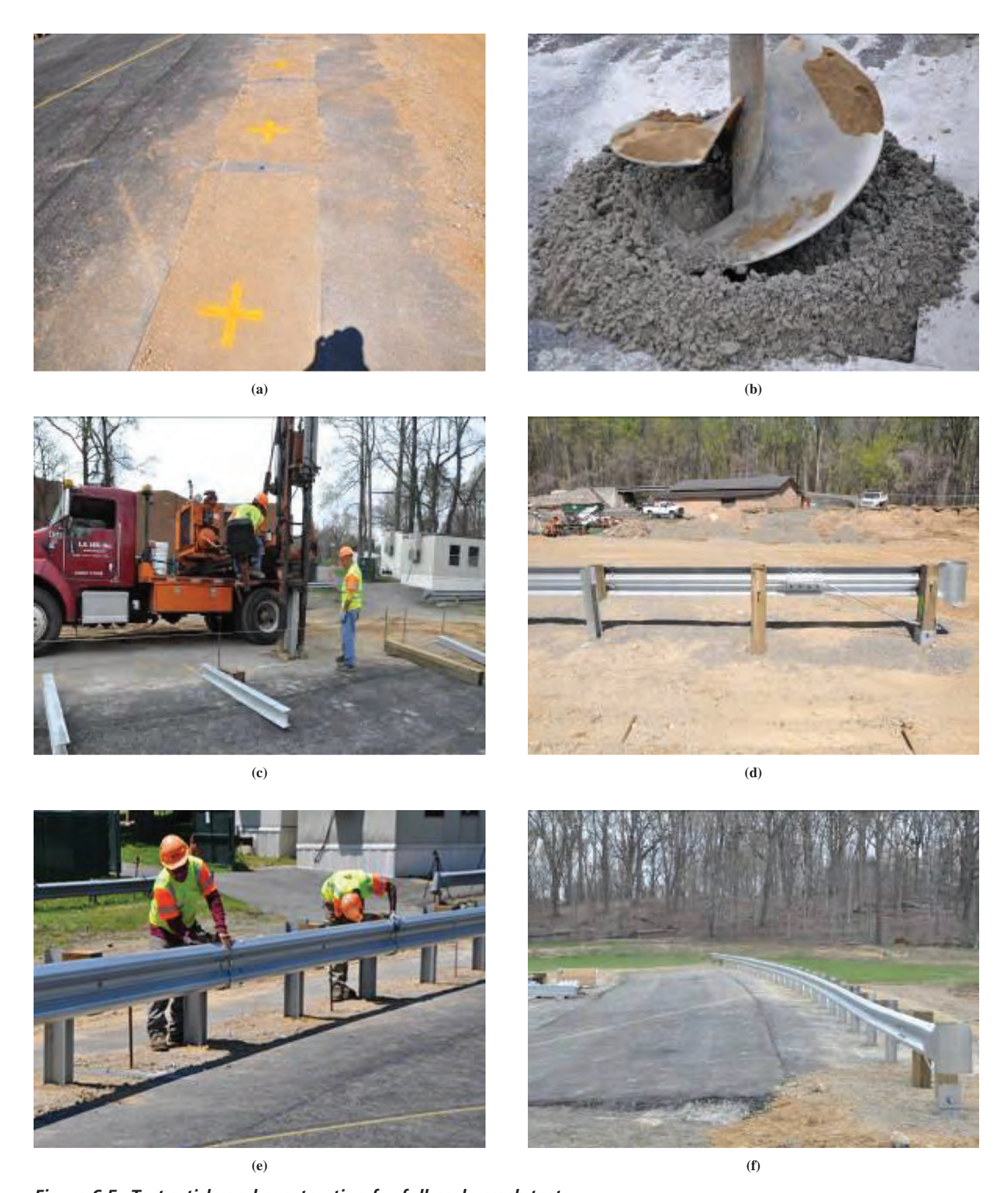


Figure 6.5. Test article and construction for full-scale crash tests.

- Test Article Design: Plan sheets showing the dimensions, connections, and configurations of the test article are provided.
- Test Article Installation: Descriptions of the efforts to construct or install the test article are provided along with all relevant support documentation (e.g., compaction metrics).
- Test Vehicle: The condition, mass, size, tires, and features of each test vehicle are noted.
- Impact Description: The nature of the impactor and its speed are documented.
- Test Article Damage: Images and measurements of damage, deflections, and ruptures of the test article (e.g., barrier) are described and images stored.
- Test Vehicle Damage: The location and nature of the damage to the test vehicle is described and recorded.
- Performance Assessment: Comparisons of test results to MASH requirements are provided to evaluate barrier performance.
- Test Summary: A MASH requirement is that a crash test summary diagram be created that shows a sequential view of the test and provides all pertinent data derived.
- Digital Impact Data: Digital impact data is provided.
- Video Images: Video images are provided.

Variations of these basic elements occurred as necessary to capture the unique nature of these tests.

# **6.5 Preliminary Tests**

Given the nature of these tests, a series of non-destructive tests were conducted to determine the following:

- Launch Speeds: It was critical to be certain that the vehicle propulsion system was set to the appropriate parameters to ensure that a vehicle would impact the barrier at the desired speed. Several tests measured the speed at possible impacts points. Vehicles were instrumented to capture accelerations and roll, pitch, and yaw rates for comparison with the vehicle dynamics results and to determine the effects of CSRS on vehicle-to-barrier interface.
- Trajectories: The paths of the vehicles were monitored to determine if the road and shoulder slopes caused the vehicle to deviate from the desired trajectory to the impact point.

Figure 6.6 shows a top view of one of the preliminary tests that was conducted to determine the appropriate launch speeds and drift effects on vehicle trajectory. The yellow line on the road surface reflects the direct extension of the track axis. The vehicle drift is the distance between the centerline of the vehicle (indicated by the green line) and the yellow line.



Figure 6.6. Top view from typical preliminary test.

Multiple runs were made for varying launch speeds to determine the average drift.

The graphs in Figure 6.7 show typical results from these tests. The top graph shows the changes in the z-axis displacement measured from a string potentiometer placed in the front-right suspension of the vehicle. The z-axis displacements from three repeat tests are shown in the graph. Time zero indicates the time the vehicle would first come in contact with the barrier. Note that as the vehicle accelerates down the track, the z-displacement increases as the acceleration pitches the vehicle up then reaches a stable level. Once the vehicle is released, the suspension starts to return to its zero value. As the vehicle reaches the transition section and enters the superelevated road section, the front suspension starts to compress leading to a decrease in the z-displacement (negative). Once all four wheels are on the road section, the suspension starts to recover again, and the z-axis displacement goes back to zero. After time zero, the side slope is encountered, causing another disruption in the front suspension. The important aspect of this is the indication of the z-axis displacement at the projected impact point. It is near zero suggesting that the vehicle is at the position of equilibrium.

Figure 6.8 shows the decrease in velocity as the vehicle free wheels to the impact point. For the tests that had a launch speed of 100 km/h (62 mph), only about 2 km/h (1.25 mph) were lost as the vehicle climbed the inclined transition section. These tests provided the information necessary to set the launch speed target for the vehicle to meet the goal of having it impact the barrier at 62 mph (100 km/h) after traveling up the incline of the CSRS to impact the barrier at the critical speed. The release speed for all three actual tests was targeted for 102 km/h (63.25 mph).

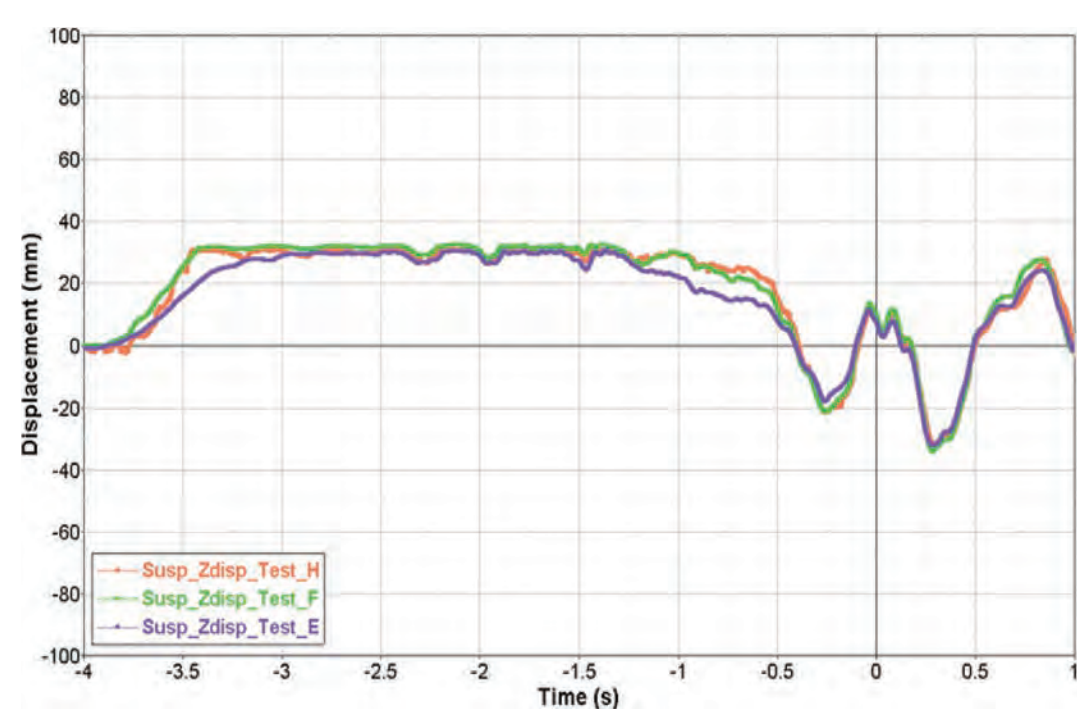


Figure 6.7. Suspension z-displacement from preliminary test.

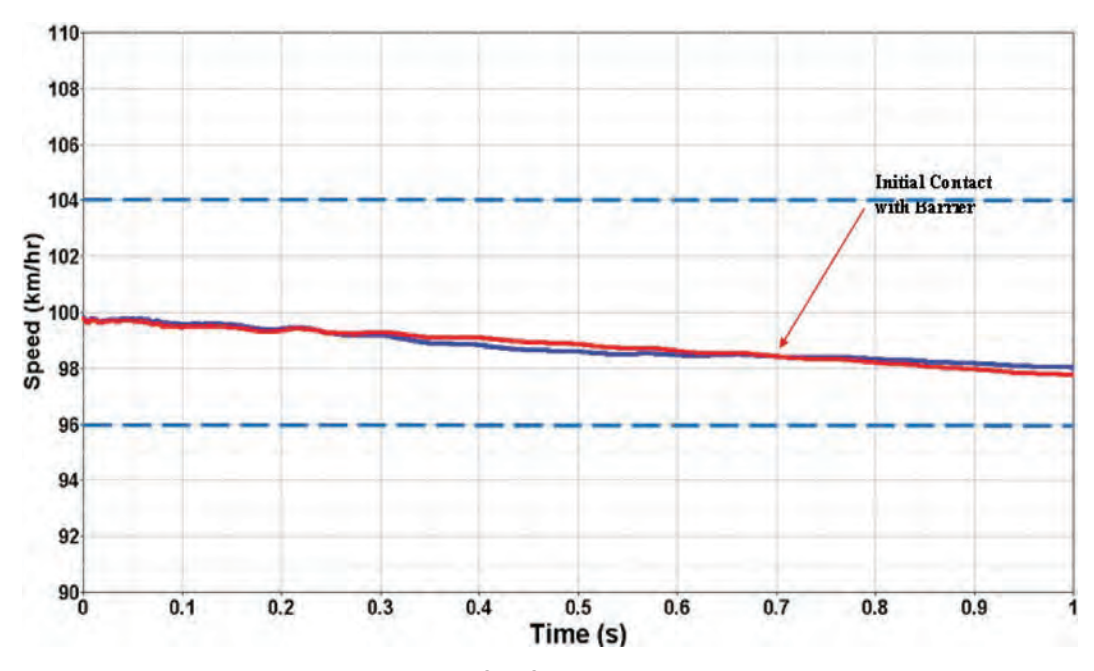


Figure 6.8. Typical vehicle speed profile from preliminary test.

# **6.6 Full-Scale Crash Testing Results**

Three full-scale tests were conducted to reflect MASH Test 3-11 requirements simulated for a 254-m (833-ft) radius CSRS with a 6% superelevation for a G4(1S) W-beam barrier with the 2270P test vehicle. Note that conditions were similar for all these tests except for the wider shoulder width in the last test. There were also some normal variations in the vehicle and impact parameters. More details are provided for each test in the following subsections.

#### 6.6.1 Test 16004

This test was performed using specifications for MASH Test 3-11. This test consisted of a 2009 Chevrolet Silverado weighing 2,315 kg (5,104 lb) impacting a G4(1S) W-beam guardrail barrier with two Type-T anchor assembly end

terminations on a 254-m (833-ft) radius curve with a 6% superelevation on an asphalt roadway/shoulder surface. The G4(1S) W-beam guardrail barrier was placed at the end of a 1.2-m (4-ft) shoulder with a –2% slope. The barrier was installed to follow the curvature of the roadway/shoulder. The set up is shown in Figure 6.9. Figure 6.10 and Figure 6.11 provide sequential views of the behavior of the vehicle in the impact. Additional test details and photos are provided in Appendix E.

The test vehicle began impacting the G4(1S) W-beam guardrail barrier at post 11. The impact was approximately 19.1 m (62.5 ft) downstream from the beginning of the barrier installation and 34.3 m (112.5 ft) upstream from the end of the barrier installation. This was approximately 0.75 m (2.5 ft) upstream from the desired critical impact point. When the barrier was impacted some snagging occurred, but the vehicle was redirected.









Figure 6.9. Vehicle and barrier set up for Test 16004.

(d)



Figure 6.10. Sequential photographs for Test 16004 (rear isometric view).



Figure 6.11. Sequential photographs for Test 16004 (front isometric view).

100

There was significant damage to the impacted area of the G4(1S) W-beam guardrail barrier. The damage to the barrier was contained between post 10 and post 16. There was considerable flattening of the W-beam guardrail with tearing. Also, there was significant twisting of the posts and broken blockouts. The damage to the barrier is shown in Figure 6.12.

The 2009 Chevrolet Silverado had significant damage as shown in Figure 6.13. The majority of the damage came on the right-hand side of the vehicle because that was the impacted side. There was major denting to the passenger side of the vehicle. The front passenger side tire became detached during the impact and the passenger rear tire was flat after impact. The front and rear bumper had considerable damage to the passenger side but the driver's side received minimal to no damage. The tires on the driver's side remained undamaged during the impact.





Figure 6.12. Damage to test article for Test 16004.

Table 6.2 contains the specific features of the test and the computed metrics from the various digital recording devices. The test vehicle was within the mass tolerance range (±50 kg) for testing requirements. The impact speed and angle were also within tolerance limits. The vehicle was redirected, although it experienced a high degree of yaw, pitch, and roll, and came to rest on its wheels. The vehicle had the front wheel sheared off and significant damage. The barrier was severely damaged, but the rail remained connected. The crash metrics computed from the instrumentation on the vehicle are provided below.

#### 6.6.2 Test 16010

This test was performed using specifications for MASH Test 3-11. This test consisted of a 2009 Chevrolet Silverado





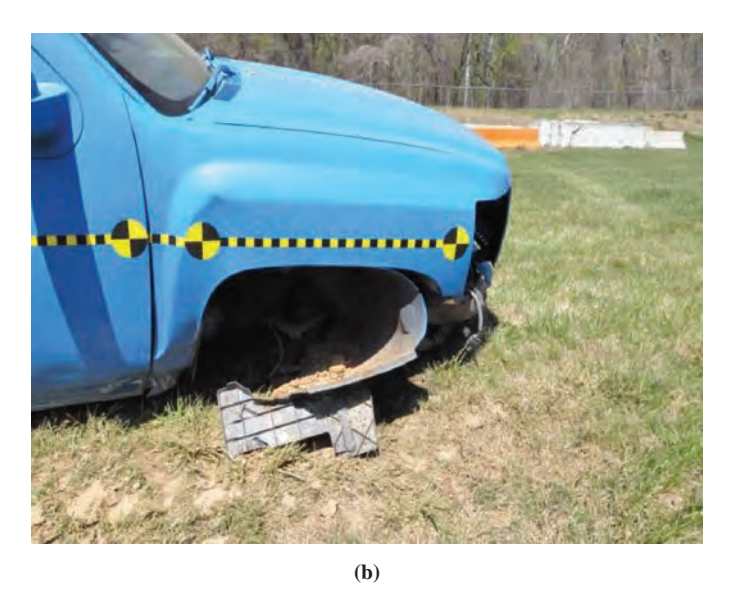


Figure 6.13. Damage to test vehicle for Test 16004.

weighing 2,283 kg (5,033 lb) impacting a G4(1S) W-beam guardrail barrier with two Type-T anchor assembly end terminations on a 254-m (833-ft) radius curve with a 6% superelevation on an asphalt roadway/shoulder surface. The G4(1S) W-beam guardrail barrier was placed at the end of a 1.2-m (4-ft) shoulder with a -2% slope. The barrier was

Table 6.2. Data and results for Test 16004.

General Information			
Test Agency:	FOIL		
Test Number:	16004		
Test Date:	04/14/201	6	
Test Article:	G41S W-E	3eam	Guardrail
Test Vehicle			
Description:			2270P Silverado
Test Inertial Ma	ass:		2,315 kg
Gross Static Ma	ass:		3,085 kg
Impact Conditions			
Speed: 100.0 k	m/h		
Angle: 25.0°			
Occupant Risk Factors			
Impact Velocity	y (m/s)		at 0.1701 s
x-direct	tion 4.9	9	
y-direct	tion 4.5	5	
THIV (km/h):	24	1.7	at 0.1721 s
THIV (m/s):	6.9	9	
Ridedown Acceleration	s (g)		
x-direct	tion –7	7.5	(0.9691 to 0.9791 s)
y-direct	tion –7	7.7	(0.2571 to 0.2671 s)
PHD ( <i>g</i> ):	10	).1	(0.2536 to 0.2636 s)
ASI:	0.7	71	(0.2518 to 0.3018 s)
Max. 50msec Moving A	Avg. Accele	eration	ns (g)
x-direction	-5	5.7	(0.9402 to 0.9902 s)
y-direction	-6	6.0	(0.2517 to 0.3017 s)
z-direction	-3	3.6	(0.9490 to 0.9990 s)
Max Roll, Pitch, and Ya	aw Angles (	(degre	ees)
Roll	-2	23.9	(0.9487 s)
Pitch	-3	36.5	(1.2232 s)
Yaw	2	25.4	(9.9888 s)



installed to follow the curvature of the roadway/shoulder. The set up is shown in Figure 6.14. Figure 6.15 and Figure 6.16 provide sequential views of the behavior of the vehicle in the impact.

The test vehicle began impacting the G4(1S) W-beam guardrail barrier between post 11 and post 12. The impact was approximately 20 m (65.6 ft) downstream from the beginning of the barrier installation and 33.4 m (109.4 ft) upstream from the end of the barrier installation. When the barrier was impacted, it was flattened out and allowed vehicle override. The vehicle came to rest on the opposite side of the barrier.

There was significant damage to the impacted area of the G4(1S) W-beam guardrail barrier. The damage to the barrier was contained between post 11 and post 15. There was a significant amount of flattening of the W-beam guardrail with tearing that allowed the vehicle to pass to the other side of the barrier. There were also broken blockouts, bolts at the posts pulled through, and significant post twisting at the impact area. The damage to the barrier is shown in Figure 6.17.

The 2009 Chevrolet Silverado had significant damage. During the initial impact, the majority of the damage came on the right-hand side of the vehicle because that was the impacted side. The front passenger side tire became detached during impact; however, the other three tires remained intact and were undamaged. When the vehicle went to the opposite side of the barrier, it rolled onto its roof causing damage to the roof. The vehicle had significant damage to the cab, suspension parts, truck bed, and a broken windshield. The vehicle damage is shown in Figure 6.18.



Figure 6.14. Vehicle and barrier set up for Test 16010.

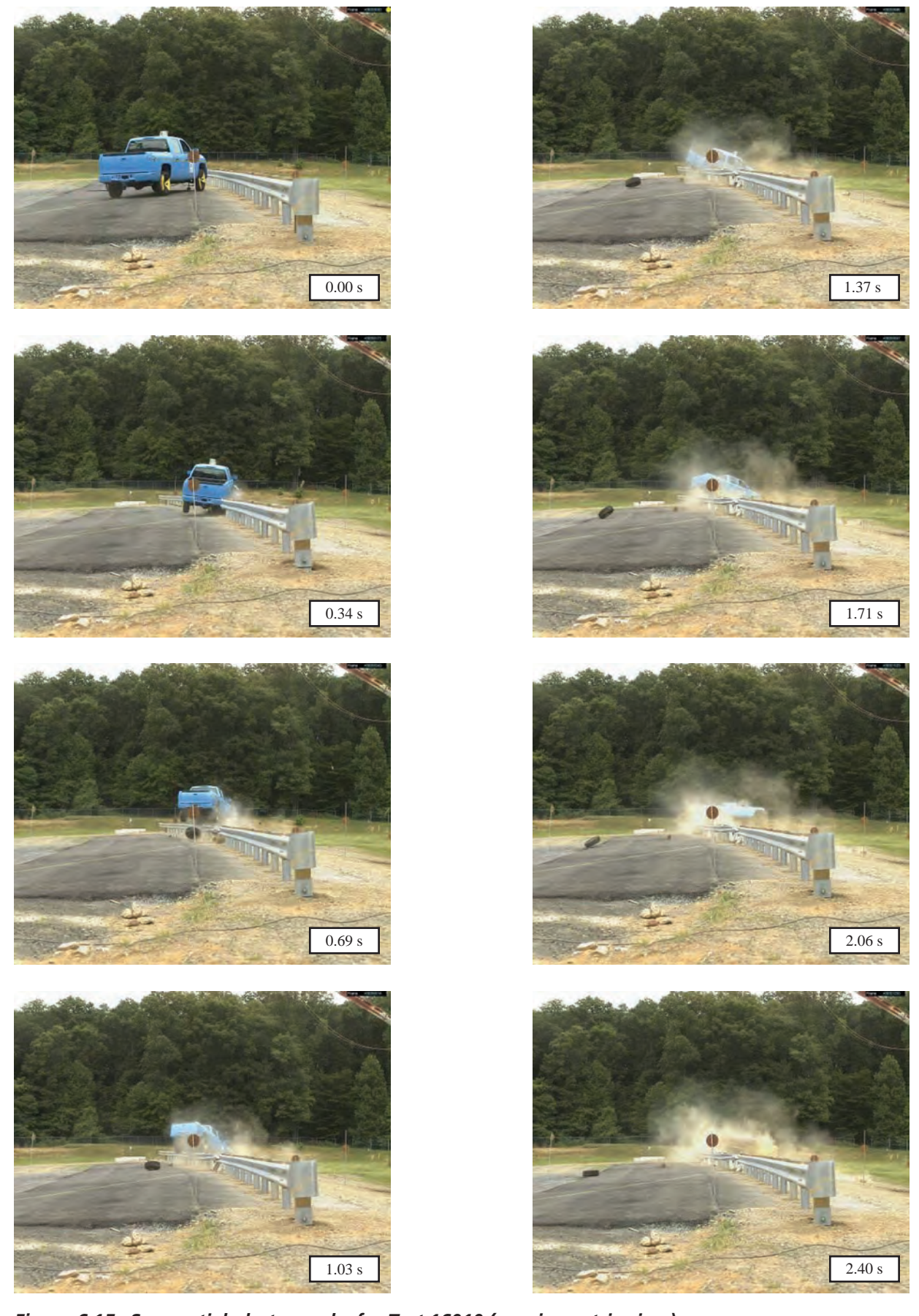


Figure 6.15. Sequential photographs for Test 16010 (rear isometric view).



Figure 6.16. Sequential photographs for Test 16010 (front isometric view).



Figure 6.17. Damage to test article for Test 16010.



Figure 6.18. Damage to test vehicle for Test 16010.



106

Table 6.3 provides the specific features of the test and the computed metrics from the various digital recording devices. The test vehicle was within the mass tolerance range  $(\pm 50~\mathrm{kg})$  for testing requirements. The impact speed and angle were also within tolerance limits. The vehicle was not redirected. It experienced a high degree of yaw, pitch, and roll, and came to rest on its roof after vaulting over the barrier. The vehicle had the front wheel sheared off and significant damage. The barrier was severely damaged, but the rail remained connected. The crash metrics computed from the instrumentation on the vehicle are provided below.

#### 6.6.3 Test 16015

This test was performed using specifications for MASH Test 3-11. This test consisted of a 2009 Chevrolet Silverado 2,268 kg (5,000 lb) impacting a G4(1S) W-beam guardrail barrier with two Type-T anchor assembly end terminations on a 254-m (833-ft) radius curve with a 6% superelevation on an asphalt roadway/shoulder surface. The G4(1S) W-beam guardrail barrier was placed at the end of a 1.2-m (4-ft) shoulder with a -2% slope. The barrier was installed to follow the curvature of the roadway/shoulder. The set up is shown in Figure 6.19. Figure 6.20 and Figure 6.21 provide sequential views of the behavior of the vehicle in the impact.

Table 6.3. Data and results for Test 16010.

```
General Information
       Test Agency:
                       FOIL.
                       16010
       Test Number:
       Test Date:
                       Times New Roman
       Test Article:
                       G41S W-Beam Guardrail
Test Vehicle
                                      2270P Silverado
       Description:
       Test Inertial Mass:
                                       3,085 kg
                                       2,283 kg
       Gross Static Mass:
Impact Conditions
       Speed: 100.0 km/h
       Angle: 25.0°
Occupant Risk Factors
       Impact Velocity (m/s)
                                       at 0.2100 s
               x-direction
                               4.8
               y-direction
                               3.8
       THIV (km/h):
                               22.7
                                      at 0.2149 s
       THIV (m/s):
                                       6.3
       Ridedown Accelerations (g)
                                      (0.2730 to 0.2830 s)
               x-direction
                               -6.1
               y-direction
                               -6.0
                                      (0.2153 to 0.2253 s)
       PHD (g):
                                      (0.2339 to 0.2439 s)
                                8.0
       ASI:
                                0.56
                                      (0.1288 to 0.1788 s)
Max. 50msec Moving Avg. Accelerations (g)
                                      (0.1249 to 0.1749 s)
       x-direction
                               -5.1
       v-direction
                               -3.7
                                      (0.1952 to 0.2452 s)
                                3.5
                                      (3.5260 to 3.5760 s)
       z-direction
Max Roll, Pitch, and Yaw Angles (degrees)
                               -51.4 (2.3602 s)
       Roll
       Pitch
                               -50.0 (4.1601 s)
                              -168.5 (3.8266 s)
```

The 2270P vehicle began impacting the G4(1S) W-beam guardrail barrier at post 13. The impact was approximately 24.8 m (81.3 ft) downstream from the beginning of the barrier installation and 28.6 m (93.7 ftp) upstream from the end of the barrier installation. When the vehicle impacted the barrier, the barrier was crushed allowing the vehicle to redirect. The vehicle came to rest on the impacted side of the barrier.

There was significant damage to the impacted area of the G4(1S) W-beam guardrail barrier. The damage to the barrier was contained between post 13 and post 18. There was a significant amount of crushing of the W-beam guardrail. There were also broken blockouts, bolts at the posts pulled through, and significant post twisting at the impact area. The damage to the barrier is shown in Figure 6.22.

The 2009 Chevrolet Silverado had significant damage. The majority of the damage came on the right-hand side of the vehicle because that was the impacted side. There was major denting to the passenger side of the vehicle. The front passenger side tire became detached during the impact due to broken suspension parts and the passenger rear tire was flat after impact. The front and rear bumper had considerable damage to the passenger side but the driver's side received minimal damage. The tires on the driver's side remained undamaged during the impact. The vehicle damage is shown in Figure 6.23.

Table 6.4 contains the specific features of the test and the computed metrics from the various digital recording devices. The test vehicle was within the mass tolerance range (±50 kg) for testing requirements. The impact speed and angle were also within tolerance limits. The vehicle was redirected, although it experienced a moderate degree of yaw, pitch, and roll, and came to rest on its wheels. The vehicle had the front wheel sheared off and significant damage. The barrier was severely damaged, but the rail remained connected. The crash metrics computed from the instrumentation on the vehicle are provided below.

#### **6.7 Test Results Evaluation**

The results from the tests are shown in Table 6.5 for the relevant MASH criteria to determine overall safety performance for G4(1S) W-beam barriers on CSRS tested. Note that the first and third tests were considered to "Pass," although the first test did not have the proper impact point. The vaulting/rollover in the second test "failed."

In Test 16004, the impact point on the barrier was about 0.75 m (2.5 ft) off from the computed critical point based on MASH recommended methods. After additional preliminary testing, the test was repeated (Test 16010) and the vehicle impacted the barrier at the desired location. Test 16015 was then performed on the wider shoulder (8 ft) and again the desired impact location was achieved. The results from Tests 16010 and 16015 confirm the simulations results.



Figure 6.19. Vehicle and barrier set up for Test 16015.

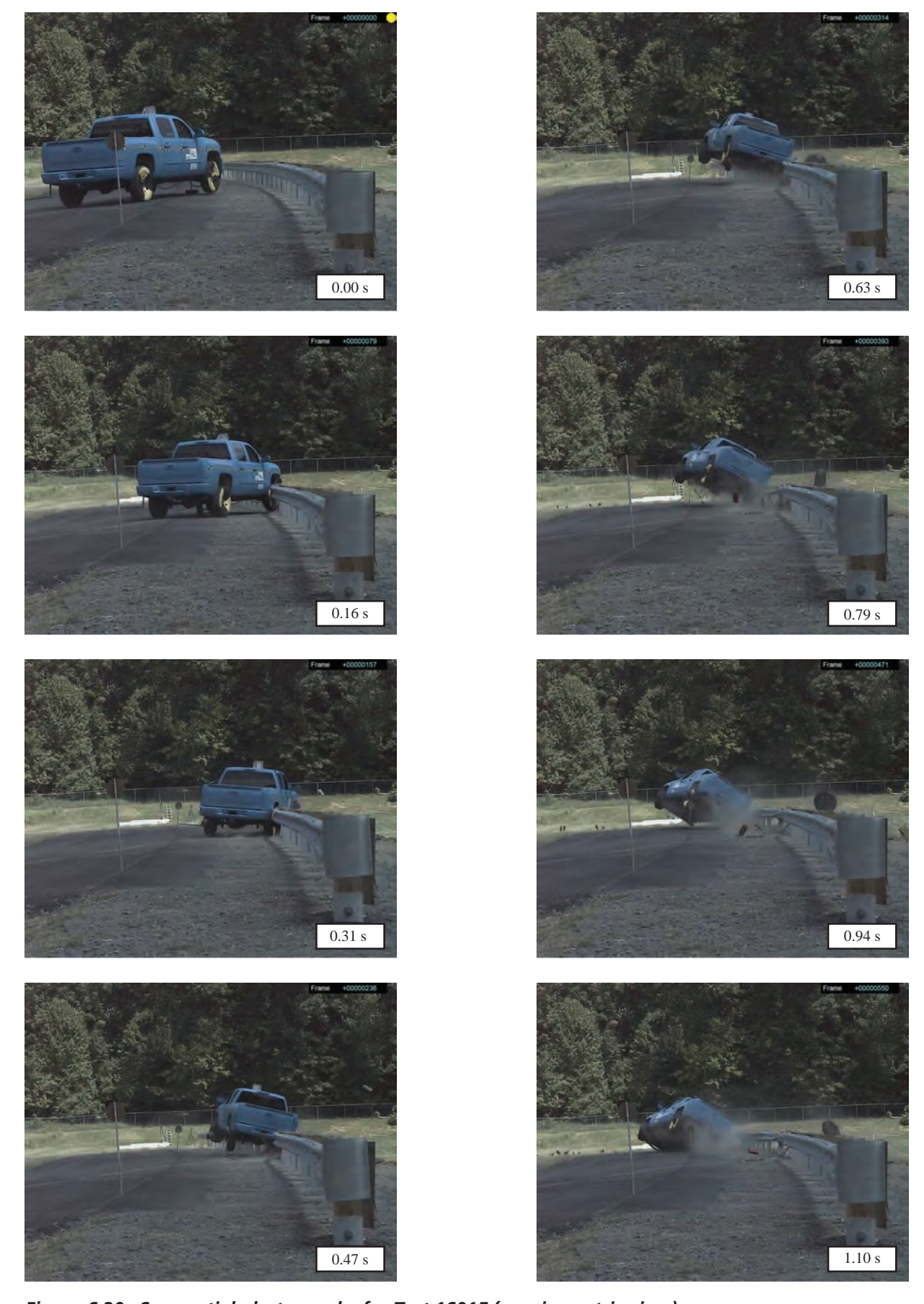


Figure 6.20. Sequential photographs for Test 16015 (rear isometric view).



Figure 6.21. Sequential photographs for Test 16015 (front isometric view).

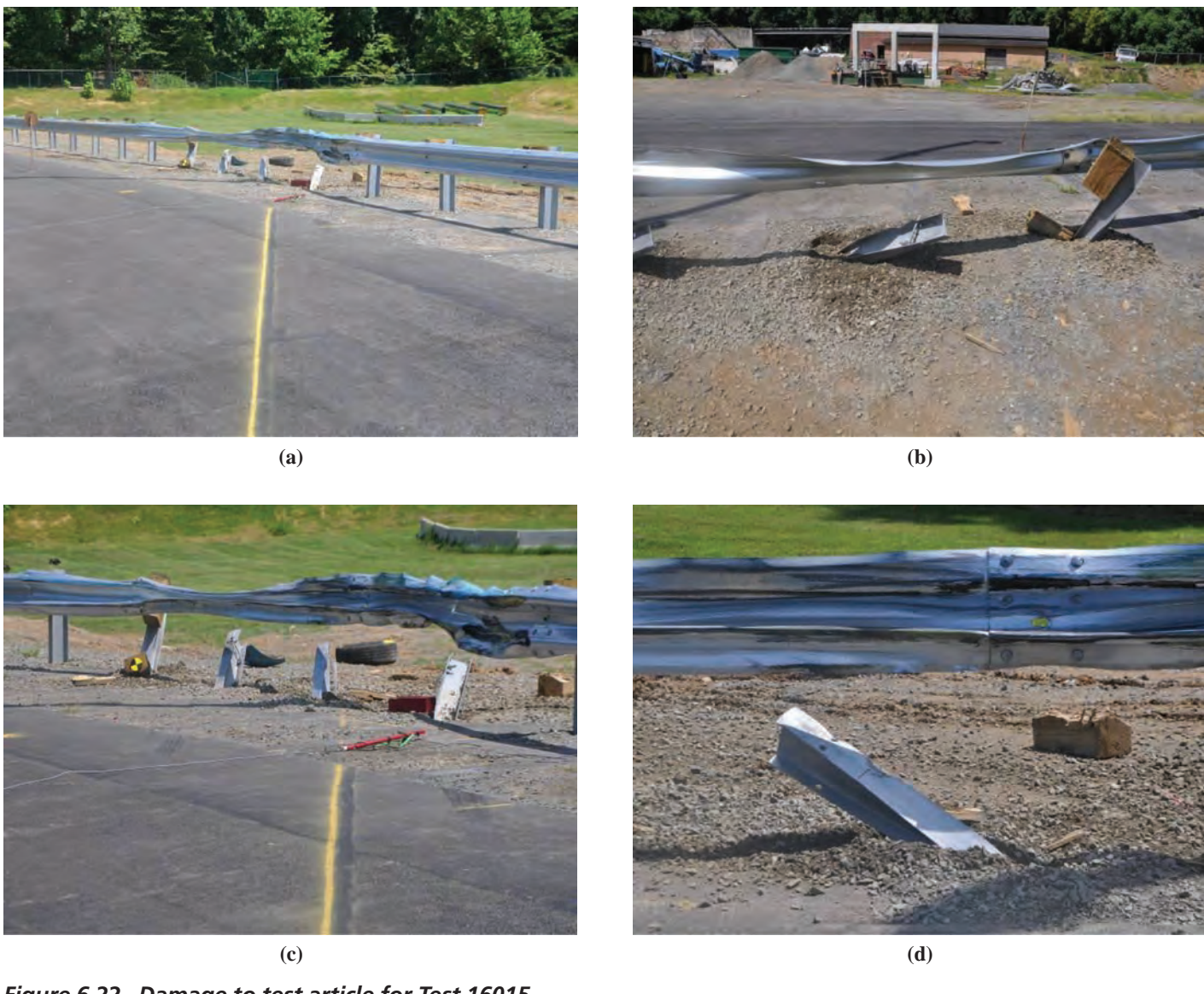


Figure 6.22. Damage to test article for Test 16015.

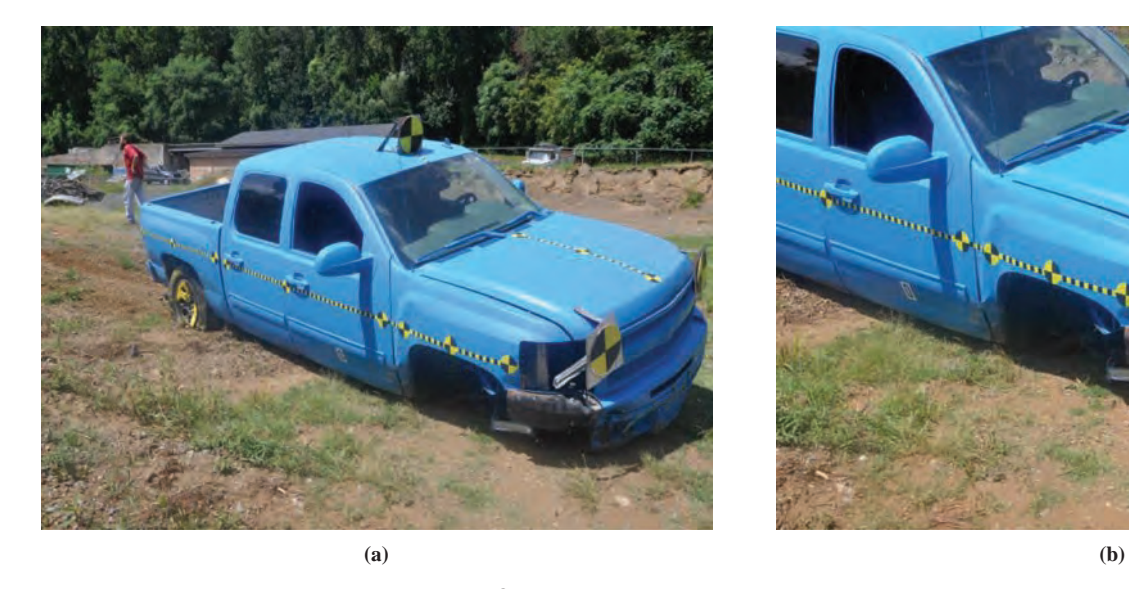


Figure 6.23. Damage to test vehicle for Test 16015.

Table 6.4. Data and results for Test 16015.

```
General Information
       Test Agency: FOIL
       Test Number: 16015
       Test Date:
                     08/18/2016
       Test Article: G41S W-Beam Guardrail
Test Vehicle
                                   2270P Silverado
       Description:
       Test Inertial Mass:
                                   2,268 kg
                                   3,085 kg
       Gross Static Mass:
Impact Conditions
      Speed: 100.0 km/h
       Angle: 25.0°
Occupant Risk Factors
       Impact Velocity (m/s)
                                   at 0.2728 s
              x-direction
                           4.7
              y-direction
                            4.2
       THIV (km/h):
                            24.3
                                   at 0.2780 s
       THIV (m/s):
                            6.8
       Ridedown Accelerations (g)
              x-direction
                            -5.9
                                   (0.3182 to 0.3282 s)
              v-direction
                            -6.7
                                   (0.2804 to 0.2904 s)
       PHD (g):
                             8.8
                                   (0.2805 to 0.2905 s)
       ASI:
                            0.60
                                   (0.2014 to 0.2514 s)
Max. 50msec Moving Avg. Accelerations (g)
                            -4.9 (0.2012 to 0.2512 s)
       x-direction
       y-direction
                            -5.1
                                   (0.3687 to 0.4187 s)
       z-direction
                             1.9
                                   (0.5016 to 0.5516 s)
Max Roll, Pitch, and Yaw Angles (degrees)
                                   (0.9998 s)
       Roll
                           -31.6
       Pitch
                           -34.5
                                   (0.8023 s)
       Yaw
                            51.3
                                   (0.9998 s)
```

#### **6.8 Conclusions**

The three full-scale crash tests were conducted at the FOIL located at the FHWA Turner-Fairbank Highway Research Center in McLean, Virginia. The tests were conducted according to MASH requirements for Test 3-11 involving 2270P vehicles. The evaluation criteria appropriate for longitudinal barriers were used as the performance benchmark. An inclined surface was constructed to represent a CSRS with the features of a 254-m (833-ft) radius curve with 6% superelevation. An asphalt shoulder was installed with a 2° declination from the edge of the roadway. The test bed was set up for all barrier placements for shoulder widths of 4 ft and 8 ft. The barrier was placed just at the edge of the shoulder. An appropriate length of G4(1S) longitudinal barrier with end treatments was installed by a certified barrier contractor for each test. The two shoulder widths required that the positioning of the posts consider the prescribed impact points determined to be the most critical. The tests involved launching the vehicle at a speed that allowed it to be at the MASH impact speed when the barrier was reached after traversing the inclined roadway surface and the down sloping shoulder.

Table 6.5. Summary of MASH evaluation of crash test results.

	Test	1000	Test
	16004	16010	16015
Structural Adequacy			
<b>A:</b> Test article should contain and redirect the vehicle; the vehicle should not penetrate, underride, or override the installation although controlled lateral deflection of the test article is acceptable.	Pass	Fail	Pass
Occupant Risk	•		
<b>D:</b> Detached elements, fragments, or other debris from the test article should not penetrate or show potential for penetrating the occupant compartment, or present an undue hazard to other traffic, pedestrians, or personnel in a work zone.	Pass	Pass	Pass
<b>F:</b> The vehicle should remain upright during and after the collision although moderate roll, pitch, and yaw are acceptable.	Pass	Fail	Pass
<b>H:</b> The occupant impact velocity in the longitudinal direction should not exceed 40 ft/s and the ORA in the longitudinal direction should not exceed 20 g.	Pass	Pass	Pass
<b>I:</b> Longitudinal and lateral ORA should fall below the preferred value of 15.0 $g$ , or at least below the maximum allowed value of 20.49 $g$ .	Pass	Pass	Pass
Vehicle Trajectory			
For redirective devices the vehicle shall exit within the prescribed box.	Pass	Fail	Pass
Overall	Pass	Fail	Pass
	1		

The results reflected outcomes predicted in the simulations. The first test was expected to result in a failure due to excessive vehicle roll (and possibly vaulting). In the first test, the vehicle did not impact the barrier at the expected critical impact point just beyond the post because there was less drift than anticipated in traversing the inclined surface. The vehicle followed the rail and was redirected because the early impact with the post kept the rail in an upright position, allowing better capture of the vehicle. The second and third tests impacted the barrier at the computed critical location using the procedure included in MASH and confirmed the simulation results. In the second test, the simulation accurately predicted (for the tested curvature, superelevation, and shoulder angle) that the vehicle would vault the barrier and not meet MASH criteria for a 1.22-m (4-ft) shoulder. In the third test, the simulation accurately predicted (for the tested curvature, superelevation, and shoulder angle) that the vehicle would get redirected and meet the MASH criteria for a 2.44-m (8-ft) shoulder.

### CHAPTER 7

# Development of Guidance for Improved Longitudinal Barrier Design, Selection, and Installation on CSRS

#### 7.1 Background

This research investigated the safety performance of barriers installed on CSRS with the intent of developing improved guidance for their design, selection, and installation. The literature review, state DOT survey, and analysis of crash data found little specific guidance for the use of longitudinal barriers on CSRS. In this research, a comprehensive analysis of vehicle trajectories was undertaken to determine the influence of a broad spectrum of superelevation, shoulder slope, shoulder width, and barrier placement on interface effectiveness (see Chapter 4). A large number of detailed crash simulations were subsequently undertaken to determine whether possible interface problems could adversely affect crashworthiness (see Chapter 5). The validity of these simulations was confirmed by the results of full-scale crash tests (see Chapter 6). These efforts have produced a wealth of results. Translating the findings into meaningful guidance is the final task of this research.

It is necessary to start by carefully defining the meanings of the following three guidance aspects that were included in the research objectives:

- **Design**. The basic design of a barrier must accommodate the nature of the impacts that might be expected. The features of the design include materials, dimensions, shape, connections, and anchorage. These need to be appropriate for the type of service (i.e., crashworthiness) the hardware is expected to provide.
- Selection. Decisions on which barrier to use in a given situation is a function of factors ranging from the road geometry, superelevation, grade, shoulder configuration, and roadside environment. Selection must also consider the nature and speed of traffic, environmental conditions, and crashworthiness requirements (i.e., test level).
- Installation. A properly designed and selected device must be appropriately installed and maintained to meet its performance expectations. Barriers must be properly placed on the roadside, given the intended orientation, and effectively

connected to other barrier elements. Barriers may need maintenance and repairs after critically damaging impacts. Frequent impacts may indicate that there are other conditions that need attention or that an upgrade is warranted.

The ultimate safety performance of a barrier is a function of the appropriate combination of these three aspects. These are important for developing construction plans for new facilities, as well as assessing the appropriateness of deployed barriers. The following sections describe trends or patterns from the results that can be translated into guidance for each of these aspects. The focus was on crashworthiness; however, the guidance will need to be adapted to practices and policies in each state.

CSRS are routinely used for the design of all types of curved road of all classifications. Superelevation (i.e., curve banking) is used to make it easier or more comfortable for drivers to navigate their vehicles through curves at higher speeds. While the *Green Book* provides criteria for the selection of superelevation rates as a function of curvature radius and highway speeds, there is no guidance provided relative to treatments for the adjacent roadsides. The *Roadside Design Guide* provides only general guidance for the design, selection, and placement of longitudinal barriers and does not offer specific barrier guidance for CSRS. It is appropriate from a comprehensive safety perspective to ask whether curve and superelevation design influence barrier performance, and if so, why and by how much.

#### 7.2 Research Questions

Many questions can be posed about safety performance of longitudinal barriers on CSRS. Concerns arise when longitudinal barriers are installed on CSRS because of the influence the curve has on the angle of impact of a vehicle with respect to the barrier. For example, the angle can increase or decrease as a result of the impact occurring on the inside or outside of the curve. Increases in impact angle may also increase the potential for vehicle instability resulting from

wheels snagging on posts and may reduce the barrier's ability to contain and redirect the impacting vehicle, thus resulting in vehicle penetration or override of the barrier. Variations in the nature of the impact may increase the impact forces that potentially exceed the load capacity of barriers designed for impacts along tangent roadway sections. These conditions may also adversely influence occupant risk.

There may be design concerns about rain and melting snow on the shoulders running onto the traveled way, where it could refreeze. For superelevated sections, then, it is common practice to slope the shoulders so that melting snow will drain away from the pavement. The use of higher rates of superelevation limits the shoulder slope options that would allow drainage away from the roadway surface on the high

side of the curve. Additional drainage concerns arise for concrete barriers that trap water along the base of the barrier if there are no adequate drain ports.

Another concern related to barrier orientation is when the barrier is installed in true-vertical orientation. The analyses presented in Section 5.6.3 indicated that, under some circumstances, this orientation resulted in a greater propensity to override the barrier. Better containment seems to be provided when the barrier is installed with an orientation perpendicular to the road surface. There may be additional orientation complications for barriers installed on the lower inside of a superelevated curve. These concerns were addressed in this research.

Table 7.1 contains key questions identified at the outset of the research to be addressed when developing the guidance;

Table 7.1. CSRS research questions.

Category	Question:
Safety	What are the characteristics of CSRS crashes?
	How effective are police crash records for identifying CSRS safety problems?
	What are the states' perspectives on this safety issue?
	What is the relative influence of design, surface, placement, and side slope on safety?
	Do longitudinal barriers on CSRS have similar safety performance as on straight, flat roads?
	Are some vehicle types more prone to crashes on CSRS?
	Are there regional differences in safety performance?
Curve	How does superelevation affect safety for varying radii?
Features	How much change (if any) is a function of the curve features (e.g., superelevation, radius, shoulder)?
	What are the relative effects of curve features?
	What is the influence of vertical grades on CSRS?
Design	What design analyses have been undertaken for barriers on CSRS?
	How much difference is there in safety performance related to height? Interface?
	To what degree is snagging influenced by placement on CSRS?
	Is snagging influenced by placement and shoulder hinge on CSRS?
	What is the difference in impacts between barriers on level terrain and those on CSRS?
	What is the propensity for higher angle impacts on CSRS?
	What are the retrofit options that would compensate for interface problems?
	What is the influence of roadway features (e.g., curvature, grade, cross section, side slopes)?
	Where barrier performance is found to be inadequate, are there options to improve the barrier
	to meet requirements?
Placement	What are the influences of shoulder width and slope?
	Does true vertical or normal to road surface orientation work best?
	How much adverse effect is noted for placement perpendicular versus true vertical?
	What is the effect of curbs?
Vehicle	How do CSRS features influence the roll, pitch, and yaw behavior of errant vehicles?
	How does this roll, pitch, and yaw effect translate to changes in the interface point on the
	barrier? What are the differences for curve features and vehicle types?
	How does vehicle size and weight affect behavior on CSRS? Trucks?
	Are there VDA metrics that indicate variations in effects on the vehicle?
Evaluation	What would be the critical test conditions for assessing barriers on CSRS?
	How sensitive are the effects for any case?
	Will NCHRP Report 350 and MASH approved barriers meet crashworthiness requirements on CSRS?
	Would MASH barriers perform better on CSRS than those in NCHRP Report 350?
	What is the difference in impact severity between barriers on level terrain and those on CSRS? What is the influence of roadway features (e.g., curvature, grade, cross section, side slopes)?
	What PIRTs should be considered for crashworthiness evaluation?

#### 114

however, addressing them all was beyond the scope of this effort. Therefore, this research focused on these critical or fundamental questions about longitudinal barrier performance on CSRS:

- What is the effect of curvature and superelevation on longitudinal barrier performance?
- What is the effect of shoulder width and slope on barrier performance for various curvature and superelevation conditions?
- Are all barriers equally effective in deployments on CSRS?
- Is barrier performance influenced by vehicle type?
- Does barrier orientation influence its performance on CSRS?

#### 7.3 Summary of Findings

A considerable amount of information can be drawn from these results. Key observations from the simulation results are noted below for concrete (rigid) and W-beam (semi-rigid) barriers.

#### 7.3.1 Concrete Barriers

- Most failures occurred when barriers were in true-vertical orientation. Simulations showed only one failure when the barrier was oriented normal to the shoulder for the 1100C vehicle and one when the barrier was normal to road for the 2270P vehicle.
- More failures were noted with higher superelevation: 12% superelevations had more failures than the 8%, and the 6% superelevation had the fewest failures.
- There were more failures on roadways with narrower shoulder widths than on those with wider shoulder widths.
- Larger shoulder angles (i.e., a greater difference in the angle between the road and shoulder) led to more failures.
- Simulations showed the F-shape concrete barrier had a moderately improved performance over the NJ concrete barrier.

#### 7.3.2 W-Beam Barriers

- There were more failures on roadways with narrower shoulder widths than on those with wider shoulders.
- Larger shoulder angles (i.e., a greater difference in the angle between the road and shoulder) led to more failures.
- G4(1S) W-beam barriers at 27¾ in. high did not meet MASH requirements for the range of conditions simulated. It was

- concluded that their performance would not be acceptable for CSRS conditions.
- The G4(1S) W-beam barriers at 29 in. high did meet MASH requirements for most cases where there were wider shoulders.
- The higher MGS met the MASH requirements for all cases. The 11 simulations covered a valid cross section of CSRS conditions without a failure.

# 7.4 Translating Findings and Observations into Guidance

The research focused on a representative set of features for CSRS for three types of longitudinal barriers, varying shoulder configurations, and different barrier placement and orientation conditions. This allowed analysis of a broad range of interface and impact scenarios to answer the critical questions and provide a basis for the development of guidelines for the safe and effective deployment of longitudinal barriers on CSRS.

In an attempt to translate these results into guidance, summary tables were generated for the three areas where guidance was sought: design, selection, and installation. The guidance is derived based on findings from the vehicle-to-barrier interface evaluations as well as the crash simulation analyses. In addition, it was considered useful to cite other areas where guidance may be needed or to highlight future research needs.

Table 7.2, Table 7.3, and Table 7.4 address specific subtopics for design, selection, and installation, respectively, with rows in each table. For each subtopic there is a column that cites (in an abbreviated form) the findings and a second column that cites the related implications and guidance. The possible elements of guidance are indicated in bold.

The following caveats apply to Table 7.2, Table 7.3, and Table 7.4:

- The findings focused on two types of MASH vehicles: 1100C and 2270P. Vehicles of other sizes were not explicitly analyzed.
- Not all possible CSRS conditions were analyzed, but a representative cross section was provided.
- Impacts were oriented to the MASH speed and angle requirements for testing longitudinal barriers at TL-3.
- Barriers were typically selected after the roadway alignments had been established.
- Agencies have more latitude relative to setting shoulder width and slope.

Table 7.2. Design guidance extracted from the simulation results.

Design Guidance		
Findings by Topic	Implications and Guidance Elements	
<ul> <li>General</li> <li>Interface areas are a function of the type of vehicle, its speed, the nature of the road, shoulder, and roadside slope surfaces conditions.</li> <li>There are differences in the interface effectiveness for the three types of barriers.</li> <li>The effective interface area is unique for each barrier type for any curvature, superelevation, shoulder width, and shoulder slope for each vehicle.</li> <li>Barriers on CSRS with higher superelevations tend to be prone to failures.</li> <li>Failures occur more frequently for narrower shoulders.</li> </ul>	<ul> <li>Poor vehicle-to-barrier interface limits the barrier functions in a crash.</li> <li>Good interface is a necessary but not sufficient condition for selection of a barrier type. Increases in impact severity need to be assessed.</li> <li>Consider the differences in interface area provided by available barriers and, to the extent possible, select the type that offers a capture area consistent with the expected traffic.</li> <li>Consider a higher barrier to better accommodate larger vehicles like SUVs and SUTs.</li> </ul>	
<ul> <li>More failures occur with steeper shoulders.</li> <li>Concrete Barriers</li> <li>NJ concrete barriers higher than 32 in. did not have a direct override issue at TL-3 because the interface area only varies by 2 in.</li> <li>The possibility of vaulting exists if the face slope of the barrier promotes vehicle ride-up (true vertical more prone to vehicle vaulting and rollover).</li> <li>F-shape concrete barriers have moderately improved performance over the NJ concrete barriers.</li> </ul>	Use concrete safety shape barriers to avoid underride problems.  Use higher concrete barriers where there is a concern about overrides associated with CSRS features (e.g., sharp curves).  Concrete barriers with an appropriate face slope may be considered the most universally effective design.  Design concrete barriers with minimum face slope to limit vehicle ride-up and maintain a viable interface area overlap.	
<ul> <li>G41S W-Beam Barriers</li> <li>G41S at 27¾ in. high shows a propensity to be overridden, but there were no indications of underride issues. Poor interface indicated by VDA was reflected in simulation results.</li> <li>The 29-inhigh barrier reduces the potential for vaulting compared with those at 27¾ in.</li> <li>The VDA indicated that there could be underride interface issues for the small car. Poor interface effects were not reflected in MGS crash simulation results.</li> <li>The 31-inhigh W-beam barrier provided the best override protection for most CSRS and shoulder conditions.</li> </ul>	The need for a higher barrier is apparent, but increasing the rail height necessitates review of the underride potential.  Give priority to low barriers on CSRS over similarly low barriers elsewhere. Increased heights are most important for tight curves where excessive speeds are likely to occur (e.g., off-ramps, downhill).  Consider 31-inhigh W-beam barrier designs for CSRS situations to further reduce the potential for override.	

Table 7.3. Selection guidance extracted from the simulation results.

Selection Guidance		
Findings by Topic	Implications and Guidance Elements	
Curvature and Superelevation     Longer radius curves with lower superelevations tend to have better interfaces with barriers.     Barriers on CSRS with higher superelevations tend to be prone to failures.     It is more likely that barriers will have a lower safety performance for the higher speed superelevation designs.	<ul> <li>Conduct further analysis of short-radius, high superelevation situations.</li> <li>Limit the use of tight curves with high superelevations.</li> <li>Consider using higher barriers on CSRS with appropriate underride protection.</li> </ul>	
Shoulder Width and Angle  VDA indicated that the greater the change in the slope from the traveled way to the shoulder surface, the greater the influence on the vehicle's suspension and hence on the potential interface with the barrier.  The width of the shoulder influences the time for spring response to limit bounce and undesirable interfaces.  For the 62-mph impacts studied, failures occurred more frequently for 4-ft shoulders than for 8-ft or 12-ft shoulders.  More failures occurred on roadways with steeper shoulders.	<ul> <li>Limit the use of major changes in shoulder slope to avoid impacting the barrier when the spring effect maximizes the interface area.</li> <li>Use wider shoulders where slope changes must be large to allow the suspension to stabilize the vehicle.</li> </ul>	
Roadside Slope     Changes in slope of the shoulder to the roadside surface can influence vehicle dynamics and the interface with barriers that need to be located further from the edge of the shoulder.	Limit the variation of slope change on the roadside for situations where the barrier is not placed adjacent to the shoulder to provide an acceptable interface.	
<ul> <li>Barrier Type</li> <li>The 29-inhigh barrier greatly reduces the potential for vaulting compared with the 27¾-inhigh barrier.</li> <li>The 31-inhigh W-beam barrier provided override protection for most CSRS and shoulder conditions.</li> <li>F-shape concrete barriers have a moderately improved performance over the NJ concrete barriers.</li> </ul>	<ul> <li>Consider 31-inhigh W-beam barrier designs for CSRS situations.</li> <li>Increase barrier height for tight curves where excessive speeds are likely to occur.</li> <li>Consider using concrete barriers with minimum face slope (e.g., single slope, over NJ or F-shape) to reduce the risk of rollover.</li> </ul>	

Table 7.4. Installation guidance extracted from the simulation results.

Installation Guidance	
Findings by Topic	Implications and Guidance Elements
Barrier Orientation     Concrete barriers installed in true-vertical orientation are more prone to vehicle vaultings and rollovers.     Barrier vertical orientation had less effect on Wbeam barrier performance.	Promote the use of orientation perpendicular to the roadway surface for concrete barriers.
Placement  Barriers further from the edge of the shoulder will be influenced by the change in angle of the shoulder slope to the back slope.  Barriers seem to function better for wider shoulders with the least angle relative to the road.	<ul> <li>Limit the placement of the barrier to the edge of shoulder on CSRS, particularly where there is a slope change going to the side slope.</li> <li>Use wider shoulder with gentler angle relative to the road on CSRS with short radii and high superelevation.</li> </ul>
Roadside Slope     Changes in slope of the shoulder to the roadside surface can influence vehicle dynamics and the interface with barriers that need to be located further from the edge of the shoulder.	Limit the variation of slope change on the roadside for situations where the barrier is not placed adjacent to the shoulder to provide an acceptable interface.
Maintenance     Posts knocked out of alignment, settlement, and other damage were not explicitly analyzed, but are likely to influence crashworthiness.	<ul> <li>Analysis on the effectiveness of damaged barriers on CSRS is needed.</li> <li>Further analysis of the relative priorities for barrier maintenance on CSRS may be needed.</li> </ul>

## CHAPTER 8

# **Conclusions**

In the first phase of this research, the analyses tended to confirm that crashes occur more frequently on curves than on tangent sections. However, the limitations of available data did not allow much mining into the effects of the various design features associated with basic curves, much less superelevated ones, on the propensity for crashes. Given that vehicles are known to leave the road on curves more frequently (e.g., due to loss of side friction, visibility issues, etc.), it is logical to question whether barriers deployed on CSRS on high-speed highways face demands greater than those same barriers do on tangent, normal sections and whether they provide adequate safety. The available sources of crash data do not typically include sufficient details about either the roadway curvature or the nature of barrier type, dimensions, and placement relative to the shoulder for barriers that were impacted. Thus, crash data does not allow barrier safety performance analysis for curves. Further, even when state DOTs have roadway geometry and barrier inventories, they may not be able to create the linkages necessary for safety performance analysis. Various sources of data were explored, but none were found to be useful for analyzing the safety of longitudinal barriers installed on CSRS. The review of previous efforts did not reveal specific knowledge or insights about the safety performance of longitudinal barriers on CSRS.

The state DOT survey conducted in the first phase sought relevant information pertaining to the safety performance of longitudinal barriers on curved and superelevated road sections. The information from the state DOTs revealed that specific design standards and practices, and/or in-service performance analyses did not exist. These efforts revealed that most states use the same design, selection, and installation guidance for longitudinal barriers on either tangent or CSRS. Further, the states did not cite concerns that this was inappropriate. There has been an improving understanding of vehicle dynamics and its role in crash occurrence and outcomes, so it was recognized that CSRS effects could lead to vehicle-to-barrier interface problems. These facets made

it apparent that it would be useful to address the question of whether there were safety issues associated with longitudinal barriers on CSRS.

The second phase of the research began with VDA. Several recent efforts used commercially available VDA tools to effectively analyze the effects of surface conditions on vehicle trajectories when considering vehicle type, suspension, and speed. The VDA simulations focused on vehicles departing the traveled way on CSRS of high-speed highways. While it was recognized that there could be an unlimited number of vehicle road departure paths, these efforts focused on two types of vehicles on roads at speeds of 60 mph. The departures were all considered to leave the roadway toward the high side of the superelevated section, under the assumption that vertical forces would be more likely to cause vaulting or underride if a barrier impact occurred. The curvature and superelevation rates for six categories of curves defined in the Green Book were considered, as were varying shoulder widths and slopes. It was assumed that the barriers would be placed immediately adjacent to the outer edge of the shoulder. Three common types of longitudinal barriers were analyzed: NJ concrete barriers, G41S W-beam guardrail, and MGS W-beam guardrail.

VDA provided information on how the vehicles departing the roadways would interface with the barriers across a broad spectrum of conditions. The results of this analysis were tabulated to show situations where underride or override issues might exist. Full understanding of the interface was not considered necessary, but VDA was useful for highlighting CSRS conditions where there could be potential barrier safety performance problems.

FE simulations were then undertaken to investigate the impact performance (i.e., physics) of the selected vehicles hitting the barriers for the critical CSRS conditions. These simulations focused on the impact conditions and standards for evaluation of barrier performance as prescribed in MASH. The simulations used validated FE models of barriers

and vehicles. More than 200 detailed simulations were undertaken to analyze those CSRS that were indicated as potentially critical in the VDA efforts. The simulations focused on MASH TL-3 evaluation requirements.

A considerable amount of information was generated in the simulations. The outcomes were summarized in a series of tables for each barrier and MASH test condition across the range of conditions simulated. For each CSRS condition (i.e., curve radius and superelevation; and shoulder width and shoulder angle), the results of the simulation runs for impacts with specific types of barriers identified possible situations where barrier safety was an issue.

Insights were drawn from these summaries and the following findings emerged:

- After approximately 60 simulations for the NJ concrete barrier, the results indicated that most passed MASH Test 3-11 (the most critical test) requirements for CSRS conditions when the barrier was installed normal to road or shoulder. The simulations of impacts with the NJ concrete barrier indicated that it was more prone to fail the crashworthiness requirements for situations where the superelevation was 8% or greater and the shoulder angle was 6% to 8%.
- Barriers on less severe CSRS conditions were more likely to meet MASH requirements. This might suggest that current applications of concrete barriers are viable for non-severe CSRS conditions.
- Efforts to simulate G4(1S) W-beam barriers for various conditions analyzed showed that the 27¾-in.-high barriers did not perform as well as other barriers with greater heights.
- The simulations of G4(1S) barriers at 27¾ in. for CSRS applications showed a propensity for override, as the VDA results also suggested. There were fewer cases of vaulting for the 29-in.-high G4(1S). There were no cases where underride was indicated to be a problem.
- Simulations of the MGS barriers (31 in. high) showed no propensity for underride issues with the small car and good performance for limiting override.
- Additional simulations for F-shape concrete barriers indicated improved performance over the NJ concrete barriers.

The simulation efforts included some additional runs to add depth to the analyses and provide a better understanding of the incremental performance differences between conditions. These confirmed the findings reported here but were not documented.

The project included a budget for full-scale crash testing to verify the findings of the VDA and simulation efforts. There was considerable discussion about which crash tests to conduct. There were many interesting options, but a very limited testing budget. Ultimately, three tests were conducted. These tests were conducted for the most common type of W-beam barrier and bracketed the pass/fail limits indicated by the simulations. Since the test results were considered similar to those of the simulations, they are believed to confirm that the simulations reflected real-world safety performance of barriers on CSRS.

#### 8.1 Proposed Guidance

A considerable amount of information was derived from the VDA, FE simulation analyses, and crash testing. In the end, the challenge was to translate these results into guidance for the design, selection, and installation of longitudinal barriers on CSRS. Table 8.1 contains the significant implications and guidance derived for the barriers and CSRS conditions analyzed. Guidance implies an understanding of the implications of vehicle-to-barrier impacts on CSRS. These are included along with the critical elements of guidance (in bold) that evolved from this research. These are subject to further vetting, rewording, and editing consultation with AASHTO committees. It is hoped that this construct offers a useful means to summarize the findings of the multifaceted analyses and those related findings that support the proposed guidance for barrier design, selection, and installation.

#### **8.2 Implications for Current Practice**

The research did not identify issues with the safety performance of longitudinal barriers installed on CSRS for situations with larger radii and small shoulder angles. There was evidence that barrier safety performance was more likely to be compromised on short-radius, high superelevation CSRS situations. These are most often found on ramps for interchanges. While it was suggested that more research be undertaken for these situations, state DOTs can provide added degrees of safety by applying the guidelines for design, selection, and installation as summarized in Table 8.1. It is hoped that there will be efforts to incorporate the findings of this research into future versions of the Roadside Design Guide. This will increase the awareness of potential safety issues and allow agencies to make the appropriate improvements in project designs, particularly for special situations, but also for their design standards.

The findings are also likely to lead to increased awareness by state DOTs of potential safety issues in design, construction, and maintenance operations. Awareness of the safety issues will enhance the recognition of them in the field and ultimately highlight the need to alter practices to mitigate potential safety problems. For example, state DOTs aware that tight, superelevated curves need special design, operations, and maintenance considerations can incorporate appropriate guidance in their manuals. There will be a need to track safety

Table 8.1. CSRS implications and guidance derived based on the results.

Aspect	Implications and Guidance Elements
Barrier Design	
General	<ul> <li>Poor vehicle-to-barrier interface limits the barrier functions in a crash.</li> <li>Good interface is a necessary, but not a sufficient condition for selection of a barrier type. The degree of increased impact severity needs to be further assessed.</li> <li>Consider using interface analyses (i.e., VDA) to evaluate special cases or other types of barriers to increase the confidence in the design.</li> <li>Consider higher barriers to better accommodate larger vehicles for CSRS applications.</li> </ul>
Concrete Barriers	<ul> <li>Concrete safety shapes do not have underride problems, but face slopes can induce rollovers.</li> <li>Use higher concrete barriers where there is a concern about overrides associated with CSRS features.</li> <li>Concrete barriers with an appropriate face slope may be considered the most universally effective design for CSRS conditions.</li> <li>Design concrete barriers with minimum face slope to limit vehicle ride-up and maintain a viable interface area overlap.</li> </ul>
W-Beam Barrier	<ul> <li>The need for a higher barrier is apparent, but increasing the rail height necessitated review of underride potential.</li> <li>Increases in barrier height are most important for tight curves where excessive speeds are likely to occur (e.g., off-ramps, downhill).</li> <li>Follow the FHWA Technical Memorandum (dated May 5, 2010) that recommends the nominal height for new installations of G4(1S) barriers be 29 in. for CSRS (Nicol 2010).</li> <li>Consider 31-inhigh W-beam barrier designs for CSRS situations.</li> </ul>
Selection	
Curvature and Super- elevation	<ul> <li>Conduct deeper analysis of short-radius, high superelevation CSRS situations.</li> <li>Limit the use of tight curves with high superelevations.</li> <li>Consider using higher barriers on CSRS with appropriate underride protection.</li> </ul>
Shoulder Width and Angle	<ul> <li>Limit major changes in shoulder slope to avoid impacting the barrier when the suspension effects can maximize the potential interface area.</li> <li>Use wider shoulders where slope changes must be large to allow the suspension to stabilize the vehicle before impact.</li> <li>Limit shoulder angle to comply with AASHTO recommendations to ensure the melting snow flows away from the road.</li> </ul>
Roadside Slope	Limit the variation of slope change on the roadside for situations where the barrier is not placed adjacent to the shoulder to provide an acceptable interface.
Barrier Type	<ul> <li>Consider higher (e.g., 31-in.) W-beam barrier designs for CSRS situations.</li> <li>Select barriers with increased height for tight curves where high speeds are likely to occur.</li> <li>Consider using concrete barriers with minimum face slope (e.g., F-shape) to reduce risk of rollover.</li> </ul>
Installation	
Orientation	Promote use of barrier orientation perpendicular to the roadway for concrete barriers.
Placement	<ul> <li>Limit the placement of barriers to only the edge of shoulder on CSRS, particularly where there is a slope change going to the side slope.</li> <li>Use wider shoulders with lower shoulder angles relative to the road on CSRS with short radii and high superelevation.</li> </ul>
Maintenance	<ul> <li>Analysis of the effectiveness of damaged barriers on CSRS is needed.</li> <li>Further analysis of the relative priorities for barrier maintenance on CSRS may be needed.</li> </ul>

performance along with changes in highway design, vehicle fleet characteristics, driver behavior, and other factors known to influence safety.

#### **8.3 Needs for Future Research**

This research successfully analyzed many questions related to the performance of longitudinal barriers on CSRS. The effort effectively demonstrated the usefulness of the VDA to understand the potential vehicle-to-barrier interfaces that are critical to safety performance for a range of CSRS conditions. The VDA efforts analyzed the effects of vehicle type, surface profile changes, and speeds across the range of curve, shoulder features, and roadside slopes relative to interface effectiveness. These provided a basis for barrier height and placement guidelines. These efforts also highlighted the design conditions, barrier types, and placement options that were likely to be problematic, as a focus for the more time-consuming, physicsbased FE analysis of the impacts between vehicles and barriers on CSRS. These simulations demonstrated that the variations in design, barrier, and placement could be accurately analyzed using simulation tools. Over 250 simulations were undertaken to determine those conditions where safety performance might not be adequate. These results were successfully verified by crash tests involving impacts for typical CSRS conditions.

The vehicle dynamics analyses and crash simulations results provided a sound basis for new guidance for the design, selection, and placement of longitudinal barriers on CSRS. While the research efforts answered many questions, some remain and others become apparent. Some questions that may warrant future research are listed below by importance:

#### Strong Need

- Assess design issues associated with the short-radii (tight) curves and high superelevation cases subject to vehicle traveling too fast (e.g., tight ramps prone to over-speed vehicles).
- Analyze the implications for SUTs impacting longitudinal barriers on CSRS (e.g., TL-4).
- Analyze the implications for tractor-trailer impacts on CSRS (i.e., TL-5 and TL-6).

- Consider CSRS barrier performance for short wheelbase SUVs (or vehicles known to be prone to rollovers). Additional simulations or testing for other vehicle types (e.g., mid-sized sedans, very small cars).
- Sensitivity analysis to determine if barriers on CSRS warrant special damage severity and repair priorities (e.g., when rails separate from posts, more slack is introduced into the system, which may reduce the ability to hold or redirect vehicles).

#### **Important**

- Determine effects of impacts of barriers on inner or downside of CSRS. Are there differences in effects for impacts with barriers on the outer or inner sides of the curve?
- Assess the effects of CSRS placed on vertical grades.
- Conduct detailed analysis of vehicle orientation traversing road departure path on CSRS.
- Develop protocol for special MASH testing requirements for CSRS.

#### Other

- Determine the sensitivity of barrier performance for other impact speeds and angles.
- Determine length of need requirements for longitudinal barriers on CSRS.
- Determine implications of reduced side friction on CSRS barrier impacts.
- Are there differences in performance where the barrier is adjacent to transition sections?
- Determine barrier performance for variations in blockouts, rub-rails, and so forth.
- Conduct specific vehicle dynamics and impact force analyses not presented to compare impacts on level terrain with those on CSRS.

Such research efforts would need to reflect the ongoing changes in road design, traffic characteristics, vehicle fleets, driver behavior, and federal and state policies and practices.

# References

- AASHTO (2011a). A Policy on Geometric Design for Highways and Streets. Washington, D.C.
- AASHTO (2011b). Roadside Design Guide. Washington, D.C.
- AASHTO (2009). Manual for Assessment of Safety Hardware. Washington, D.C.
- Brennan, S. N., and Hamblin, B. C. (2007). Utilization of Vehicle Dynamic Simulations as Predictors of Highway Safety. ASME International Mechanical Engineering Congress and Exposition, IMECE2007-42195.
- Bronstad, M. E., and Kimball, C. E., Jr. (1986). Bridge Rail Retrofit for Curved Structures. Report prepared for FHWA by Southwest Research Institute, San Antonio, TX.
- Bullard, D. L., Jr., Bligh, R. P., and Menges, W. L. (1996). NCHRP Report 350 Compliance Test 3-11 for the Modified G4(1S) Guardrail with Timber Blockouts. Report prepared for FHWA by Texas Transportation Institute, College Station, TX.
- Bullard, D. L., Jr., Bligh, R. P. and Menges, W. L. (2009). MASH Testing and Evaluation of the New Jersey Safety Shape Barrier. Report prepared under NCHRP Project 22-14 by Texas Transportation Institute, College Station, TX.
- CarSim (2006). Mechanical Simulation Corporation. http://www.carsim.com.
- Claar, P. W., Buchele, W. F., and Sheth, P. N. (1980). Off-Road Vehicle Ride: Review of Concepts and Design Evaluation with Computer Simulation. SAE International 801023, Warrendale, PA.
- Day, T. D., and Garvey, J. T. (2000). Applications and Limitations of 3-Dimensional Vehicle Rollover Simulation. SAE International 2000-01-0852, Warrendale, PA.
- Engineering Dynamics Corporation (2005). HVE Software (Human, Vehicle, and Environment). Beaverton, OR. http://www.edccorp.com.
- Esfahani, E. S., Marzougui, D., and Opiela, K. S. (2009) Safety Performance Evaluation of Concrete Median Barriers under Updated Crashworthiness Criteria. *SAE Journal*, January.
- Hadden, J. A., Everson, J. H., Pape, D. B., and Narendran, V. K. (1997). Modeling and Analysis of Driver/Vehicle Dynamics with Run-Off-Road Crash Avoidance System. 30th International Symposium on Automotive Technology and Automation. Paper No. 97SAF020, pp. 343–350, Florence, Italy, June 16–19.
- Hallquist, J. O. (1997). LS-DYNA Theoretical Manual. Livermore Software Technology Corporation, Livermore, CA.
- Hallquist, J. O. (2006). LS-DYNA Keyword User's Manual. Livermore Software Technology Corporation, Livermore, CA.
- Mancosu, F. (2002). Vehicle-Road-Tyre Interaction in Potential Dangerous Situations: Results of VERT Project. SAE International 2002-01-1181, Warrendale, PA.

- Marzougui, D., Kan, C. D., and Opiela, K. S. (2007). Effects of Shoulder Drop-off on W-Beam Guardrail Performance. National Crash Analysis Center, George Washington University, Virginia Campus, Ashburn.
- Marzougui, D., Kan, C. D., and Opiela, K. S. (2008a). Evaluation of the Influences of Cable Barrier Design and Placement on Vehicle to Barrier Interface. NCAC Document 2008-W-001, National Crash Analysis Center, George Washington University, Virginia Campus, Ashburn.
- Marzougui, D., Kan, C. D., Opiela, K. S. (2008b). Safety Performance Evaluation of Portable Concrete Barriers. Working Paper NCAC 2007-W-004. Prepared for FHWA by the National Crash Analysis Center, George Washington University, Virginia Campus, Ashburn.
- Marzougui, D., Kan, C. D., and Opiela, K. S. (2009a). Analyzing the Effects of Cable Barriers Behind Curbs Using Computer Simulation. Report 2009-W-008. Prepared for FHWA by the National Crash Analysis Center, George Washington University, Washington, D.C.
- Marzougui, D., Kan, C. D., and Opiela; K. S. (2009b). Component and Full-Scale Tests of the 2007 Chevrolet Silverado Suspension System. NCAC 2009-R-004. National Crash Analysis Center, George Washington University, Virginia Campus, Ashburn.
- Marzougui, D., Kan, C. D., Opiela, K. S. (2009c). Evaluation of Rail Height Effects of the Safety Performance of W-Beam Barriers. Working Paper NCAC 2007-W-002. Prepared for FHWA by the National Crash Analysis Center, George Washington University, Virginia Campus, Ashburn.
- Marzougui, D., Kan, C. D., and Opiela, K. S. (2010a). Using Vehicle Dynamics Simulation as a Tool for Analyzing Cable Barrier Effectiveness. Report 2010-W-006. Prepared for FHWA by the National Crash Analysis Center, George Washington University, Virginia Campus, Ashburn.
- Marzougui, D., Kan, C. D., and Opiela, K. S. (2010b). Safety Performance Evaluation of Portable Concrete Barriers. NCAC 2007-R-004. Prepared for FHWA by the National Crash Analysis Center, George Washington University, Virginia Campus, Ashburn.
- Marzougui, D., Kan, C. D., Esfahani, E. S., and Opiela, K. S. (2010c). Safety Performance of Concrete Median Barriers under Updated Crashworthiness Criteria. Working Paper NCAC 2008-W-002. Prepared for FHWA by the National Crash Analysis Center, George Washington University, Virginia Campus, Ashburn.
- Marzougui, D., Kan, C. D., and Opiela, K. S. (2010d). Safety Performance Evaluation of W-Beam Guardrail with Raised Blockouts. Working Paper NCAC 2009-T-002. Prepared for FHWA by the National Crash Analysis Center, George Washington University, Virginia Campus, Ashburn.

- Marzougui, D., Mahadevaiah, U., and Opiela, K. S. (2011a). Development of a Modified MGS Design for Test Level 2 Impact Conditions Using Crash Simulation. Working Paper NCAC 2010-W-005. Prepared for FHWA by the National Crash Analysis Center, George Washington University, Virginia Campus, Ashburn.
- Marzougui, D., Kan, C. D., and Opiela, K. S. (2011b). Comparison of the Crash Test and Simulation of an Angle Impact of a 2007 Chevrolet Silverado Pick-Up Truck into a New Jersey-Shaped Concrete Barrier for MASH Conditions. Working Paper NCAC 2010-W-001. Prepared for FHWA by the National Crash Analysis Center, George Washington University, Virginia Campus, Ashburn.
- Marzougui, D., Mahadevaiah, U., Tahan, F., Kan, C. D., McGinnis, R., and Powers, R. (2012a). NCHRP Report No. 711: Guidance for the Selection, Use, and Maintenance of Cable Barrier Systems. Transportation Research Board of the National Academies, Washington, D.C.
- Marzougui, D., Kan, C. D., Samaha, R. R.; Cui, C., and Nix, L. (2012b). Extended Validation of the Finite Element Model for the 2007 Chevrolet Silverado Pick-Up Truck (MASH 2270kg Vehicle). NCAC 2012-W-003. National Crash Analysis Center, George Washington University, Virginia Campus, Ashburn.
- Marzougui, D., Samaha, R. R., Nix, L., and Kan, C. D. (2012c). Extended Validation of the Finite Element Model for the 2010 Toyota Yaris Sedan (MASH 1100kg Vehicle). NCAC 2012-W-005. National Crash Analysis Center, George Washington University, Virginia Campus, Ashburn.
- Marzougui, D., Kan, C. D., and Opiela, K. S. (2012d). Safety Performance Evaluation of Concrete Barriers on Curved and Superelevated Roads. Working Paper NCAC 2011-W-005. Prepared for FHWA by the National Crash Analysis Center, George Washington University, Virginia Campus, Ashburn.
- McMillan, N. J., Pape, D. B., Hadden, J. A., Narendran, V. K., and Everson, J. H. (1997). Statistics-Based Simulation Methodology for Evaluating Collision Countermeasure Systems Performance. Presented at the IEEE Conference on Intelligent Transportation Systems, Boston, MA, Nov. 9–12.
- National Crash Analysis Center (2009). Modeling, Testing, and Validation of the 2007 Chevy Silverado Finite Element Model, NCAC 2009-W-005. George Washington University, Virginia Campus, Ashburn.
- National Crash Analysis Center (2011). Development and Validation of a Finite Element Model for a 2010 Toyota Yaris Sedan. NCAC 2011-T-001. Prepared for FHWA by the National Crash Analysis Center, George Washington University, Virginia Campus, Ashburn.
- National Crash Analysis Center (2012a). NCAC Finite Element Vehicle Models Update 2012, 2012-T-002. George Washington University, Virginia Campus, Ashburn.
- National Crash Analysis Center (2012b). Development and Validation of a Finite Element Model for a Geo Metro Sedan. NCAC 2007-T-008. George Washington University, Virginia Campus, Ashburn.
- National Crash Analysis Center (2012c). Development and Validation of a FE Model of a 1994 Chevy C2500 Pick-up Truck. NCAC 2007-T-009. George Washington University, Virginia Campus, Ashburn.
- National Crash Analysis Center (2012d). Development and Validation of a FE Model of a 2010 Toyota Yaris Passenger Sedan. NCAC 2011-T-001. George Washington University, Virginia Campus, Ashburn.
- National Crash Analysis Center (2012e). Development and Validation of a Model of a 2007 Chevy Silverado Pick-up Truck. NCAC 2009-T-005. George Washington University, Virginia Campus, Ashburn.
- Nicol, D. A. (2010). FHWA Memorandum: Roadside Design: Steel Strong Post W-Beam Guardrail. Washington, D.C., May 17.

- Pape, D. B., Narendran, V. K., Koenig, M. J., Hadden, J. A., and Everson, J. H. (1996). Dynamic Vehicle Simulation to Evaluate Countermeasure Systems for Run-Off-Road Crashes. SAE International, 960517, Warrendale, PA.
- Polivka, K. A., Sicking, D. L., Rohde, J. R., Bielenberg, R. W., Faller, R. K., Reid, J. D., Holloway, J. C., and Kuipers, B. D. (2004). Development of the Midwest Guardrail System for Standard and Reduced Post Spacing in Combination with Curbs. Prepared for Midwest States Pooled Fund Program by Midwest Roadside Safety Facility, Lincoln, NE.
- Polivka, K. A., Sicking, D. L., Rohde, J. R., Bielenberg, R. W., Faller, R. K., and Reid, J. D. (2006a). Performance Evaluation of the Modified G4(1S) Guardrail—Update to NCHRP 350 Test No. 3-11 with 28" C.G. Height (2214WB-2). Prepared for NCHRP Project 22-14(2) by Midwest Roadside Safety Facility, Lincoln, NE.
- Polivka, K. A., Sicking, D. L., Rohde, J. R., Bielenberg, R. W., Faller, R. K., Reid, J. D., and Coon, B. A. (2006b). Performance Evaluation of the Permanent New Jersey Safety Shape Barrier—Update to NCHRP 350 Test No. 3-10 (2214NJ-1). Prepared for NCHRP Project 22-14(2) by Midwest Roadside Safety Facility, Lincoln, NE.
- Polivka, K. A., Sicking, D. L., Rohde, J. R., Bielenberg, R. W., Faller, R. K., and Reid, J. D. (2006c). Performance Evaluation of the Midwest Guardrail System—Update to NCHRP 350 Test No. 3-10 (2214MG-3). Prepared for NCHRP Project 22-14(2), Midwest Roadside Safety Facility, Lincoln, NE.
- Polivka, K. A., Sicking, D. L., Rohde, J. R., Bielenberg, R. W., Faller, R. K., and Reid, J. D. (2006d). Performance Evaluation of the Modified G4(1S) Guardrail—Update to NCHRP 350 Test No. 3-11 with 28" C.G. Height (2214MG-2). Report prepared for NCHRP Project 22-14(2), Midwest Roadside Safety Facility, Lincoln, NE.
- Ray, M. L., Plaxico, C. A., Anghileri, M. (2010). NCHRP Web-Only Document 179: Procedures for Verification and Validation of Crash Simulations Used in Roadside Safety Applications. TRB, National Research Council, Washington, D.C.
- Ross, H. E., Jr., Sicking, D. L., Zimmer, R. A., and Michie, J. D. (1993). NCHRP Report 350: Recommended Procedures for the Safety Performance Evaluation of Highway Features. TRB, National Research Council, Washington, D.C.
- Sheikh, N. M., and Alberson, D. C. (2005). Comparative Simulation Evaluation Bridge Parapet Orientations. Report 9-8132-5. Texas Transportation Institute, Texas A&M University, College Station.
- Sheikh, N. M., and Bligh, R. P. (2006). Analysis of the Impact Performance of Concrete Median Barrier Placed on or Adjacent to Slopes. Report 0-5210-1. Texas Transportation Institute, Texas A&M University, College Station.
- Sheikh, N. M., Bligh. R. P., and Menges, W. L. (2008). Crash Testing and Evaluation of F-Shape Barriers on Slopes. Report 0-5210-3. Texas Transportation Institute, Texas A&M University, College Station.
- Sicking, D. L., and Mak, K. K. (2004). Improving Roadside Safety by Computer Simulation. A2A04: Committee on Roadside Safety Features, Transportation Research Board of the National Academies, Washington, D.C.
- Stout, D., Hughes, W., and McGee, H. (1993). Traffic Barriers on Curves, Curbs, and Slopes. FHWA Report FHWA-93-01. McLean, VA, August.
- Torbic, D. J., Harwood D. W., Gilmore D. K., Pfefer R., Neuman T. R., Slack, K. L. and Hardy, K. K. (2004). NCHRP Report 500: Guidance for Implementation of the AASHTO Strategic Highway Safety Plan—Volume 7: A Guide for Reducing Collisions on Horizontal Curves. Transportation Research Board of the National Academies, Washington, D.C.

# APPENDIX A

# State Dot Survey Instrument and Instructions

Appendix A contains the state DOT survey and instructions. It can be found on the TRB website (www.trb.org) by searching for "NCHRP Research Report 894".

## APPENDIX B

# Vehicle Dynamics Simulation Results

Appendix B contains the vehicle dynamics simulation results. It can be found on the TRB website (www.trb.org) by searching for "NCHRP Research Report 894".

## APPENDIX C

# **Finite Element Model Validations**

Appendix C contains the FE model validations. It can be found on the TRB website (www.trb.org) by searching for "NCHRP Research Report 894".

# APPENDIX D

# **Finite Element Simulation Results**

Appendix D contains the FE simulations results. It can be found on the TRB website (www.trb.org) by searching for "NCHRP Research Report 894".

## APPENDIX E

# **Full-Scale Crash Testing Report**

Appendix E contains full-scale crash test report. It can be found on the TRB website (www.trb.org) by searching for "NCHRP Research Report 894".

ADA

Abbreviations and acronyms used without definitions in TRB publications:

A4A Airlines for America

AAAE American Association of Airport Executives AASHO American Association of State Highway Officials

Americans with Disabilities Act

AASHTO American Association of State Highway and Transportation Officials

ACI–NA Airports Council International–North America ACRP Airport Cooperative Research Program

APTA American Public Transportation Association
ASCE American Society of Civil Engineers
ASME American Society of Mechanical Engineers
ASTM American Society for Testing and Materials

ATA American Trucking Associations

CTAA Community Transportation Association of America CTBSSP Commercial Truck and Bus Safety Synthesis Program

DHS Department of Homeland Security

DOE Department of Energy

EPA Environmental Protection Agency FAA Federal Aviation Administration

FAST Fixing America's Surface Transportation Act (2015)

FHWA Federal Highway Administration

FMCSA Federal Motor Carrier Safety Administration

FRA Federal Railroad Administration FTA Federal Transit Administration

 HMCRP
 Hazardous Materials Cooperative Research Program

 IEEE
 Institute of Electrical and Electronics Engineers

 ISTEA
 Intermodal Surface Transportation Efficiency Act of 1991

ITE Institute of Transportation Engineers

MAP-21 Moving Ahead for Progress in the 21st Century Act (2012)

NASA National Aeronautics and Space Administration
NASAO National Association of State Aviation Officials
NCFRP National Cooperative Freight Research Program
NCHRP National Cooperative Highway Research Program
NHTSA National Highway Traffic Safety Administration

NTSB National Transportation Safety Board

PHMSA Pipeline and Hazardous Materials Safety Administration RITA Research and Innovative Technology Administration

SAE Society of Automotive Engineers

SAFETEA-LU Safe, Accountable, Flexible, Efficient Transportation Equity Act:

A Legacy for Users (2005)

TCRP Transit Cooperative Research Program TDC Transit Development Corporation

TEA-21 Transportation Equity Act for the 21st Century (1998)

TRB Transportation Research Board
TSA Transportation Security Administration
U.S. DOT United States Department of Transportation

Washington, DC 20001

500 Fifth Street, NW

TRANSPORTATION RESEARCH BOARD

The National Academies of SCIENCES · ENGINEERING · MEDICINE

The nation turns to the National Academies of Sciences, Engineering, and Medicine for independent, objective advice on issues that affect people's lives worldwide.
www.national-academies.org



NON-PROFIT ORG. U.S. POSTAGE **PAID**COLUMBIA, MD
PERMIT NO. 88